Development of the sea urchin apical organ:

cellular mapping of gene expression and FGF signalling

Avigdor Lerner

Research Department of Genetics, Evolution and Environment

UCL

Submitted for the Degree of Doctor of Philosophy

September 2013

Declaration

I, Avigdor Lerner confirm that the work presented in this thesis is my own. Where information has been derived from other sources, I confirm that this has been indicated in the thesis.

Signed:

Abstract

The sea urchin apical organ constitutes a fundamental part of the larval nervous system and forms a neuro-sensory structure capable of sensing environmental cues and coordinating swimming behaviour. However, the gene regulatory network (GRN) that underlies the specification of this structure is poorly understood. The first step in building an apical organ GRN, is the high-resolution characterisation of regulatory genes in both *time and space*. This information then allows the regulatory states of the apical domain to be determined and identifies the existence of different spatial domains.

In this study, spatial and temporal expression data of regulatory genes were overlaid onto cellular maps of the apical domain at different developmental stages. These cellular maps were then used to establish the different regulatory states that occur in the apical domain and their dynamics during development. This analysis illustrated that the spatial organisation of the apical domain is far more complex and dynamic than previously thought.

The rest of the thesis focuses on functional analysis, and addresses the role of FGF signalling in the development of the apical organ. Embryos injected with a *fgfr1* morpholino or incubated with SU5402, a common chemical inhibitor of FGFR1, show an upregulation in a limited group of apical organ genes. Surprisingly, the two methods of disrupting FGFR1 did not affect similar genes, and suggests that an unspecific perturbation is occurring. Functional analysis was also carried out on *zic2*, an apical organ transcription factor upregulated by SU5402 treatment. The results show that *zic2* represses itself and is required for a normal complement of serotonergic neurons.

Acknowledgements

I would like to thank my supervisor Paola Oliveri for all the intellectual discussions, valuable help, patience and guidance (both in and outside the lab) she has given me over the past few years. Thank you for taking notice of a keen, bright-eyed, second year undergraduate and giving him the opportunity to do a summer research project, and for letting me stick around to do my PhD! It has been a great experience watching the lab grow from the very beginning.

I am very grateful to Claudio Stern and Hazel Smith for their guidance and advice throughout my PhD. Also to Kevin Fowler and the research department of GEE for their support and funding. I am grateful to the BBSRC for providing the financial support necessary for me to undertake a PhD.

The Rosh Yeshivah for among so many things, teaching me how to recognise what a good question is.

To past and current members of the Oliveri lab, especially Edmondo, David, Liberio and Anna. Thank you all so much for the assistance, lively and enthusiastic discussions, and most importantly for making the lab a much more amusing place then it would otherwise be.

My summer project and undergraduate students. It has been a privilege to have had the opportunity to supervise and work with you. A special thanks goes to Isabelle Blomfield for her excellent work during a summer project and for collaborating with me again for her undergraduate research project, as well as doing a great and unbelievable patient job proof reading this thesis. Also to Riina and Agnieszka for their help working with the *dcry* gene.

I would like to thank all my family. My parents for giving me the freedom to always make the educational choices I wanted and for all their support. Granny for her love and support, especially when it was needed most, it is appreciated beyond words. Booba for

making Maida Vale my second home and always being there for me. Rutie for taking an interest in my thesis and all her encouragement. Chaim for his general cuteness. My parents in laws, for the chocolate liquor, cold Diet Coke, but most importantly for taking me in like one of their own.

Finally, achron achron choviv, I would like to thank my eishes chayil of a wife, Rachelli for the love, support, encouragement and general looking after she has given me over the past three years. No one has suffered more from my hermit like existence than her and I hope this will make her proud.

Gurglem est squarkus

To Victor Wacks

Table of contents

List of figures

List of tables

Chapter 1:
Introduction

In the closing pages of *Ontogeny and Phylogeny,* Stephan Jay Gould predicted "that an understanding of regulation must lie at the center of any rapprochement between molecular and evolutionary biology; for a synthesis of the two biologies will surely take place, if it takes place at all, on the common field of development" (Gould, 1977). Since the modern synthesis was proposed and the structure of DNA elucidated, it has become clear that species diverge from common ancestors through changes in their DNA. A precise understanding of these changes and how they account for today's morphological diversity is less clear.

Over several decades, developmental and evolutionary studies have shown that animals, irrespective of body plan and level of divergence, share specific families of genes that regulate the development of body plan (Carroll *et al.,* 2005). This common genomic "toolkit" for animal development, contains many of the transcription factors and signalling pathways that provide the basis for animal diversity (Carroll*.,* 2000). Importantly, these transcription factors and signalling molecules combine with downstream differentiation genes to form networks. These relatively simple regulatory sub-circuits consist of a highly conserved set of "linkages" between a few genes encoding transcription factors and the binding sites of genes encoding differentiation proteins (Erwin and Davidson, 2002). Other classes of network sub-circuits are also common to all bilaterians, and hence are part of the shared genomic regulatory heritage from the last common bilaterian ancestor (Erwin and Davidson, 2002). The different elements of this regulatory toolkit are employed to construct a diverse array of body plans, as can be observed throughout the bilaterians. Ultimately, it is the genomic program for development that explains in a mechanistic manner how a fertilised egg gives rise to dozens or even hundreds of different cell types and goes on to form the adult body plan (Tabou-de-Leon and Davidson, 2007).

The specification and patterning of the nervous system has received particular attention from developmental biologists, as it is such a defining feature of the body plan. Animal nervous systems are hugely diverse both structurally and functionally; from the complex brain and major nerve tracts of vertebrates to the much simpler nerve nets and rings of more basal invertebrates (Holland, 2003). Many marine invertebrates are indirect developers and acquire an adult body plan via a distinct larval stage followed by metamorphosis into an adult. The relative simplicity of this embryonic stage and assorted nervous systems makes these marine larvae appealing models for genomic and network-level studies. The knowledge of how the genome encodes the development of such diverse nervous systems is integral to understanding, not only a fundamental aspect of embryonic development, but also to gaining insight into nervous system evolution.

1.1 What is an apical organ?

In the late nineteenth century, Conklin, (1897) undertook a study of the embryology of *Crepidula,* a marine mollusc, and noticed a thickened epithelium at the apical pole, which he named the apical plate. This apical plate proceeded to form what he described as an "apical sensory organ" (figure 1.1). Its role in development and larval function is poorly understood, but is assumed to be a neuro-sensory structure of some type (Lacalli, 1994). Because the apical organ is only present in the free-swimming larvae and disappears after metamorphosis, it is thought to be required for the detection of settlement cues and the induction of metamorphosis, as well as to direct larval swimming (Rentzsch *et al.,* 2008). Two aspects of apical organs lend support for a sensory function. Firstly, apical organs are usually associated with a tuft of long cilia known as an apical tuft (figure 1.2; Nakajima, *et al*., 1993; Hadfield *et al.,* 2000). Secondly, most apical organs include neural elements and are involved in the establishment of neural tracts (figure 1.2; Chia and Koss, 1979; Lacalli, 1994; Kempf *et al.,* 1997).

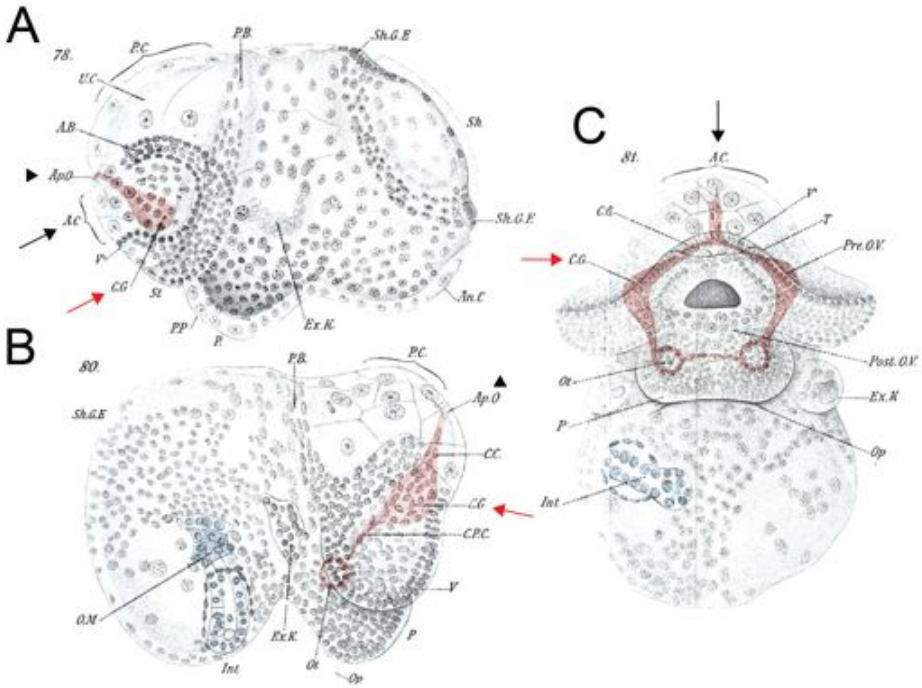

Figure 1.1. Anatomy of the marine mollusc *Crepidula fornicata*
Aspects relevant for this study are indicated in the figure. The apical cell plate (AC, black arrow); the cerebral ganglion (CG, red arrow) and the apical organ cells (ApO, black arrowhead; adapted from Conklin, 1987).

The neuronal basis of the apical organ

The phylogenetic distribution of apical organs with associated ciliary tufts, includes marine larvae of basal metazoans (*e.g.* cnidarians) as well as protostomes (*e.g.* molluscs and annelids) and deuterostomes (*e.g.* echinoderms and hemichordates). Neuronal distribution within the apical organ is illustrated here in a number of phylogenetically distinct examples.

As a sister group of Bilateria, cnidarians hold a key phylogenetic position for understanding nervous system evolution. During the planula stage, the cnidarian *Nematostella vectensis* develops an apical organ with an associated apical tuft (figure 1.2 A). Larvae swim with this apical organ facing forward and ultimately settle and metamorphose on this pole. Recently, Nakanishi *et al.,* (2012) showed that at mid-planula stage, the neurites of most ectodermal neurons extend towards the base of the

apical organ, suggesting that sensory information from the ectoderm is being integrated into the apical organ. However, there is no accumulation of neurons or a ganglion-like structure commonly found in other bilaterian apical organs. This is strange and fails to support the idea that the apical organ is a “neuro” structure.

In contrast, bilaterians show a much greater innervation of the apical organ. Within the protostomes, however, only the Lophotrochozoa develop apical organs. Below are three examples of lophotrochozoans that show this greater lever of innervation. Firstly, the phoronid *Phoronopsis harmeri* develops an apical organ with an associated apical tuft, that contains a number of serotonergic neurons (figure 1.2 B,C). These neurons differentiate simultaneously into flask-shaped cells each bearing a cilium that extends from the embryo surface. Later during development, the basal parts of these neurons form short processes that form a neuropil in the centre of the apical organ (figure 1.2 C white arrow). In addition to serotonergic neurons, the apical organ also contains neurons positive for the neuropeptide FMRFamide (figure 1.2 D; Temereva and Wanninger, 2012). Secondly, similarly to phoronids, the brachiopod, *Terebratalia transversa* has a thickened apical plate which develops an apical organ with associated ciliary tuft. As development progresses, the apical organ contains a large number of monociliated sensory neurons with at least two morphological types (figure 1.2 E white arrows labeled SN1 and SN2), that extend axonal projections to a central neuropil (Santagata *et al.,* 2011). A third Lophotrochozoa example, is the polychaete annelid *Sabellaria alveolata,* that produces a well defined apical organ and associated apical tuft early in development (Brinkmann and Wanninger, 2008). The number of serotonergic neurons increases as development progresses, and they go on to form an apical nerve ring, directly underneath the apical tuft (figure 1.2 F). Cells positive for the neuropeptide FMRFamide are also located in the apical organ and extend fine neural processes that also form an apical nerve ring (Brinkmann and Wanninger, 2008).

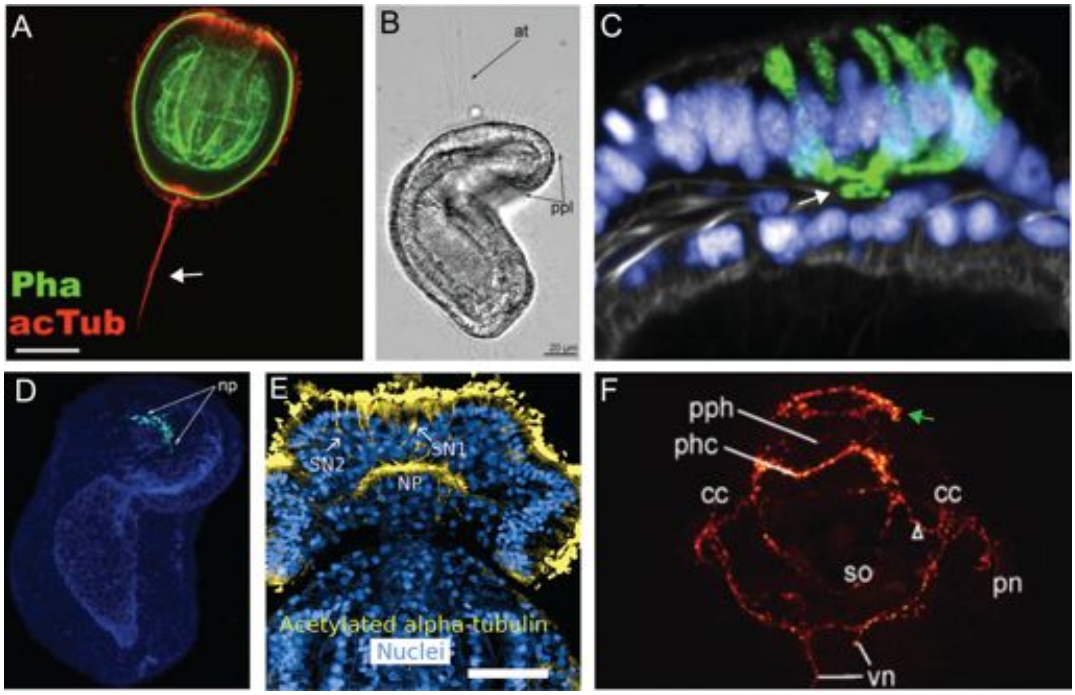

Figure 1.2. Apical organs in cnidarians and protostomes
(A) The apical tuft (white arrow) in the cnidarian *Nematostella vectensis.* Labeled with phalloidin (Pha, green) and acetylated tubulin (acTub, red; adapted from Nakanishi *et al.,* 2012). (B, C, D) The phoronid, *Phoronopsis harmeri*. (B) The apical tuft (black arrow, labled at). (C) Serotonergic neurons (green) can be seen in the apical organ, neuropile (white arrow), cells labeled with Hoechst (violet). (D) FMRFamide positive cells (cyan) can be seen as a horseshoe-shaped neuropil (np, double white arrows), co-stained with phalloidin (blue; adapted from Temereva *et al.,* 2012). (E) The brachiopod *Terebratalia transversa*, two morphological types of sensory neurons (SN1 and SN2) extend axonal projections to a central neuropil (NP). Labelled with acetylated α tubulin (yellow) and DAPI stained nuclei (blue; adapted from Santagata *et al.,* 2012). (F) The polychaete annelid *Sabellaria alveolata, s*erotonergic neurons (red) form a apical nerve ring (green arrow; adapted from Temereva *et al.,* 2012). Scale bars: 100 μm in A; 25 μm in B.

Hemichordates are deuterostomes and the sister group to echinoderms, and are closely related to chordates. *Ptychodera flava* is an indirect-developing hemichordate that has an apical organ and small apical tuft (figure 1.3 A pink arrow; Nielsen *et al.,* 2007). More detailed neurological studies have been carried out in another indirect-developing hemichordate, *Balanoglossus proterogonius* that has an apical ganglion containing serotonergic neurons and a basiepithelial neuropil (figure 1.3 B black arrow). In addition, a large number of FMRFa-immunoreactive cells were detected in the apical organ and in the epithelium of the stomach (figure 1.3 C black arrow and arrowheads respectively; Nezlin *et al.,* 2004). The larval stages of echinoderms all have apical organs

and apical tufts, although they differ in level of neurulation and types of neurons (figure 1.3 D; Byrne *et al.,* 2007). In conclusion, the larvae of many marine organisms possess an apical organ, which is usually associated with a tuft of long cilia and neuronal structures. Both serotonergic and FMRFamide positive cells, are commonly found within the apical organ and these often extend processes that form neuropile in the apical organ.

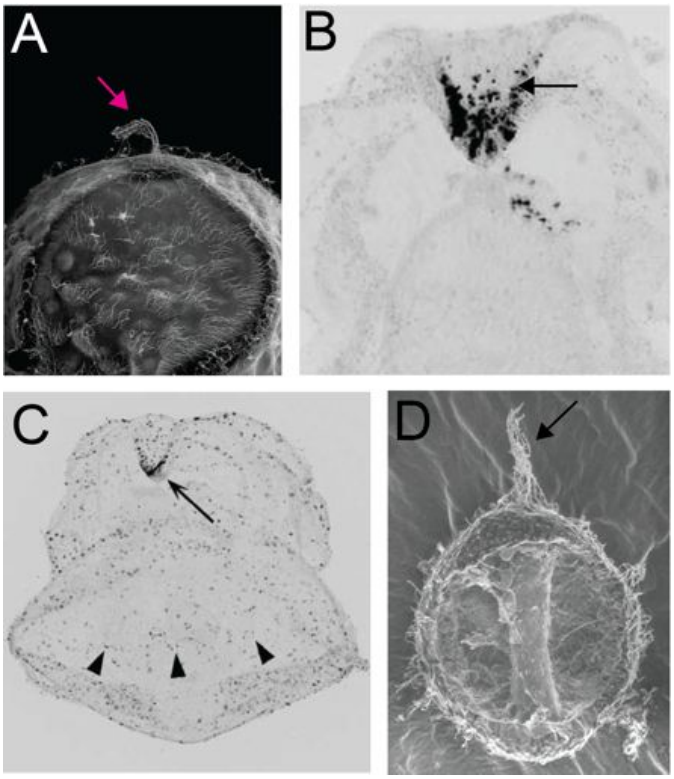

Figure 1.3. Apical organs in deutrostomes
(A) The apical tuft (pink arrow) can be seen in the hemichordate, *Ptychodera flava* (adapted from Nielsen *et al.,* 2007). (B) Serotonergic neurons in the apical organ (black arrow). (C) FMRFamide neurons in the apical organ (black arrow) and the stomach (black arrow heads; adapted from Nezlin *et al.,* 2004). (D) The apical tuft (black arrow) can be seen in the sea urchin, *Lytechinus variegatus* (adapted from Morrill and Marcus, 2005).

The sensory basis of the apical organ

The presence of a tuft of long cilia and neurons in the apical organs of marine larvae, led to the hypothesis that the apical organ functions as a neuro-sensory structure (Lacalli, 1994). In the previous section, I brought a number of examples showing that the apical organ in general was a neuronal structure. I will now bring two further examples showing how the apical organ functions to sense the external environment and is linked to organism behaviour.

Most marine invertebrates produce free-swimming larvae that undergo the process of metamorphosis, a morphogenetic event that transforms the larvae into the juvenile form of the species (Ruiz-Jones and Hadfield, 2011). Metamorphosis is often triggered by the presence of specific chemical cues that are associated with requisite prey, microbial films, or linked to a suitable habitat (Hadfield *et al.,* 2000). Many marine larvae exhibit a range of "testing" and "sampling" behaviours prior to settlement. One common behaviour involves swimming near the substratum so that the apical tuft brush es or touches the substratum (Barnes and Gonor, 1973; Wodicka and Morse, 1991). Hadfield *et al.,* (2000) impaired the function of apical organ cells in the nudibranch *Phestilla sibogae* through the use of the vital dye DASPEI and irradiation. The resulting death of the apical organ cells, caused the otherwise healthy larvae to no longer respond to usual metamorphic cues.

Recently, Conzelmann *et al.,* (2013) identified a neuropeptide, allatostatin-B, that signals via a G protein-coupled receptor, in the marine polychaete annelid *Platynereis dumerilii*. Interestingly, both allatostatin-B and its receptor are expressed in the chemosensory–neurosecretory cells in the apical organ. Morpholino antisense oligonucleotide (MASO) knockdown of the specific G protein-coupled receptor resulted in a loss of settlement behaviour. In contrast, the addition of synthetic allatostatin-B caused the larvae to mimic normal settlement behaviour, including sustained exploratory crawling and frequent touching of the apical tuft to the substrate. In addition, several other neuropeptides are expressed in sensory neurons in the apical organ and regulate larval swimming depth during the free-swimming phase of the life cycle (Conzelmann *et al.,* 2011).

1.2 Gene regulatory networks in development

The body plan of an animal, and hence its exact mode of development, is a property of its species and is thus encoded in the genome (Davidson, 2010). Embryonic development is the process that converts the inherited regulatory program encoded in the genome, into the three dimensional morphology that ultimately forms an embryo (Peter and Davidson, 2011; Ettensohn, 2013). Gene regulatory networks (GRN) underlie all of life's processes, from the initial development of the animal body plan to determining the main events of post-embryonic development, including organogenesis, formation of different cell types, and eventually development to the adult form. Beyond development, GRNs control a vast array of physiological phenomena and how the organism responds to environmental fluctuation and stimuli (Davidson, 2010). Simply put, GRNs are models that describe how regulatory genes interact with one another and control a biological process *e.g.* development. If we want to understand how the genome encodes for the development of an embryonic structure *e.g.* the apical organ we need to study the underlying GRN.

Properties of developmental GRNs

GRNs consist of regulatory genes, defined by Eric Davidson and colleagues as transcription factors and signalling molecules (Davidson, 2001). As regulatory genes interact with one another, as well as other downstream genes, and because every regulatory gene has multiple inputs and outputs, the total map of their interactions has the form of a network (figure 1.4; Davidson, 2006). The genes in the network are regulated by clusters of DNA sequences called *cis*-regulatory elements, that serve as binding sites for transcription factors (Arnone and Davidson, 1997). The *cis*-regulatory elements present in a gene, determine which transcription factors bind to it and as a result when and where the gene will be expressed. These *cis*-regulatory elements are typically found in modules several hundred base pairs in length that on average contains 10 or more binding sites (figure 1.4; Small *et al*., 1992; Arnone and Davidson, 1997, Oliveri and Davidson, 2004; Levine and Davidson, 2005)

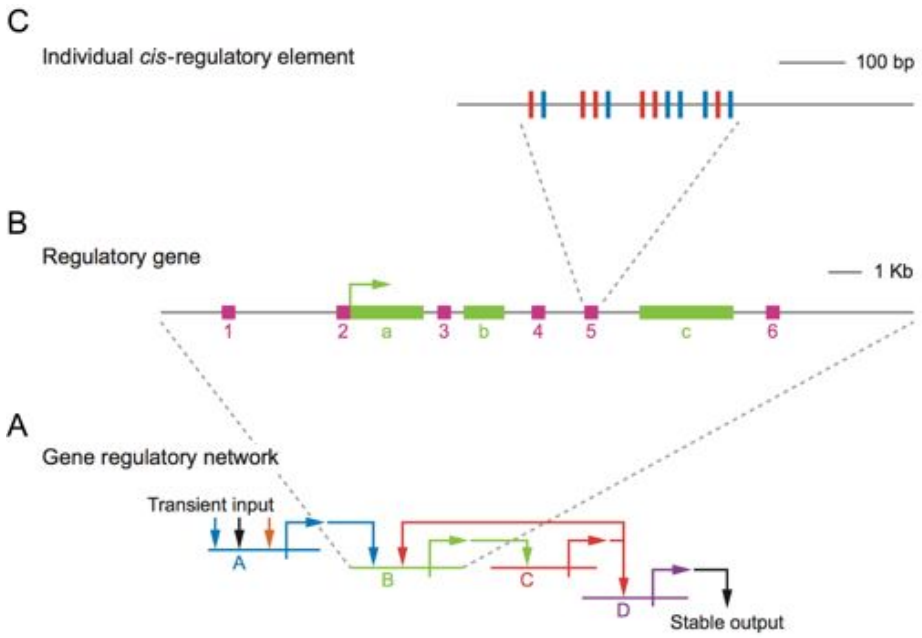

Figure 1.4. *cis*-regulatory aspects of a GRN
(A) Transcription factors and signalling molecules interact to form a network. (B) A gene contains a number of *cis*-regulatory modules (pink boxes) that control its expression in time and space. The exons are indicated in light green boxes. (C) An individual *cis*-regulatory module contains a cluster of several transcription factor binding sites, indicated in red and blue boxes. In this diagram the colour codes of the three levels match, so panel C represents the *cis*-regulatory module of gene B, which has binding sites of transcription factors A (blue) and C (red; adapted from de Leon and Davidson, 2007).

A fundamental characteristic of GRNs is that they are modular. GRNs are composed of multiple sub-circuits that each carry out a specific developmental task *e.g.* cell specification. Therefore the types of sub-circuit a GRN contains, is an indication of the biological tasks it carries out (Davidson and Levine, 2008). The architecture of a GRN sub-circuit defines the developmental task it carries out (Davidson, 2010). Table 1.1 gives some common examples of GRN sub-circuits and what developmental task they perform. Interestingly, GRN sub-circuits with a similar architecture but different regulatory genes are repeatedly encountered doing the same tasks in different GRNs (Davidson, 2009 and 2010).

Table 1.1. Types of common sub-circuits found in developmental GRNs. The left column shows the type of sub-circuit and the right column shows the effect associated with that sub-circuit (adapted from (Davidson and Levine, 2008). Further explanation of a double negative gate and the community effect can be found on pages 39-41.

GRN subcircuit design feature	Developmental control logic
Double negative gate	Exclusive spatial derepression and repression
Intraterritorial repression	Exclusion of alternative regulatory states
Ligand gene response to own signal transduction system	Community effect: enforce transcriptional conformity within territory
Auto and cross regulatory feedback	Dynamic regulatory state lockdown
Regulatory auto-repression	Temporal expression peak/oscillation
Regulatory auto-repression controlling expression of signal ligand genes	Dynamic spatial wave of signaling

Another important characteristic of GRNs is that they are hierarchical. Parts of the GRN controlling the initial stages of development are at the top of the hierarchy and influence everything else downstream, while the part of the GRN controlling intermediate processes of spatial subdivision or the formation of future morphological pattern are in the middle, and finally the parts controlling the detailed functions of cell differentiation and morphogenesis are at the bottom (Erwin and Davidson, 2009). According to Erwin and Davidson (Davidson and Erwin, 2006; Erwin and Davidson, 2009) GRNs are constructed from several key components (summarised in figure 1.5):

1. "Kernels" are a set of genes that are highly conserved and the loss of any gene within the kernel will stop its function and likely result in a lack of the body part. For example the heart-field specification kernel that is conserved in both *Drosophila* and vertebrate development (reviewed by Davidson and Erwin, 2006).
2. Plug-in(s) are GRN sub-circuits that are often re-deployed in a non-conserved way, although the sub-circuit architecture remain the same. Typical plug-ins are signal transduction systems for example Wnt signalling.
3. Switches are smaller control circuits that permit or forbid the activity of a whole sub-circuit and act as input/output (I/O) devices within the GRN. For example, *hox* genes in specification of vertebral morphology in vertebrates (Wellik and Capecchi, 2003).

4. Differentiation gene batteries encode proteins required for differentiated cell function and are under regulatory control of a small group of transcriptional drivers. A good example are the downstream gene batteries that form the sea urchin skeleton (Oliveri *et al.,* 2008; Rafiq *et al.,* 2012).

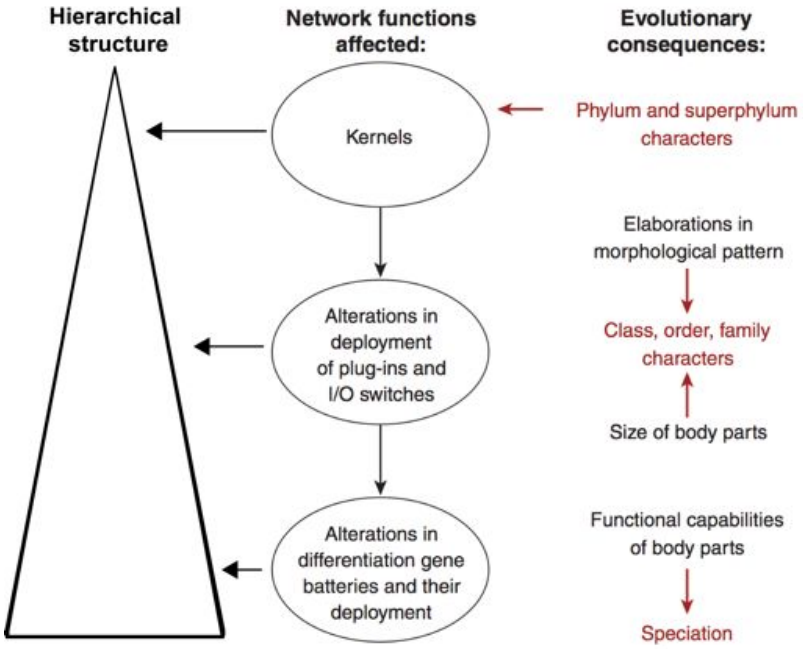

Figure 1.5. The components and hierarchy of a GRN
The hierarchical structure of a GRN can be seen, showing kernels at the top, plug-ins and I/O switches in the middle and finally differentiation gene batteries at the bottom of the GRN. The right column shows evolutionary consequences of changes at different parts of the GRN (adapted from Davidson and Erwin, 2006).

One important consequence of the hierarchical nature of GRNs is that the individual levels of the hierarchy differ in evolutionary lability (He and Deem, 2010). Therefore, the ramifications of a mutation will depend entirely on the location within the GRN hierarchy (Erwin and Davidson, 2009; Peter and Davidson, 2011). He and Deem (2010) suggest that the highly conserved kernels relate to the phylum and superphylum level characteristics; the plug-ins and I/O devices relate to the class, order, and family characteristics; and the batteries might relate to the speciation characteristics, leading them to propose that the slow evolution of the top components and fast evolution of the bottom components of the hierarchy is a universal phenomenon in the evolution of gene regulatory networks.

GRNs and regulatory states

So far, I have focussed on the importance of GRNs to understanding the development of an embryonic structure. I have discussed how the *cis*-regulatory elements of a gene determine the transcription factors that bind to it and thus control the gene's expression in space and time. I will now examine how gene expression dynamics drive the process of development.

The sum of the transcription factors and signalling molecules present in any given cell defines its "regulatory state" (Davidson, 2001). Working backwards, development relies on specific proteins appearing in a given domain of the embryo, interacting and carrying out their normal functions. How these proteins arrive at their correct location depends directly on the differential expression of the genes that encode these proteins, which in turn depends on the regulatory state of the cells. Furthermore, the regulatory state is the direct output of the GRNs encoded in the *cis*-regulatory modules controlling gene expression of regulatory genes (Oliveri *et al*, 2008). Thus development is precisely driven by the transition from one regulatory state to the next (Davidson, 2006).

The embryo is made up from a number of multicellular regions in which a given regulatory state is expressed. As development progresses, these regions will usually be sub-divided into more refined, regionally specific domains (Davidson, 2006). The GRN controls this partitioning of the embryo into specific regulatory state sub-domains, and as mentioned before, this is what causes the process of cell specification within these sub-domains. Recent studies of the sea urchin ectoderm GRN, have shown that a progression and subdivision of spatial regulatory states precedes the spatial resolution of the cell fates, to which the territory eventually gives rise (Peter and Davidson, 2011). Furthermore, an understanding of regulatory states illustrates the true level of spatial complexity and allows the identification of what domains exist, at any developmental stage. For example, the sea urchin aboral ectoderm, which until recently was viewed as a single territory, is now thought to exist as multiple different regulatory domains, even if the functional biological significance of these regulatory domains might not be played out until later stages of larval development (de Leon *et al*., 2013).

Visualisation and analysis GRN data

As I described above, GRNs are typically large-scale, multi-layered, and organised in a modular and hierarchical fashion. The networks usually represent a multicellular organism and as development progresses, the network architecture constantly changes. Reconstruction of developmental GRNs requires unique computational tools that support the above representational requirements. Based on these observations, the Davidson lab have developed a freely available, platform-independent, open source software package (BioTapestry) which supports both the process of model construction and also model visualisation, analysis, documentation, and dissemination (Longabaugh *et al*., 2005). BioTapestry supports a symbolic representation of genes, their products, and their interactions. Furthermore, the GRN needs to be viewable at a number of different levels, from the whole, to the subcircuits, to the cis-regulatory DNA, and to the nucleotide sequence. The same underlying GRN behaves differently in different cell types, spatial domains, and environmental conditions, and at different times. BioTapestry uses a three-level hierarchy to describe a GRN (figure 1.6 shows a representative GRN): (A) The *View from the Genome* provides a summary of all inputs into each gene, regardless of when and where those inputs are relevant. Only one copy of each network element is shown. (B) The *View from all Nuclei* is derived from the *View from the Genome*, and contains the interactions present in different regions over the entire time period of interest. Each region, in a *View from all Nuclei,* is a subset of the *View from the Genome*, and sub-networks may be duplicated in different regions. (C) The *Views from the Nucleus* describes a specific state of the network at a particular time and place. Inactive portions of the network are indicated in gray, while the active elements are shown coloured.

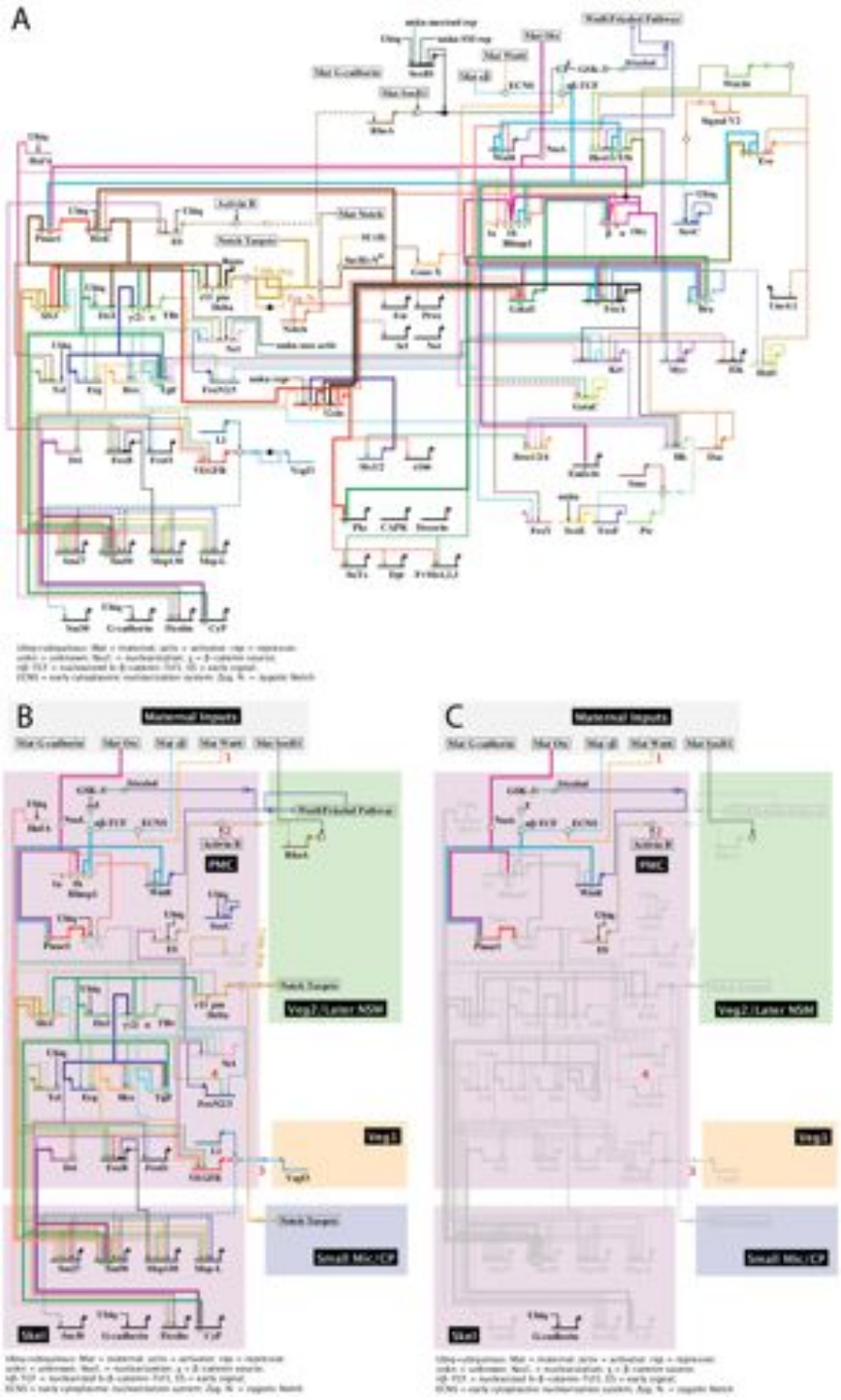

Figure 1.6. Different "views" of a GRN model in BioTapestry

The endomesoderm GRN as seen using the (A) *View from the Genome*, (B) *View from All Nuclei* (C) the *View from the Nucleus* (http://www.spbase.org/endomes/).

1.3 The sea urchin as a developmental model

Fertilisation is the essential process by which most sexually reproducing individuals begin. The German biologist Oskar Hertwig, (1876) first published his observations of the fusion of sperm and egg nuclei at fertilisation during the nineteenth century and paved the way for the sea urchin as a leading model organism for the study of embryology and development. Until the last quarter of the 19th century, the field of developmental biology was based principally on visual examination; the excellent optical clarity of sea urchin eggs and embryos made them a natural model (Ernst, 2011). Hans Driesch, (1891) discovered that a fully formed sea urchin larva can arise from an isolated blastomere at either the two or four-cell stage, and therefore part of an egg has the ability to develop into a full organism. Some of the most important investigations and contributions to modern biology from the early 20th century, were from Theodor Boveri. In one study using sea urchin embryos, he concluded that "normal development is dependent on the normal combination of chromosomes and this can only mean that the individual chromosomes must possess different qualities" (Boveri, 1902).

With molecular biology beginning to flourish in the late 1960s, Britten and Davidson, (1969) produced a model explaining genetic regulation for higher organisms involving regulatory elements that activate batteries of genes. Eric Davison, recognising the benefits and extensive knowledge that already exists for the sea urchin, selected it for large-scale analysis of gene expression and regulation during development and differentiation (Ernst, 2011). With advancing technology and a greater understanding of sea urchin development, extensive examination of the *cis*-regulatory region of the *endo16* gene identified those elements that are responsible for the temporal and spatial expression of this gene (Yuh *et al.,* 1996). In 2002, Davidson *et al*. (2002) produced a "provisional regulatory gene network for the specification of the endomesoderm of the sea urchin embryo", a major achievement in understanding how the genome encodes the development of an embryonic territory. Further advantages to using sea urchins as model organisms, are that the adults are easy to obtain and maintain and can readily be induced to spawn copious quantities of eggs that upon fertilisation divide synchronously; the genome was published in 2006 (Sodergren *et al.,* 2006) and a

transcriptome in 2012 (Tu *et al.,* 2012). High-resolution temporal expression profiles from nanostring data are available (Materna *et al.,* 2010) and high-throughput methods exist for *cis*-regulatory analysis. A wide variety of biochemical and molecular biological approaches, from protein purification to cDNA library construction, can also be used in the sea urchin. The sea urchin is also highly amenable to modern light microscopy, as well as other methods of visualisation, including fluorescence-based methods for monitoring gene expression, protein localisation, protein-protein interaction, and biochemical activity.

Moreover, the sea urchin is proving to be an excellent model for studying the evolution of development. The echinoderm phylum branched from the chordate lineage prior to the Cambrian explosion, more than 500 million years ago. They have been classified as deuterostomes by early systematists, due to their developmental feature of the mouth forming from the second invagination. Modern phylogenetic tools have repeatedly verified this classification (Swalla and Smith, 2008; Edgecombe *et al.,* 2011). Sea urchins and other echinoderms are invertebrate deuterostomes (figure 1.7), yet still have a close phylogenetic relationship with chordates, as shown by the sequence of the genome (Sodergren *et al.,* 2006). This phylogenetic position provides an excellent basis for evolutionary and comparative studies.

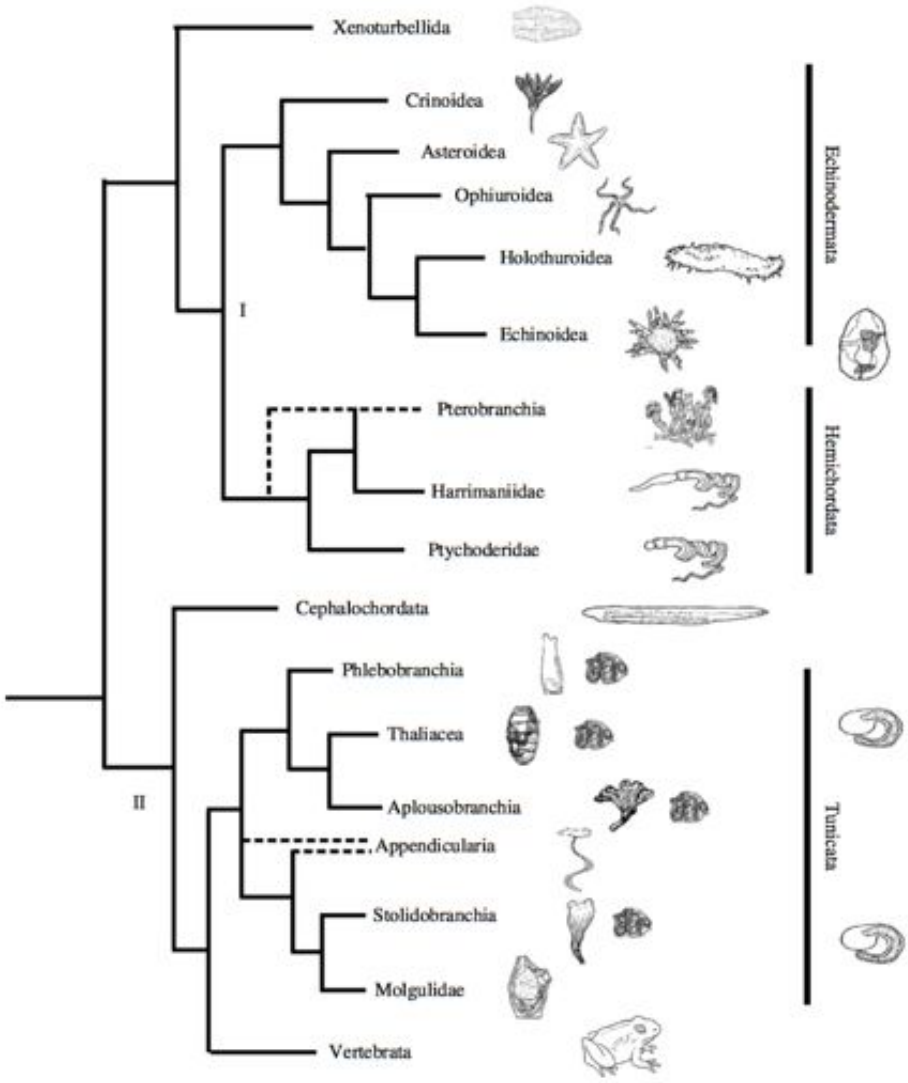

Figure 1.7. A current deuterostome phylogeny

(I) The Ambulacraria include the echinoderms and the hemichordates. The sea urchins are echinoderms. Genomic evidence suggests that xenoturbella may be a sister group to the Ambulacraria, but its position is unclear (for a more detailed discussion of this see Edgecombe *et al.,* 2011; Telford and Copley, 2011). (II) Chordates are a monophyletic group that share a specific body plan, but mitochondrial and genomic evidence are in conflict about the position of some of the members (adapted from Swalla and Smith, 2008).

1.3.1 Sea urchin development

Sea urchins are marine invertebrates and use external fertilisation by the release of gametes into the environment. The eggs of the sea urchin used in this thesis, *Strongylocentrotus purpuratus,* are approximately 80μm in diameter, with a 10-30-nm thick fibrous extracellular matrix, known as the vitelline layer, bonded to the plasma membrane. Surrounding the vitelline layer is a second extracellular matrix, the egg jelly layer (Glabe and Vacquier, 1977). Unlike almost all other animal eggs, sea urchins have completed meiotic divisions associated with oogenesis when eggs are released from the ovary. They have a haploid interphase nucleus of de-condensed chromatin surrounded by a complete nuclear envelope (Trimmer and Vacquier, 1986). The much smaller spermatozoa consists of conical head, containing the acrosomal vesicle and the haploid nucleus, a single mitochondrion and a single flagellum. The fusion of the egg and sperm initiates a number of important processes: a *fast* and *slow* block to polyspermy and the formation of the fertilisation membrane and hyaline layer (Hylander and Summers, 1982; Wong and Wessel, 2008).

Early development and fate map

After fertilisation is complete, development starts with a series of mitotic cleavage divisions, that divide the mass of the egg into smaller, nucleated cells. The sea urchin undergoes radial, holoblastic cleavage and exhibits stereotypic cleavage for the first seven divisions. The first two cleavages are both meridional and are perpendicular to each other (figure 1.8 A, B and C). The third cleavage is equatorial, and divides the embryo into animal and vegetal halves (figure 1.8 D). In contrast to earlier symmetrical divisions, the fourth cleavage is asymmetrical. The four animal cells divide equally and meridionally into eight equal cells, called mesomeres (figure 1.8 E), while the four vegetal cells divide equatorially in an unequal fashion to produce four larger cells, called macromeres and four smaller cells, called micromeres at the vegetal pole (figure 1.8 E). In the fifth cleavage, the eight mesomeres in the animal half divide equatorially to produce two tiers called an1 and an2, then the macromeres divide meridionally to form

a tier of 8 cells below an1 called veg (figure 1.8. F). The micromeres slow down and skip one cell division. In the sixth cleavage, the animal cells divide meridionally while the vegetal cells divide equatorially producing a veg1 and veg2 tiers each of 8 cells and respectively in contact with the animal half and with the micromeres. At this stage the micromeres divide again unequally, to produce a cluster of four small micromeres and four larger micromeres in direct contact with the veg2 tier (figure 1.8 F) and produces a ~60-cell blastula (Pehrson and Cohen, 1986; Cameron and Davidson, 1991; reviewed by Wolpert, 2007; Gilbert, 2010; McClay, 2011).

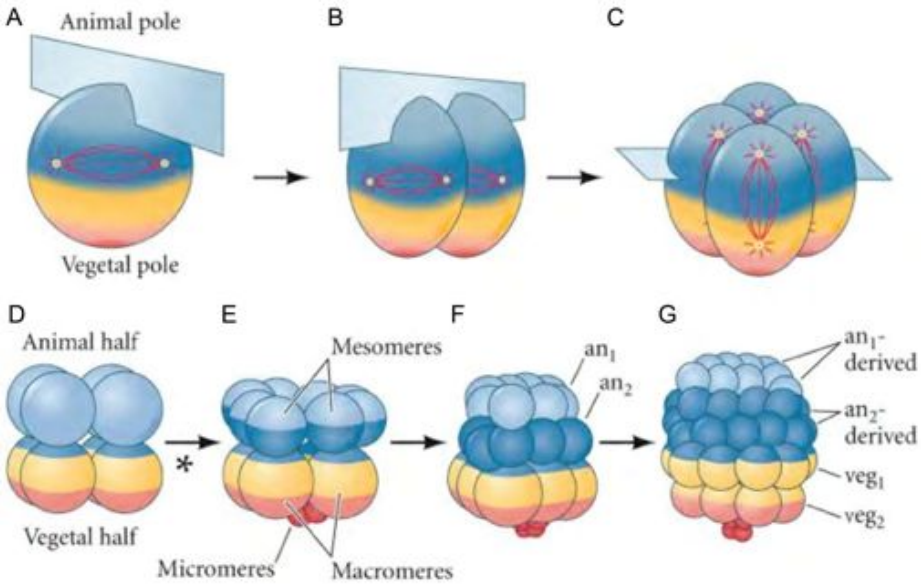

Figure 1.8. Sea urchin cleavage
Cartoon representing first six stereotypical cleavages of the develoment of sea urchin. All the embryo in the diagram are oriented with animal pole up. The three different embryological layers are colorcoded. Mesoderm red, endoderm yellow and ectoderm blue. Animal (an1 and an2) and vegetal (veg1 and veg2) cell tiers emerging during cleavage are indicated (adapted and modified from Gilbert, 2000).

The cells divide synchronously another time to reach the 120 cell stage, with the exception of the small micromeres which will divide only once more before development of the rudiment. After this stage, the cleavages become asynchronous in the different cell lineages and they also slow down. Depending on the species, the cleavages stop after 8-10 rounds. In the sea urchin species used in this study, *Strongylocentrotus purpuratus*, cultured at 15°C the first cleavage occurs two hours after fertilisation, and all the other cleavages take place every hour. At the end of cleavage,

cells are of equal size and form a hollow sphere surrounding a central cavity; each cell is in contact on one side with the proteinaceous liquid of the blastocoel and on the other site with the outer hyaline layer and form a blastula (figure 1.9 A). At this stage, the cells become organised into a true epithelium, with permanent cell junctions and a complex extracellular matrix on both the interior and exterior surfaces. The formation of the blastocoel is accomplished by the adhesion of the blastomeres to the hyaline layer and by an influx of water that expands the internal cavity (Dan, 1960; Wolpert and Gustafson, 1961). The blastula soon acquires a single, active cilium on each blastomere and at the animal pole an apical tuft of long cilia appears. The ciliated embryo begins to rotate with the fertilisation membrane. A specific protease, the hatching enzyme, is synthesised and secreted from the animal half of the embryo to digest the fertilisation membrane and releases the motile embryo (Gilbert, 2010). This occurs at 15 hours after fertilisation in *S. purpuratus*.

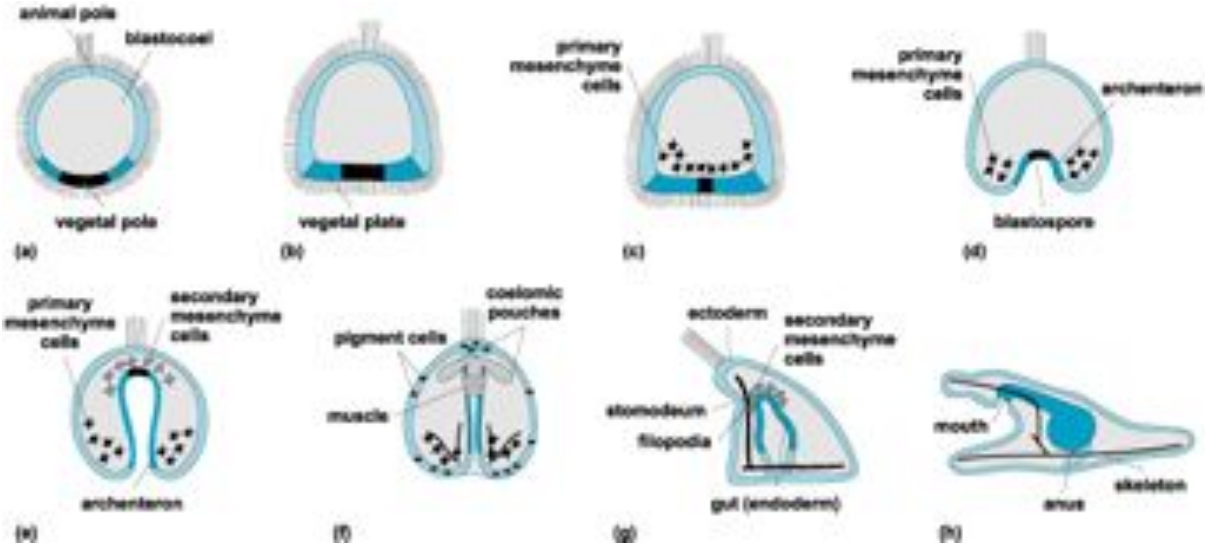

Figure 1.9. Sea urchin development and timings
The major stages of sea urchin development are depicted. Times are given for *S. purpuratus* (the model used in this study). (a) hatching blastula - 15 hours. (b) hatched blastula - 18 hours. (c) mesenchyme blastula - 24 hours. (d) early gastrula - 30 hours. (e) mid-gastrula - 36-40 hours. (f) late gastrula (oral view) - 48 hours. (g) late gastrula (lateral view) - 48 hours. (h) early pluteus larvae - 72 hours).

The blastula-stage sea urchin embryo can be considered to be composed of different territories. These are conceived as polyclonal assemblages of contiguous blastomeres, characterised by a unique regulatory state and that will give rise to one or multiple cell types (Cameron and Davidson 1991). A long series of lineage tracing experiments (Cameron *et al.,* 1987; Davidson, 1989, Cameron and Davidson, 1991; Cameron *et al.,* 1990) show that five major embryonic territories are already segregated in the sea urchin embryo at the 60-cell stage as shown in figure 1.10: the oral ectoderm (yellow), the aboral ectoderm (green), the small micromere (purple), the skeletogenic large micromere (red) and the vegetal territory (blue) derived from the macromeres, each of them correspond exactly with a definitive polyclonal lineage compartment that has segregated by 6th cleavage. The ectodermal territories have not been fully segregated at this stage, as indicated by the white colour in figure 1.10 (Davidson *et al*., 1998). Each of these territories has a unique fate that has been established with precision with many fate map experiments: The four small micromeres will divide only once more during embryogenesis and go onto form the coelomic pouches and ultimately the adult rudiment; the skeletogenic large micromeres, on the other hand, are the only autonomously specified cell type and they will only contribute to the formation of the larval skeleton. The macromere descendants at late blastula stage acquire a particular morphology and form a thickened vegetal plate. Different regions of the vegetal plate go on to form the mesoderm and endoderm territories after receiving instructive signals from the adjacent large micromeres. Opposite the vegetal plate a thickening of the animal pole also occurs and forms the animal plate. As mentioned above, at the 60-cell stage the ectodermal territories are not fully segregated, and although the apical domain forms between the oral and aboral ectodermal territories, the exact cells that will go on to form the apical domain are not fully known. Takacs *et al.,* (2004) showed the expression of *nk2.1* marks this additional apical organ territory. Many genes have since been found to be expressed in the apical organ (see the Sea Urchin Genome issue of Developmental Biology, 2006; reviewed by Angerer *et al.,* 2011).

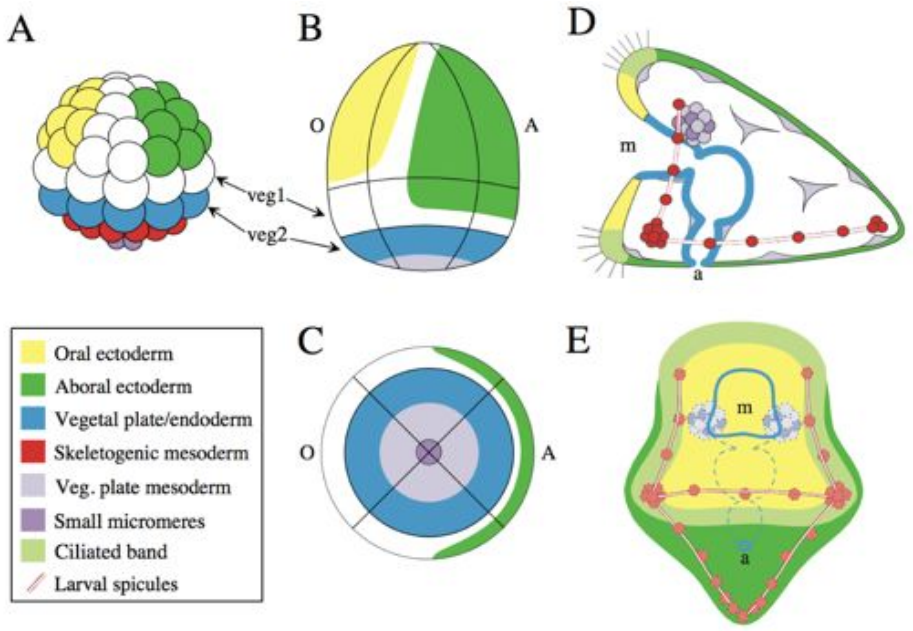

Figure 1.10. The sea urchin cell specification map
(A) 60-cell stage, lateral view. (B) Mesenchyme blastula (24 hours), external lateral view. (White region are not yet specified). (C) Vegetal view of a mesenchyme blastula (24 hours), vegetal view. The central region of the vegetal plate is now divided radially into a central mesodermal territory (light purple), consisting of cells destined to give rise to secondary mesenchyme and coelomic pouches and an endodermal territory that will produce foregut and midgut (blue). (D) Early pluteus-stage larva (~72 hours), lateral view and (E) same stage, oral view. Showing final state of specification. The skeletogenic mesenchyme, shown secreting the bilaterally organised skeletal structure (red). Coelomic pouches are depicted as circular arrays of purple cells at the side of the foregut, pigment cells are shown embedded in the aboral ectoderm, and fusiform blastocoelar cells are illustrated (adapted from Davidson *et al*., 1998).

Morphogenetic movements and early pluteus larva

The sea urchin blastula, after hatching from its fertilisation membrane, consists of a single layer of about 250 cells that form a hollow ball, flattened and thickened at the vegetal side (figure 1.9 b). The first cells to move are the descendants of the large micromeres, that undergo an epithelial-to-mesenchymal transition followed by migration within the blastocoel, and are subsequently termed primary mesenchymal cells (Gustafson and Wolpert, 1961). They will give rise only to the skeletogenic mesoderm and will differentiate into the skeleton of the pluteus larva (red in figure 1.10); in *S. purpuratus* the primary mesenchymal cells ingress around 22 hours. Immediately after the primary mesenchymal cell have ingressed into the blastocoel, gastrulation starts. In *S. purpuratus,* this occurs at 30 hours. The general process of

gastrulation in the sea urchin can be divided into the following steps: (1) The central part of the thickened vegetal plate bends inwards and gives rise to a short stub-like gut rudiment, the archenteron, in what is called the primary invagination; (2) after primary invagination is completed, the length of the archenteron barely changes for several hours. At this stage, the secondary mesenchyme cells become visible at the tip of the archenteron. They will give rise to many mesodermal cell types (*e.g.* muscle andpigment cells, communally called the non-skeletogenic mesoderm). Secondary mesenchyme cells extend long and thin filopodia toward the animal pole, while remaining attached to the archenteron and pull it upwards towards the animal pole; (3) the archenteron is then converted from a small stub-like to a slender tube-like structure via convergent extension cell movements; (4) the archenteron tilts toward the future mouth (the oral ectoderm). At this point, the secondary mesenchyme cells disperse in the blastocoel forming mesodermal structures, while the archenteron fuses with the stomodeum to form a continous digestive tube. (reviewed by Kominami and Takata, 2004; Gilbert, 2010).

At the end of gastrulation, a pluteus larva emerges. The primary mesenchyme cells, now fused in a syncytium, form the elongated larval skeleton, which starts to be deposited as a triradiate skeletal rudiment in the ventrolateral clusters at the late gastrula stage. The extension of the skeleton forces the ectoderm to change shape and drives the classic form found in the sea urchin pluteus larvae. Concurrently, a band of cilia develops surrounding the oral ectoderm, and the apical tuft disappears (Nakajima, 1986; Ettensohn, 2013). The gut subdivides into the foregut, midgut and hindgut, with muscular sphincters forming at the compartment junctions. This regionalisation becomes evident, not only morphologically, but also by patterns of specific gene expression (Cole *et al.,* 2009). Two coelomic pouches outpocket laterally of the foregut, and progeny of the non-skeletogenic mesoderm and small micromeres bulge to either side. The pluteus larva differentiates to produce a number of cells necessary for the skeleton, for neural transmission and for feeding. The pluteus is locomotive and feeds on plankton using coordinated beating of cilia of the ciliary band (Gustafson and Wolpert, 1963; Bisgrove and Burke, 1987).

1.3.2 Genomic control of the sea urchin ectoderm

The apical organ develops from one of the animal cell tiers, an1. The animal half of the embryo will give rise to several structures including mouth, ciliary band and flat ectodermal epithelium. The specification of the apical organ lies at the crossroad of the primary, animal-vegetal axis and the secondary embryonic oral-aboral axis.

Oral-aboral axis formation

Unlike the animal-vegetal axis, which is already fixed in the unfertilised egg (Boveri, 1901), the oral-aboral axis is far less stable and is open to physical manipulation (Horstadius, 1938). Cell lineage analysis shows that in *S. purpuratus* the oral-aboral axis is specified with reference to the first cleavage plane (Cameron and Davidson, 1991). Morphologically, the oral-aboral axis is only recognisable during the gastrula stage and it is during this stage that the embryo begins to flatten on the presumptive oral side and simultaneously, the primary mesenchyme cells form two ventrolateral clusters and the archenteron bends towards the oral side (Horstadius, 1967; Duboc *et al.,* 2004). Duboc *et al.,* (2004) showed that the zygotic expression of *nodal* is found in the presumptive oral ectoderm as early as late cleavage (figure 1.11 A). *nodal,* a member of the transforming growth factor beta (TGFβ) superfamily of signalling molecules, is both necessary and sufficient to specify the oral ectoderm. In fact, ectopic expression of *nodal* converts the entire ectoderm into oral ectoderm and induces ectopic expression of oral ectoderm genes including *goosecoid (gsc)*, *brachyury (bra), bone morphogenetic protein* (*bmp*) *2/4*, and *antivin* (Duboc *et al.,* 2004). A asymmetric distribution of mitochondria in the egg, predates the prospective oral-aboral axis; it creates an ox-redox gradient and regulates transcription factors required for *nodal* activation (Coffman and Davidson, 2001). p38, a stress-activated protein kinase, responds to reactive oxygen species and appears to be a positive input into nodal expression and therefore the development of oral ectoderm (for review see Coffman *et al.,* 2009). *lefty,* a *nodal* antagonist is directly downstream of nodal and locks down the initial expression of *nodal* to the oral ectoderm through an autoregulative loop called the community effect model (figure 1.11

B; for more details and modelling of interaction see Bolouri and Davidson, 2010). *bmp2/4* is also expressed in the oral ectoderm and is downstream of *nodal.* However *bmp2/4* is required for the specification of the aboral ectoderm. In fact, despite its oral ectoderm expression, the BMP2/4 ligand binds to receptors only in the aboral ectoderm through the action of *chordin,* which is largely responsible for the restriction of *bmp2/4* signalling to the aboral side (figure 1.11 C; Angerer *et al.,* 2000; Bradham *et al,* 2009; Lapraz *et al.,* 2009).

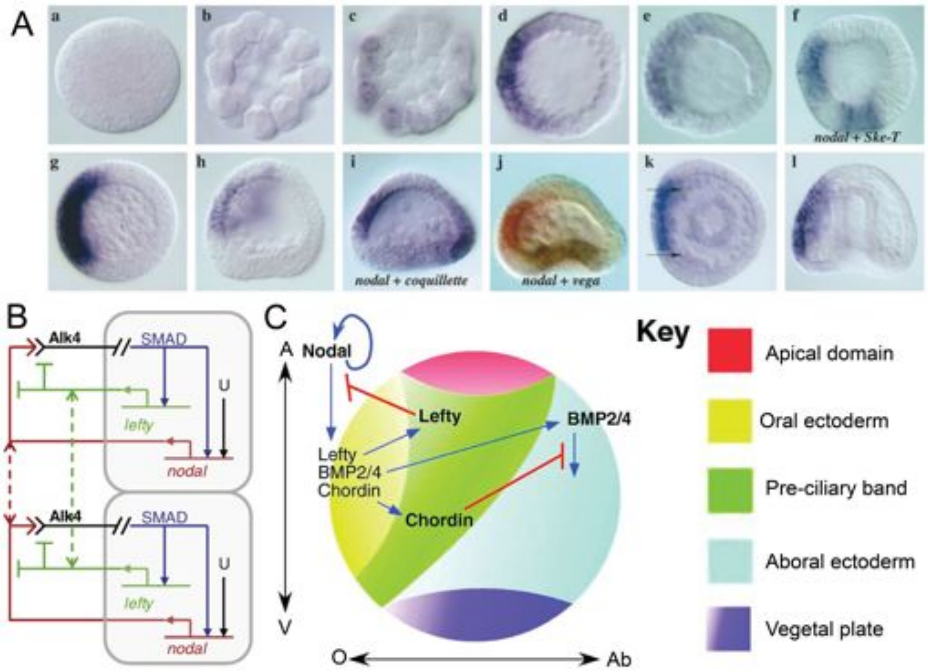

Figure 1.11. Oral-aboral axis formation

(A) Spatial expression pattern of *nodal* in the sea urchin (*P. lividus).* (a) Unfertilised egg (b) 32-cell stage (c) 60-cell stage (d) early blastula stage (e) swimming blastula stage (f) swimming blastula stage, double stained with *nodal* and *ske-T*/*Tbx1* (a primary mesenchyme cell marker) (g) mesenchyme blastula stage, apical view (h) mesenchyme blastula stage, lateral view (i) mesenchyme blastula stage, double stained with *nodal* and *coquillette/Tbx2/3* (a aboral ectoderm marker) (j) mesenchyme blastula stage, double stained with *vega* (a marker of presumptive endoderm) in blue and *nodal* in red (k) gastrula stage, vegetal view, *nodal* is expressed on the oral (left) side of the embryo where the two primary mesenchyme cell clusters are located (arrows) (l) gastrula stage, lateral view (oral side on left; adapted from Duboc *et al.,* 2004). (B) Lefty–Nodal community effect modelled in two cells (rounded rectangles; adapted from Bolouri and Davidson, 2010). (C) TGFβ signalling specifies ectodermal fates along the oral-aboral axis. Animal (A), vegetal (V), oral (O) and aboral (Ab; adapted and modified from Angerer *et al.,* 2011).

The sea urchin ectoderm GRN

The sea urchin embryo endomesoderm GRN is at present the most complete, predictively useful, and validated large scale developmental GRN available (Davidson, 2010). A major objective over the past five years or so, has been to extend GRN analysis to other territories of the sea urchin embryo, especially the ectoderm. An initial perturbation model of the gene regulatory network for oral and aboral ectoderm specification in the sea urchin embryo was published by Su *et al*., (2009). As discussed previously, *nodal* is an early input and uses an auto-regulatory feedback system to drive expression of the initial nodal-dependent regulatory states found in the oral ectoderm. The GRN predicts two direct targets of the Nodal signalling pathway, one a transcriptional repressor and one a transcriptional activator. The repressor is the transcription factor *gsc,* which has been previously shown to be an obligate transcriptional repressor, essential for oral ectoderm specification (Angerer *et al.,* 2001). The activator is the transcription factor *foxG*, and plays a newly discovered role as a pivotal early player in oral ectoderm specification. Together, this predicts a double negative regulatory gate (figure 1.12 A), similar to the *pmar1* mechanism, that accounts for the installation of the specific regulatory state of the skeletogenic micromere lineage (Oliveri *et al.,* 2002). Perturbation and expression data obtained by Su and collaborators, (2009) shows that the oral ectoderm is formed from a number of regulatory and spatial domains. More recently, Li *et al.,* (2012) identified more regulatory genes that contribute to the oral ectoderm regulatory state during specification and interestingly show that many of these genes are expressed in different spatial patterns. These spatial expression patterns are highly dynamic and progressively sub-divide the oral ectoderm into sub-domains of gene expression (figure 1.12 B). *not*, a novel downstream target of *nodal* was also identified. *not* activates *gsc* and is thought to be direct target of *nodal* and *nk1* (Li *et al.,* 2012).

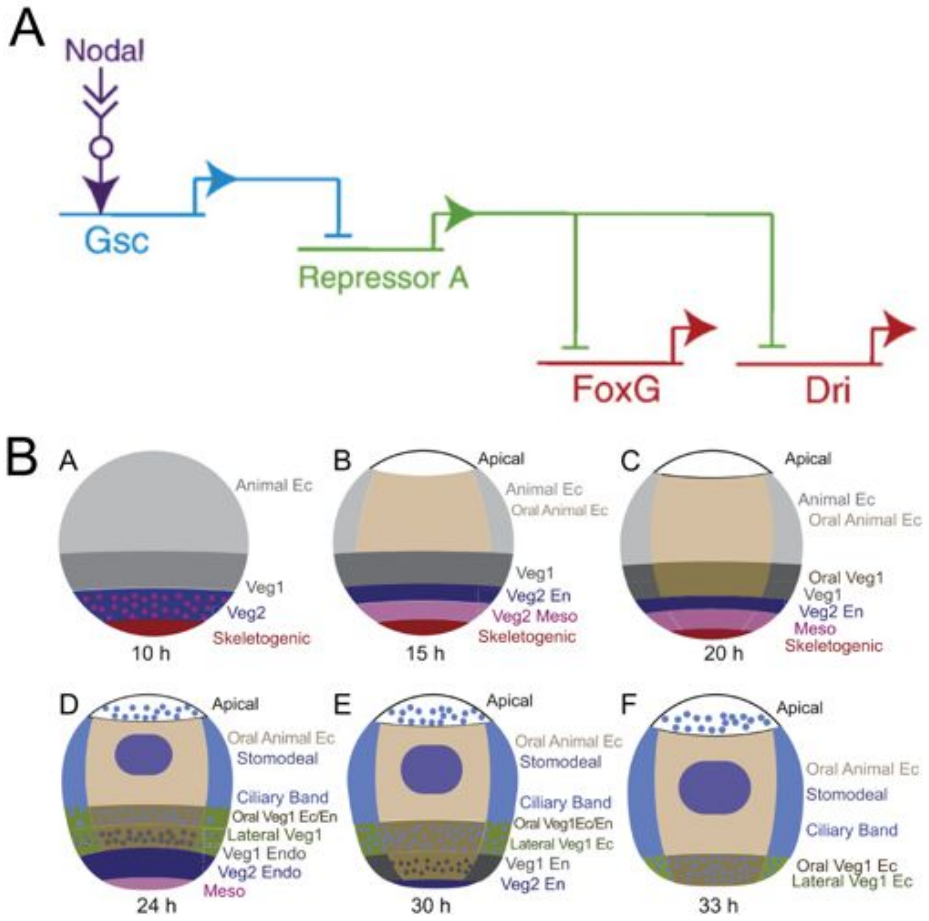

Figure 1.12. Aspects of the oral ectoderm GRN
(A) In the oral ectoderm, *gsc* represses the expression of a yet unknown Repressor A, which otherwise represses the expression of *foxG*, *deadringer* (*dri*), and other oral regulatory genes (adapted from Su*.,* 2009). (B) A diagram highlighting ectodermal gene expression domains of early sea urchin embryos, viewed from the oral ectoderm. As development progresses there is an increase in spatial complexity and the existence of multiple gene expression domains can be observed (adapted from Li *et al.,* 2012).

Regulatory genes involved in the specification of the aboral ectoderm are far less understood than that of the oral ectoderm. Su *et al.,* (2009) showed that like so many other GRNs, a feedback circuit is used for dynamic lockdown of aboral regulatory state (figure 1.13 A) The first gene to be expressed in the aboral ectoderm is *tbx 2/3,* and it activates four homeodomain genes, *iroquois homeobox A* (*irxA*), *apterous* (*lhx2.9*), *dlx,* and *hox7*. *irxA* then feeds back and activates *tbx 2/3.* Furthermore, Chen *et al.,* (2011) showed that the spatial complexity of the aboral ectoderm is far greater than previously thought (figure 1.13 B) and based on the gene expression patterns, the authors conclude that the aboral ectoderm contains at least three sub-domains by the mesenchyme

blastula stage. Recently de-Leon *et al.,* (2013) illustrated that the initial activation of aboral genes (*i.e. tbx 2/3* and *max*) depends directly on the redox sensitive transcription factor hypoxia inducible factor 1α (*hif-1α*). *cis*-regulatory analysis of the aboral ectoderm gene, *tbx 2/3* shows that *hif-1α* is a direct input and initiates aboral ectoderm specification. Interestingly, what used to be viewed as a simple, single territory is far from it and it is clear that a number of sub-domains exist and that a progression of spatial regulatory states precedes the emergence of the cell fates to which the territory eventually gives rise to.

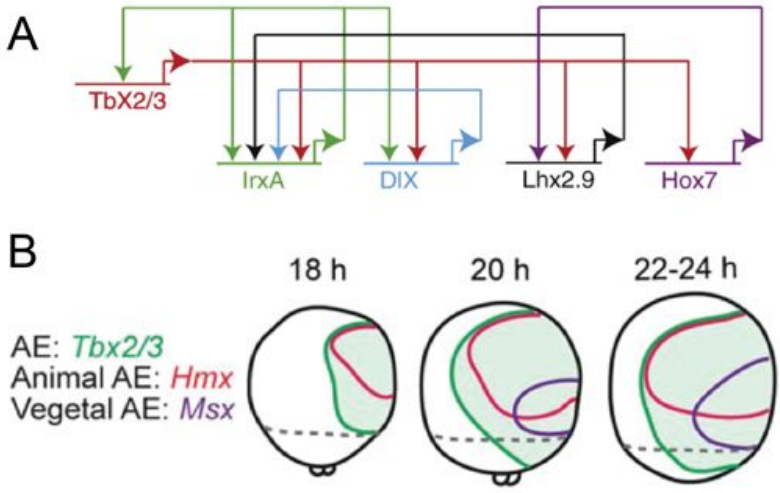

Figure 1.13. Aspects of the aboral ectoderm GRN
(A) Feedback relationships in the aboral ectoderm GRN. The four homeodomain genes *irxa*, *lhx2.9*, *dlx*, and *hox7* are all locked together in a feedback loop, and *irxa* feeds back on *tbx2/3*, the first gene to be expressed in the aboral ectoderm (adapted from Su, 2009). (B) Different gene expression pattern domains in the aboral ectoderm. The overall aboral ectoderm is marked by *tbx2/3*. The animal aboral ectoderm is marked by *hmx* and the vegetal aboral ectoderm is marked by *msx* (adapted from Chen *et al.,* 2010).

The ciliary band forms a 4 to 5-cell wide strip of columnar cells, that is in between the oral and aboral ectoderm (figure 1.14 A; Davidson *et al*., 1998; Yaguchi *et al*., 2006). This structure is specified quite late (at the start of gastrulation) in the development of the sea urchin, relative to many other territories. The transcription factor *hepatocyte Nuclear Factor 6* (*hnf6*) is the first molecular marker for ciliary band and is expressed in the presumptive ciliary band by mesenchyme blastula stage (Otim *et al.,* 2004). The oral and aboral boundaries of the ciliary band are controlled by *nodal* and *bmp2/4* signalling respectively (Yaguchi *et al.,* 2010a). Saudemont *et al.,* (2010) recently showed that *lefty*

and *chordin,* which are antagonists of *nodal* and *bmp 2/4,* are thought to prevent conversion of the ciliary band into oral or aboral ectoderm and that the default state of ectoderm is ciliary band in the absence of Nodal and BMP signalling (figure 1.14). This is in contrast to data previously published by Su *et al., (*2009). The literature is unclear about the territorial origin of the ciliary band; Davidson and collaborators (1991) considered it just an unspecified set of cells between the oral and aboral ectoderm (figure 1. 10), while according to Su *et al.,* (2009) it appears as a separate domain within the oral ectoderm and forms part of the oral ectoderm GRN, at least initially. This is supported by the fact that from early gastrula onwards, genes initially expressed throughout the oral ectoderm such as *hnf6, foxG* and *orthodenticle homeobox β1* (*otxβ1*) begin to be expressed in the ciliary band only (Su *et al.,* 2009).

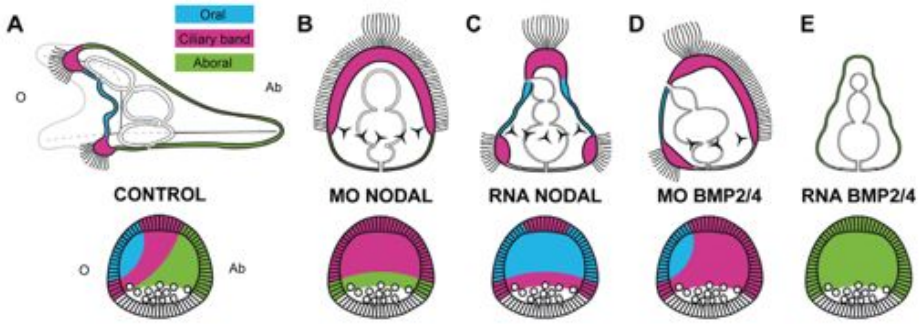

Figure 1.14. Patterning of of the ciliary band
(A) The thick ciliated epithelium of the ciliary band is restricted to a belt of cells at the interface between the oral and aboral ectoderm in control embryos. (B) *nodal* MASO causes an expanded ciliary band. (C) *nodal* RNA causes an expanded oral ectoderm, although a poorly positioned ciliary band still forms. (D) *bmp2/4* MASO causes an ectopic ciliary band to form in the aboral ectoderm. (E) *bmp2/4* RNA causes the entire embryo to consist of aboral ectoderm. Oral ectoderm (blue); aboral ectoderm (green); ciliary band (red; adapted and modified from Saudemont *et al.,* 2010).

1.4 Nervous system development in the sea urchin

The fully developed pluteus larvae, is a free living planktonic organism, that lives in the ocean for several months before undergoing metamorphosis. For this reason, the larva is equipped with an efficient nervous system to monitor and interact with its environment. Here I shall describe the major characteristics of the sea urchin nervous system and its development, with particular emphasis on the apical organ.

Several different types of neurons have been identified in the sea urchin in the past by immunolocalisation of neurotransmitters and other molecular markers. For instance, in *Strongylocentrotus droebachiensis*, dopamine is first detected quite late in development in the four-armed plutei. At this stage, 6 to 8 anti-dopamine immunoreactive cells are located in an oral ganglion spanning the lower lip, and 7 cells in the ganglia at the base of the post-oral arms with processes that contribute to axons underling the ciliary band (figure 1.15 A-C). The number and size of anti-dopamine immunoreactive cells increases throughout development, reaching around 30 cells in the eight-armed larvae (Bisgrove and Burke, 1987). Interestingly, inhibiting the formation of dopamine decreased the swimming activity of blastula stage embryos in a dose-dependent manner, indicating an early function of dopamine even before neurons fully differentiate (Katow et al., 2010). Cells positive for glyoxylic acid-induced fluorescence of catecholamine are expressed in *S. droebachiensis* in a similar fashion to dopaminergic neurons (Bisgrove and Burke, 1987). GABAergic neurons on the other hand, first appear in the four-arm pluteus of *S. droebachiensis* and are restricted to the dorsal surface of the oesophagus and extend a single axon on either side of the oesophagus (Fig 1.15 A-C; Bisgrove and Burke, 1987). In the six-arm pluteus, the number of GABAergic neurons greatly increase and are now found in the upper lip and as a plexus across the oesophagus.

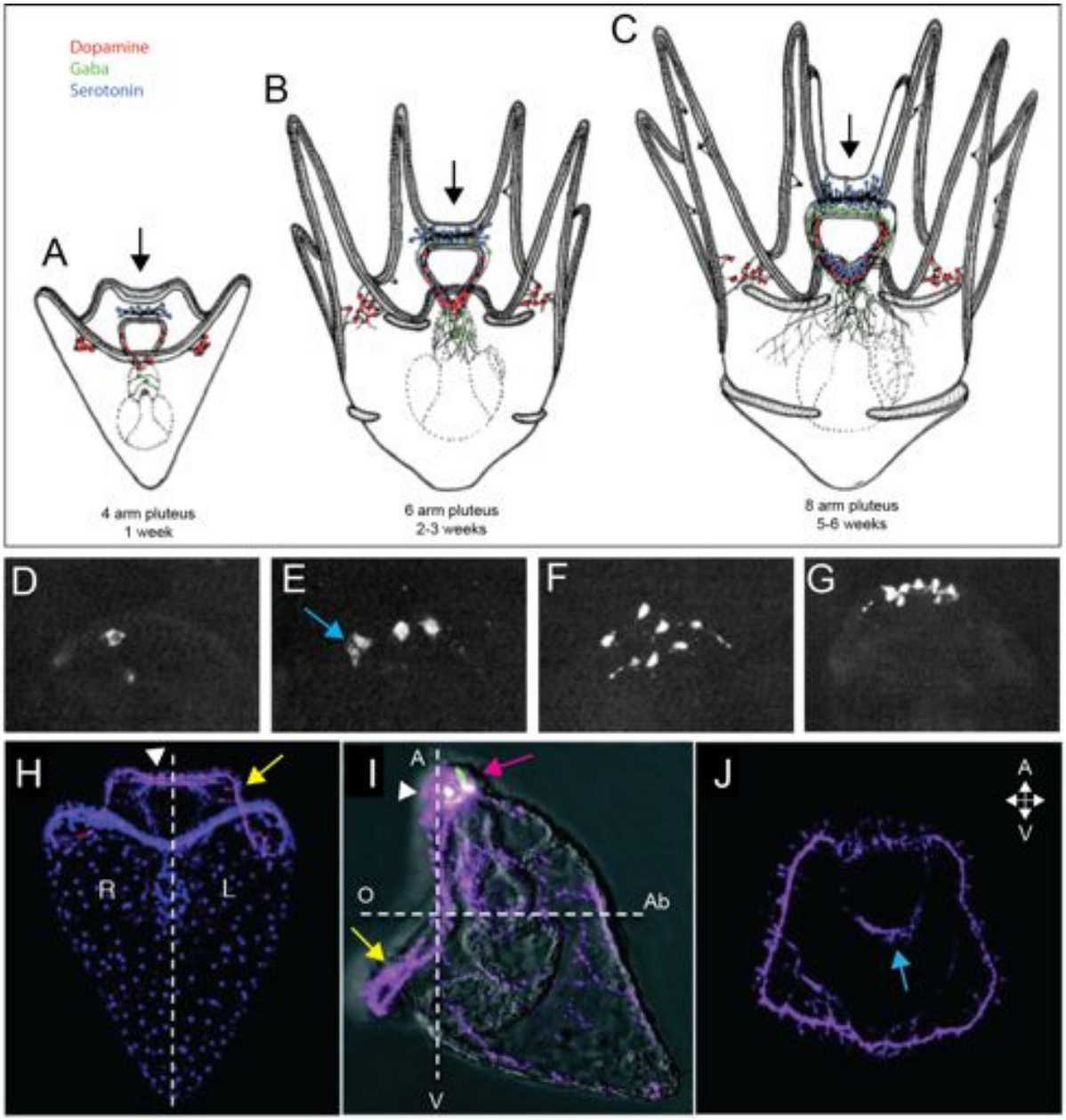

Figure 1.15. Neuronal diversity in the sea urchin larvae

(A-C) Distribution of dopamine, GABA and serotonin immunoreactive cells during larval development in *S. droebachiensis*. Black arrow indicates location of apical organ (adapted and modified from Bisgrove and Burke, 1987). (D-G) The apical domain showing the appearance of serotonergic neurons (E) Blue arrow indicates what appears to be a pair of recently divided cells (adapted and modified from Bisgrove and Burke , 1986). (H-J) Sea urchin larvae showing the position of all neurons (magenta) and serotonergic neurons (green). The apical organ (white arrowhead), serotonergic neurons (pink arrow), ciliary band (yellow arrow) and pharyngal neurons (blue arrow). R, right; L, left; A, Animal; V, vegetal; O, oral; Ab, aboral (adapted and modified from Angerer *et al*., 2011).

The first serotonergic neuron appears as a single neuroblast in the apical domain of the late gastrula (figure 1.15 D, Bisgrove and Burke, 1986). Later in development, more

neuroblasts can be detected in the apical domain. These are roughly spherical in shape and about 9μm in diameter and have no cellular processes or immunoreactive extensions (figure 1.15 E). As development continues, the serotonin positive cells become less regular in shape and begin to extend projections, and in some cases can be seen dividing (figure 1.15 E turquoise arrow, F). At pluteus larvae, a ganglion of 6 to 8 neurons has formed; these neurons now take on a flask-like shape with the apical end extending to the embryo surface. Axons extend from the base of each neuron and together form a plexus of axons that lie beneath the apical domain (Figure 1.15 G; Bisgrove and Burke, 1986). With development, the number of serotonergic neurons increases in the apical organ and neurons are now also found in the lower lip of the six-arm pluteus larvae (Figure 1.15 A-C; Bisgrove and Burke, 1987). Finally, in the late larvae, the apical organ ganglion extends axons along the base of the epidermis that overlies the blastocoel.

Traditionally, neurons were always thought to be derivatives of the ectodermal germ layer (Gilbert, 2010). However, Wei *et al.,* (2011) recently discovered that some of the pharyngal neurons of the sea urchin embryo originate not from the ectoderm as expected, but from the endoderm. The pharynx forms from both the oral ectoderm and the foregut endoderm. Using the photo-activated protein KikGR to track ectodermal cells, they proved that ectodermal cells are non-migratory and their derivatives do not go on to form the pharyngal neurons. Interestingly, the transcription factors *six3* and *nkx3.2* are both expressed in the apical domain and the foregut, and are both required for the specification of the pharyngal neurons.

The nervous system in the late gastrula embryo (48 hours) and pluteus larvae (72 hours) of the model used in this thesis, *S. purpuratus*, is relatively uncomplicated and is easier to relate back to embryonic development. Neuron number increases throughout larval development and the fully formed, eight-arm pluteus contains a great diversity of neuron types, as well as a highly complex array of sensory neurons, interneurons, and tracts of axons (As seen in *S droebachiensis* Figure 1.15 C; Bisgrove and Burke, 1987). For the purpose of this thesis, I will be concentrating on the simpler and more basic nervous system that appears in the first 3 days of development. In the early pluteus larvae, the nervous system is organised into two main territories; the apical organ and

the ciliary band (figure 1.15 H,I white arrowhead and yellow arrow; summarised in figure 1.16). The neurons of the early larval nervous system originate as neuroblasts in the apical domain and ciliary band in the late gastrula stage. At pluteus stage, the apical organ is a bilaterally symmetrical group of neurons at the anterior end of the larva positioned between the pre-oral arms. It comprises 4-6 bilaterally positioned serotonergic neurons, a central cluster of 10-12 non-serotonergic neurons and several non-neural support cells (Burke *et al.,* 2006). The ciliary band neurons are arranged at regular intervals on the side closest to the mouth and contribute axons to a central tract that runs the length of the ciliary band (figure 1.15 H-J; Burke *et al.,* 2006). Figure 1.16 summarises the relevant aspects of the nervous system in the early pluteus larvae.

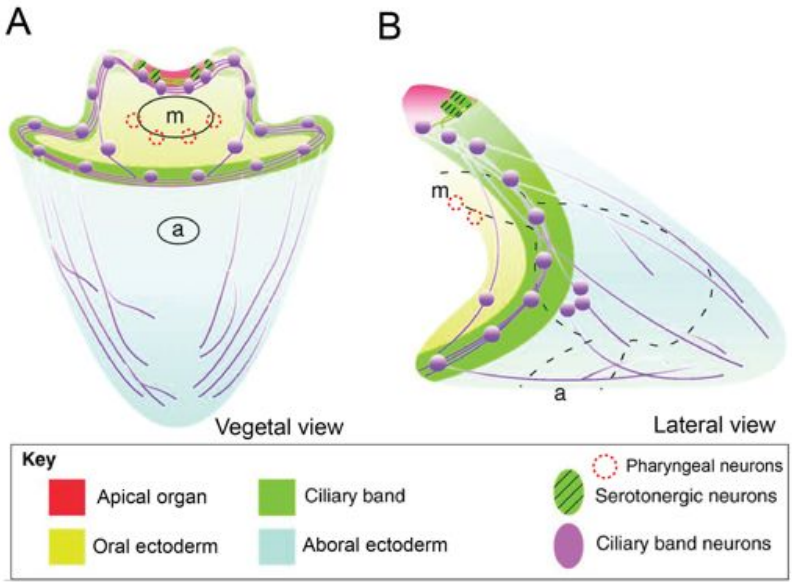

Figure 1.16. Summary of the nervous system in a sea urchin pluteus larvae
Pluteus larvae. (A) Vegetal view (B) Lateral view. Non-serotonergic neurons can be seen throughout the ciliary band as well as the apical organ. These neurons extend long axons towards the posterior of the larvae. Serotonergic neurons can be seen in the aboral half of the apical organ and produce axons, forming a ganglion and pharyngal neurons can be seen in the mouth (m, mouth and a, anus; adapted and modified from Angerer *et al.,* 2011)).

Tryptophan 5-hydroxylase (TPH) is the rate-limiting enzyme in the biosynthesis of serotonin. *tph* is detected in the apical domain of late gastrula and shows expression in serotonergic neurons of the apical organ (Yaguchi and Katow, 2003). To investigate the role of the serotonergic neurons on ciliary beating and thus swimming behaviour, the authors used the chemical *p*-Chlorophenylalanine to inhibit the synthesis of serotonin.

p-Chlorophenylalanine-treated larvae did not swim, despite the occurrence of ciliary beating, suggesting that proper serotonin synthesis is required for normal swimming behaviour in the larvae. Furthermore, the addition of serotonin to embryo cultures has been shown to increase cilia beat frequency, while in contrast adding dopamine decreases cilia beat frequency (Wada *et al.,* 1997).

Initial specification of the apical domain

Classical experiments carried out by Hörstadius in the early twentieth century, involved separating a 16-cell sea urchin embryo into animal and vegetal halves. He found that a cultured animal-half produced only a ciliated ball of epithelium, known as a dauerblastula (figure 1.17 B). On the other hand, the animal half develops into a morphologically normal pluteus when combined with micromeres (figure 1.17 C). These results show clearly, that the differentiation of the animal hemisphere is not completely autonomous and requires signals from the vegetal half to develop normally (figure 1.17; Hörstadius, 1973).

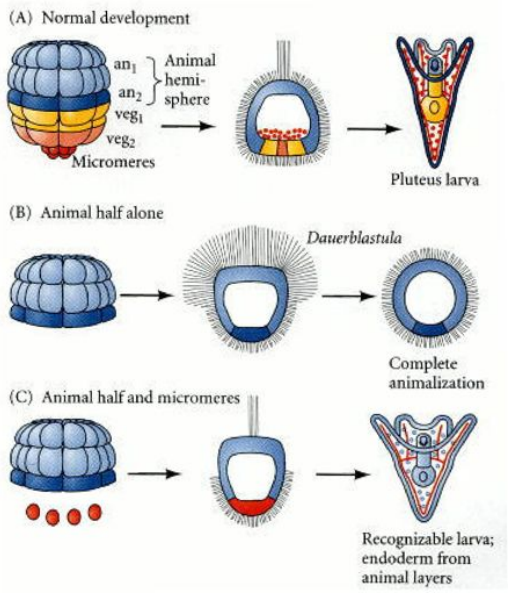

Figure 1.17. Vegetal signalling is required for ectoderm development
(A) Normal development of a 64-cell embryo. Coloured layers indicate cell fates. (B) An isolated animal hemisphere becomes a ciliated ball of cells. (C) When the isolated animal halves are combined with isolated micromeres a recognisable pluteus larvae is formed, with all the endoderm derived from the animal hemisphere (adapted from Gilbert, 2000).

Modern molecular biology has given a new insight into this classical experiment and shows that β-catenin first enters nuclei of the vegetal-most blastomeres by late 4th cleavage (Oliveri *et al*., 2002) and activates a wave of vegetal-to-animal cell-cell signalling that successively specify the mesoderm and endoderm (Davidson *et al.,* 2002). This wave of signalling is also thought to be responsible for the initial restriction of apical domain genes towards the animal pole (Yaguchi *et al.,* 2008). In fact, when nuclear entry of β-catenin is blocked during cleavage, endomesoderm specification fails, and apical organ genes such as *foxQ2* and *six3* expand to occupy the whole embryo and produce a greatly increased number of serotonergic neurons (figure 1.8; Wikramanayake *et al*., 1998; Logan *et al*., 1999; Yaguchi *et al*., 2006, Wei *et al.,* 2009 reviewed by Angerer *et al.,* 2011). Recently, Range *et al.,* (2013) have shown that the restriction of *foxQ2* and other apical organ genes to the animal pole is not dependent simply on Wnt/β-catenin signalling, highlighting that Wnt/Frizzled5/8-JNK and Frizzled1/2/7-PKC pathways are also required. When Wnt/Frizzled5/8-JNK signalling is disrupted, apical organ genes expand to cover the entire ectoderm, although not the endomesoderm. In contrast, the Frizzled1/2/7-PKC pathway antagonises the restriction of the apical organ genes to the animal pole, and disruption results in the loss of apical organ gene expression. In conclusion, these experiments support the importance of Wnt signalling originating in the vegetal hemisphere for the restriction of the apical organ to the animal pole.

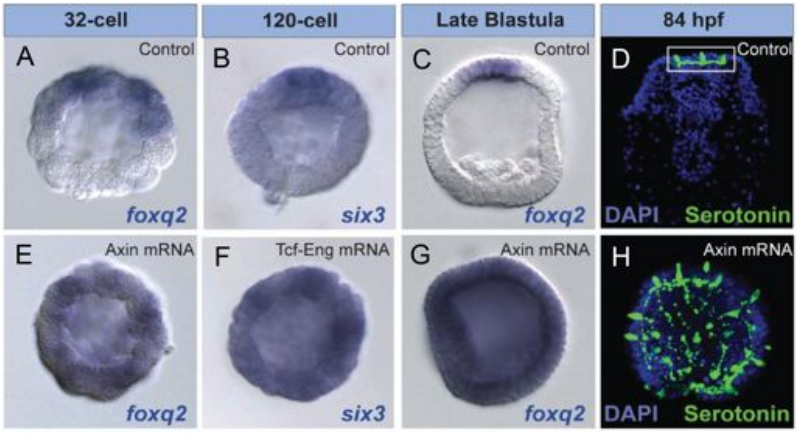

Figure 1.18. Blocking Wnt/β-catenin
(A-D) *foxQ2, six3* and serotonergic neurons in control embryos. (E-H) Embryos treated with either Axin mRNA or Tcf-Eng mRNA that blocks Wnt/β-catenin and results in expansion of *foxQ2, six3* and serotonergic neurons (adapted from Range *et al.,* 2013).

Development of the apical tuft

In both protostomes and deuterostomes, the apical organ develops from a thickened epithelium at the animal pole of the larval body, generally called the animal plate, and is usually associated with a neuronal ganglion and long cilia, termed the apical tuft. One of the first genes to be specifically expressed in the sea urchin apical domain is the homeodomain transcription factor *nk2.1* (Takas *et al.,* 2004). Expressed solely in the apical domain from hatched blastula stage, Nk2.1 protein is not co-expressed with serotonin and an *nk2.1* MASO knockdown has no effect on neurogenesis (Takas *et al.,* 2004). Dunn *et al.,* (2007) performed subtractive hybridisation screens designed to isolate downstream targets of *nk2.1* and successfully identified several downstream structural cilia genes, including *radial spoke 3, tecktin3,* and *radial spoke head p63.* Whole Mount in-situ Hybridisation (WMISH) was performed on these and two other cilia genes, *alpha 2 tubulin* and *dynein p33,* and showed that all five genes are expressed in the apical domain. Furthermore, an *nk2.1* MASO proves that all fives genes are downstream targets of *nk2.1*. *alpha 2 tubulin, radial spoke 3,* and *tecktin 3* were no longer detected in the apical domain, while *radial spoke head p63* and *dynein p33* become expressed ectopically in the oral ectoderm (figure 1.19 A,B). *nk2.1* is also required for the correct development of the apical tuft and in embryos treated with a *nk2.1* MASO, the apical tuft is lost. In addition, *nk2.1* knockdown embryos did not swim normally and sat at the bottom of the dish (Dunn *et al.,* 2007). Therefore, while *nk2.1* does not play a role in the development of serotonergic neurons, it seems clear that *nk2.1* controls the development of the ciliary tuft that exists in the apical organ. Another gene restricted in the apical domain of the sea urchin embryo is *foxQ2*, and is the earliest regulatory gene to be expressed exclusively in the apical domain (Tu *et al.,* 2006). It has been shown that *foxQ2* is required for both the normal development of serotonergic neurons but also for the differentiation of the apical tuft (Yaguchi *et al.,* 2010b). Yaguchi *et al.,* (2010b) showed that a gene called *ankyrin-containing gene apical tuft-1* (*ankat-1*) encoding a protein with ankyrin repeats in its N-terminal domain, was immediately downstream of *foxQ2* and expressed in the apical domain (figure 1.19 C). *ankat-1* MASO caused a loss of the apical tuft (figure 1.1. D) but did not affect the normal motility of embryos.

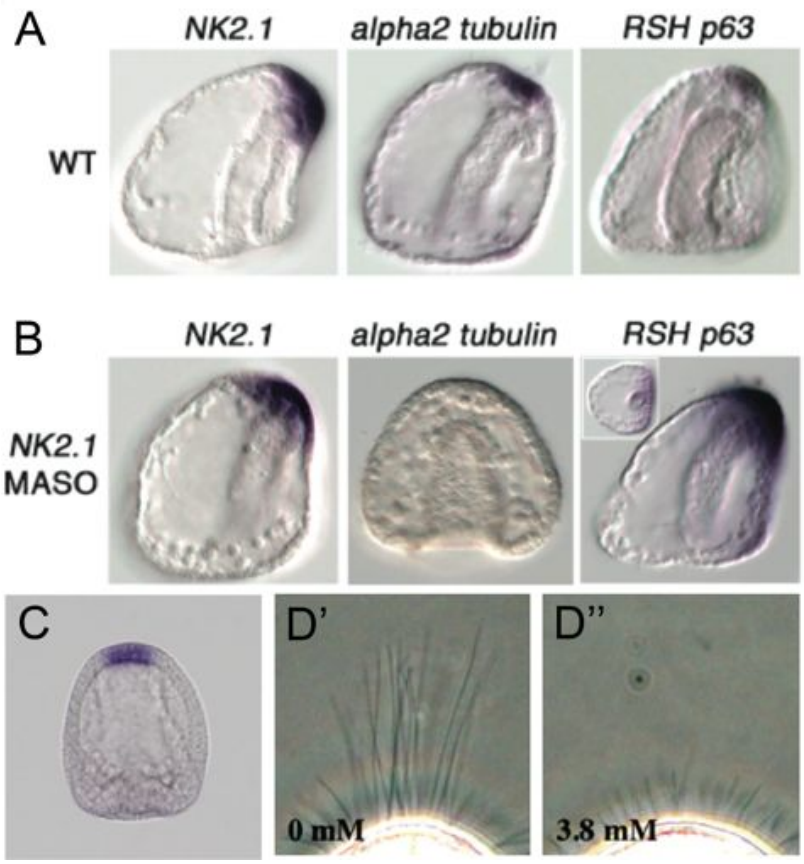

Figure 1.19. Regulation of the apical tuft in the sea urchin apical organ
(A,B) The expression of *nk2.1* and two downstream cilia genes; alpha2 tubulin and RSH p63 in wild type embryos and embryos treated with a *nk2.1* MASO (adapted from Dunn *et al.,* 2007). (C) expression of *ankAT* in the apical domain. (D) The apical tuft in control and embryos treated with a *ankAT* MASO (adapted from Yaguchi *et al.,* 2010b).

Neuroectoderm pattering and neuronal specification

One of the most important steps in the development of the nervous system, is the partitioning of ectoderm into neuroectoderm and non-neuroectoderm. During early development, Nodal and BMP 2/4 signalling act to specify the non-neurogenic oral and aboral ectoderm. Therefore, robust mechanisms are required to protect the apical domain and the ciliary band from these signals, in order to allow the formation of these two neuro-ectodermal territories. Yaguchi *et al.,* (2011) used a microarray approach to identify genes strongly down-regulated in embryos treated with a *foxQ2* MASO. One of these genes is *forebrain embryonic zinc finger* (*fez)*, a transcription factor, that begins to be expressed in the apical domain after hatching and is co-expressed with *foxQ2* until

mid-gastrula stage. During late gastrula stage, *fez* expression fades from the apical domain and is replaced by three to five individual *fez* positive cells along the aboral edge of *foxQ2* (figure 1.20 A). Double fluorescent WMISH shows that *fez* is co-expressed with *tph,* a marker for serotonergic neurons (figure 1.20 A). Embryos treated with a *fez* MASO have fewer serotonergic neurons (figure 1.20 B) and have a smaller apical domain as seen by a reduction in the size of the *foxQ2* domain (figure 1.20 C). *fez* is thought to control the size of the apical domain by inhibiting the action of an apical domain inhibitor, BMP 2/4. Therefore, embryos treated with both a *fez* MASO and a *bmp 2/4* MASO show no effect on the size of the *foxQ2* domain (figure 1.20 C,D).

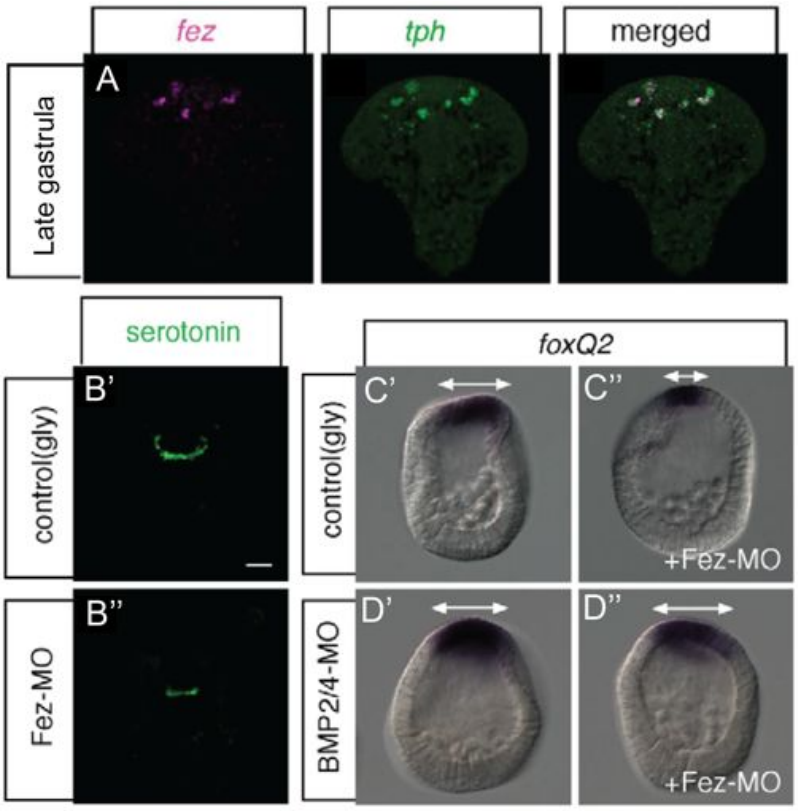

Figure 1.20. Expression and role of *fez* in the sea urchin apical organ
(A) *fez* is co-expressed with *tph*. (B) Embryos treated with *fez* MASO have a reduced number of serotonergic neurons. (C) Embryos treated with *fez* MASO have a smaller apical domain as seen by *foxQ2* expression when compared to controls. (D) Combined *fez* and *bmp 2/4* MASO help to explain how fez controls apical domain size (adapted from Yaguchi *et al.,* 2011).

As described above, serotonergic neurons are the first neurons to differentiate in the sea urchin embryo, appearing at the aboral edge of the apical domain in late gastrula.

Therefore, it is clear that any apical organ GRN must help explain how these neurons are specified and correctly positioned. Recently, Yaguchi, *et al*., (2012) have shown that *zinc finger homeobox (zfhx1),* a zinc-finger homeodomain transcription factor, also called s*madIP* (Howard-Ashby *et al*., 2006)*,* is expressed in the precursors of serotonergic neurons. Embryos treated with a *zfhx1* MASO produce a reduced number of serotonergic neurons, although those specified, form a normal, if smaller, ganglion. Interestingly, *zfhx1* is co-expressed with the gene that encodes the Delta ligand, and interfering with the Delta-Notch signalling using either DAPT, a γ-secretase inhibitor (Hughes *et al*., 2009), or *delta* MASO results in upregulation of *zfhx1* and an increase in the number of serotonergic neurons (Yaguchi *et al.,* 2012). This implies a mechanism of lateral inhibition (Simpson, 1990) in which the cells receiving the Delta-Notch signalling turn off *zfhx1, delta* and are not specified as serotonergic neurons.

six3 and *foxQ2* function at the top of an apical organ GRN

Another important transcription factor involved in the development of the sea urchin apical organ, and one that is evolutionarily conserved with other organisms, is *six3* (Steinmetz *et al*., 2003). In the sea urchin, like *foxQ2*, *six3* is expressed in the animal half of cleavage stage embryos and in the apical domain by hatched blastula stage (Poustka *et al.,* 2007). Embryos treated with a *six3* MASO, lack the thickened epithelium in the animal plate and lack serotonergic neurons (figure 1.21; Wei *et al.,* 2009). The absence of *six3* results in the strong down regulation of many apical domain genes *e.g. retinal homeobox* (*rx*), *achaet-scute* (*ac-sc*)*,* and *homeobrain* (*hbn*). As a result of this phenotype, and the early expression of *six3*, Wei *et al.,* (2009) proposed that *six3* functions at the top of an apical organ GRN. In support of this hypothesis, ectopic expression of *six3* obtained by mRNA injection, resulted in an extreme change in morphology and expansion of the apical domain, into a strange horseshoe band of cells. This band of cells contains a greatly expanded set of serotonergic neurons and non-serotonergic neurons, and also express the *nk2.1* gene. Burke *et al.,* (2006) have shown that *rx, ac-sc,* and *hbn* are all expressed specifically in the apical domain from early mesenchyme blastula stage and predict that together, they form a second tier in the hierarchy of the apical organ GRN.

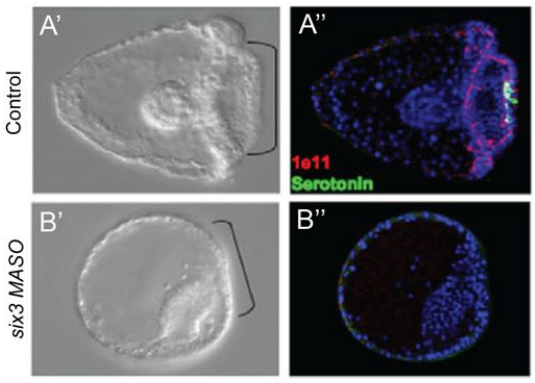

Figure 1.21. Importance of *six3* in the apical organ
(A) Control embryo showing a normal apical organ (black bracket) and normal neuronal structures including serotonergic neurons. (B) Embryos treated with *six3* MASO show a reduced apical plate and lose all neuronal structures (adapted from Wie *et al.,* 2009).

foxQ2 is the earliest known gene to be expressed specifically in the apical domain of the sea urchin embryo (figure 1.22 A-D; Tu *et al.,* 2006). Initially expressed in the animal half during cleavage stage, its expression is rapidly restricted to the apical domain in early blastula. At this stage, the border of *foxQ2* is immediately adjacent to the oral ectoderm marker *nodal* (figure 1.22 E). The absence of nuclearization of β-catenin, obtained by cadherin injection (Logan and McClay 1996), results in loss of *nodal* and thus loss of the oral-aboral ectoderm specification. Interestingly, removing foxQ2 protein by morpholino re-establishes oral-aboral polarity (Yaguchi *et al.,* 2008). On the contrary, ectopic ectodermal expression of *foxQ2* represses *nodal* and oral-aboral polarity, although the absence of *foxQ2* does not result in *nodal* expression in the apical domain (figure 1.22 F) Furthermore, the absence of both *lefty*, a nodal antagonist and *foxQ2* results in an expansion of *nodal* into the apical domain (figure 1.22 G,H) (Yaguchi *et al.,* 2008). Thus, the apical domain appears to be protected from Nodal signalling by the presence of both *foxQ2* and *lefty*.

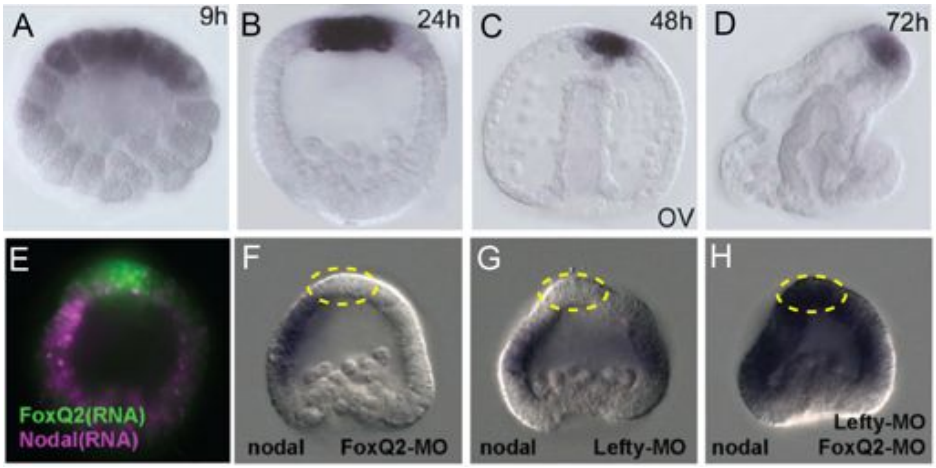

Figure 1.22. Expression and function of *foxQ2* in the apical domain
(A-D) Embryonic expression pattern of *foxQ2* (adapted from Tu *et al.,* 2006). (E) Double fluorescent WMISH showing relative position of *nodal* and *foxQ2.* (F-H) The effect on *nodal* expression in the apical domain (yellow dashed circle) when embryos are treated with *foxQ2* MASO, *lefty* MASO or both (adapted from Yaguchi *et al.,* 2008).

One of the most interesting results shown by Yaguchi *et al.,* (2008) is that in the absence of *foxQ2,* embryos lose oral-aboral polarity and serotonergic neurons are no longer restricted to the aboral edge of the apical domain. Recently, Yaguchi *et al.,* (2012) showed that *zfhx1* is expressed in serotonergic precursors along the aboral edge of the apical domain. When *nodal* translation is blocked by use of a *nodal* morpholino, individual cells that express *zfhx1* and *tph* are no longer located at the aboral edge of the apical domain, but rather surround it. In contrast, if Nodal signalling is expanded into the aboral ectoderm by the use of a *lefty* morpholino or by inhibiting *bmp2/4*, expression of both *zfhx1* and *tph* are lost from the apical domain. These findings have begun to help elucidate the regulatory pathway, that results in the specification of serotonergic neurons, as shown in the diagram in figure 1.23. According to Yaguchi and collaborators, *six3* and *foxQ2* sit at the top of an apical organ/neurogenic GRN and are required for the formation of the apical domain (Wei *et al.,* 2009; Yaguchi *et al.,* 2008, 2011). They activate genes such as *fez, nk2.1* and *ankAT-1* (Takas *et al.,* 2004; Dunn *et al.,* 2007; Yaguchi *et al.,* 2010b). *nk2.1* and *ankAT-1* are involved in the specification of the apical tuft and play no role in neurogenesis. *fez* on the other hand, is required for controlling the size of the apical organ and as a result the number of serotonergic

neurons, but is not required for the actual differentiation of serotonergic neurons. Initially, *delta,* followed by *zfhx1* and *fez,* are all expressed in serotonergic precursors. Finally, *zfhx1* is switched on by *foxQ2* and is required for *tph* expression, which in turn is required for the synthesis of serotonin (Yaguchi *et al.,* 2012).

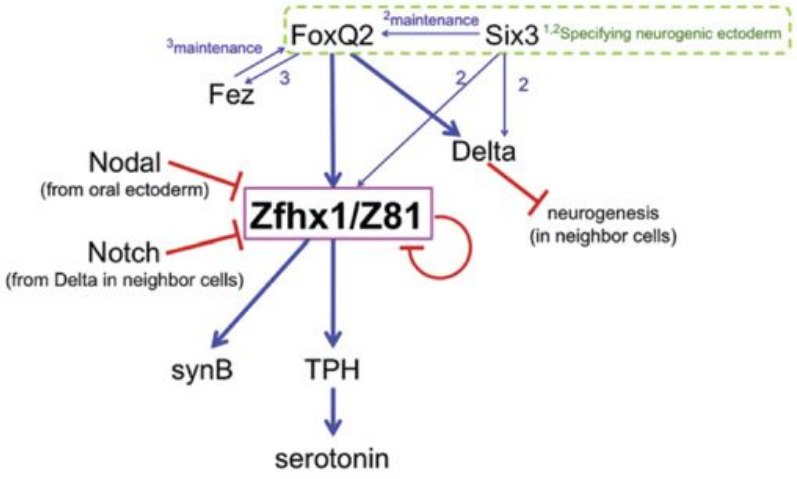

Figure 1.23. Regulatory mechanisms controlling differentiation of serotonergic neurons in the sea urchin embryo

Important aspects of the model are as follows: FoxQ2 and Six3 interact in the early specification of the apical domain and both regulate *zfhx1/z81* and *delta* expression. Zfhx1/z81 is required for the expression of *tph*, which is required for serotonin synthesis, and for synaptotagminB (synB). Delta-Notch signalling controls the number of neurons and Nodal inhibits neural development on the oral side. FoxQ2 is required for the expression of *fez* and Fez controls the size of the apical domain. References within the figure - 1, Yaguchi *et al*., 2008; 2, Wei *et al*., 2009; 3, Yaguchi *et al*., 2011. Adapted from Yaguchi *et al.,* (2012).

1.5 Aims of this thesis

The introduction above has given some background into the general biology of the apical organ and how it may function as a neuro-sensory structure. The sea urchin apical organ forms at the anterior end of the embryo and is home to the serotonergic neurons and apical tuft. As I have reviewed, the GRN specifying the apical organ is in its early stages and fundamentally, the apical domain is still treated as a spatially simple and homogenous territory. My investigations therefore, are directed by two main objectives: identifying the regulatory states and spatial domains that exist in the apical domain during development, and expanding the functional linkages that make up apical organ GRN.

I address the first of these objectives in chapters 3 to 5. In the first half of chapter 3, I compile a large dataset of regulatory and downstream genes that are expressed in the apical organ during development. Using a molecular landmark for the apical organ, I created cellular maps of the apical domain at different stages of development. I carried out a high-resolution, spatial analysis of this landmark using fluorescent WMISH and overlaid these data onto cellular maps. In the second half of chapter 3, I begin a detailed expression study of regulatory genes in order to identify their position relative to the apical organ landmark in blastula stages. In chapter 4 and 5, I extend this study from mesenchyme blastula stage to late gastrula stage.

I address the second objective in chapter 6. I start with disrupting Fibroblast growth factors (FGF) signalling using two methods: SU5402, a commonly used chemical inhibitor of FGF receptor 1 (FGFR1), and specific *fgfr1* MASOs. I also carry out a third perturbation study involving *zic2*. These three functional studies were analysed using a range of quantitative and qualitative methods. Finally, I searched the sea urchin genome and subsequently characterised novel members of the FGF signalling family.

In chapter 7, I present a discussion of the work presented in this thesis. I integrate all the mapping data and use the cellular maps to identify the different regulatory states that exist in the apical domain at each developmental stage. I then attempt to explain some surprisingly different results between the SU5402 treatments and *fgfr1* MASO experiments. Finally, I present the results of my thesis in a wider context, and touch upon the evolutionary implications of this work.

Chapter 2:
Materials and methods

I will now present the general materials and methods that were used in this thesis. They comprise of the bioinformatic tools (section 2.1), molecular cloning and sequencing (section 2.2), embryological techniques (section 2.3) and RNA quantification techniques (section 2.4)

2.1 Bioinformatics

Identification of apical organ genes

In order to identify as many genes as possible that may contribute to the apical organ GRN, I compiled a set of regulatory and downstream genes previously shown to be expressed in the apical organ (see chapter 3 table 3.1). This was obtained by an extensive search of the published literature and the Max Planck *S. purpuratus* WMISH database (http://goblet.molgen.mpg.de/eugene/cgi/eugene.pl). In most cases, each sea urchin gene is identified by a unique SPU_0NNNN number, which has been assigned during the genome assembly and annotation process and corresponds to the predicted gene model in the *S. purpuratus* genome (http://www.spbase.org; Sodergren *et al.,* 2006). Alternatively, when no "SPU" gene model was available, accession numbers were used to retrieve nucleotide sequence data from the National Center for Biotechnology Information (NCBI) Entrez database: http://www.ncbi.nlm.nih.gov/Entrez/.

Genes potentially expressed in the sea urchin apical organ

To identify sea urchin homologues of chick neural genes and *Nematostella* apical organ genes, BLAST (Basic Local Alignment Search Tool; Altschul*, et al.*, 1990) search was performed against the sea urchin genome protein database (http://www.spbase.org/blastx).

Multiple-alignments

Multi-alignments were used to identify and compare functional domains in different proteins. Amino acid sequences were obtained mostly using NCBI Entrez Protein database (http://www.ncbi.nlm.nih.gov/entrez/query.fcgi?db=Protein) and SpBase (http://www.spbase.org) and were aligned using the ClustalW function in Mega5 (Larkin *et al*., 2007; Tamura *et al*., 2011). Protein domains were identified using Pfam and/or SMART (Punta *et al*., 2012; Schultz *et al*., 1998).

2.2 Molecular cloning and sequencing

Primer design

All primers were designed using Primer3 (Rozen and Skaletsky, 2000, http://frodo.wi.mit.edu/primer3/). When designing primers for cloning, all settings were left as defaults and the product size to the desired length of fragment to clone. For QPCR primers, the following changes were made: product size was set to 120-180 nucleotides to guarantee optimal amplification efficiency, max 3' stability was changed to 8 and max Poly-X was changed to 3, optimal Tm was set at 60°C. It has been established in sea urchin that for WMISH probes, larger fragments give better signal, thus the primers were designed to amplify the largest fragment as possible based on the coding sequence of the gene of interest. Primers were ordered from MWG eurofins (http://www.eurofinsgenomics.eu) and 100 mM stock solutions were prepared from lyophilised product. Suggested primers were checked against the sea urchin genome using BlastN, to check for promiscuous binding to any other part of the genome. For a complete list of primers used and their corresponding nucleotide sequence, see appendix A.

PCR amplification

Polymerase chain reaction (PCR) was used to amplify a discrete fragment of a desired gene to clone into plasmid vectors for different purposes. Each PCR reaction was set up using the Expand High Fidelity PCR system kit (Roche, Indianapolis, IN) in a final volume of 25 µl containing: 2.5 µl of Expand High Fidelity 10X buffer with final concentration of 1.5 mM $MgCl_2$, 0.4µl Expand High Fidelity enzyme mix (2.5 units per

reaction), 1.25 µl of both forward and reverse primer at 10 mM, 0.5 µl of dNTP at 10 mM of each dNTP, 3 µl of template DNA (16.8 ng) and 16.1 µl of sterile double-distilled water. Amplification was carried out using a BioRad C1000 thermal cycler using the following cycle conditions: Initial denaturation at 94°C for 2 minutes, 10 amplification cycles as follows: denaturation at 94°C for 15 seconds, annealing at 45-65°C for 30 seconds depending on the Tm of the primers, elongation at 72°C for 0.5-3 minutes depending on the length of the fragment to amplify (based on 1 minute per kb of fragment size). This is followed by 15-20 amplification cycles of denaturation at 94°C for 15 seconds, annealing at 45-65º°C for 30 seconds, elongation at 72°C for 0.5-3 minutes (based on 1 minute per kb of fragment size) with a 5 second extension for each successive cycle. Finally, an extension cycle was carried out at 72°C for 10 min as a repair step. In many cases a gradient of 45, 50, 55, 60°C was used to optimise the amplification.

PCR clean up and gel extraction

To determine the outcome of the PCR reaction, 5 µl of the reaction was checked on an agarose gel (see below). If a single band of the desired molecular weight (MW) was detected, the PCR product was purified to remove primer dimers, polymerase and unincorporated nucleotides using the NucleoSpin® Extract II kit (Macherey-Nagel) following the manufactures instructions. In cases where a number of PCR products were amplified, the band corresponding to the predicted molecular weight was excised from the gel, extracted and purified with the same NucleoSpin® Extract II kit as per the manufactures instructions.

DNA ligation

In order to have a stable clone of the desired gene, the purified PCR products were ligated into the pGEM®-T Easy Vector (Promega) ideal for cloning PCR products with an A-nucleotide overhang, left by the Taq polymerase. The ligation reaction was set up using 5 µl of 5X Rapid Ligation Buffer, 1 µl (50 ng) of pGEM®-T Easy Vector, 1 µl of T4 DNA ligase and an ideal ratio of vector to fragment of 1:3 or 1:6, with nuclease free water (Ambion) to a final volume of 10 µl. The reaction was incubated at room temperature (RT) for 2 hours or at 12°C over night.

Transformation into competent bacterial cells

In order to select and propagate in a large scale, the desired fragment ligated into a bacterial plasmid vector, bacterial chemical competent cells were transformed with the ligation reaction. Briefly, 5 µl of ligated DNA was transformed into chemical competent DH5-α E.coli bacteria (Invitrogen). A 50 µl aliquot of competent cells was thawed on ice and 5 µl of ligated DNA was added, gently mixed and incubated on ice for 30 minutes. The cells where then heat shocked at 42°C for 20 seconds and cooled on ice for 2 minutes. 950 µl of pre-warmed SOC broth (Sigma) was added to the tube and incubated at 37°C for 1 hour at 150 rotations per minute (RPM). 100µl and 900µl of the transformed bacteria were plated on two separate Luria Broth (LB) plates containing Tryptone (pancreatic digest of casein) 10 g/L, Yeast extract 5 g/L, and NaCl 5 g/L (Sigma) with additional 100µg/ml of ampicillin and incubated overnight at 37°C. To select transformants using blue/white screening 50 µg/ml X-gal was added to each plate.

Screening of recombinant colonies (Colony PCR)

In order to screen a large number of colonies for transformants with the desired length of fragment, colony PCR was used to amplify the fragment from primers at each side of the cloning site. Single colonies were inoculated onto 20 µl of LB broth containing 100 µg/ml ampicillin and incubated for 1 hour at 37°C. A PCR reaction was set up using the Taq DNA Polymerase (Invitrogen) in a final volume of 20µl containing: 2 µl of 10X PCR buffer with final concentration of 1.5 mM $MgCl_2$, 0.1 µl Taq DNA Polymerase (5 Units/ µl), 0.8 µl each of 10mM T7 and SP6 primer, 0.4 µl of 10 mM dNTP mixture (2.5 mM each), 1 µl of LB containing the picked colony with transformed plasmid and 14.9µl of Nuclease-free water (Ambion). Amplification was carried out using a BioRad C1000 thermal cycler using the following cycle conditions: Initial denaturation at 98°C for 5 minutes, 25 amplification cycles as follows: denaturation at 94°C for 30 seconds, annealing at 55°C for 30 seconds, elongation at 72°C for 1 minutes (based on 1 minute per kb of fragment size) and a final extension step of 72°C for 5 minutes. The amplified fragments were visualised on an agarose gel (see below) and the MW was determined in comparison to the 1kb Plus molecular weight marker (Invitrogen). The recombinant colonies were then selected for further analysis.

Plasmid DNA preparation (mini-Prep)

A single bacterial colony containing the desired recombinant plasmid vector was inoculated into 4 ml of LB broth containing 100 µg/ml ampicillin and incubated over night at 37°C at 225 RPM. In cases when a colony PCR was carried out, 5 µl of the inoculum of the colony that contains a fragment of desired length was used to inoculate 4 ml of LB broth as described above. The overnight culture was spun down and the NucleoSpin® Plasmid kit (Macherey-Nagel) was used to extract and purify plasmid according to the manufacturer's instructions. The DNA quantity and quality was determined with a NanoDrop® 2000c Spectrophotometer.

DNA digestion

To confirm the MW of the DNA fragment incorporated into the plasmid, a restriction enzyme digestion was used, utilising the two EcoRI digestion sites at each side of the pGEM®-T Easy Vector cloning site. A digestion reaction was set up using the EcoRI (Roche) in a final volume of 20 µl containing: 2 µl of 10X buffer H, 0.2 µl EcoRI enzyme (12 Units/µl), 2 µl purified plasmid at variable concentration (40-500 ng/µl), and 15.8 µl of nuclease-free water. The reaction was incubated for at least 1 hour at 37°C and the MW of the digest checked by gel electrophoresis.

Gel electrophoresis

To visualise and check the MW of nucleic acids, gel electrophoresis was performed by running a suitable quantity of DNA/RNA solution with 6X gel loading buffer (0.25% (w/v) Bromophenol Blue, 50% (v/v) Glycerol, 0.25% (w/v) Xylene Cyanol FF) in a 0.8% - 1.2% agarose gel (depending on the MW) in 0.5% TBE (manufacture) containing 0.5 µg/ml Ethidium Bromide (Sigma) with a current of 80 – 120 volts.

DNA sequencing

The correct sequence of a stable clone was determined by the public service of the Scientific Support Service Wolfson Institute for Biomedical Research at UCL (http://www.ucl.ac.uk/wibr/services/rnai/sequence).

2.3 Embryological techniques

Animals and culture of embryos

Adult sea urchins of the species *Strongylocentrotus purpuratus* were obtained from Pat Leahy (Kerchoff Marine Laboratory, California Institute of Technology, USA). On arrival, the animals were kept in large tanks of artificial seawater (Instant Ocean Acquarium Sea Salt Mixture) at 12-13°C, and fed regularly with seaweed (*Ulva lactuca*) from the Mediterranean sea. When sea urchin embryos or larvae were required, mature adults were initially induced to spawn by vigorous shaking and if necessary intracoelomic injection of 0.55M potassium chloride into the soft tissue around the mouth. Sea urchins show no sexual dimorphism so it is only possible to identify male and female individuals after they have spawned. Eggs were collected by placing a female upside down in a glass beaker filled with filtered artificial seawater (FASW; containing 28.3g NaCl, 0.77g KCl, 5.41g $MgCl_{2\cdot 6}H2O$, 3.42g $MgSO_4$, 0.2g $NaHCO_3$, 1.56g $CaCl_2$ dehydrate in 1 litre of deionized H_20 and adjusted to a pH to 8.2 and a salinity of 34 parts per thousand; this was then filtered through a 0.45 µm filter unit (Nalgene) and allowed to settle by gravity. All glassware and plastic used for animals and embryos cultures were kept free from any detergent and washed only with deionized H_2O as detergent can disturb normal development of the embryos. Concentrated sperm (dry sperm) was collected using a pipette and kept on ice until it was used for fertilisation or alternatively, stored at 4°C for up to two weeks. Collected eggs were passed through a 70 µm nitrex mesh to remove debris and washed twice with FASW. Sperm was activated by dilution of 5-10 µl of concentrated sperm in 10 ml of FASW and used to fertilise the eggs. Embryos that were required for microinjection or were fixed before hatching, were fertilised in 2mM Para Amino Benzoic Acid (PABA) in FASW, to avoid the hardening of the fertilisation membrane. Successful fertilisation was checked by elevation of the fertilisation membrane and then two washes were carried out to remove remaining sperm. Developing embryos were cultured in FASW at 15°C and a mixture of Streptomycin (50 µg/ml) and Penicillin (20 U/ml) were used as antibiotics to stop bacterial growth.

Embryo fixation and storage

Sea urchin embryos develop synchronously up to pluteus larval stage and achieve a desired developmental stage at the same time after fertilisation, if cultured at the same temperature. To fix embryos for WMISH and serotonin antibody staining, embryos were collected at the right developmental stage and left to settle on ice; in some cases embryos were helped to settle by addition of a few microliters of fixative solution (4% paraformaldehyde (Electron Microscopy Sciences Cat. #15710), 32.5% filtered seawater, 32.5 mM MOPS at pH7, 162.5 mM NaCl). Once the embryos had settled, the FASW was removed and the embryos washed in fixative solution twice. The embryos were left in fresh fixative solution overnight at 4°C with a 1:10 ratio of embryos pellet volume to fixative solution. The embryos were then washed 5 times in cold MOPS buffer (0.1M MOPS pH7, 0.5M NaCl, 0.1% Tween-20 in DEPC- treated H_2O) and stored in 70% ethanol at −20°C indefinitely. For acetylated tubulin staining to visualise the cilia, embryos were fixed in 1% glutaraldehyde (Sigma) in FASW for 10 minutes and then washed in PBST (137 mM NaCl, 2.7 mM KCl, 1.5 mM KH_2PO_4, 6.5 mM Na_2HPO_4, pH7.4, 0.02% (v/v) Tween).

Probe template preparation

PCR was used to amplify the desired fragment from a clone using primers that sit outside both RNA polymerase promoter sites, using the primers pSPORT Forward and pSPORT Reverse (GTGCTGCAAGGCGATTAA and TGTGGAATTGTGAGCGGATA). Each PCR reaction was set up using the Expand High Fidelity PCR system kit (Roche, Indianapolis, IN) in a final volume of 50 µl containing: 5 µl of Expand High Fidelity 10X buffer with final concentration of 1.5 mM $MgCl_2$, 0.5 µl Expand High Fidelity enzyme mix (2.5 units per reaction), 1.5 µl of both pSPORT forward and pSPORT reverse primers 10 µM, 1µl of dNTP with a final concentration of 200 µM of each dNTP, 5 µl of template DNA (5 ng) and 35.5µl of nuclease-free water (Ambion). Amplification was carried out using a BioRad thermal cycler C100 using the following cycle conditions: Initial denaturation at 95°C for 5 minutes, 10 amplification cycles as follows: denaturation at 95°C for 30 seconds, annealing at 55°C for 30 seconds, elongation at 72°C for 0.5-3 minutes (based on 1 minute per kb of fragment size). This is followed by 20 amplification cycles of denaturation at 95°C for 30 seconds, annealing at 55°C for 30 seconds, elongation at

72°C for 0.5-3 minutes (based on 1 minute per kb of fragment size) with a 5 second extension for each successive cycle and a final elongation step of 72°C for 8 minutes. Gel electrophoresis was performed to check the MW of the PCR product and that a single band was obtained, then the template was purified using NucleoSpin® Extract II kit (Macherey-Nagel) following the manufactures instructions.

Probe synthesis for WMISH

In order to hybridise to the target mRNA, a single stranded probe had to be synthesised from the antisense strand and either labelled with Digoxigenin (DIG), Fluorescein (Fluo) or Dinitrophenol (DNP). The orientation of the insert in the vector was judged from the sequencing products and the correct polymerase to synthesise the antisense strand was chosen. Transcription reactions were carried out in a total volume of 20 µl using either SP6 RNA Polymerase set (SP6 RNA polymerase and 10x transcription buffer; Roche) or T7 RNA Polymerase set (T7 RNA polymerase and 10x transcription buffer; Roche) depending on the clone. To prevent RNA degradation, Protector RNase inhibitor (Roche) was used in all reactions. Synthesising DNP labelled probes is a two-step process. Firstly, a non-labelled (cold) probe is synthesised using a ribo-nucleotide mix (NTP; Promega) as follows:

Template DNA	1 µg
2.5mM NTP mix (Promega)	8 µl
10x transcription buffer	2 µl
T7 or Sp6 RNA polymerase 2 Units/µl	2 µl
RNase Inhibitor 2 Unit/µl	1 µl
Nuclease-free H_2O	up to 20 µl

All transcription reactions were incubated for at least 2 hours at 37°C; in the case of Sp6 polymerase the reaction was left longer, up to 5 hours. To stop the reaction and remove the template DNA, 1 µl of DNAseI RNase free was added to the reaction and incubated at 37°C for 15 min. The newly synthesised transcripts were cleaned from unincorporated nucleotides by precipitation using 10 µl of 7.5M LiCl (Ambion), the reaction was incubated at −20°C overnight. The probe mixture was then centrifuged for 30 min at

maximum speed in a microcentrifuge (Eppendorf, model 5424). The pellet was observed and washed twice with 1 ml 80% ethanol. The pellet was air dried until all residual ethanol had evaporated. Probes were dissolved in 30 µl of nuclease-free H_2O and the concentration was determined using NanoDrop® 2000c Spectrophotometer and stored at -80°C. Gel electrophoresis using a 1% agarose gel was used to confirm successful synthesis and absence of probe degradation. Secondly, the DNP labelling reaction was carried out using the Label It DNP labeling Kit (Mirus corporation) in a total volume of 20 µl using the following reagents:

Cold RNA probe	1 µg
10X Mirus Labelling Buffer A	5 µl
Label It DNP reagent	5 µl
Nuclease-free H_2O	to 50 µl

The DNP labelling reaction was incubated for 2 hours at 37°C. To remove any unincorporated DNP, the RNA probes were purified using the Mini Quick Spin RNA Columns G-50 Sephadex (Roche), following manufacturer's instructions. Aliquots of the probe were made at the concentration of 50 ng/µl and stored at -80°C. DIG and Fluo labelled probes were synthesised in one step using 10X DIG RNA labelling mix (Roche) or 10X Fluorescein RNA labelling mix (Roche) respectively, as follows:

Template DNA	0.5 µg
10X DIG or fluorescein mix	8 µl
10x transcription buffer	2 µl
T7 or Sp6 RNA polymerase (2 Units/µl)	1.6 µl
RNase Inhibitor (1 Unit/µl)	0.4 µl
Nuclease-free H_2O	to 20 µl

The transcription reaction was incubated for 2-7 hours at 37°C. To remove template DNA from the transcription reaction, 1 µl of DNAse/RNAse free (1 Unit/µl; Roche) was added and incubated for 15 minutes at 37°C. To precipitate the RNA, 30 µl of DEPC H_2O and 10 µl of 7.5 M LiCl was added, and the reaction incubated at −20°C overnight. To wash the probe, the mixture was centrifuged for 30 min at maximum speed before removing the supernatant and adding 1 ml 80% ethanol. The mixture was centrifuged for 15 min at maximum speed and washed a second time with 1 ml 80% ethanol and centrifuged at maximum speed. The ethanol was removed and the pellets air dried until residual ethanol had evaporated. Probes were dissolved in 50 µl of DEPC H_2O. Gel electrophoresis using a 1% agarose gel was used to confirm successful synthesis and absence of degradation. The probe was diluted to 50 ng/µl and aliquots of the probe were made and stored at -80 °C.

Whole mount *in situ* hybridisation

To detect the spatial pattern of gene expression, *in situ* hybridisation techniques were employed on whole embryos at different developmental stages or those that have been differently treated. Two WMISH protocols were used in this thesis and are named “long” and “short”. The “long” protocol was modified from Arenas-Menas *et al.,* (2000) and Minokawa *et al.,* (2004). Embryos were removed from −20°C and roughly 50 embryos for each stage were transferred into 1.5 ml tubes (Eppendorf) containing fresh 70% ethanol. The embryos were first washed four times with 1 ml MOPS buffer. Embryos were then pre-hybridised in 500 µl of fresh hybridisation buffer (70% formamide, 0.1M MOPS pH7, 0.5M NaCl, 0.1% Tween-20, 1mg/ml BSA) for 3 hours at 60°C. Embryos were then hybridised for one week at 60°C in fresh hybridisation buffer containing 0.1 ng/µl of probe.

Post-hybridisation

Embryos were washed five times with 1 ml MOPS buffer at room temperature and then incubated in 500 µl of hybridisation buffer for 3 hours at 60°C to remove excess of probe. Embryos were washed a further three times with 1 ml MOPS buffer at room temperature.

Single probe detection

Detection of the hybridised probe began with incubating the embryos in 1 ml of blocking solution 1 (0.1M MOPS pH7, 0.5M NaCl, 10mg/ml BSA, 0.1% Tween-20) for 20 minutes at room temperature and then in 1 ml blocking solution 2 (0.1M MOPS pH7, 0.5M NaCl, 10% sheep serum, 1mg/ml BSA, 0.1% Tween-20) for 30 minutes at 37°C. The embryos were then incubated with 1/1000 dilution of anti-DIG-AP Fab fragments (Roche) or Anti-FLOU-AP Fab fragments (Roche) in 1 ml of antibody solution (0.1M MOPS pH7, 0.5M NaCl, 1% sheep serum, 0.1 mg/ml BSA, 0.1% Tween-20) overnight at room temperature. The excess of antibody was removed by washing the embryos six to eight times with 1 ml MOPS buffer at room temperature for 30 minutes. Embryos were then washed twice with alkaline phosphatase buffer (0.1M Tris pH9.5, 50mM $MgCl_2$, 0.1M NaCl, 1mM Levamisole) for 30 minutes at room temperature. At this point embryos were stained in 500 µl of staining buffer (10% dimethyl formamide, 0.1M Tris pH9.5, 50mM $MgCl_2$, 0.1M NaCl, 1mM levamisole) containing 4 µl of NBT/BCIP stock solution (Roche) or INT/BCIP stock solution (Roche). Staining was developed in the dark, at room temperature. Staining could take from a couple to several hours depending on the probe length and level of gene expression. To monitor the development of the stain, embryos were regularly inspected under a dissecting microscope. If needed, embryos were left to stain over night at 4°C. When a suitable level of staining had developed, the staining reaction was stopped by washing three times in MOPS buffer containing 0.05M EDTA and transferred initially to 25% glycerol and then 50% glycerol and stored at 4°C indefinitely.

Double probe detection

The protocol used for the simultaneous detection of two different genes (Minokawa *et al.,* 2005) is largely the same as the standard single *in-situ* hybridisation with the following modifications: Embryos were hybridised for one week at 60°C in fresh hybridisation buffer containing 0.1 ng/µl of each probe labelled with DIG, Fluo or DNP in a non-overlapping combination of the two. During detection steps, the higher expressing gene is processed first and embryos are incubated with 1/1000 dilution of either Anti-Digoxigenin-AP Fab fragments (Roche) or Anti-Fluorescein-AP Fab fragments, depending on which label has been used. The first staining was carried out

with NBT/BCIP, which produces a purple precipitate. When a suitable level of staining had developed, the staining reaction was stopped by washing three times in 1 ml of MOPS buffer, and to completely eliminate the alkaline phosphatase activity, the embryos were washed in gylcine solution (0.1M glycine hydrochloride pH2.2, 0.1% Tween-20) and then washed four times with 1 ml MOPS buffer. Embryos were then blocked and incubated overnight with the second relevant antibody as described in the standard single *in-situ* hybridisation. The second gene is stained with INT/BCIP, which produces a yellow precipitate. Stains were developed in the dark at room temperature or 4°C. The development of the stain was regularly monitored under a dissecting microscope. The second staining reaction was stopped by washing three times in MOPS buffer containing 0.05M EDTA and transferred initially to 25% glycerol and then 50% glycerol.

The "short" WMISH protocol

A shorter WMISH protocol was carried out according to the protocol of Dr. Cynthia Messier (adapted from Croce *et al.,* 2010) with a number of modifications. Fixed embryos were removed from storage at –20°C and transferred into 1.5 ml tubes (Eppendorf) or to curved-bottom 96 well plates (Nunc) containing 50% ethanol. All the following steps were carried out in 1 ml volume for 1.5 ml tubes and 200 µl if a 96 well plate was used, unless otherwise specified. The embryos were then washed five times in TBST (0.2M Tris pH 7.5, 0.15M NaCl, 0.1% Tween-20). Embryos were transferred to 1:1 ratio of TBST:hybridisation buffer (50% deionized formamide, 10% polyethelene glycol (PEG; Sigma), 0.6M NaCl, 0.02M Tris pH 7.5, 0.5mg/ml yeast tRNA, 1X Denhardt's soultion, 0.1%Tween-20, 5mM EDTA). Embryos were pre-hybridised in 500 µl (200 µl in wells) of fresh hybridisation buffer for 1 hour at 60°C (65°C in wells). A hybridisation buffer containing 50 ng/ml probe final concentration was incubated for 10 minutes at 95°C, then 10 minutes on ice and left at 60°C (65°C in wells) until ready to use. Embryos were then hybridised overnight at 60°C (65°C in wells) in hybridisation buffer/ probe mix.

Post-hybridisation and antibody

Embryos were washed in a 1:1 ratio of TBST:hybridisation buffer at 60°C (65°C in wells), then washed four times (twice in wells) in TBST at 60°C (65°C in wells). This was followed by two washes in 1X SSC at 65°C and then a single wash in 0.1X SSC at 65°C

when using wells only (to reduce unspecific binding of the probe in the smaller volumes of a well). The embryos were then re-equilibrated in TBST at room temperature (2X washes) and probe detection started with incubation of the embryos for 30 minutes in blocking buffer (TBST, 5% sheep serum) at room temperature. The embryos were incubated with 1/2000 dilution of Anti-Digoxigenin-AP, Fab fragments (Roche) or Anti-Fluorescein-AP, Fab fragments (Roche) in blocking buffer for 1 hour at room temperature.

Probe detection

To remove excess antibody, embryos were washed six times with TBST buffer at room temperature. After TBST buffer washes, embryos were washed twice with alkaline phosphatase buffer (0.1M Tris pH9.5, 50mM $MgCl_2$, 0.1M NaCl, 1mM Levamisole, 0.1% Tween-20) for 30 minutes at room temperature. Embryos were then stained in 500 µl (100 µl in 96 well plates) of staining buffer (alkaline phosphatase Buffer, 10% dimethyl formamide,) containing 0.8 µl of NBT/BCIP stock solution (Roche) or INT/BCIP stock solution (Roche). Stains were developed in the dark at room temperature or 4°C. To monitor the development of the stain, embryos were regularly inspected under a dissecting microscope. When a suitable level of staining had developed, the staining reaction was stopped by washing three times in TBST buffer containing 0.05M EDTA and transferred initially to 25% glycerol and then 50% glycerol. Embryos were stored at 4°C.

The "short" double fluorescent WMISH protocol

The protocol is largely the same as the standard "short" single *in situ* hybridisation, with the following modifications. The fluorescent detection was carried out with the Tyramide Signal Amplification (TSA) Systems (Perkin Elmer) using antibodies conjugated with peroxidase (POD). After over night hybridisation with each probe at 50 ng/ml final concentration, and one wash to remove the excess of probe, embryos were incubated with 1/2000 dilution of Anti-DIG-POD Fab fragments (Roche) or Anti-FLUO-POD, Fab fragments (Roche) or Anti-DNP horseradish peroxidase (Perkin Elmer) in Perkin Elmer blocking buffer (0.5M in TBST according to manufacturer's instructions) for 1 hour at room temperature for anti-DIG and anti-Fluo antibodies, and overnight at

room temperature for anti-DNP antibody. Embryos were washed six to eight times with 1 ml of TBST, and then incubated in amplification wash diluent (TBST, 0.0015% H_2O_2) for 30 min at room temperature. Embryos were then stained with 1X amplification diluent containing 1:400 dilution of CY3, for 45 min or with 1X amplification diluent containing 1:400 dilution of CY5, for 90 min. Stains were developed in the dark, at room temperature and stopped by washing four times in TBST buffer. The embryos were stored at 4°C. For double fluorescent *in situ*, CY5 was usually used to stain the DNP labelled probe. After washing with TBST to remove background staining, the horseradish peroxidase activity had to be completely eliminated to allow the second staining. To this purpose, the embryos were washed once in 1% H_2O_2, once in TBST, then once in glycine solution (0.1M glycine hydrochloride pH2.2, 0.1% Tween-20) and then washed three times with 1 ml TBST. Embryos were then blocked and incubated overnight, with the second antibody as described above. To stain the second probe, embryos were washed six to eight times with 1 ml TBST, and then incubated again with the amplification wash diluent for 30 min, at room temperature. Embryos were then stained again, as mentioned above, using CY3 or CY5. Stains were developed in the dark at room temperature. The embryos were then washed four times in TBST buffer checked for staining under epifluorescent microscope and washed further if required and stored at 4°C.

Immunohistochemistry

Immunohistochemical methods were used to visualise serotonergic neurons and ciliated structures in the sea urchin embryo. Roughly 50-100 embryos, were fixed (see above), and removed from −20°C and transferred into 1.5 ml tubes (Eppendorf) containing fresh 70% ethanol or, if freshly fixed, were transferred into PBST. Embryos were washed three times with PBST and incubated in 500 µl of blocking buffer (PBST, 2.5% BSA) for 30 minutes at room temperature. For serotonin staining, the embryos were then incubated for 1 hour at room temperature with anti-serotonin produced in rabbit (Sigma) diluted 1:1000 in PBST. For acetylated tubulin staining, the embryos were then incubated for 1 hour at room temperature with anti-acetylated tubulin produced in mouse produce in goat (Sigma) diluted 1:500 in blocking buffer. To remove excess antibody, embryos were washed three times in 1 ml of PBST. For serotonin, the

embryos were incubated for 1 hour at room temperature with 500 µl of PBST containing 1:250 anti-Rabbit Alexa 488 (Invitrogen) and for acetylated tubulin the embryos were incubated for 1 hour at room temperature with 500µl of PBST containing 1:250 Fab anti-Mouse (Invitrogen) Alexa 488. The embryos were then washed three times with PBST and checked under the fluorescent microscope.

Differential Interference Contrast (DIC) & epi-fluorescent microscopy.

35-40 µl of embryos in glycerol were collected using a P200 Gilson pipette and deposited on a microscope slide under a dissecting scope (Zeiss). Small balls of plasticine were placed on the four corners of a cover slip, in order to lift it from the slide, which was carefully placed over the solution containing the embryos. In some cases, the slide was sealed using transparent nail varnish. Bright-field and DIC images were taken with a Zeiss AxioImager M1 coupled to a Zeiss AxioCam HRc using 20X and 40X magnification. Images were usually taken at different focal planes and often the same embryo was rolled to enable images to be taken from different perspectives. Photoshop CS5 (Adobe) was used to make basic adjustments to brightness and contrast, and for cropping. For fluorescent stained embryos, each embryo was imaged multiple times using different channels and DIC. Photoshop was then used for basic image processing and adjustments in order to merge the multiple channels into the same image using liner dodge tool.

Confocal microscopy

Up to 100 µl of embryos were collected using a P200 Gilson pipette and placed on a 35 mm petri dish with a glass bottom (Wilco). Images were collected using an inverted Zeiss confocal laser scanning microscope LSM 510, with Z-stacks of 1 µm collected for all channels required. Optical sections were stacked and analysed using ImageJ software package (NIH) and the final merged images were produced using Photoshop CS5 (Adobe).

Microinjection

To microinject sea urchin embryos, unfertilised eggs were immobilised on protamine-coated plates. Lids of 60 mm plastic Petri-dish (Flacon) were filled for one minute with 1% W/V protamine sulphate (Sigma, CAT 53597-25-4) solution in distilled H_2O. Following protamine coating, the lids were washed thoroughly with distilled water to remove excess of solution, and air dried over night at room temperature.

Microinjection needle preparation

Needles for microinjection were prepared from 1.0 mm outside diameter, 0.75 mm inside diameter, borosilicate glass supplied by Sutter Instrument Co. Novato, CA (No. B100-75-10). Fine-tipped microinjection needles were pulled on a Sutter P-97 micropipette puller (P=300; H=560; Pu=140; V=80; T=200). To avoid clogging of needles, all solutions to be microinjected were filtered through 0.2 µm filters and centrifuged for 15 minutes.

Glass pipettes

Glass Pasteur pipettes were pulled in a Bunsen flame and broken off at the end to obtain a desired size to collect eggs and embryos. The internal diameter of a "rowing" pipette should be roughly the same as the egg diameter (~70 µm) to warrant optimal rowing of eggs.

Morpholino Injection solution

Sequence specific Morpholino antisense oligonucleotides (MASO) were designed and ordered by Gene-Tools (for sequences see Appendix A). The lyophilised oligos were resuspended in a 500mM or 1mM stock solution and incubated at 55°C for 10 min before preparing the injection solution, which is kept at room temperature. To ensure specificity of the MASO

Solution	Volume	Final Concentration
MASO	X µl	50 µM to 300 µM
1M KCL	1.2 µl	120 mM
Rhodamin Dextran 5 mg/ml (MW 10.000; Sigma)	1 µl	0.5 mg/ml
H_2O	Up to 10 µl	N/A

Eggs and sperm were collected from adult urchins, and a small fertilisation test was carried out to make sure the gametes were healthy. For microinjection, eggs were de-jellied by passing throw a 60µm nitrex mesh several times and stored at 15°C in ASW in a Petri dish coated with 1% agarose. The eggs were then rowed using a pulled glass pasteur pipette onto protamine-coated plates and kept covered at 15°C in 2 mM PABA-ASW until they were ready to be injected. The microinjection needles were loaded with morpholino solution. The rowed embryos were then fertilised and injected with the appropriate MASO using a picospitzer III. Following injection, embryos were incubated in protamine plates in PABA-ASW at 15°C, until 15 hours (just before hatching), the percentage of injected embryos (fluorescence of Rhodamine Dextran) noted, and transferred by mouthpiece to agar-coated (1% w/v) plates filled with a mixture of Streptomycin (50 µg/ml) and Penicillin (20 U/ml) in FASW, and again incubated at 15°C. Embryos were observed for phenotypic change and imaged at various time points. At selected times, 50 embryos, were collected and transferred to a tube (Eppendorf) using a mouthpiece, centrifuged at maximum speed for 30 seconds, then the supernatant was removed and the embryos prepared for RNA extraction (as described in the following section). The morpholinos targeting FGFR1 translation were provided by Dr. Yi-Hsien Su at the Institute of Cellular and Organismic Biology, Academia Sinica (Taiwan). To estimate the accuracy of the microinjection, Rhodamine Dextran was co-injected with the morpholino solution and subsequently visualised using fluorescence microscopy: an average of 90-95% of embryos (n>50) were successfully injected in each experiment. In all experiments, as a negative control, embryos were injected with the standard control morpholino, at equal or greater concentration than the test morpholino, and compared side-by-side with uninjected and MASO-injected embryos. All newly designed morpholinos were acquired from Gene Tools (Corvallis, OR). To select for the most

specific antisense oligos, the designed oligo sequence was checked against the sea urchin genome and transcriptome using BlastN and discarded if more than one sequence was tagged at 80% of identity. In the case of FGFR1, two independent MASO were used further confirm specificity.

Inhibition of FGFR1 (receptor kinase) signalling using SU5402

SU5402 (Calbiochem) was prepared as 5 mM stock in DMSO and stored at -20°C. A pilot study was performed using 10 µM or 20 µM SU5402. Subsequent experiments all used 20 µM. Embryos were fertilised and cultured in 10 ml Petri dishes (Falcon) with 5 ml of culture (1000 embryos/ml). SU5402 was added to the embryos, which were allowed to develop normally at 15°C. Further embryos were cultured in FASW and DMSO in parallel, and were used as controls. Embryos were collected in the same manner as the MASO experiments (described above).

2.4 RNA quantification techniques

Extraction of total RNA

To eliminate RNAase contamination, all the procedures were carried out in a dust free environment, using gloves and RNAase free plastic instruments. Embryos at the right developmental stage were collected in a tube and centrifuged at 2000 RPM for 5 minutes to remove all the water. The pellet of embryos was then processed for RNA extraction. Total RNA purification was carried out using RNeasy micro RNA extraction kit (Qiagen) according to the manufacturer protocol with the following modifications. The embryo pellet corresponding to 50-1000 embryos was resuspended in 350 µl of RLT buffer (Ambion) including 1% β-mercaptoethanol. The solution was either stored at -80°C or processed immediately. 1 µl of carrier RNA (39.7 ng/µl) was added to the RNA sample. To ensure no contamination of genomic DNA occurred, a DNAseI step was added as suggested by the manufacturer. The wash with 500 µl 80% ethanol was done twice to increase the quality of the RNA. The sample was eluted using 14 µl or 20 µl of RNAse free water depending on the initial starting material. The total RNA samples

were generally processed directly for cDNA synthesis.

First strand cDNA synthesis

The first strand cDNA synthesis was optimised for subsequent quantitative PCR analysis (QPCR). The cDNA was synthesised in a 20 µl reaction from up to 1 µg of total RNA using the iScript™cDNA Synthesis Kit (BioRad), which uses a mixture of both oligo(dT) and random primers in order to guarantee an unbiased copy of different target sequences. The reagents are kept on ice but the reaction is set up at room temperature as follows:

5X iScript Reaction Mix	4 µl
Template total RNA	14 µl
iScript Reverse Transcriptase	1 µl
Nuclease-free H_2O	Up to 20 µl

The reaction was incubated in a BioRad thermal cycler using the following conditions: 25°C for 5 minutes, 42°C for 30 minutes, 85°C for 5 minutes, and finally 4°C forever. cDNA was diluted to the correspondent of 1 embryo/µl using DEPC H_2O and stored at −20.

Quantitative PCR

To quantify gene expression levels at different developmental stages or at different conditions, QPCR was used to monitor the abundance of PCR products intercalated with a fluorescent dye, SYBR Green. All QPCR reactions were carried out in triplicates or quadtriplicates in 384 well plates (Applied Biosystems) using 2X Power SYBR Green (Applied Biosystems) on a 7900HT Fast Real-Time PCR system (Applied Biosystems). In each well, a 9 µl reaction was set up as follow: 0.55 µl of forward and reverse primers (2.5 pmol/µl), 5 µl of 2X Power SYBR green, 0.4 µl of cDNA (1.12ng) and 3 µl of sterile double-distilled water. The PCR was done as two steps PCR: after an initial denaturating

step at 95°C for 10 min, 40 cycles of 1 min at 60°C and 15 sec at 95°C were used. A final dissociation step was added to ensure a single fragment was amplified.

To ensure accuracy of quantification across different biological samples each mRNA was normalised against an internal, invariant standard. *ubiquitin* (*ubq*) has been previously shown to be expressed at a constant level in early sea urchin development (Nemer *et al.,* 1991) and it has been extensively used with the same efficiently as 18S ribosomal RNA (Oliveri *et at.*, 2002; Revilla-i-Domingo *et al.*, 2007; Materna *et al.,* 2010) as internal standard. *ubq* was thus selected as both the internal standard and quality control in each experiment, while no cDNA samples (H_2O) was used as negative control to assess potential contaminations. The cycle number (Ct) at which the fluorescence crosses a chosen threshold during the exponential phase of the amplification is proportional to the amount of starting material. To ensure technical reproducibility, four replicas were conducted for each combination of cDNA and primers and were then averaged for further calculation and standard deviation was calculated. Experimental points in which replicas had a standard deviation higher than 1 were discarded. To quantify the effect of a perturbation on a given gene the QPCR data were treated as described in Oliveri and Davidson (2006). Briefly, each average replica value was initially normalised to the *ubq* average value for each plate: the Ct of the internal standard is subtracted from the Ct of the gene of interest ($\Delta Ct_{(ubq)}$). After normalisation, then the different experimental conditions are compared: the ΔCt value of the perturbed sample (perturbed-$\Delta Ct_{(ubq)}$) is subtracted from the ΔCt of the control (Control-$\Delta Ct_{(ubq)}$). The cycles-difference (ΔΔCt) between the two samples after normalisation to the internal standard is indicative of the change of level of transcripts caused by the perturbation. ΔΔCt is converted into folds of change using the following formula:

fold change = primer efficiency$^{\Delta\Delta C^t}$.

It has been shown that using our methods of primer design and SYBR Green (Applied Biosystems) the efficiency of amplification of primers range from 1.90 to 1.95 and thus 1.9 has been previously found to be a good approximation and this value has been used in all experiments (Rast *et al*., 2004; Materna and Oliveri, 2008).

Diagrams, graphs and line drawings

Figures were made using Adobe Illustrator CS5 or Adobe Photoshop CS5. Graphs showing temporal and other data were created using Microsoft Excel 2008 and OmniGraphSketcher.

Chapter 3

Regulatory state analysis:

gene expression mapping and the early embryo

3.1. Building an apical organ developmental gene set

Ultimately, the aim of this project is to extend the comprehensive GRN of the sea urchin embryo, to include the neurogenic apical organ. The first step in building a developmental GRN, and the initial starting point of my PhD research, was to identify as many of the regulatory genes as possible that are involved in apical organ development. A comprehensive list of the transcription factors and signalling molecules expressed in the apical domain during development, provides a list of components for the GRN model. However, regulatory genes that are ubiquitously expressed, while important, contribute less to the specification of a particular territory (Materna and Oliveri, 2008) and are generally not included in GRN models. Non-regulatory genes are also valuable, as they can be used to study the downstream transcriptional activation of differentiation genes. They are usually structural or metabolic in nature and reflect the specialised biological function and final specification of the cells types.

Our first aim was to build a comprehensive apical organ gene set (Table 3.1); the resultant list consists of two main parts: confirmed apical organ genes and potential apical organ genes. Confirmed apical organ genes have been previously characterised as being expressed in the apical organ during development, while the potential apical organ genes, represent strong candidate genes identified due to their expression in apical organs or the neurogenic tissues of other organisms.

Table 3.1. Sea urchin apical organ gene set

First two columns show gene name and unique ID. The next three columns show functional data based on a custom ontology published for the sea urchin (Tu *et al.*, 2012). The last column is a reference.

Gene name	SPU identifier	Class. Level 1	Class. Level 2	Class. Level 3	Reference
ac-sc	SPU_028148	Nervous	Nervous_TF	Nervous_TF	Burke et al., 2006
armadillo	SPU_004121	Unkown			Sinigaglia et al., 2013b
bmp 2/4	SPU_000669	Signaling	Signaling_TGFB	Signaling_TGFB_Ligand	Lapraz et al., 2006
cwle4df3	SPU_004702	TF	TF_bHLH	TF_bHLH	Jackson et al., 2010
crim1-like	SPU_027369	Signaling	Signaling_TGFB	Signaling_TGFB_Modulator	Wei et al., 2009
dmy	SPU_000282	Nervous	Nervous_Circadian	Nervous_Circadian	This thesis
delta	SPU_016129	Signaling	Signaling_Notch	Signaling_Notch	Walton et al. 2009
dispatched	SPU_020459	Signaling	Signaling_Hedgehog	Signaling_Hedgehog	Wei et al., 2009
dkk-3	SPU_012506	Signaling	Signaling_WnTFst	Signaling_WnTFst	Wei et al., 2009
dynein heavy chain	SPU_030227	Cytoskeleton	Cytoskeleton_Dynein	Cytoskeleton_Dynein	Sinigaglia et al., 2013b
dynein p33	SPU_015320	Cytoskeleton	Cytoskeleton_Dynein	Cytoskeleton_Dynein	Dunn et al., 2007
e2f3	SPU_006753	TF	TF_Other	TF_Other	Howard-Ashby et al., 2006
egflike	SPU_012362	Adhesion	Adhesion_ReceptorGPCR	Adhesion_ReceptorGPCR	Sinigaglia et al., 2013b
egr/zf60	SPU_015358	TF	TF_ZNF	TF_ZNF	Materna et al., 2006
ets1/2	SPU_002874	TF	TF_Ets	TF_Ets	Francesca Rizzo Thesis
fezl/133	SPU_027491	TF	TF_ZNF	TF_ZNF	Materna et al., 2006
fgf 9/16/20	SPU_006342	Signaling	Signaling_RTK	Signaling_RTK_Ligand	Röttinger et al., 2008
fgfr like-1	SPU_020660	Signaling	Signaling_RTK	Signaling_RTK_Receptor	Bertrand et al., 2009
fgfr1	SPU_020677	Signaling	Signaling_RTK	Signaling_RTK_Receptor	Lapraz et al., 2006
fgfr2	SPU_004747	Signaling	Signaling_RTK	Signaling_RTK_Receptor	Röttinger et al., 2008
nb74	SPU_021429	Cytoskeleton			Max Planck WMISH database
foxd	SPU_016418	TF	TF_Forkhead	TF_Forkhead	Tu et al., 2006
foxg	SPU_009711	TF	TF_Forkhead	TF_Forkhead	Tu et al., 2006
foxj1	SPU_027969	TF	TF_Forkhead	TF_Forkhead	Tu et al., 2006
foxk	SPU_025010	TF	TF_Forkhead	TF_Forkhead	Tu et al., 2006
foxq2	SPU_019002	TF	TF_Forkhead	TF_Forkhead	Tu et al., 2006
frizzled 5/8	SPU_022916	Signaling	Signaling_WnTFst	Signaling_WnTFst	Max Planck WMISH database
gsx/x2	SPU_007599	TF	TF_ZNF	TF_ZNF	Oliveri unpublished
gremlin	SPU_020330	Signaling	Signaling_TGFB	Signaling_TGFB_Modulator	Sinigaglia et al., 2013b
hbn	SPU_023177	TF	TF_Homeo	TF_Homeo	Burke et al., 2006
hes	SPU_006814	TF	TF_bHLH	TF_bHLH	Minokawa et al., 2004
hesc	SPU_021608	TF	TF_bHLH	TF_bHLH	Revilla-i-Domingo et al., 2007
hlf	SPU_006414	TF	TF_bZip	TF_bZip	Howard-Ashby et al., 2006
hmg2	SPU_005572	TF	TF_SoxHMG	TF_SoxHMG	Max Planck WMISH database
hnf6	SPU_016449	TF	TF_Homeo	TF_Homeo	Otim et al., 2004
hp1	SPU_012729	Unkown			Max Planck WMISH database
huntingtin	SPU_011485	Unkown			Max Planck WMISH database
id	SPU_015374	TF	TF_bHLH	TF_bHLH	Oliveri unpublished
kf13/c1/68	SPU_023727	TF	TF_ZNF	TF_ZNF	Materna et al., 2006
lhx2.9	SPU_004021	TF	TF_Homeo	TF_Homeo	Howard-Ashby et al., 2006
meg1	SPU_002300	Unkown			Max Planck WMISH database
mitr	SPU_025486	TF	TF_Homeo	TF_Homeo	Poustka et al., 2007
neurod	SPU_024918	TF	TF_bHLH	TF_bHLH	Burke et al., 2006
neurogenin	SPU_007147	TF	TF_bHLH	TF_bHLH	Burke et al., 2006
nk2.1	SPU_000757	TF	TF_Homeo	TF_Homeo	Takacs et al., 2004
nkx3-2	SPU_013047	TF	TF_Homeo	TF_Homeo	Wei et al., 2011
nodal	SPU_011064	Signaling	Signaling_TGFB	Signaling_TGFB_Ligand	Duboc et al., 2004
obelix	SPU_026467	Unkown			Pinto et al., 2011
ovo/z157	SPU_012448	ZNF	ZNF	ZNF	Materna et al., 2006
pacrg	SPU_004619	Cytoskeleton			Max Planck WMISH database
pacrglike1	SPU_012917	Cytoskeleton			Sinigaglia et al., 2013b
pax2/5/8	SPU_014539	TF	TF_Homeo	TF_Homeo	Lapraz et al., 2006
pax6	SPU_006786	TF	TF_Homeo	TF_Homeo	Burke et al., 2006
pax-c	SPU_000276	TF	TF_Homeo	TF_Homeo	Max Planck WMISH database
pea	SPU_014576	TF	TF_Ets	TF_Ets	Francesca Rizzo Thesis
pitx2	SPU_004099	TF	TF_Homeo	TF_Homeo	Duboc et al., 2005
radial spoke 3	SPU_014801	Cytoskeleton			Dunn et al., 2007
dpn	SPU_003137	Cytoskeleton	Cytoskeleton_Dynein	Cytoskeleton_Dynein	Sinigaglia et al., 2013b
rep3	SPU_023615	Unkown			Max Planck WMISH database
rfx1/2/3	SPU_007611	TF	TF_Other	TF_Other	Neugebauer et al., 2009
rsh p63	SPU_012045	Cytoskeleton			Dunn et al., 2007
rx	SPU_014289	TF	TF_Homeo	TF_Homeo	Burke et al., 2006
sFrp	SPU_026015	Signaling	Signaling_WnTFst	Signaling_WnTFst	Max Planck WMISH database
sFrp1/5	SPU_011271	Signaling	Signaling_TGFB	Signaling_TGFB_Modulator	Poustka et al., 2007
sFrp3/4 r	SPU_004062	Signaling	Signaling_WnTFst	Signaling_WnTFst	Illies et al., 2002
six3	SPU_018908	TF	TF_Homeo	TF_Homeo	Wei et al., 2009
sox/d1	SPU_022820	TF	TF_SoxHMG	TF_SoxHMG	Kenny et al., 1999
sox/b2	SPU_025113	TF	TF_SoxHMG	TF_SoxHMG	Kenny et al., 2003
sox/c	SPU_002603	TF	TF_SoxHMG	TF_SoxHMG	Howard-Ashby et al., 2006
span-like4	SPU_004117	Metalloprotease	Metalloprotease	Metalloprotease	Angerer et al., 2006
sprouty	SPU_025476	Signaling	Signaling_RTK	Signaling_RTK_Modulator	Röttinger et al., 2008
tektin 3	SPU_023618	Cytoskeleton	Cytoskeleton_MicrotubuleAssociated	Cytoskeleton_MicrotubuleAssociated	Dunn et al., 2007
tektin-2	SPU_020728	Cytoskeleton	Cytoskeleton_MicrotubuleAssociated	Cytoskeleton_MicrotubuleAssociated	Dunn et al., 2007
tph	SPU_003725	Nervous	Nervous_NeurotransmitterRelated	Nervous_NeurotransmitterRelated	Yaguchi et al., 2003
tubulin alpha 2	SPU_004143	Cytoskeleton	Cytoskeleton_Tubulin	Cytoskeleton_Tubulin	Dunn et al., 2007
unc-4/4	SPU_024961	Cytoskeleton			Yaguchi et al., 2010
unc4.1	SPU_001739	TF	TF_Homeo	TF_Homeo	Howard-Ashby et al., 2006
univin	SPU_000668	Signaling	Signaling_TGFB	Signaling_TGFB_Ligand	Lapraz et al., 2006
vmd9	SPU_017609	Unkown			Max Planck WMISH database
vitellogenin2	SPU_016052	Oogenesis	Oogenesis	Oogenesis	Max Planck WMISH database
vijv vha pol	SPU_027021	Unkown			Max Planck WMISH database
z167	SPU_015362	TF	TF_ZNF	TF_ZNF	Poustka et al., 2007
z467	SPU_002140	TF	TF_ZNF	TF_ZNF	Materna et al., 2006
z55	SPU_014197	TF	TF_ZNF	TF_ZNF	Materna et al., 2006
zfhx1	SPU_022242	TF	TF_ZNF	TF_ZNF	Yaguchi et al., 2010
zic2	SPU_029583	TF	TF_ZNF	TF_ZNF	Materna et al., 2006

Confirmed apical organ genes

An extensive literature review was undertaken to find genes that are expressed in the apical organ during embryonic development. In addition, genes that are specifically excluded from the apical organ are included in the gene set, as these may act as repressors whose disappearance are required for specification to occur. A number of publications provided a rich source of genes for the apical organ gene set. Many of these are included in the Sea Urchin Genome: Implications and Insights. A special edition in Developmental Biology (2006). Another useful publication is Wei *et al*., (2009) who showed that the transcription factor *six3* operates at the top of an apical organ GRN and affects a large number of genes in an early apical organ gene set. The Max Planck sea urchin WMISH expression database (http://goblet.molgen.mpg.de/eugene/cgi/eugene.pl) is a publicly available resource containing sea urchin gene expression patterns. The database facilitates the search for genes, based on a specific domain of expression, in our case "apical organ".

Potential apical organ genes

The apical organ GRN, in the sea urchin embryo is thought to contain many conserved metazoan elements. A comparative approach, using both vertebrate and invertebrate model organisms, was used to identify apical organ genes that may have escaped previous investigations.

The chick embryo has been an important model for neural development for many years, and in particular, illustrates the importance of FGF signalling in neural induction (Streit *et al*., 2000). From an evolutionary perspective, it would be interesting to see if aspects of FGF signalling and its role in neural development are conserved in echinoderms. The sea urchin apical organ gene set, already includes an FGF ligand gene, *fgf 9/16/20* and one receptor, *fgfr1.* Table 3.2 shows a number of genes involved in chick neural development, the sea urchin homologues if they exist, and what expression data are available. To identify sea urchin homologues of chick neural genes, a BLASTX search of

the sea urchin protein data base (www.spbase.org) was carried out. Sea urchin *soxB1* (*sox2* and *sox3* in chick) is expressed in the entire ectoderm (Kenny *et al.,* 1999), but because regulatory genes with ubiquitous or pan-ectodermal expression usually provide less information at the level of the GRN, I shall not be discussing *soxB1* any further in this thesis. *msx* has been previously characterised in sea urchin and is expressed in the aboral ectoderm (Su *et al.,* 2009) and appears not to be involved in apical organ development. Both *geminin* and *churchil* were characterised by WMISH and are ubiquitously expressed in the sea urchin embryo (data not shown). The remaining genes have yet to be characterised and nothing is known about their expression pattern.

Table 3.2. Common neural genes in chick
The left column lists a number of neural genes in the chick (C Stern, personal communication). The middle and right column are details of the sea urchin homologues if they exist.

Gene Name (Chick)	Gene Name (Sea urchin)	Gene ID
sox2	*soxB1*	SPU_022820
sox3	*soxB1*	SPU_022820
geminin	*geminin*	SPU_005762
erni	no match found	N/A
msx1	*msx (not msx1)*	SPU_022049
churchill	*chuchill1*	Glean_13399
bert	no match found	N/A
sip1	*sip1*	SPU_026620
brm	*brg1(brm)*	SPU_025657
hp1alpha	*leishmanolysin-like*	SPU_002117
hp1gamma	*similar to chromobox homolog 1*	SPU_020586

The cnidarian, *Nematostella vectensis,* forms a swimming larva with an apical organ and tuft, and shares many characteristics in common with sea urchins. In a related project, we have been working in collaboration with Chiara Sinigaglia and Fabian Rentzsch from the Sars Centre for Marine Molecular Biology, University of Bergen, investigating homology between the apical organ in the sea urchin, *S. purpuratus* and the sea anemone, *Nematostella.* Based on the premise of shared homology, genes found in the apical organ of *Nematostella* are likely to also be expressed in the apical organ of sea urchin. A screen carried out in *Nematostella,* recovered 78 genes with expression in the apical organ (C Sinigaglia, personal communication). To identify sea urchin homologues, a BLASTX search of the sea urchin protein database (www.spbase.org) was carried out in conjunction with a reciprocal BLAST search (Rivera *et al.,* 1998). For 3 of the

Nematostella genes, no sea urchin gene could be identified. Several *Nematostella* genes found the same sea urchin gene as its closest match. Out of the remaining 65 genes, only 9 have been properly characterised and their spatial expression patterns known (see appendix B for *Nematostella* gene list and all sea urchin homologues).

Analysis of the gene set

The apical organ gene set consists of over 90 genes. This includes 71 regulatory genes, made up of 51 transcription factors and 20 signalling molecules from 5 different pathways (figure 3.1). Several components of the Wnt signalling pathway were identified in the gene list *e.g. frizzled 5/8, secreted frizzled-related protein 1/5* (*sFRP1/5*). Wnt signalling is already known to play an important role in the development of the apical organ, especially in the early spatial restriction of genes to the animal pole (Range *et al.,* 2013; reviewed by Angerer *et al.,* 2011). As previously mentioned, two components of the FGF signalling pathway were identified in the gene set. FGF signalling is involved in neural induction in a number of phylogenetically distinct animals, including humans and other vertebrates (Stern *et al*., 2005). The majority of the downstream markers fall into two categories; The first are involved in ciliogenesis, for example tubulins and dyneins, and are important structural genes for the formation of cilia; the second are involved in neural differentiation, for example *tph.* Interestingly, our gene set contains many homologues of genes involved in neurogenesis, both in deuterostomes and protostomes. This provides a good foundation for comparative and evolutionary studies into an ancient and conserved neurogenic GRN that could predate the bilaterian split. Whereas this list includes many genes, it represents only a starting point, since more candidate genes will undoubtedly be found as experimentation and analysis progress.

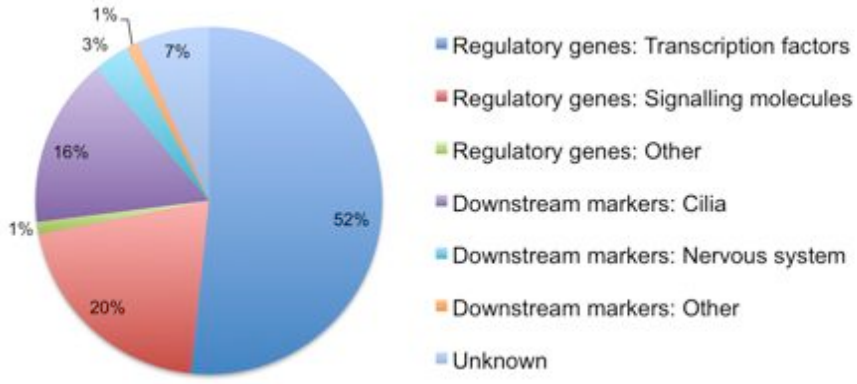

Figure 3.1. Different functional classes of genes found in the apical organ gene set
A graphical representation of the apical organ gene set showing the different functional classes. Nearly three quarters are regulatory genes consisting of either transcription factors (blue) or signalling molecules (red). Interestingly, a large proportion of genes are involved in cilia (purple). Functional class data is based on a custom sea urchin ontology published with the sea urchin transcriptome (Tu *et al.*, 2012).

3.2. Landmark-based gene expression mapping

After identifying as many of the regulatory genes and downstream markers as possible, the next stage in building a GRN and the main focus of my PhD work was characterising gene expression, both in time and space. GRN models describe the regulatory interactions between transcription factors and signalling molecules, which drive the partitioning of the embryo into compartments of specific regulatory state, and the progression of specification within these compartments. Mapping of regulatory gene expression is essential for understanding the dynamic of compartment partitioning, and the identity of its regulatory state. However, accurately characterising gene expression in relation to underlying anatomical and cellular morphology is difficult, as the apical organ shows little or no distinctive morphology at early stages of development. To circumvent this problem, a molecular marker was chosen as a landmark. Working in a similar way to an anatomical or morphological landmark, it provides a reference point to judge the expression of one gene relative to another. A good landmark should fulfil two important criteria; it should be as stable as possible, and should allow for the easy establishment of location. For the purpose of mapping regulatory gene expression in the apical domain, the transcription factor *foxQ2* was identified from the literature as a clear choice for use as a molecular landmark

foxQ2 as an apical organ landmark

foxQ2 is particularly well suited as a landmark for the apical organ. It is expressed specifically in a single domain in the animal hemisphere and never in the vegetal hemisphere (Tu *et al.,* 2006). Additionally, of all the regulatory genes expressed solely in the apical domain, *foxQ2* is transcribed the earliest and remains expressed in the apical domain until the embryo reaches pluteus larva stage (Tu *et al.*, 2006). To use *foxQ2* as a landmark for the apical organ, and to gain a better understanding of its spatial and temporal dynamic, I carried out a high-resolution fluorescent WMISH (figure 3.2). *foxQ2* is a member of the Forkhead family of transcription factors and its expression in the apical organ is highly conserved in invertebrates (Santagata *et al*., 2012; Sinigaglia *et al.,* 2013). The *foxQ2* in sea urchin contains an engrailed homology-1 motif, known to mediate physical interaction with transcriptional corepressors of the TLE/Groucho family and suggests that it could play a role as a repressor in the sea urchin (Yaklichkin *et al.,* 2007).

foxQ2 expression (figure 3.2 U) begins during mid-cleavage stage (6 hours) and increases rapidly until it reaches 1748 transcripts per embryo at hatched blastula stage (18 hours). Transcript levels fluctuate between 1701 to 1877 transcripts per embryo until the start of gastrulation (30 hours). At early gastrula stage, (30-33 hours) there is a dramatic and steep decrease in transcript number to around 1120 transcripts per embryo. Transcripts then remain fairly stable until the end of gastrulation (48 hours). Spatially, *foxQ2* is initially expressed in all mesomeres in the late cleavage embryo (Tu *et al.,* 2006). The expression of *foxQ2* then becomes restricted to the apical domain by the start of blastula stage (figure 3.2 A-F). *foxQ2* expression remains in the apical domain throughout gastrulation, however its expression domain shrinks concurrently with gastrulation (figure 3.2 compare J to L), and subsequently remains expressed until the pluteus larva, when it begins to be down regulated. In conclusion, *foxQ2* is remarkably stable, and our results confirm that *foxQ2* is expressed in the apical domain and in no other region of the embryo. These high-resolution data strongly support the choice of *foxQ2* as a suitable landmark for mapping the sea urchin apical organ.

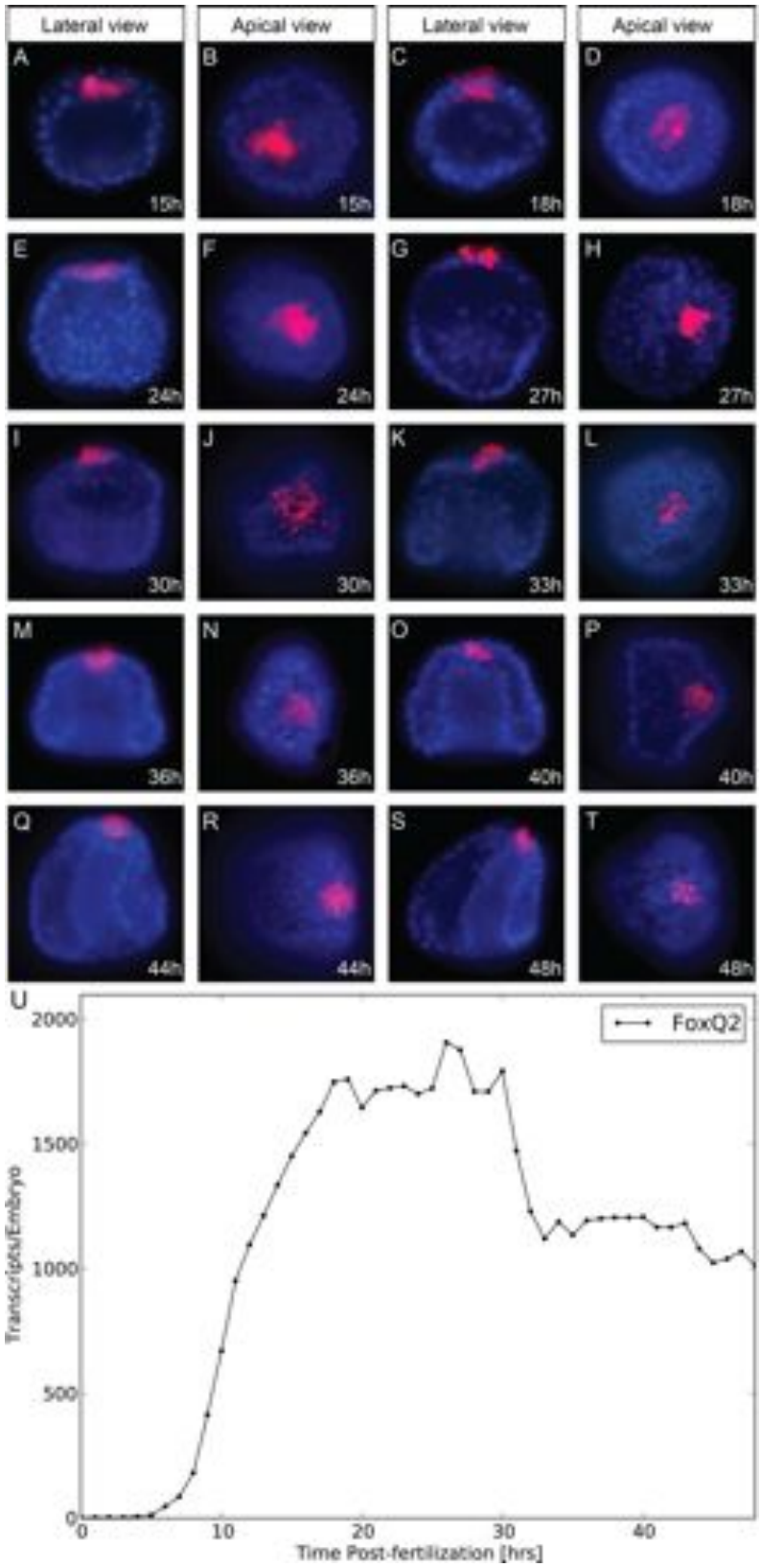

Figure 3.2. High-resolution temporal and spatial expression data for *foxQ2*

(A-T) Single fluorescent WMISH of *foxQ2* (red) at 3 to 4 hour intervals. *foxQ2* is expressed in only the apical domain during development. Nuclei are labeled blue with DAPI. Embryos are presented in lateral and apical views with the oral side to the right. (U) High-resolution temporal expression profile of *foxQ2* as revealed by nanostring data (Materna *et al.,* 2010).

Creating apical view cellular maps of different developmental stages

Displaying gene expression data and relating gene expression to specific embryonic territories is a difficult task. To overcome this Davidson, (2006) has used widely available schematic sections of sea urchin embryos at different stages of development, colour coding embryonic territories or gene expression to make them clear. These schematic sections are taken from a lateral perspective, and while providing a useful resource, prove difficult to accurately depict gene expression in the apical domain, highlighting the need for a schematic representation of the sea urchin embryo from an apical domain perspective. I set out to create a realistic diagram that represents, at a cellular level, a standard embryo at different developmental time points when viewed from an apical perspective. Four stages of development were chosen to make cellular maps and were picked to give a broad coverage of development: (1) hatched blastula, (2) mesenchyme blastula. (3) mid-gastrula and (4) late gastrula.

To start, a single fluorescent WMISH was carried out on embryos representing these four stages, using *foxQ2* as a probe, stained with cy3, and nuclei counterstained with DAPI. The embryos were placed in 50% glycerol, below a coverslip and viewed under an epi-fluorescence microscope. A 20-200 microliter tip was used to manipulate the coverslip and indirectly manoeuvre the embryos to ensure the apical domain faced the objective with the *foxQ2* expression centred. The microscope was then focused on the very top of the apical organ and a short Z-series of images were taken using both DIC optics and with the DAPI channel, at different focal planes, with a 40X objective (figure 3.3 B). These images were arranged in Adobe Photoshop (figure 3.3 C-E) and the DAPI and DIC superimposed for each focal plane, then each cell was marked using an electric Wacom tablet and pen; by using the different focal planes it was easier to identify the true cells. The outline of each cell was then carefully traced and used to produce a cellular map (figure 3.3 F). The image was then transferred to Adobe Illustrator and adjusted to produce the final graphic of the cellular map (figure 3.3 G). This process was then repeated for the remaining three stages (figure 3.4). The cellular map that was created for hatched blastula stage (18h) embryos can in fact also be used to represent earlier hatching blastula stage (15h) embryos (figure 3.4), due to the fact the cell number does not change between these two stages (Cameron *et al.,* 1987).

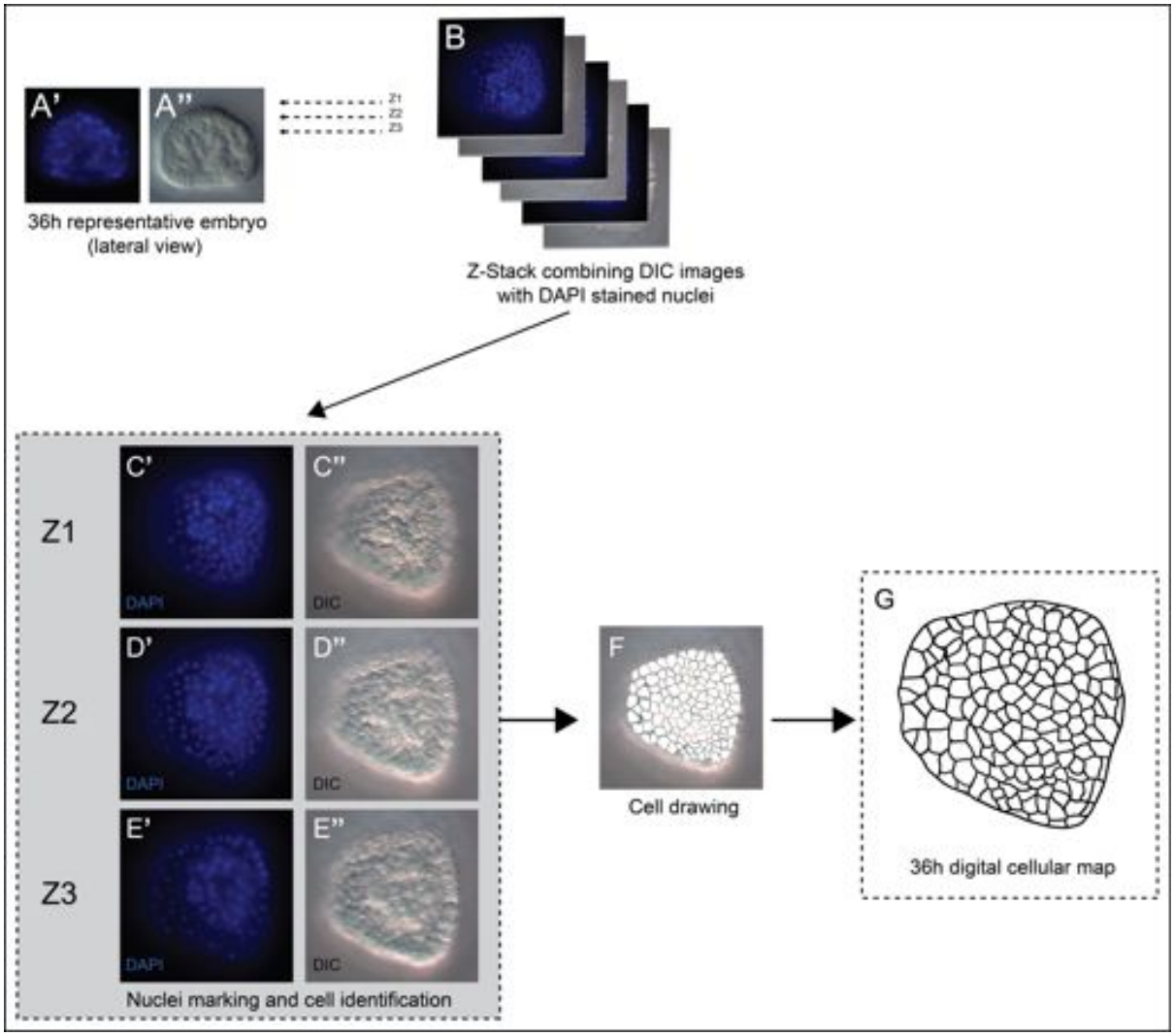

Figure 3.3. Creating an apical view cellular map

(A) DIC and DAPI stained images of a lateral view representative mid-gastrula embryo (36 hour). (B) A series of Z-stack images was taken at different focal planes through the apical domain of the embryo. (C) Each Z-stack slice is comprised of a DAPI and DIC image and was superimposed using photoshop. Individual cells were then identified and marked. (F) Once the cells have been identified the cell outlines were traced. (G) A completed apical view cellular map representing the apical domain of a mid-gastrula embryo. Nuclei are labeled blue with DAPI.

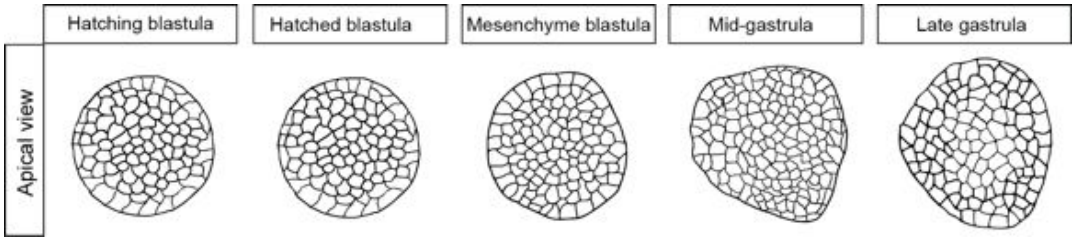

Figure 3.4. Apical view cellular map for different developmental stages

Apical view cellular maps for five different developmental stages. Oral ectoderm on the right hand side.

Once the cellular maps had been created for all stages, the next step was to map the expression of *foxQ2* onto the new cellular maps. Embryos fluorescently stained for *foxQ2* were imaged and imported into Adobe Photoshop. DAPI and the fluorescent expression data was superimposed and the domain of expression was traced (figure 3.5 A,D). The number of cells positive for *foxQ2* was counted from both a lateral and apical view (figure 3.5 C,F; number of embryos counted n=113; see appendix B for number of embryos counted for each gene). By combining all this information, it was possible to come up with a representative embryo that best shows the expression of *foxQ2 (*figure 3.5 B and C) or any other gene for that stage. The data from each stage is then combined to give a representation of the spatial dynamics of *foxQ2* throughout development (figure 3.6).

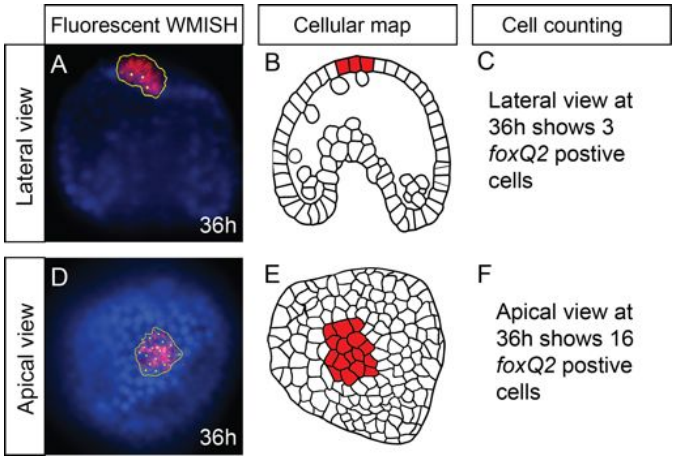

Figure 3.5. Mapping *foxQ2* expression onto apical view cellular maps
(A) *foxQ2* positive (red) cells marked (yellow) in a lateral view of a mid-gastrula stage (36 hour). (B, C) *foxQ2* positive cells counted and the information superimposed on to a lateral view mid-gastrula cellular map. (C) *foxQ2* positive (red) cells marked (yellow) in a apical view of a mid-gastrula stage (36 hour). (E, F) *foxQ2* positive cells counted and the information superimposed on to a apical view mid-gastrula cellular map. Nuclei are labeled blue with DAPI.

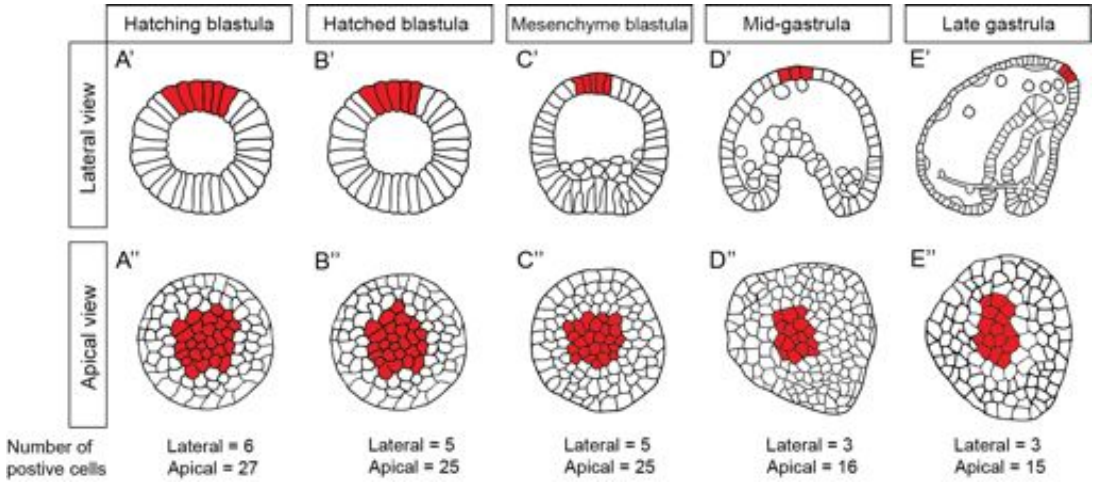

Figure 3.6. Cellular maps for different developmental stages showing *foxQ2* expression
(A-E) Lateral and apical views showing *foxQ2* (red) in the apical domain at five developmental stages. Oral ectoderm on the right hand side. Below the cellular maps is the number of *foxQ2* positive cells observed in both lateral and apical views. See appendix B for details of the number of embryos counted for these experiments.

Integration of *foxQ2* high-resolution temporal data, spatial data and cellular maps

High-resolution, hourly, temporal expression data already exists for *foxQ2* and other genes from the NanoString nCounter, an RNA counting device. This data is publicly available (http://vanbeneden.caltech.edu). and has been used in this thesis together with temporal data gathered by QPCR (for further details about the high-resolution temporal expression data or details of the NanoString nCounter see Materna *et al*., 2010). This was augmented with high-resolution spatial data from fluorescent WMISH carried out at approximately 3 hour intervals (figure 3.2). For each of the five cellular maps (figure 3.6), an in depth study of the relevant stage was carried out, accompanied with lateral and apical view cell counting. With these newly available data, it is now possible to combine and integrate this information to give a unique and highly detailed view of the *foxQ2* expression during sea urchin development (figure 3.7). Furthermore, the number of *foxQ2* transcripts per cell can be calculated by using the fact that *foxQ2* is expressed in a single territory through development and the number of *foxQ2* positive cells is known, as well as the number of individual transcripts per embryo at each time point, (figure 3.7 - green boxes).

Tu *et al.,* (2006) show that at cleavage stage, *foxQ2* is expressed in the mesomeres and becomes restricted to the apical domain by hatched blastula stage. I can now elaborate and refine this information. It is clear that already by hatching blastula stage, *foxQ2* is restricted to a circle of roughly 27 cells (n=16; figure 3.2 A,B; figure 3.7 A). The number of transcripts of *foxQ2* at the same stage is 1451 transcripts per embryo, therefore an estimated ~54 transcripts per cell can be calculated. Over the next three hours, the number of transcripts per embryo increases to 1748 by hatched blastula stage, while the number of cells that express *foxQ2* decreases slightly to 25 (n=22), resulting in an estimated 70 *foxQ2* transcripts per cell (figure 3.7 B). From hatched blastula stage, until the start of gastrulation, *foxQ2* expression is very stable, both in number of transcripts per cell and number of positive cells. A third phase of expression begins after the start of gastrulation. Between 30 and 33 hours there is a decrease in *foxQ2* transcripts in the sea urchin embryo (figure 3.7 - black arrow). This however, is concurrent with a reduction in actual cells that express *foxQ2* from 25 to 15 (n=16), meaning that although the number of transcripts fall from 1792 to 1120, the actual number of transcripts per cell remains constant at around 70. The restriction of *foxQ2* occurs along the oral-aboral axis and clears from the aboral side, thus converting a loose 5 cell by 5 cells arrangement to a 3 cell by 5 cell arrangement (compare figure 3.2 J to L; Yaguchi *et al.,* 2011). The clearance from the aboral side of the apical domain is interesting, as it is the location of the serotonergic neurons. This raises the interesting possibility, that *foxQ2* acts a repressor of neuronal differentiation and its expression must clear from the aboral apical domain at gastrulation, to allow normal neuronal differentiation. I have extended the analysis of *foxQ2* beyond the usually spatial and temporal expression profiles, to an understanding of the actual number of cells that express *foxQ2* and the number of transcripts per cell. Furthermore, combining and integrating these data has provided us with an even more useful landmark for mapping the apical organ through development.

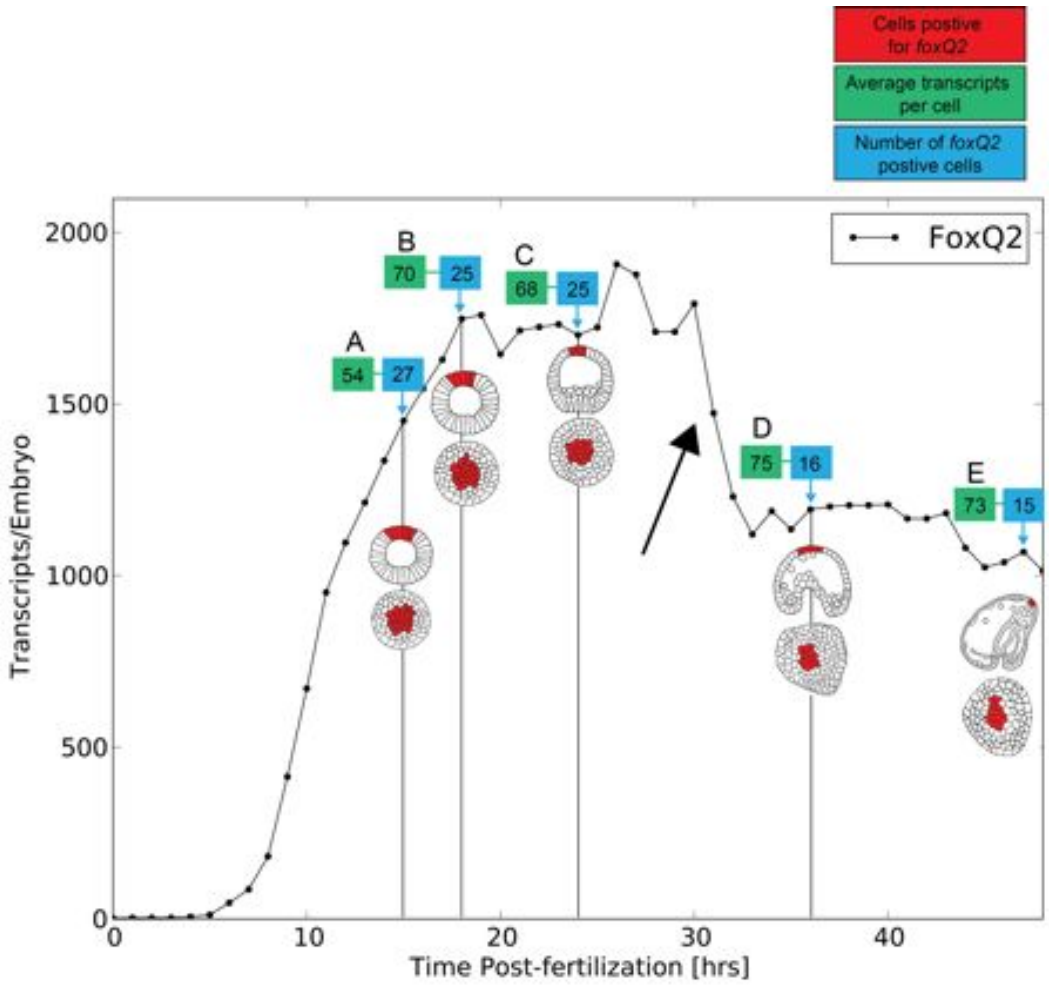

Figure 3.7. Integration of *foxQ2* expression data

I have combined high-resolution temporal data (Materna *et al.,* 2010) with cellular maps showing *foxQ2* (red) spatial expression. For each developmental stage the number of *foxQ2* positive cells is shown (blue) and the average number of transcripts per cell (green). Developmental stages shown are: (A) hatching blastula, (B) hatching blastula, (C) mesenchyme blastula, (D) mid-gastrula and (E) late gastrula. Oral ectoderm on the right hand side. After gastrulation (30 hours) a reduction in *foxQ2* expression (black arrow) can be seen.

3.3 Combinatorial gene expression studies of the apical domain at hatching blastula stage

The remainder of this chapter is dedicated to my analysis of the apical domain regulatory states. Here, I focus my efforts on the early embryo and study two developmental stages: (1) The hatching blastula, which occurs at 15 hours, just after the embryo exits the fertilisation membrane. (2) The hatched blastula, which arises at 18 hours and is characterised by the embryo swimming freely. Over the next two sections, I describe the results from a series of detailed gene expression studies. Genes were investigated individually by double fluorescent WMISH, with the apical organ landmark *foxQ2,* to identify their position relative to the apical domain. In many cases these results were augmented with counting the number of cells that express a given gene, additional double fluorescent WMISH with other apical organ genes, and tracing the outlines of gene expression to allow more accurate comparisons. This data was then combined and integrated into gene expression cellular maps. The starting point was to identify genes that are expressed early in the apical domain, based on high-resolution Nanostring (Tu *et al,* 2010) and QPCR quantitative data (this thesis). As shown in figure 3.8, a small number of genes are expressed early in the apical organ domain and these are described in detail, to help determine the regulatory state of the apical domain in the early embryo.

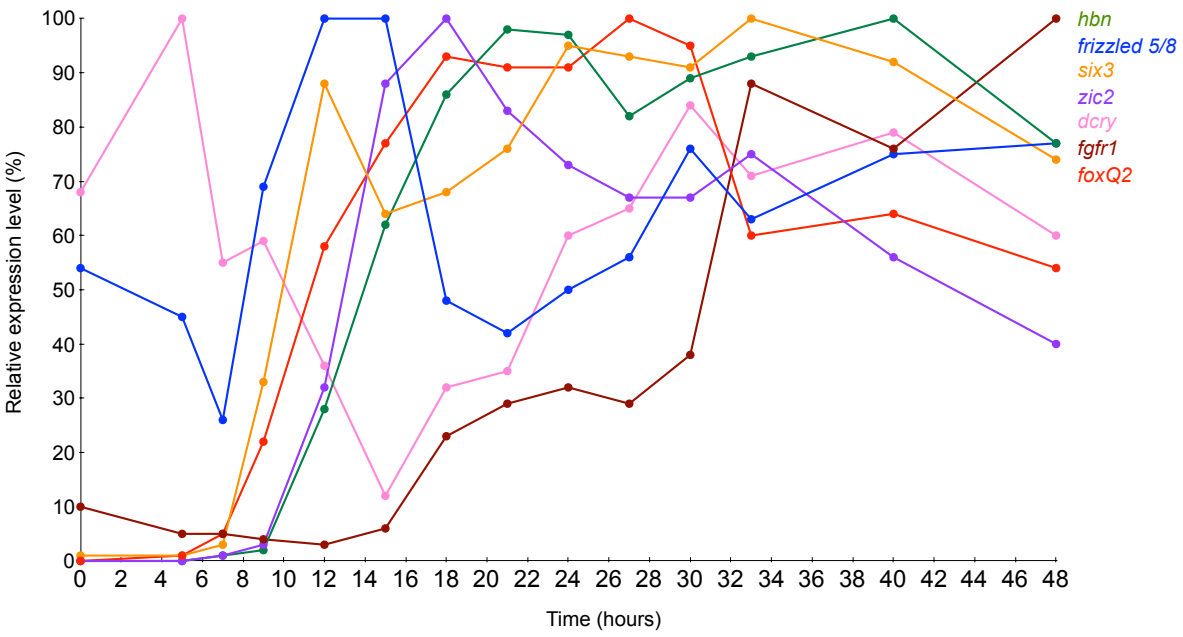

Figure 3.8. Temporal expression profiles of apical organ genes in the early embryo
Genes that appear in the apical domain by-hatched blastula stage (18 hours). Expression levels are given as a fraction of peak expression. *foxQ2, hbn, six3,* and *zic2* data were quantified using Nanostring nCounter (Materna *et al.,* 2010). *frizzled 5/8, dcry* and *fgfr1* were quantified using QPCR (see Materials and methods; see appendix B for actual number of transcripts).

Expression of *six3*

six3 is a member of the homeodomain family of transcription factors. The apical/ anterior expression of *six3* is highly conserved across bilaterians (Steinmetz *et al*., 2010) and cnidarians (Sinigaglia *et al*., 2013). Expression of *six3* has previously been studied in two species of sea urchin, *P. lividus* (Poustka *et al*., 2007) and *S. purpuratus* (Wei *et al*., 2009). The *S. purpuratus* homologue of *six3* shows high conservation to *H. sapiens six3* in the homeodomain (98% identity), the six domain (91%) and the groucho interaction domain (71%). Wei *et al*., (2009) showed that *six3* is expressed in the animal hemisphere during late cleavage stage, in the apical domain by hatched blastula stage and then in two rings, one near the periphery of the apical domain and the other in the endomesoderm during mesenchyme blastula stage. In order to better understand the expression of *six3* in the apical domain, I re-examined its expression in more detail.

six3 expression (figure 3.8 - orange line) begins almost simultaneously with *foxQ2* (figure 3.8 - red line) but increases in a more dramatic fashion until it reaches an initial

peak of 1753 transcripts per embryo at early blastula stage (12 hours), after which it is slightly reduced to 1273 transcripts per embryo by hatching blastula stage (15 hours). At this stage, *six3* expression is seen only in the apical domain when viewed from a lateral perspective (figure 3.9 D'). Counting the number of positive nuclei using DAPI counterstaining, shows that *six3* is expressed across 11 cells at its widest point (number of embryos n=14). Shifting the focal plane to the centre of the embryo, *six3* expression appears as two bilateral blocks with the central part of the apical domain showing little or weak expression (figure 3.9 E'), suggesting that *six3* is not expressed as a uniform large disc of cells at the animal pole, but rather, as a ring. To help clarify the expression pattern, I rotated the embryos and observed them from an apical perspective. This showed that *six3* is not expressed as a uniform disc, but rather as a ring in the apical domain (figure 3.9 F'). In contrast, Poustka *et al.,* (2007) previously showed that *six3* cleared from the central apical domain and formed a ring-like structure much later, at mesenchyme blastula stage. Furthermore, *six3* is not expressed as a true ring, but rather in a horseshoe pattern that is open on one side (figure 3.9 F). Without the use of oral-aboral markers it is difficult to predict if the 'opening' of the horseshoe is situated on the oral or aboral side. Data published by Wei *et al.,* (2009) shows that *six3* is expressed in the oral ectoderm at late gastrula, assuming no changes in the side of the clearance of expression, this suggests that *six3* is expressed in the oral apical domain and cleared from the aboral apical domain even at this earlier stage. In order to understand the exact location of *six3* in the apical domain, I carried out a double fluorescent WMISH with the apical organ landmark *foxQ2* (figure 3.9 C). *six3* shows no co-expression with *foxQ2* and is situated in an outer ring of cells in a region that surrounds and borders the central apical domain, marked by *foxQ2.*

To investigate *six3* expression further, and to gain a better understanding of its relative position within the apical domain, I carried out a double fluorescent WMISH with another gene expressed in the apical domain at this stage, *frizzled 5/8,* a receptor in the Wnt signalling pathway discussed in more detail later in this section. *frizzled 5/8* expression is seen only in the apical domain (figure 3.9 D'',E''). Rotating the embryos and viewing from an apical perspective shows that *frizzled 5/8* is expressed as a compact disc of cells in the apical domain (figure 3.9 F''). *six3* is clearly expressed in a larger domain than *frizzled 5/8* (figure 3.9 D-F). The outer edges of *frizzled 5/8* are co-

expressed with *six3* but there is no co-expression in the centre (figure 3.9 E'''). Interestingly, *six3* co-expression appears stronger on one side of *frizzled 5/8* (figure 3.9 E''' white arrow) but more faintly on the other side (figure 3.9 E''' turquoise arrow). This is seen more clearly when viewed from an apical perspective. *six3* is not co-expressed with the majority of *frizzled 5/8* although there is strong co-expression between *six3* and one edge of *frizzled 5/8* (figure 3.9 F''' white arrow) and weaker co-expression on the other edge (figure 3.9 F''' turquoise arrow).

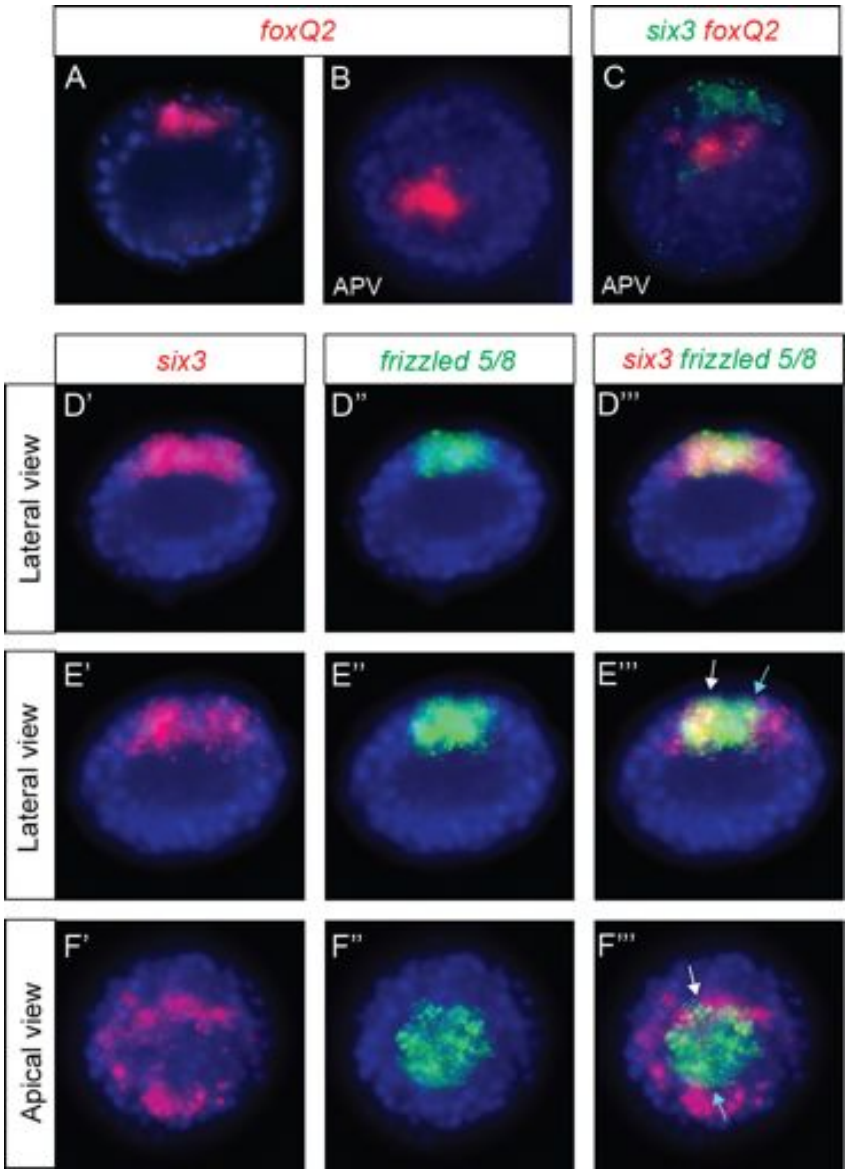

Figure 3.9. Expression analysis of *foxQ2, six3* and *frizzled 5/8* at hatching blastula stage
(A,B) Single fluorescent WMISH of *foxQ2*. (C) Double fluorescent WMISH of *six3* and *foxQ2*. (D-E) Double fluorescent WMISH of *six3* and *frizzled 5/8,* showing each channel individually and merged. DAPI stained nuclei are blue. Unless otherwise specified embryos are presented in a lateral view with the apical domain at the top. Apical view (APV). See main text for descriptions of arrows.

Expression of *frizzled 5/8*

frizzled genes encode integral membrane proteins that function as receptors for secreted Wnt proteins and have been identified in a diverse range of animals, from sponges to humans. Frizzled proteins are defined by conserved structural features, including seven hydrophobic domains and a cysteine-rich ligand-binding domain. Together with their Wnt ligands, Frizzled receptors regulate diverse cellular processes, ranging from cell fate decisions and control of proliferation to cytoskeletal rearrangements, cell adhesion and apoptosis (Huang and Klein, 2004). *Frizzled 5/8* was first characterised in the Mediterranean sea urchin, *P. lividus* by Croce *et al.,* (2006) and showed strong amino acid similarities to Frizzled 5 and Frizzled 8 receptors of vertebrates, suggesting that the sea urchin *frizzled 5/8* is an ortholog of an ancestral *frizzled 5/8* that was subsequently duplicated later during evolution. *frizzled 5/8* is ubiquitously expressed during early cleavage stages and becomes restricted to the animal hemisphere by the end of cleavage stage and the apical domain by hatched blastula stage. At mesenchyme blastula stage, *frizzled 5/8* begins to be expressed in a second domain that forms a ring of cells in the vegetal plate. As development continues through gastrulation, *frizzled 5/8 is* detected in the apical domain and at the tip of the archenteron (Croce *et al*., 2006; Range *et al*., 2013). I now present a more detailed re-examination of *frizzled 5/8* expression in the apical domain.

frizzled 5/8 expression (figure 3.8 - blue line) is maternal, with zygotic expression visible at mid-cleavage stage (8 hours). Expression increases rapidly before the start of *foxQ2* expression (figure 3.8 - red line) reaching 927 transcripts per embryo by the end of cleavage stage (9 hours) and reaching a peak of 1332 transcripts per embryo by hatching blastula (15 hours). At this stage, *frizzled 5/8* expression is seen only in the apical domain when viewed from a lateral perspective (figure 3.9 D,E and figure 3.10 A). Counting the number of positive nuclei using DAPI counterstaining shows that *frizzled 5/8* is expressed across 8 cells in the apical domain, compared to 6 cells of *foxQ2* (n=32). In order to determine the exact cells expressing *frizzled 5/8* relative to the landmark *foxQ2*, I carried out a double fluorescent WMISH. *frizzled 5/8* is expressed in the apical domain in a region that is larger than *foxQ2* (figure 3.10 A). *frizzled 5/8* and *foxQ2* show full co-expression in the central apical domain, however, *frizzled 5/8* is also expressed in

an additional cell row outside the central apical domain marked by *foxQ2.* Rotating the embryos and viewing from an apical perspective shows that the smaller *foxQ2 is* expressed within the larger *frizzled 5/8* (figure 3.9 B). Comparing the outlines of expression, shows that on two sides of *foxQ2* there is a cell row that expresses just *frizzled 5/8* (figure 3.10 B''). Examination of confocal microscopy confirmed these results and show that in both lateral (figure 3.10 C) and apical perspectives (figure 3.10 D) *frizzled 5/8* is expressed in a larger domain than *foxQ2* and that two separate regulatory states exist.

As discussed above, *six3* is not co-expressed with *foxQ2.* In contrast, *six3* is co-expressed with the outer edges of *frizzled 5/8* (compare figure 3.9 F with C). With the knowledge that *frizzled 5/8* is expressed in a larger domain than *foxQ2,* the above results can be explained quite simply. *six3* is expressed in a horseshoe pattern in cells directly abutting, but never overlapping, the central apical domain marked by the presence of *foxQ2.* On the other hand, *frizzled 5/8* is expressed in the apical domain in a slightly larger region than *foxQ2* and therefore is co-expressed with *six3* in the cell row immediately adjacent and outside of the *foxQ2* positive central apical domain. What is more complicated to understand, is the seemingly stronger co-expression of *six3* along one side of *frizzled 5/8,* suggesting the possible existence of lateral asymmetry.

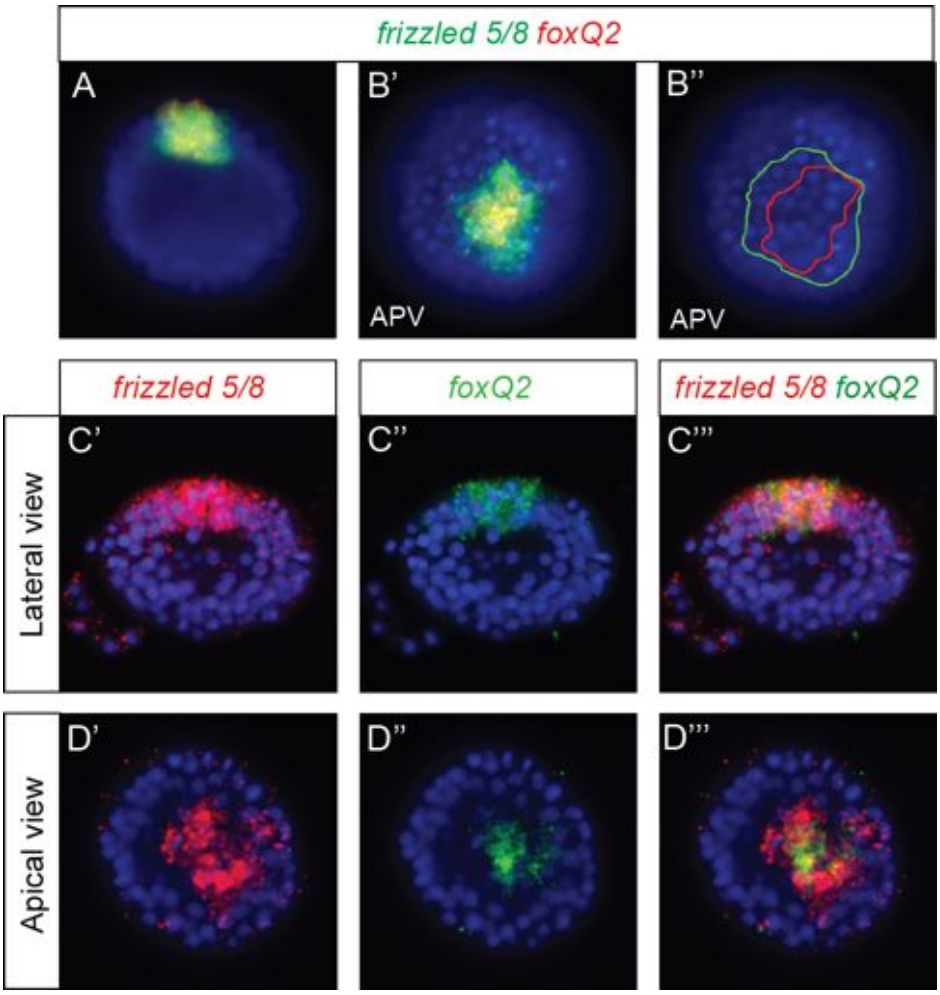

Figure 3.10. Expression analysis of *frizzled 5/8* at hatching blastula stage
(A,B) Double fluorescent WMISH of *frizzled 5/8* and *foxQ2,* (B'') Outline of gene expression of B'. (C,D) Double fluorescent WMISH of *frizzled 5/8* and *foxQ2* (images are full projections of confocal slices). DAPI stained nuclei are blue. Unless otherwise specified embryos are presented in a lateral view with the apical domain at the top. Apical view (APV). See main text for descriptions of arrows.

Expression of *hbn*

Another gene that is expressed early in the apical domain is *hbn* (*homeobrain*), a member of the paired-class homeobox family of transcription factors. *hbn* is expressed in the anterior dorsal head primordia during early development in *Drosophila* (Walldorf *et al*., 2000) and in the anterior neurogenic domains of the brachiopod, *Terebratalia transversa* (Santagata, 2012). *hbn* was initially characterised by Howard-Ashby *et al.,* (2006) and Burke *et al.,* (2006) and shows closest homology to the *hbn* of *Drosophila.* In the sea urchin, *hbn* is expressed in the apical domain from hatched blastula stage until

late gastrula stage (Howard-Ashby *et al.,* 2006) and in the oral ganglia and scattered cells in the apical organ of pluteus larvae (Burke *et al*., 2006). A more detailed analysis was carried out by Wie *et al*., (2009) showing that *hbn* and *foxQ2* are co-expressed in the same domain at mesenchyme blastula stage, and then at gastrula stages *hbn* forms a ring around *foxQ2.* To confirm this dynamic expression in the apical domain, I re-examine the spatial expression of *hbn.* .

hbn expression (figure 3.8 - green line) begins 2 to 3 hours after the activation of *foxQ2* (figure 3.8 - red line) but follows the same steep initial incline reaching 204 transcripts per embryo by early blastula stage (12 hours), and 450 transcripts per embryo by hatching blastula stage (15 hours). *hbn* expression can be seen in 6 cells (n=5) across the apical domain, when viewed from a lateral perspective (figure 3.11 A). An apical view of embryos stained with both *foxQ2* and *hbn* show that *hbn* and *foxQ2* are co-expressed in the same domain (figure 3.11 B). However, not every cell that expresses *foxQ2* also expresses *hbn* (figure 3.11 B white arrow) and likewise, not every cell that expresses *hbn* expresses *foxQ2* (figure 3.11 B turquoise arrow). The fact that both *hbn* and *foxQ2* are expressed in same number of cells (n=5) in the apical domain suggest that they are truly co-expressed and a natural cell to cell variability results in single cells expressing only one of the two genes.

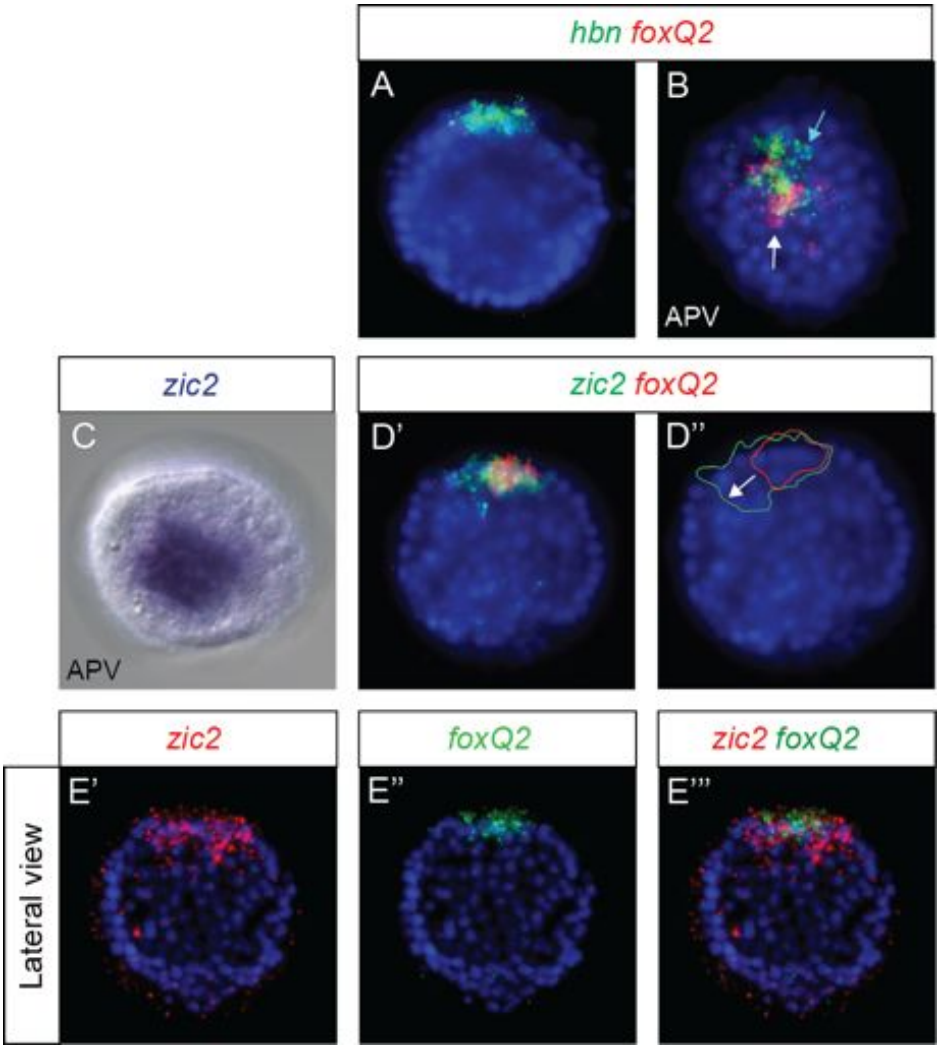

Figure 3.11. Expression analysis of *hbn* and *zic2* at hatching blastula stage
(A) Single fluorescent WMISH of *hbn* and (B) Double fluorescent WMISH of *hbn* and *foxQ2*. (C) DIC image of a NBT/BCIP WMISH of *zic2.* (D) Double fluorescent WMISH of *zic2* and *foxQ2,* (D'') outline of gene expression of D'. (E) Double fluorescent WMISH of *zic2* and *foxQ2* (images are full projections of confocal slices). DAPI stained nuclei are blue. Unless otherwise specified embryos are presented in a lateral view with the apical domain at the top. Apical view (APV). See main text for descriptions of arrows.

Expression of *zic2*

Another selected apical organ gene is *zic2. zic* genes are members of the *gli/glis/nkl/zic* transcription factor super-family and are characterised by the presence of five tandemly repeated C2H2 zinc finger DNA binding domains (Aruga *et al*., 1994). In vertebrates, many *zic* genes share a common expression pattern in the neuroectoderm and specific regions of the developing nervous system including the neural plate and anterior neural

folds in *Xenopus* (Nakata *et al*., 1998). In sea urchin a single *zic2* gene was characterised by Materna *et al.,* (2006) and is expressed in the apical domain at hatched blastula stage and at late gastrula stage.

zic2 expression (figure 3.8 - purple line) is similar to *hbn* (figure 3.8 - green line) during the early stages of development. Like *hbn* it begins 2 to 3 hours after the activation of *foxQ2* (figure 3.8 - red line) and follows the same steep initial incline reaching 160 transcripts per embryo by early blastula stage (12 hours), and 447 transcripts per embryo by hatching blastula (15 hours). At this stage, *zic2* expression is seen only as a disc of cells in the apical domain (figure 3.11 C) and is expressed across ~7 cells in the apical domain (n=13). Double fluorescent WMISH of *zic2* and *foxQ2* shows that *zic2* is co-expressed with *foxQ2* in the central apical domain but is also expressed outside *foxQ2* on one side (figure 3.11 D white arrow). A more detailed analysis of *zic2* and *foxQ2* was undertaken using confocal microscopy (figure 3.11 E). Projections of individual confocal slices confirm that *zic2* is expressed in the entire *foxQ2* domain but also in a few extra cells outside *foxQ2*. Taking these results together it suggests that *zic2* is expressed as a uniform disc that is larger and eccentric relative to *foxQ2*.

Cellular maps and summary

In this section, I have used a series of double fluorescent WMISH to identify the position of several regulatory genes in the apical domain at hatching blastula stage. All these data were combined, integrated and subsequently overlaid onto cellular maps. These maps provide the tools to begin to analyse the regulatory states that exist at each developmental stage (see Discussion). Figure 3.12 shows cellular maps for the four regulatory genes studied at hatching blastula stage. The study shows that the so called apical domain is actually formed by several cellular domains marked by unique combinations of regulatory gene expression as early as hatching blastula stage. A central domain marked by our landmark, *foxQ2* and *hbn. frizzled 5/8* forms a larger domain around the *foxQ2* central apical domain and finally *six3* forms a horseshoe domain that is not co-expressed with *foxQ2.*

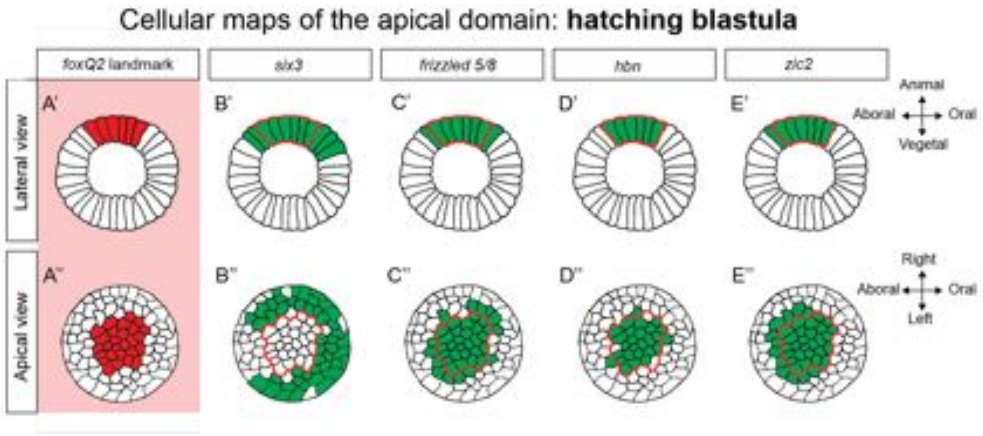

Figure 3.12. Cellular maps of gene expression at hatching blastula stage
Lateral and apical view of hatching blastula stage cellular maps. (A) *foxQ2* expression (red). (B-E) Expression of other regulatory genes (green) with outline of *foxQ2* (red line).

3.4 Combinatorial gene expression studies of the apical domain at hatched blastula stage

Although only three hours elapses between hatching blastula stage (15 hours) and hatched blastula stage (18 hours), the complexity of gene expression increases. In the following section, I expand my analysis to consider two further genes that have begun to be expressed by hatched blastula stage: *fgfr1* and *dcry.* Somewhat unexpectedly, taking into account just two additional genes, uncovers a higher complexity than predicted into the regulatory state and patterning of the apical organ.

Expression of *six3*

six3 expression (figure 3.8 - orange line) increases slightly to 1340 transcripts per embryo by hatched blastula stage (18 hours). In approximately half of the embryos studied, *six3* expression can now be seen in the vegetal plate as well as the apical domain (figure 3.13 D white arrow). Counting the number of positive nuclei shows that *six3* is expressed across 11 cells (n=9) in the apical domain. Double *in situ* with *foxQ2*

show that *six3* is expressed in the apical domain in a larger region than *foxQ2* (figure 3.13 C,D). Consistent with what was described in hatching blastula stage and as a result of the orientation with which the embryo is observed, *six3* is expressed either equally on both sides of *foxQ2* (figure 3.13 C) or unequally on one side of *foxQ2* (figure 3.13 D) seen clearly by comparing the outlines of gene expression (figure 3.13 D'' white arrow).

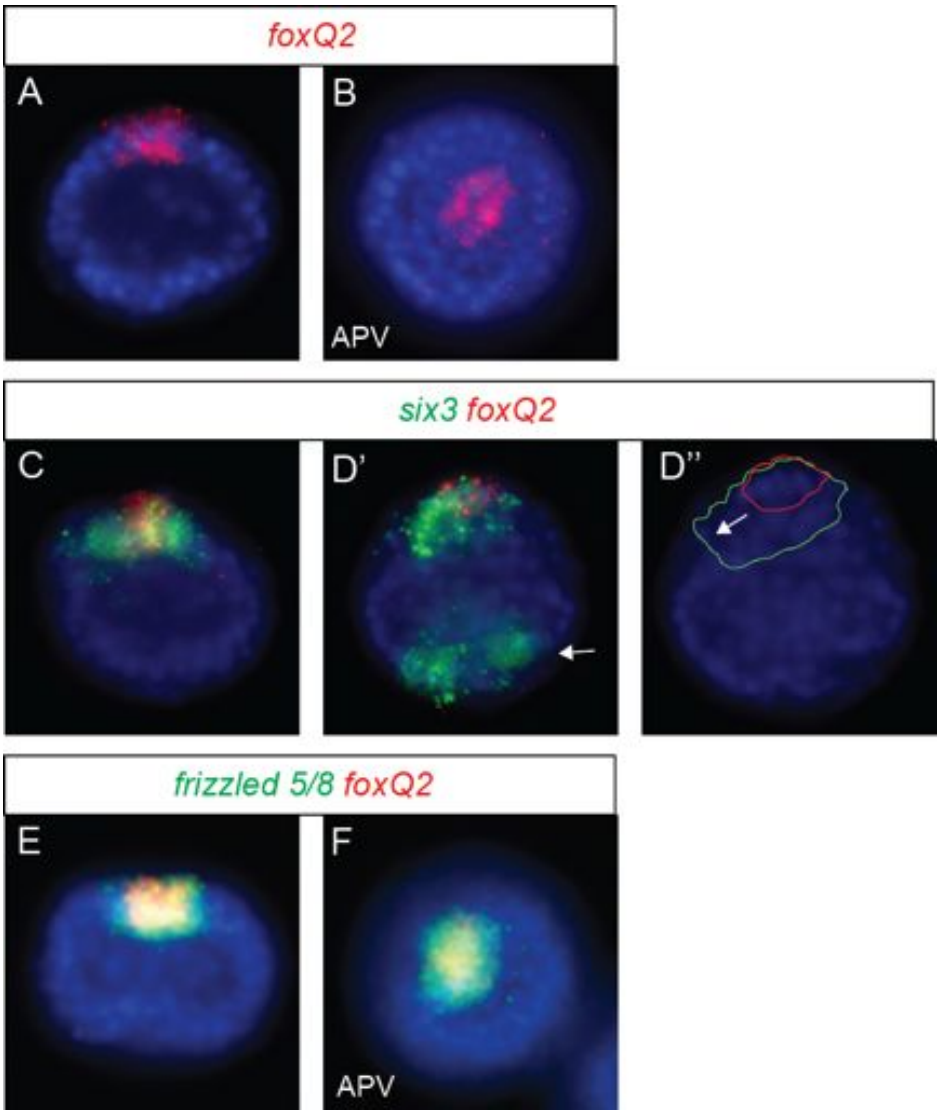

Figure 3.13. Expression analysis of *foxQ2, six3* and *frizzled 5/8* at hatched blastula stage
(A,B) Single fluorescent WMISH of *foxQ2*. (C,D) Double fluorescent WMISH of *six3* and *foxQ2*, (D'') outline of gene expression of D'. (E,F) Double fluorescent WMISH of *frizzled 5/8* and *six3.* DAPI stained nuclei are blue. Unless otherwise specified embryos are presented in a lateral view with the apical domain at the top. Apical view (APV). See main text for descriptions of arrows.

Expression of *frizzled 5/8*

frizzled 5/8 expression (figure 3.8 - blue line) dramatically falls to 644 transcripts per embryo by hatched blastula (18 hours). At this stage, *frizzled 5/8* expression is seen only in the apical domain. As shown by a lateral view (figure 3.13 E), *frizzled 5/8* is expressed across 8 cells (n=10) in the apical domain and double fluorescent WMISH with *foxQ2* (figure 3.13 E) reveals full co-expression in the central apical domain, marked by *foxQ2*, however, *frizzled 5/8* is also expressed in an additional cell row on either side of the *foxQ2* domain. An apical view shows that *foxQ2* and *frizzled 5/8* are expressed in two concentric discs, with the smaller *foxQ2* expressed within the larger *frizzled 5/8* (figure 3.13 F). Compared to the previous stage, *frizzled 5/8* is now expressed in a single extra cell row around the whole of *foxQ2* (compare figure 3.13 F to figure 3.10 B).

Expression of *hbn* and *dcry*

Temporal expression profile shows an increase of *hbn* (figure 3.8 - green line) from 450 at hatching blastula stage (15 hours) to 621 transcripts per embryo at hatched blastula stage (18 hours). *hbn* is expressed only in the apical domain and in a similar region to *foxQ2* at hatched blastula stage (figure 3.14 A). Counting the number of positive cells shows that *hbn* and *foxQ2* are both expressed across 5 cells in the apical domain (n=12). Double fluorescent WMISH showed that *hbn* is entirely co-expressed with *foxQ2* (figure 3.14 A), confirmed also from the apical view (figure 3.14 B). This is supported also by the number of *hbn* positive cells that are in average 24 per embryo (n=4), while *foxQ2* is expressed in 25 cells in the apical domain. Similar to hatching blastula stage, there appears to be a slight cell to cell variability, that results in single cells expressing only one of the two genes (figure 3.14 B white arrow).

dcry genes encode type I cryptochrome proteins, that are light responsive and generally function as blue/UV-A light photoreceptors important in circadian clocks (Cashmore *et al*., 1999). Although not strictly a regulatory gene, such as a transcription factor or a signalling molecule, *dcry* can influence gene expression via manipulation of the circadian molecular clock and associated transcriptional control (Nitabach and Tagert

2008). Although phylogenetic analysis of the sea urchin genome identified a single *dcry* gene (Rubin *et al.*, 2006), no expression data exists.

dcry temporal expression (figure 3.8 - pink line) is maternal, with zygotic expression starting at hatched blastula stage (18 hours). At this stage, *dcry* expression is seen only in the apical domain, in a similar size to *foxQ2,* when viewed from a lateral perspective (figure 3.14 C). Counting the number of positive nuclei using DAPI counterstaining, shows that *dcry* is expressed across 5 cells in the apical domain (n=6), identical to the 5 cells of *foxQ2*. Double fluorescent WMISH (figure 3.14 C) show that *dcry* is expressed in the central apical domain completely within the *foxQ2* domain, although *dcry* expression is not as uniform as *foxQ2*, and not every *foxQ2* positive cell expresses *dcry.* The apical view confirms that *dcry* and *foxQ2* are co-expressed in the central apical domain but with some cell-to-cell variability in either expression pattern (figure 3.14 D). This variability can be attributed to the fact that *dcry* is in a highly dynamic phase of expression.

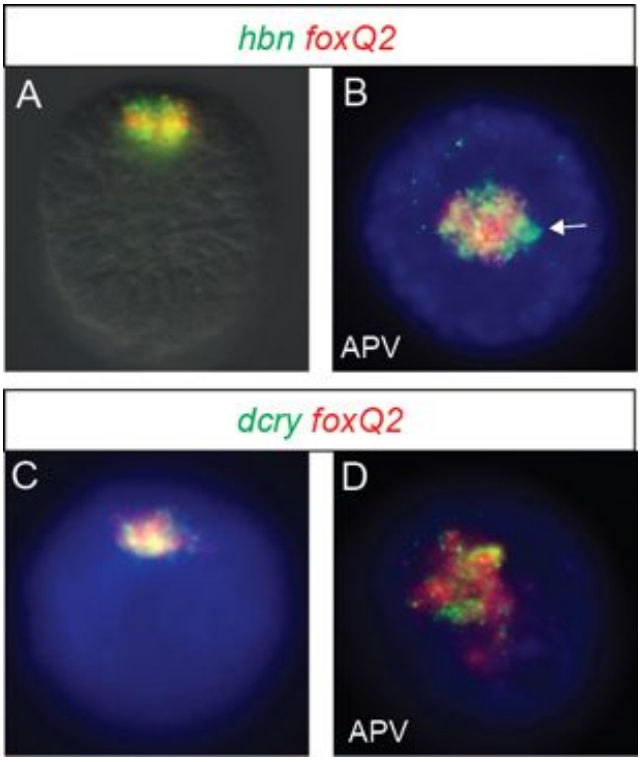

Figure 3.14. Expression analysis of *hbn* and *dcry* at hatched blastula stage
(A,B) Double fluorescent WMISH of *hbn* and *foxQ2*. (C,D) Double fluorescent WMISH of *dcry* and *foxQ2.* DAPI stained nuclei are blue. Unless otherwise specified embryos are presented in a lateral view with the apical domain at the top. Apical view (APV). See main text for descriptions of arrows.

Expression of *fgfr1*

fgfr1 encodes a protein that functions as a receptor for FGF ligands. FGF receptors are composed of an extracellular ligand-binding domain that contains three immunoglobulin (Ig)-like domains, a single transmembrane helix, and a cytoplasmic domain that contains protein tyrosine kinase activity (McCoon *et al*.,1996). FGF signalling is involved in a diverse range of developmental processes and in particular plays a role in nervous system development in vertebrates (Stern *et al*., 2005) and in the development of the apical organ in cnidarians (Rentzsch *et al*., 2008).

fgfr1 was initially characterised in *S. purpuratus* by McCoon *et al*., (1996) and subsequently in more detail in the Mediterranean sea urchin, *P. lividus* by Lapraz *et al.,* (2006). *fgfr1* is ubiquitously expressed during cleavage stages and begins to be expressed more strongly in the vegetal plate by hatched blastula stage. Starting at the blastula stage, *fgfr1* expression also becomes asymmetrical along the oral–aboral axis, with a stronger expression in the presumptive oral ectoderm. At mesenchyme blastula stage, *fgfr1* is strongly expressed in the ingressing primary mesenchyme cells, after which expression is seen in the secondary mesenchyme cells and the apical domain. During gastrulation, restricted expression of *fgfr1* persists in the apical domain and in the oral ectoderm, but *fgfr1* is now also transcribed actively in the presumptive endoderm and invaginated archenteron. Here, I confirm similar expression in *S. purpuratus.*

fgfr1 expression (figure 3.8 - brown line) is maternal, with zygotic expression already visible at hatching blastula stage (15 hours) and increasing rapidly up to 1579 transcripts per embryo by hatched blastula stage (18 hours). At hatched blastula stage, *fgfr1* shows strong expression in the apical domain and weaker expression in the oral ectoderm and vegetal plate when viewed from a lateral perspective (figure 3.15 A; see also figure 3.15 B and compare white arrow to turquoise arrow in C). Counting the number of positive nuclei using DAPI counterstaining is difficult as *fgfr1* is expressed across a number of territories on the oral-aboral axis. However, it can be seen that *fgfr1* is expressed across 6 cells along the lateral axis in the apical domain, compared to 5 cells of *foxQ2* (n=4). In order to map the *fgfr1* expressing cells in the apical domain, I

carried out a double fluorescent WMISH with *foxQ2*. *fgfr1* is co-expressed with *foxQ2* in only the oral half of the apical domain and extends into the oral ectoderm away from the apical domain (figure 3.15 B white arrow). This is particularly interesting, as it is the first example of asymmetrical gene expression along the oral-aboral axis in the apical domain and illustrates that the apical domain already has distinct differences in oral and aboral regulatory state. Rotating the embryos and viewing from an apical perspective shows *fgfr1* clearly co-expressed with *foxQ2* in one half of *foxQ2* (figure 3.15 C).

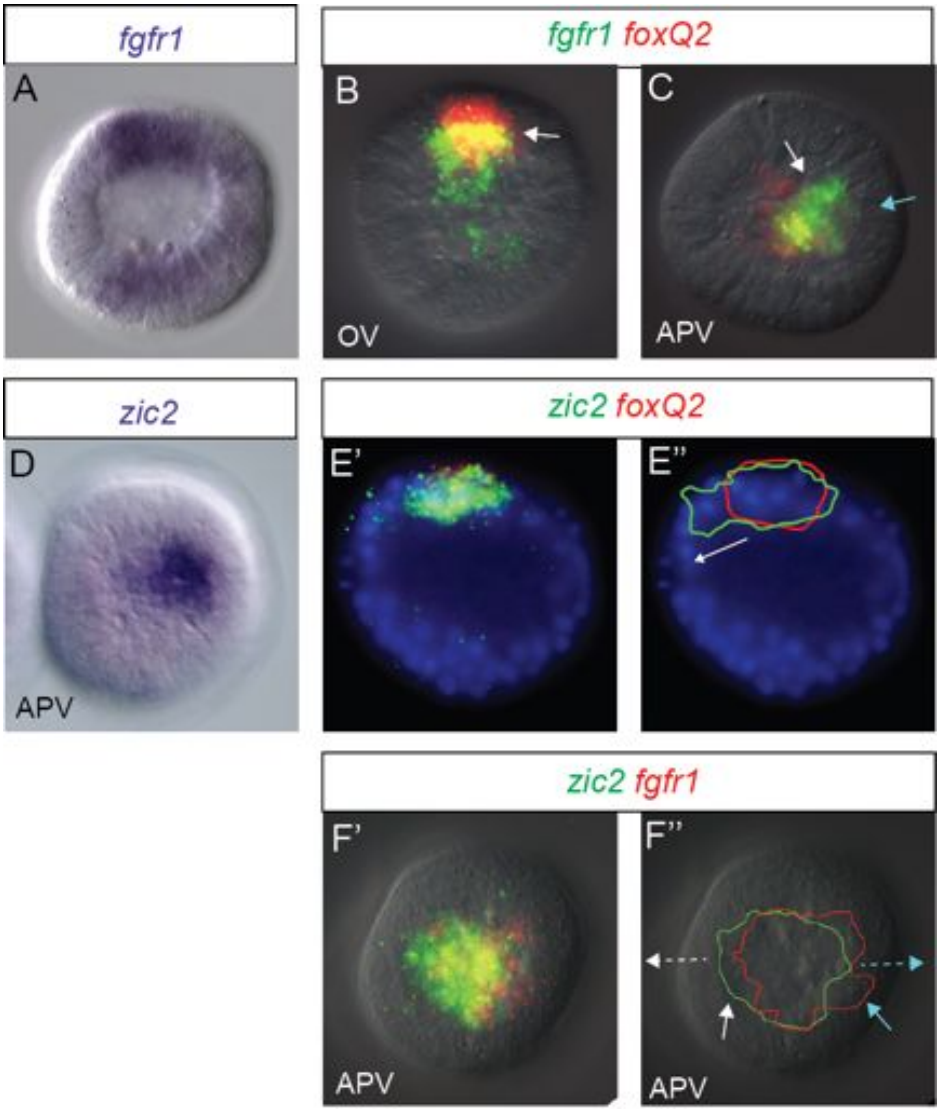

Figure 3.15. Expression analysis of *fgfr1* and *zic2* at hatched blastula stage
(A) NBT/BCIP WMISH of *fgfr1*. (B,C) Double fluorescent WMISH of *fgfr1* and *foxQ2.* (D) NBT/BCIP WMISH of *zic2.* (E) Double fluorescent WMISH of *zic2* and *foxQ2*, (E'') outline of gene expression of E'. (F) Double fluorescent WMISH of *zic2* and *fgfr1*, (F'') outline of gene expression of F'. DAPI stained nuclei are blue. Unless otherwise specified embryos are presented in a lateral view with the apical domain at the top. Apical view (APV). See main text for descriptions of arrows.

Expression of *zic2*

zic2 expression (figure 3.8 - purple line) increases to 506 transcripts per embryo by hatched blastula stage (18 hours), and is expressed only in the apical domain (3.15 D). Double fluorescent *in situ* of *zic2* and *foxQ2* shows that *zic2* is co-expressed with *foxQ2* in the central apical domain, but also expressed in two cells (n=7) on one side of *foxQ2* (figure 3.15 E' and E'' white arrow). As described above, *fgfr1* is expressed in the oral half of the apical domain and provides a good marker for understanding relative gene expression along the oral-aboral axis in the apical domain. Thus, double *in situ* of *zic2* and *fgfr1* show that these genes are expressed on opposite sides of the apical domain (figure 3.15 F dashed white and turquoise arrows), suggesting that, as *fgfr1* is known to be expressed in the oral side, then *zic2* must be expressed in the aboral side. The outlines of their expression domains (figure 3.15 F''), illustrate that three different domains are present: 1) *zic2* only in the aboral apical domain (white arrow); 2) fgfr1 in opposite oral apical domain (turquoise arrow); 3) and *zic2, foxQ2* and *fgfr1* in the central apical domain.

Cellular maps and summary

Figure 3.16 shows cellular maps for the six genes studied at hatched blastula stage. *foxQ2, hbn* and *dcry* are all expressed in the central apical domain. *frizzled 5/8* is expressed in a larger domain in and around *foxQ2. six3* expression does not overlap at all with with *foxQ2* and is expressed as a horseshoe around the central apical domain. Finally, *fgfr1* is expressed in only the oral half of the apical organ, while *zic2* is expressed in the central apical domain and few cells in the aboral apical domain.

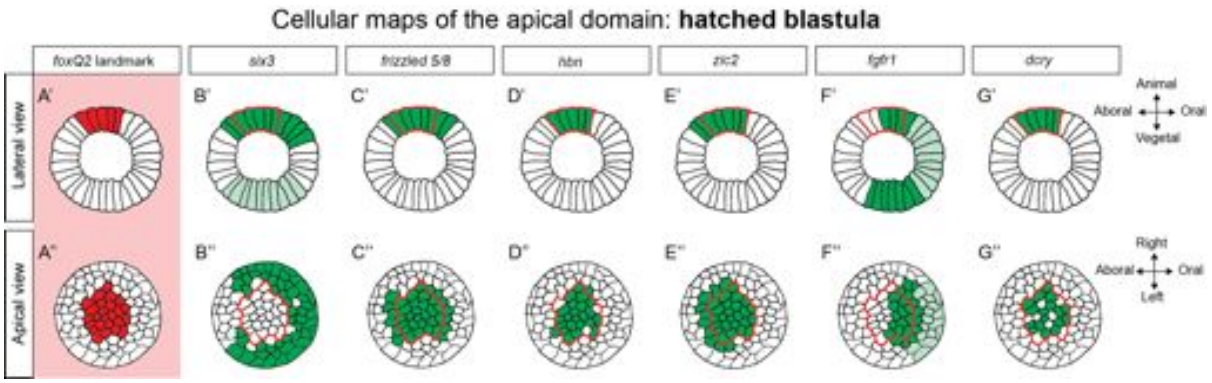

Figure 3.16. Cellular maps of gene expression at hatched blastula stage

Lateral and apical view of hatched blastula stage cellular maps. (A) *foxQ2* expression (red). (B-G) Expression of other regulatory genes (green) with outline of *foxQ2* (red line).

Chapter 4

Regulatory state analysis:

the gastrulating embryo

In this chapter, I continue my analysis of the apical domain regulatory states, as the embryo undertakes the key developmental task of gastrulation. Three developmental stages are studied in this chapter: (1) Mesenchyme blastula, which occurs at around 24 hours and is characterised by the ingression of the primary mesenchyme cells, that later go on to form the skeleton; (2) Early gastrula, which occurs around 30 hours and marks the start of the invagination of the gut; (3) Mid-gastrula, which occurs between 36-40 hours is the stage in which the extended gut can be seen in the embryo. Concurrent with these morphogenic movements, the apical domain undergoes a series of dynamic changes in gene expression. New genes appear in the apical domain during this period and there is a sharp increase in spatial complexity and number of regulatory state sub-domains. Throughout this period of development, several new genes begin to be expressed in the apical domain. Figure 4.1 shows the temporal expression profiles for six genes that are subsequently described in detail to help determine the regulatory state of the apical domain in the gastrulating embryo.

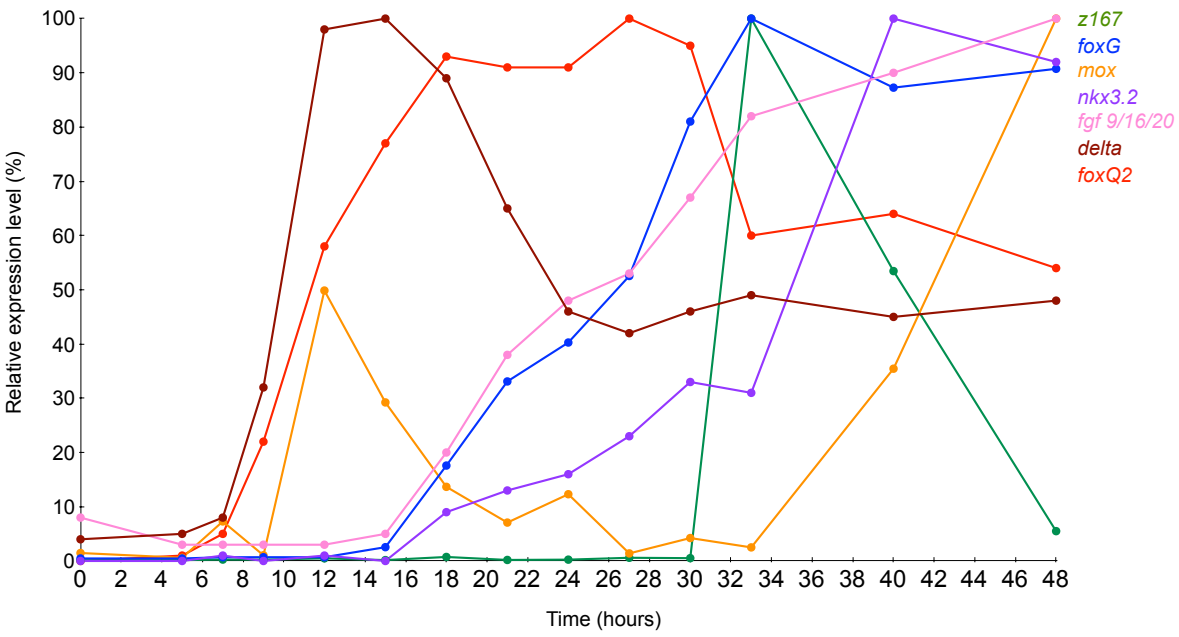

Figure 4.1. Temporal expression profiles of apical organ genes in the gastrulating embryo
Genes that appear in the apical domain by-mid-gastrula stage (36 hours). Expression levels are given as a fraction of peak expression. *foxG, fgf 9/16/20, delta,* and *foxQ2* data were quantified using Nanostring nCounter (Materna *et al.,* 2010). *z167, mox* and *nkx3.2* were quantified using QPCR (see Materials and methods; see appendix B for actual number of transcripts).

4.1. Combinatorial gene expression studies of the apical domain at mesenchyme blastula stage

Detailed studies with double fluorescent WMISH were carried out to identify the emergence of new regulatory states and to understand how existing domains are refined over time. Genes were investigated individually, by double fluorescent WMISH with the apical organ landmark *foxQ2* to identify their position relative to the apical domain. In many cases, these results were augmented with counting the number of cells that express a given gene, additional double fluorescent WMISH with other apical organ genes, and tracing the outlines of gene expression to allow more accurate comparisons.

six3 expression

six3 levels of expression (figure 3.8 - orange line) increase from 1340 at hatched blastula stage (18 hours), to 1874 transcripts per embryo by mesenchyme blastula (24 hours). At this stage, double fluorescent WMISH of *six3* and *foxQ2* shows that *six3* continues to be expressed in a ring made by several (2-3) cell rows surrounding the *foxQ2* positive apical domain but shows no co-expression (figure 4.2 C white dotted circle). Consistent with earlier stages, the ring is not complete and cells on one side do not express *six3*. *six3* marks the outer boundary of the apical domain and has increased its expression from 11 cells (in hatched blastula stage; n=9) to 13 cells (n=8), across a lateral view. Interestingly, there is a one cell row gap between *six3* and *foxQ2* but only on one side (figure 4.2 C white arrow).

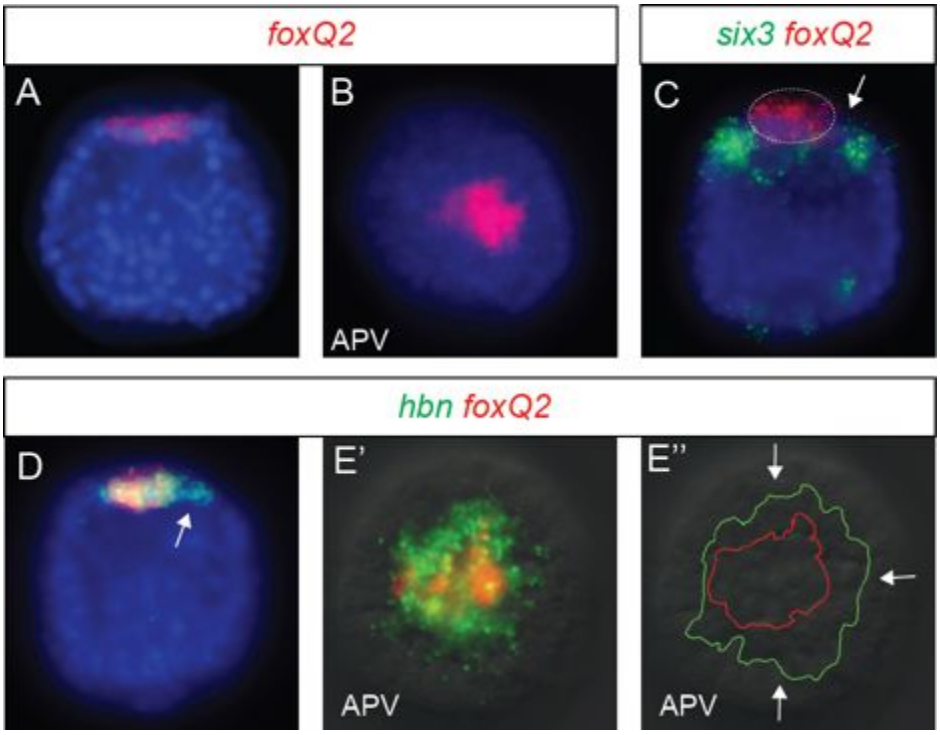

Figure 4.2. Expression analysis of *foxQ2, six3* and *hbn* at mesenchyme blastula stage
(A,B) Single fluorescent WMISH of *foxQ2*. (C) Double fluorescent WMISH of *six3* and *foxQ2*. (D,E) Double fluorescent WMISH of *hbn* and *foxQ2,* (E'') outline of gene expression of E'. Unless otherwise specified embryos are imaged with fluorescence microscopy and DAPI-labeled nuclei (blue) or DIC. Embryos are presented in a lateral view with the apical domain at the top. Apical view (APV). See main text for descriptions of arrows.

hbn expression

hbn expression (figure 3.8 A - green line) increases slightly from 621 transcripts per embryo at hatched blastula stage (18 hours) to 708 transcripts per embryo by mesenchyme blastula (24 hours). At this stage, *hbn* increases its expression in the apical domain from 5 cells (at hatched blastula; n=12) to 8 cells (n=7) across the lateral view. *hbn* is still co-expressed with *foxQ2* in the central apical domain but now is also expressed on one side of *foxQ2* (figure 4.2 D white arrow). Rotating the embryo and observing from an apical perspective, shows that the outer boundary of *hbn* has expanded beyond the *foxQ2* domain (figure 4.2 E). To clarify, I compared the outlines of their expression domains and showed that *hbn* is expressed outside *foxQ2* on three sides (figure 4.5 D''' white arrows). However, without an oral-aboral marker, it is difficult to know the direction of *hbn* expansion, however it is thought to be on the oral side (L. Angerer and Z. Wei personal communication,).

fgf 9/16/20 and *fgfr1* expression

Signalling, and in particular canonical Wnt signalling, has been proposed in the literature, to play an important role in the establishment and patterning of the apical organ (reviewed by Angerer *et al.,* 2011). However, little or no research has been undertaken to see if FGF signalling plays a role. Interestingly, I have shown that an FGF receptor, *fgfr1* is expressed in the oral side of the apical domain and in the oral ectoderm. This lends support to the suggestion that FGF signalling might be important in apical organ development and worthy of further study. FGF ligands will be discussed in more detail in chapter 6, but briefly, they form a family of extracellular signalling peptides, which are key regulators of many biological processes, ranging from cell proliferation to the control of embryonic development in metazoans. Over the past decade or so, many studies have shown the importance of FGFs in nervous system development and specifically neural induction (reviewed by Mason, 2007). A single FGF ligand has been identified in the sea urchin *S. purpuratus* genome (Lapraz *et al.,* 2006), and the protein sequence shows the most similarities with members of the FGF 9/16/20 subfamily (Röttinger *et al.,* 2008). The spatial expression for *fgf 9/16/20* has

previously been characterised by Röttinger *et al.* (2008) in the Mediterranean sea urchin *P. lividus* and I present here a detailed expressions pattern in *S. purpuratus.*

fgf 9/16/20 expression (figure 4.1 - pink line) begins at hatched blastula stage (18 hours), approximately 10 hours after the onset of *foxQ2* (figure 4.1 - red line). Expression levels are low and reach only 58 transcripts per embryo by mesenchyme blastula stage (24 hours). At mesenchyme blastula stage, *fgf 9/16/20* is expressed in two broad domains in the ectoderm (figure 4.3 A black arrows). Double fluorescent WMISH with the apical organ landmark *foxQ2* show that *fgf 9/16/20* is expressed in the lateral ectoderm either side of *foxQ2* (figure 4.3 B white arc showing a single side), but shows no co-expression. Each domain forms an approximate rectangle 6 cells wide by 2 cells deep (n=12), although at this stage *fgf 9/16/20* expression is quite weak and gene expression boundaries are relatively undefined. This expression is consistent with expression in the lateral ectoderm as shown for *P. lividus* (Röttinger *et al.,* 2008). At this time, the receptor *fgfr1* (figure 3.8 - brown line) increases its level of expression from 1579 to 2199 transcripts per embryo by mesenchyme blastula stage (24 hours) and is expressed at equal intensity in the apical domain and the oral ectoderm (compare figure 3.15 A-C to figure 4.3 C turquoise arrow). Embryos stained with both *fgfr1* and *foxQ2* show that *fgfr1* remains exclusively in the oral apical domain (figure 4.3 C white arrow) and is excluded from the entire aboral side of the embryo, including the aboral apical domain. The ligand FGF 9/16/20 must bind to the extracellular domain of FGFR1 in order to activate the receptor and transduce the FGF signal. This implies the two proteins must come into contact and therefore, I was curious to understand the spatial relationship between the two genes. I carried out a double fluorescent WMISH with *fgf 9/16/20* and *fgfr1* and compared the outline of their expression (figure 4.3 D,E). Viewed from the oral perspective, *fgf 9/16/20* is expressed in two blocks either side of *fgfr1* but there appears no overlap in expression (figure 4.3 E’’’).

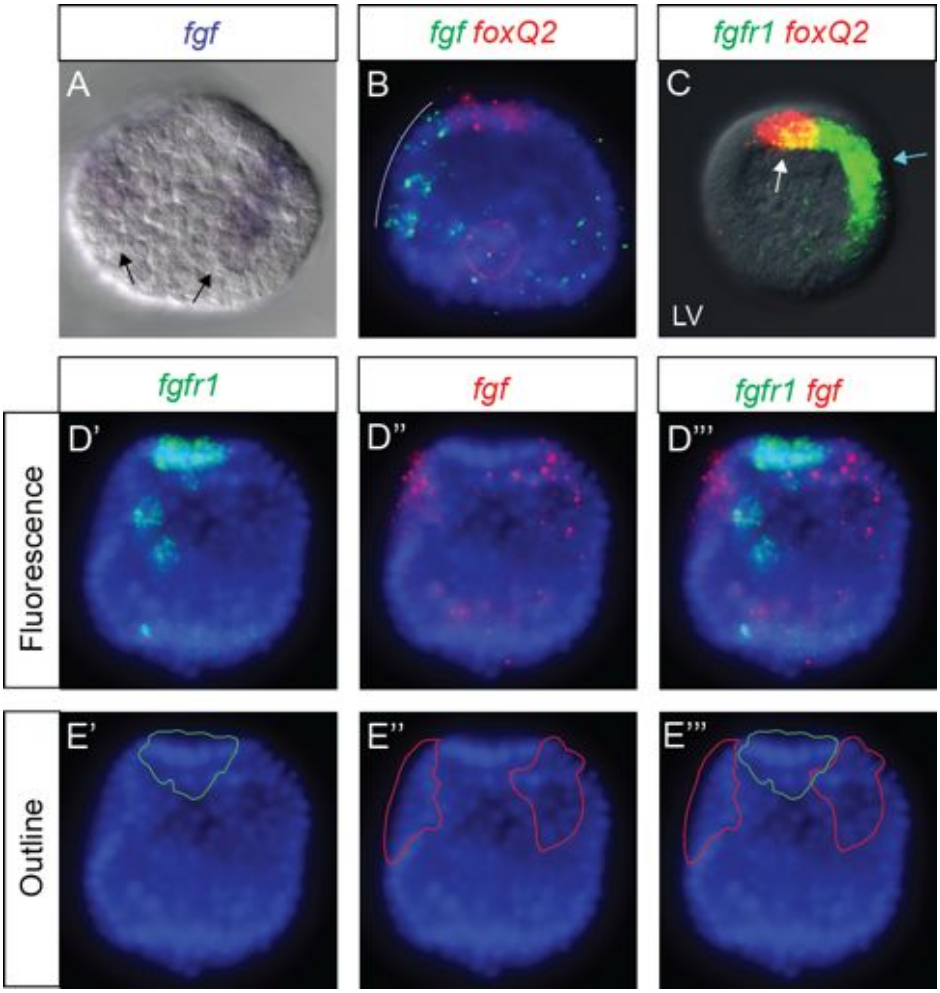

Figure 4.3. Expression analysis of *fgf 9/16/20* and *fgfr1* at mesenchyme blastula stage
(A) DIC image of a NBT/BCIP WMISH of *fgf 9/16/20*. (B) Double fluorescent WMISH of *fgf 9/16/20* and *foxQ2*. (C) Double fluorescent WMISH of *fgfr1* and *foxQ2.* (D) Double fluorescent WMISH of *fgf* and *fgfr1* showing each channel individually and merged. (E) Outline of gene expression of D. Unless otherwise specified embryos are imaged with fluorescence microscopy and DAPI-labeled nuclei (blue) or DIC. Embryos in this figure are all presented in a oral view with the apical domain at the top. Lateral view (LV) with the oral side at the right. See main text for descriptions of arrows.

frizzled 5/8 and *nkx3.2* expression

frizzled 5/8 expression (figure 3.8 - blue line) remain constant at around 650 transcripts per embryo. At mesenchyme blastula stage, *frizzled 5/8* is clearly expressed in the apical domain and the vegetal plate (figure 4.4 A). Double fluorescent WMISH with *frizzled 5/8* and *foxQ2* shows that *frizzled 5/8* is co-expressed with *foxQ2* in the central apical domain but it is also expressed in cells outside *foxQ2*, especially on one side (figure 4.4 B). Interestingly, the overall expression domain of *frizzled 5/8* increases from 8 cells (in

hatched blastula stage; n=10) to 9 cells (n=19) across a lateral view. Comparing the outline of each expression domain shows, that *frizzled 5/8* is expressed in 2-3 cell rows outside *foxQ2* on one side (figure 4.4 B''' turquoise arrow) and only 1 cell row on the opposite side (figure 4.4 B''' white arrow). This suggests that *frizzled 5/8 has* expanded its expression into the oral or aboral ectoderm territory. To help decide which of these is true, I carried out a double fluorescent WMISH with the homeobox gene *nkx3.2*, which is known to be expressed in the oral side of the apical domain and presumptive foregut and is required for the development of pharyngeal neurons (Wie *et al.,* 2009 and 2011). *nkx3.2* expression (figure 4.1 - purple line) is only 45 transcripts per embryo at mesenchyme blastula stage (24 hours), when it is expressed only in the apical domain and within a larger domain of *frizzled 5/8* (figure 4.4 C,D). The fact that *frizzled 5/8* is expressed equally around *nkx3.2,* suggests that *frizzled 5/8* is expressed more towards the oral side. I showed earlier that *fgf 9/16/20* is not co-expressed with *foxQ2* in the apical domain (figure 4.3 D,E). Since *frizzled 5/8* expression is larger than *foxQ2,* I carried out a double fluorescent WMISH with *frizzled 5/8* and *fgf 9/16/20* to see if any co-expression occurred. Apical views show, that *fgf 9/16/20* is expressed on the lateral border of *frizzled 5/8,* but is not co-expressed with it (figure 4.4 E) It is interesting to notice that while *frizzled 5/8* and *fgf 9/16/20* domain of expression are adjacent, *fgf 9/16/20* and *foxQ2* are separated by a domain of 1-2 cells not expressing any of the two genes (compare figure 4.3 D''' with figure 4.4 E''').

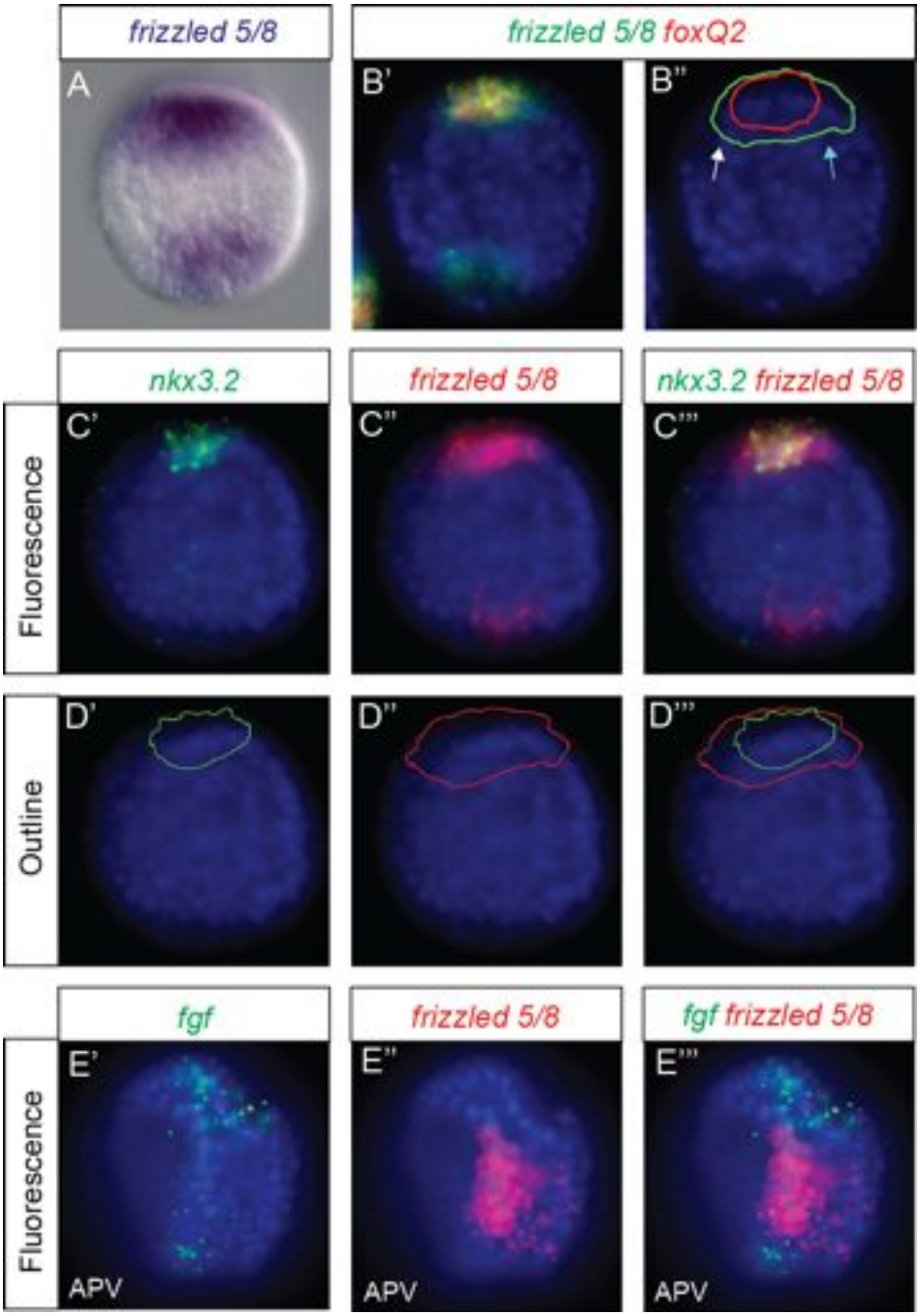

Figure 4.4. Expression analysis of *frizzled 5/8, fgf 9/16/20* and *nkx 3.2* at mesenchyme blastula stage

(A) DIC image of a NBT/BCIP WMISH of *frizzled 5/8*. (B) Double fluorescent WMISH of *frizzled 5/8* and *foxQ2*, (B'') outline of gene expression of B'. (C) Double fluorescent WMISH of *nkx3.2* and *frizzled 5/8* showing each channel individually and merged, (D) outline of gene expression domains of C. (E) Double fluorescent WMISH of *fgf 9/16/20* and *frizzled 5/8* showing each channel individually and merged. Unless otherwise specified embryos are imaged with fluorescence microscopy and DAPI-labeled nuclei (blue). Embryos are all presented in a lateral view with the apical domain at the top. Apical view (APV). See main text for descriptions of arrows.

zic2 expression

zic2 expression (figure 3.8 - purple line) shows a steady decrease from 506 transcripts per embryo at hatched blastula stage (18 hours), to 371 transcripts per embryo by mesenchyme blastula (24 hours). At this stage, *zic2* is still expressed only in the apical domain (figure 4.5 A). An apical view of embryos stained with *zic2* and *foxQ2* show that *zic2* is co-expressed with *foxQ2,* but also is expressed in additional cells outside *foxQ2* domain (figure 4.5 B). The outlines of their expression domains, clarifies the relative expression of *zic2* to *foxQ2* (figure 4.5 B''). This illustrates, that *zic2* and *foxQ2* are co-expressed in the central apical domain, but that *zic2* is also expressed on three sides of *foxQ2* (figure 4.4 B'' white arrow and turquoise arrows).

dcry expression

dcry expression (figure 3.8 - pink line) increases from 71 transcripts per embryo at hatched blastula stage (18 hours), to 185 transcripts per embryo by mesenchyme blastula (24 hours). At this stage, *dcry* remains expressed in the apical domain (figure 4.5 C). Double fluorescent WMISH of *dcry* and *foxQ2* shows, that both genes are co-expressed in the apical domain (figure 4.5 C). The apical view shows, that although *dcry* is co-expressed with *foxQ2,* its expression is not as homogenous as *foxQ2* (figure 4.5 D).

delta expression

The Delta signalling ligand, in contrast to many other signalling ligands, is bound to the cell surface, thus, limiting its effective range to cells that are in direct contact with the *delta* expressing cell. In the sea urchin *S. purpuratus,* Delta/Notch signalling is required for specification of all non-skeletogenic mesoderm cell types, such as pigment cells, blastocoelar cells, coelomic pouch cells and circumesophageal muscle (Sweet *et al.,* 2002; Materna *et al.,* 2012). Recently, Yaguchi *et al.,* (2012) have shown that the number of serotonergic neurons in the apical organ is affected by the Delta/Notch-mediated lateral inhibition. *delta* expression (figure 4.1 - brown line) starts during early cleavage

stage (6 hours) and reaches 153 transcripts per embryo by mesenchyme blastula (24 hours). At this stage, *delta* is expressed both in the apical domain and vegetal plate (figure 4.5 E) which is consistent with what has been previously published. Double fluorescent WMISH of *delta* and *foxQ2* show that *delta* is co-expressed with *foxQ2* (figure 4.5 E turquoise arrow). Rotating the embryos and viewing from an apical perspective shows, that *delta* is expressed in individual cells scattered within the *foxQ2* positive apical domain (figure 4.5 F). This is better illustrated by a comparison of the outlines of expression domains (figure 4.5 F'' white arrows).

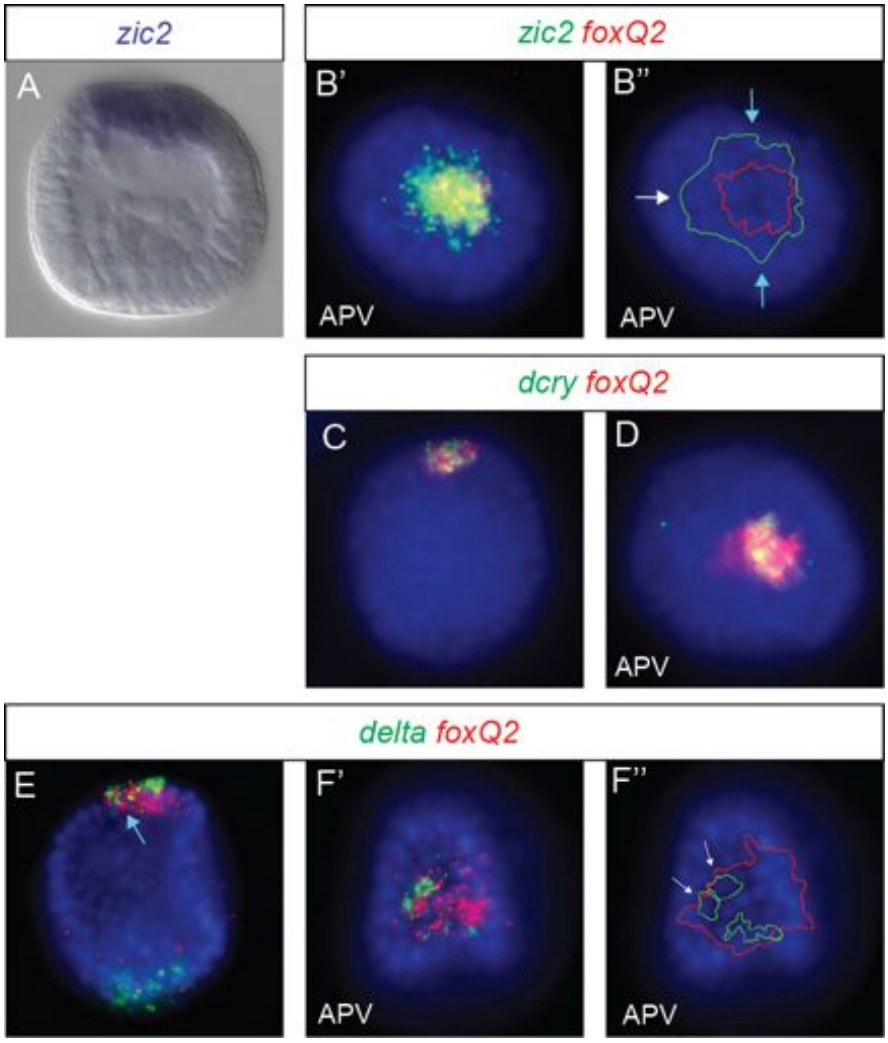

Figure 4.5. Expression analysis of *zic2*, *dcry* and *delta* at mesenchyme blastula stage
(A) DIC image of a NBT/BCIP WMISH of *zic2*. (B) Double fluorescent WMISH of *zic2* and *foxQ2,* (B'') outline of gene expression of B'. (C,D) Double fluorescent WMISH of *dcry* and *foxQ2.* (E,F) Double fluorescent WMISH of *delta* and *foxQ2*, (F'') outline of gene expression of F'. Unless otherwise specified embryos are imaged with fluorescence microscopy and DAPI-labeled nuclei (blue). Embryos are presented in a lateral view with the apical domain at the top. Apical view (APV). See main text for descriptions of arrows.

Cellular maps and summary

In this section, a series of double fluorescent WMISH were carried out to identify the position of several regulatory genes in the apical domain at mesenchyme blastula stage. All these data were combined, integrated and subsequently overlaid onto cellular maps. Figure 4.6 shows cellular maps for the eight regulatory genes studied so far at this stage. In mesenchyme blastula stage embryos some genes retain similar expression patterns as earlier such as *six3, frizzled 5/8, zic2, fgfr1* and *dcry.* New genes include *delta,* that is found in scattered cells in the central apical domain and *nkx3.2* which is located in the the oral apical domain and towards the oral boundary of *frizzled 5/8. hbn* undergoes a dramatic change and is now found outside the central apical domain in the oral and lateral apical domain. In the six hours since hatched blastula stage, and the addition of one or two genes, the number of expression domains and hence the number of regulatory states, has increased dramatically.

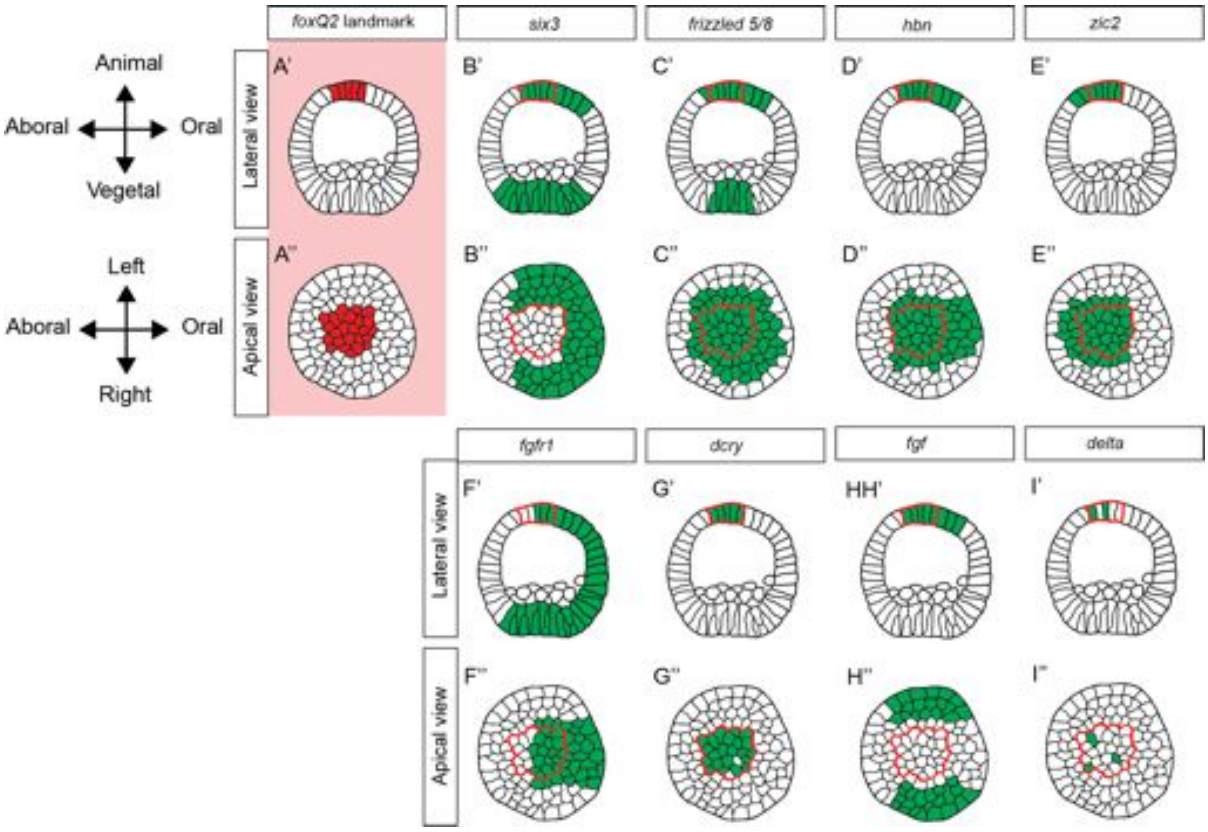

Figure 4.6. Cellular maps of gene expression at mesenchyme blastula stage
Lateral and apical view of mesenchyme blastula stage cellular maps. (A) *foxQ2* expression (red). (B-I) Expression of other regulatory genes (green) with outline of *foxQ2* (red line).

4.2. Combinatorial gene expression studies of the apical domain at early gastrula stages

As discussed in chapter 3, cellular maps of the apical domain were created for three developmental stages before gastrulation: hatching blastula (15 hours); hatched blastula (18 hours) and mesenchyme blastula (24 hours). Two further cellular maps were created for developmental stages after gastrulation: mid-gastrula (36 hours) and late gastrula (48 hours). In the following section, I present gene expression data for early gastrula stage embryos in order to help bridge the dynamics changes in gene expression that occurs at the start of gastrulation (30 hours). I also extend my analysis to consider an additional gene: *foxG.*

hbn expressions

hbn expression (figure 3.8 - green line) decreases slightly from 703 transcripts per embryo at mesenchyme blastula stage (24 hours) to 646 transcripts per embryo by early gastrula (30 hours). At this stage, *hbn* is expressed broadly in the apical domain although appears on one side to be expressed with a greater intensity (figure 4.7 C black arrow). Similarly to mesenchyme blastula, double fluorescent *in situ* with *foxQ2* shows that *hbn* is co-expressed with *foxQ2* in the central apical domain and also outside the *foxQ2* domain (figure 4.7 D white and turquoise arrows).

six3 expression

The levels of s*ix3* expression (figure 3.8 - orange line) remain constant from mesenchyme blastula stage (24 hours) to early gastrula (30 hours). At this stage, *six3* is expressed in the apical domain and the vegetal territories (figure 4.7 E). Double fluorescent WMISH of *six3* and *foxQ2* shows that *six3* is not co-expressed with *foxQ2* but surrounds the *foxQ2* central apical domain with one side particularly faint and one side that doesn't express any *six3* (figure 4.7 F white arrow).

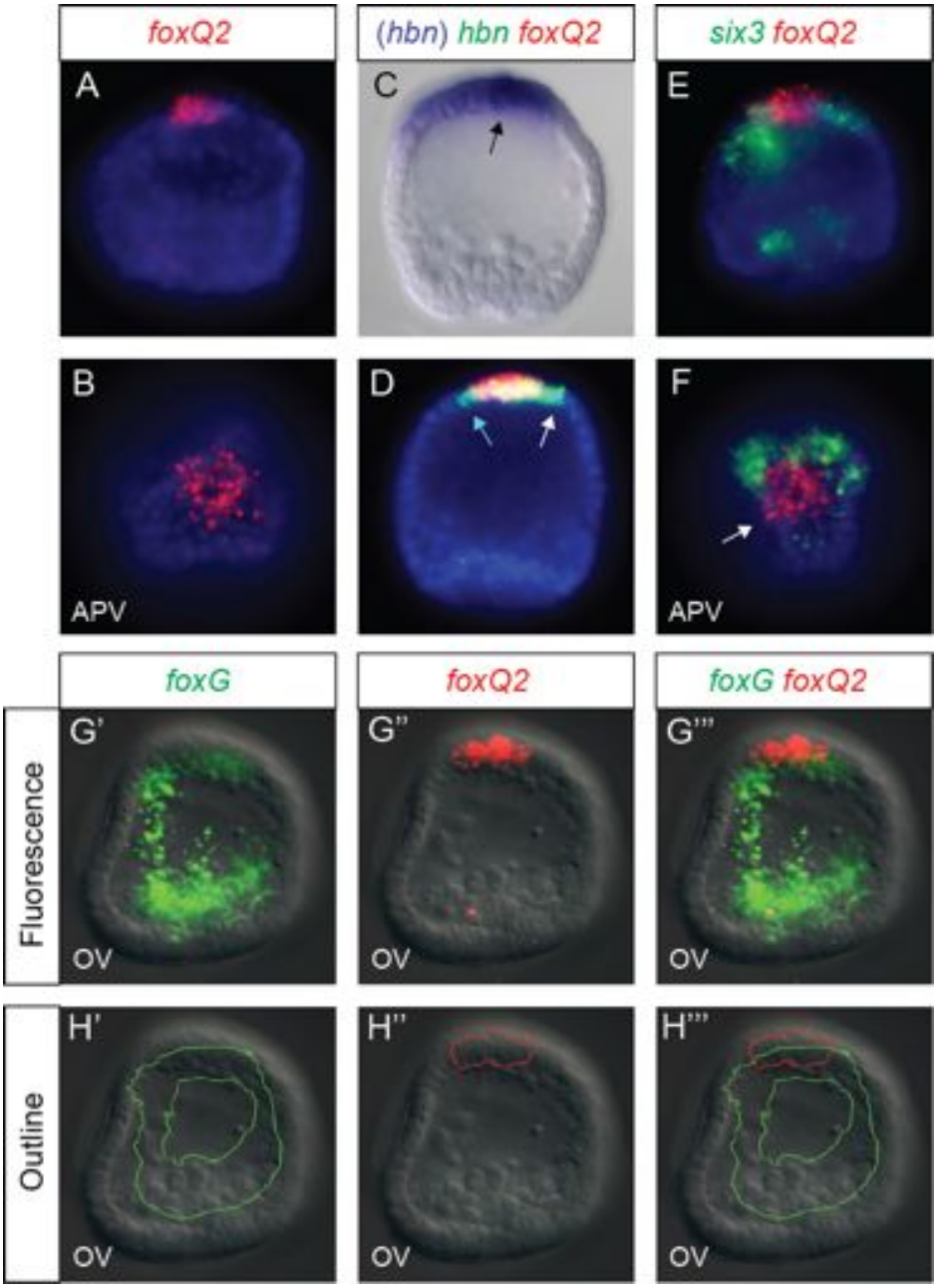

Figure 4.7. Expression analysis of *foxQ2, hbn, six3* and *foxG* at early gastrula stage
(A,B) Single fluorescent WMISH of *foxQ2*. (C) DIC image of a NBT/BCIP WMISH of *hbn*. (D) Double fluorescent WMISH of *hbn* and *foxQ2.* (E,F) Double fluorescent WMISH of *six3* and *foxQ2*. (G) Double fluorescent WMISH of *foxG* and *foxQ2* showing each channel individually and merged. (H) Outline of gene expression domains of G. Unless otherwise specified embryos are imaged with fluorescence microscopy and DAPI-labeled nuclei (blue) or DIC. Embryos in this figure are all presented in a lateral view with the apical domain at the top. Apical view (APV), oral view (OV). See main text for descriptions of arrows.

foxG expression

foxG is a member of the forkhead family of transcription factors and is known to be widely expressed in the nervous systems of invertebrates (Santagata *et al*., 2012). Similar to *foxQ2, foxG* contains an engrailed homology-1 motif, known to mediate physical interaction with transcriptional co-repressors of the TLE/Groucho family and suggests that it could play a role as a repressor in the sea urchin (Yaklichkin *et al.,* 2007). Initially characterised by Tu *et al.,* (2006) in the sea urchin *S. purpuratus,* it is expressed faintly in the oral ectoderm at hatched blastula stage. This oral expression persists until the start of gastrulation, after which *foxG* expression is restricted to the presumptive ciliary band domain. *foxG* expression reaches 432 transcripts per embryo at early gastrula stage (figure 4.1 - blue line). As *foxG* is a marker for the ciliary band, a double fluorescent WMISH with *foxG* and *foxQ2* will help elucidate the position of the ciliary band relative to the apical domain (figure 4.7 G,H). From an oral perspective, *foxG* is clearly expressed in the ciliary band and appears to show little co-expression with the edge of *foxQ2* (figure 4.7 G'''). This is better illustrated by a comparison of the expression outlines, shown in figure 4.7 H''', and illustrates that *foxG* overlaps with the oral edge of *foxQ2* at this stage.

fgf 9/16/20 and *fgfr1*

fgf 9/16/20 expression (figure 4.1 - pink line) steadily increases to 80 transcripts per embryo by early gastrula stage (30 hours). *fgf 9/16/20* is now expressed in the lateral ectoderm on either side of the apical domain (figure 4.8 A,C) as well as in the primary mesenchyme cells (figure 4.8 B black arrow) and adjacent ectoderm (figure 4.8 B red arrow). Interestingly, double *in situ* with our landmark *foxQ2* shows that *fgf 9/16/20* is never co-expressed in the central apical domain and actually, the two domains of expression, are separated by one or two cells (figure 4.8 D white arrows). On the contrary, at early gastrula stage, the receptor *fgfr1* is expressed in an 8-10 cell wide band (n=9) in the oral half of the apical domain and the oral ectoderm, as well as the the vegetal plate (figure 4.7 E,F).

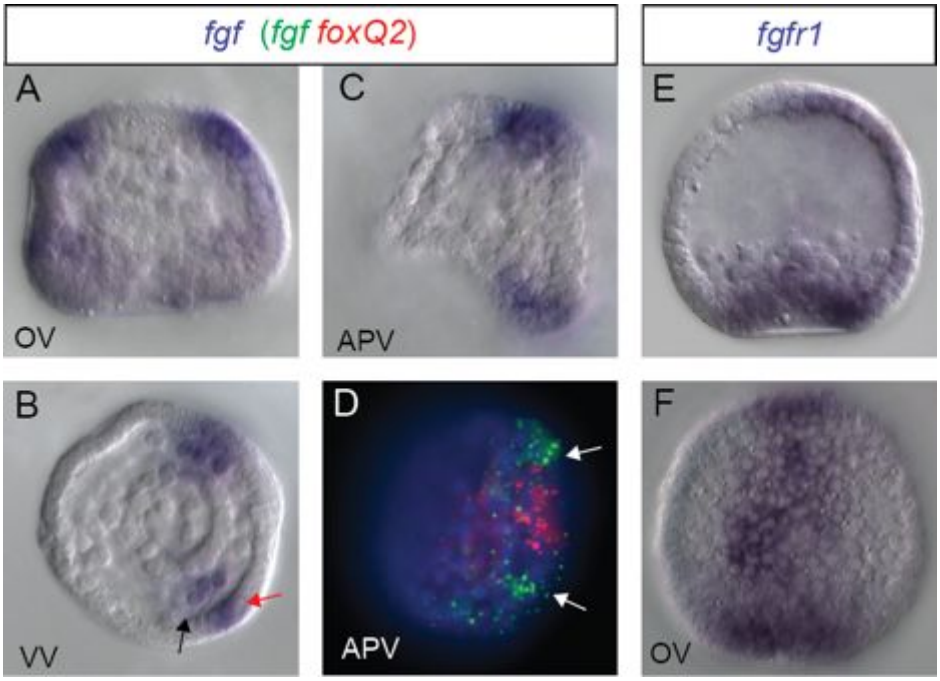

Figure 4.8. Expression analysis of *fgf 9/16/20* and *fgfr1* at early gastrula stage
(A-C) DIC images of a NBT/BCIP WMISH of *fgf 9/16/20*. (D) Double fluorescent WMISH of *fgf 9/16/20* and *foxQ2.* (E,F) DIC images of a NBT/BCIP WMISH of *fgfr1*. Unless otherwise specified embryos are imaged with fluorescence microscopy and DAPI-labeled nuclei (blue). Embryos in this figure are presented in a lateral view the oral side at the right and the apical domain at the top. Apical view (APV), oral view (OV), vegetal view (VV). See main text for descriptions of arrows.

frizzled 5/8 and *nkx3.2* expression

frizzled 5/8 (figure 3.8 - blue line) increases its expression from 655 transcripts per embryo at mesenchyme blastula stage (24 hours), to 1010 transcripts per embryo by early gastrula (30 hours). At this stage, *frizzled 5/8* is expressed in the apical domain and non-skeletogenic mesoderm (figure 4.9 A). To identify the position of *frizzled 5/8,* relative to the apical organ landmark *foxQ2,* double fluorescent WMISH was carried out and shows that *frizzled 5/8* is expressed in a larger domain than *foxQ2* and appears in cells outside *foxQ2* especially on one side (figure 4.9 B'' white arrow). Double fluorescent WMISH of *frizzled 5/8* and either *fgf 9/16/20* or *nkx3.2*, which are expressed with a oral apical domain/ectoderm bias, allow us to determine the exact position of the *frizzled 5/8* cells outside the *foxQ2* region. Interestingly, there is a one cell wide overlap between the edges of *frizzled 5/8* and *fgf 9/16/20* (figure 4.9 C'' white arrows). This is confirmed when observed from an apical perspective (figure 4.9 D''). The double

fluorescent using *nkx3.2,* shows that *frizzled 5/8* and *nkx3.2* are expressed as concentric circles (figure 4.9 E''''). Both of these pieces of data, suggest that *frizzled 5/8* is expressed in a larger disc than *foxQ2* but is not concentric and is shifted along the oral-aboral axis towards the oral side.

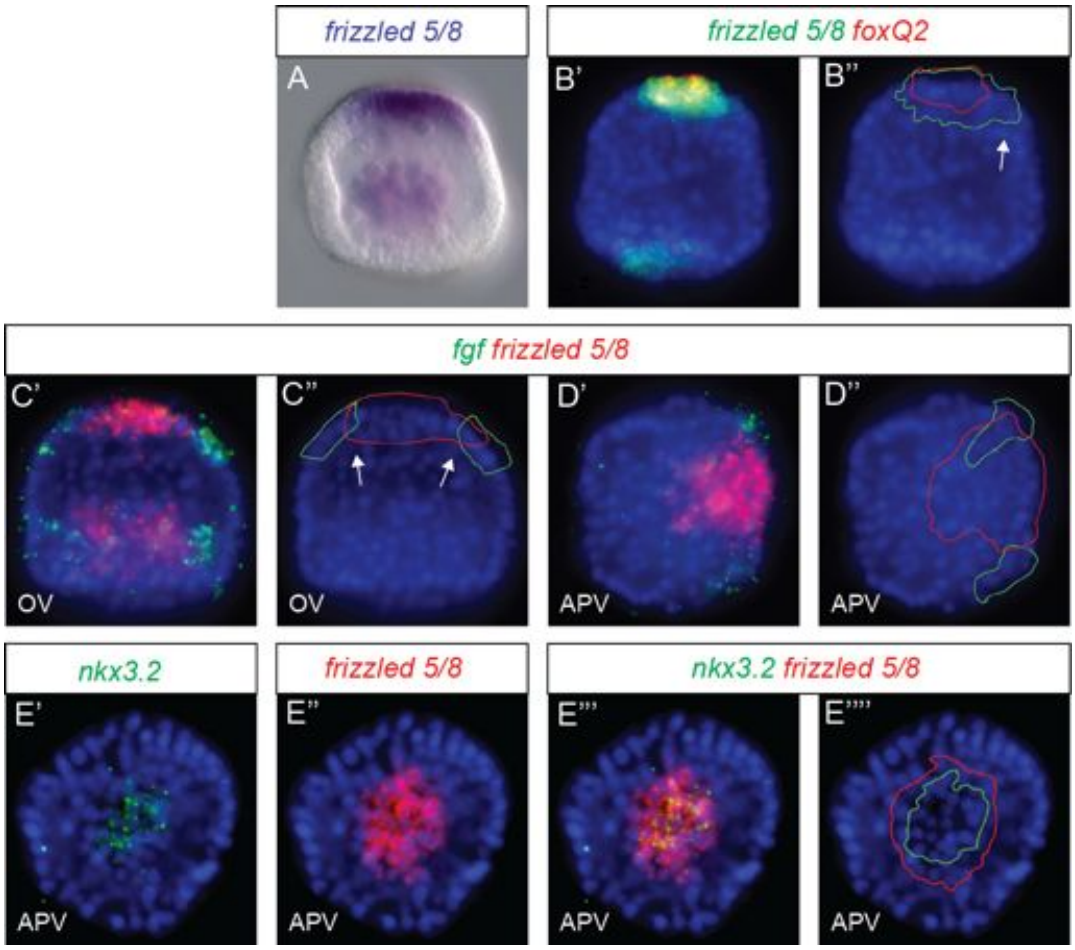

Figure 4.9. Expression analysis of *frizzled 5/8, fgf 9/16/20* and *nkx3.2* at early gastrula stage
(A) DIC images of a NBT/BCIP WMISH of *frizzled 5/8*. (B) Double fluorescent WMISH of *frizzled 5/8* and *foxQ2,* (B'') outline of gene expression of B'. (C,D) Double fluorescent WMISH of *fgf 9/16/20* and *frizzled 5/8,* (C'') outline of gene expression of C' and (D'') outline of gene expression of D'. (E) Double fluorescent WMISH of *nkx3.2* and *frizzled 5/8* showing each channel individually and merged, (E''') outline of gene expression of E'''. Unless otherwise specified embryos are imaged with fluorescence microscopy and DAPI-labeled nuclei (blue). Embryos are presented in a lateral view with the apical domain at the top. Apical view (APV; image D oral side is at the right), oral view (OV). See main text for descriptions of arrows.

zic2 expression

zic2 expression (figure 3.8 - purple line) remains fairly constant from mesenchyme blastula stage (24 hours) to early gastrula stage (30 hours), when *zic2* is expressed only in the apical domain (figure 4.10 A). A double fluorescent WMISH with *zic2* and *foxQ2* shows, that *zic2* is co-expressed with *foxQ2* in the central apical domain but also in 2-3 cells (n=6) on one side of *foxQ2* (figure 4.10 B white arrow). Double fluorescent WMISH with the oral marker *fgfr1* (figure 4.10 C,D), show that *fgfr1* is co-expressed with one third of the *zic2* domain (figure 4.10 D''' white line). This shows that *zic2* extends 2-3 cells outside *foxQ2* on the aboral side and it is consistent with data so far shown, that *fgfr1* is co-expressed with the oral half of *foxQ2* (figure 4.10 D white dotted circle shows approximate location of *foxQ2*).

delta and *dcry* expression

delta is the first gene to be expressed in "scattered" cells in the apical domain already from mesenchyme blastula stage. At early gastrula stage, a second gene, *dcry* also begins to be expressed in scattered cells. *delta* expression (figure 4.1 - brown line) shows constant levels of transcription from mesenchyme blastula stage (24 hours), to early gastrula stage (30 hours). Double fluorescent WMISH with *foxQ2* confirms what was observed at mesenchyme blastula stage (figure 4.10 E white arrow), although at this stage *delta* is no longer expressed in the vegetal plate. Rotating the embryos and viewing from an apical perspective shows that *delta* is expressed as individual scattered cells along one side of *foxQ2* but is not co-expressed with *foxQ2* (figure 4.10 F') The outlines of their expression domains, illustrates this even more clearly and shows that *delta* cells are now no longer expressed within the domain of *foxQ2* and are found lined up along one side (figure 4.10 F'').

dcry expression (figure 3.8 - pink line) increases from 135 transcripts per embryo at mesenchyme blastula stage (24 hours), to 189 transcripts per embryo by early gastrula stage (30 hours). Double fluorescent WMISH with *foxQ2* shows, that *dcry* is becoming

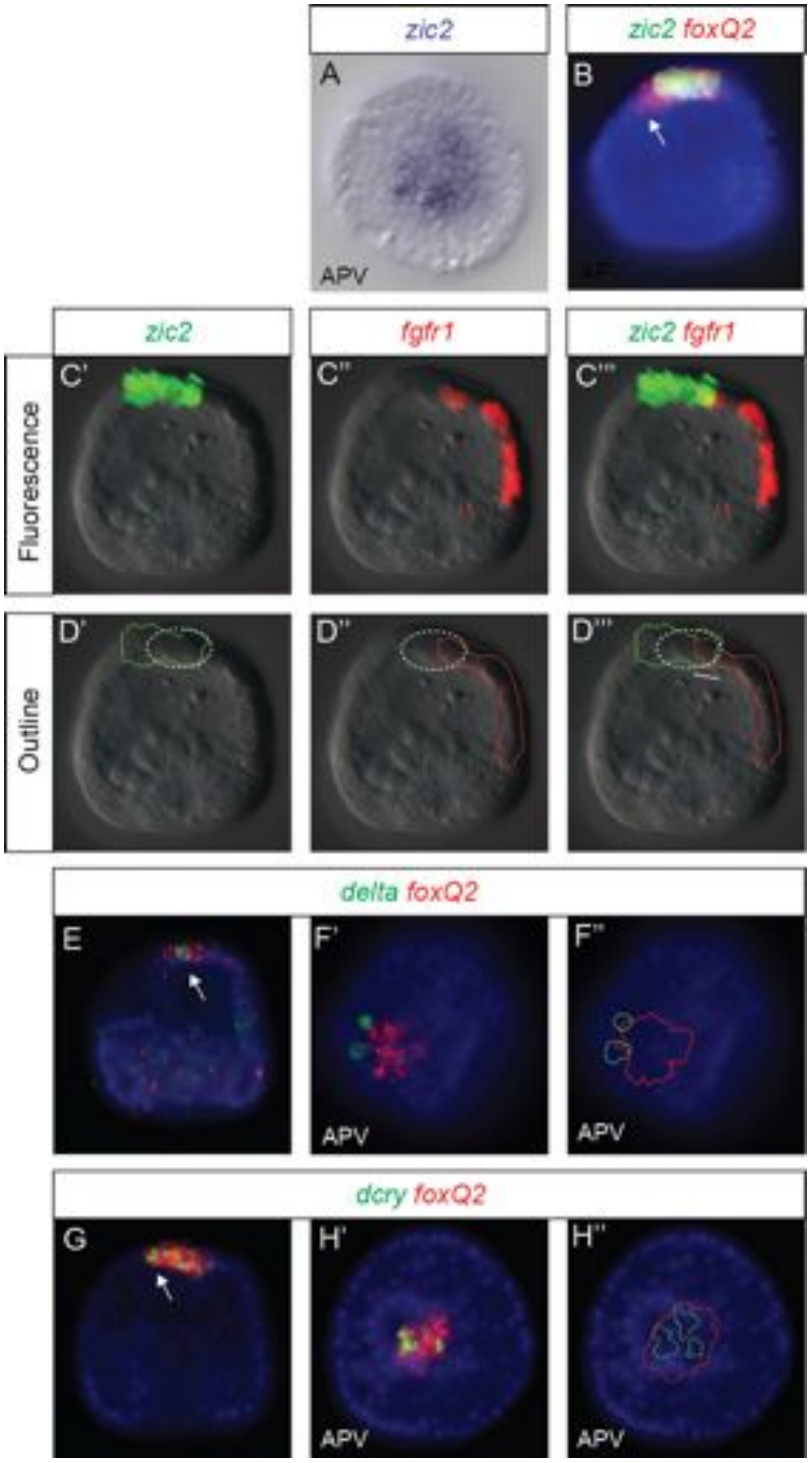

Figure 4.10. Expression analysis of *zic2*, *delta* and *dcry* at early gastrula stage
(A) DIC images of a NBT/BCIP WMISH of *zic2*. (B) Double fluorescent WMISH of *zic2* and *foxQ2.* (C,D) Double fluorescent WMISH of *zic2* and *fgfr1* showing each channel individually and merged, (D) outline of gene expression of C. (E,F) Double fluorescent WMISH of *delta* and *foxQ2,* (F'') outline of gene expression of F'. (G,H) Double fluorescent WMISH of *dcry* and *foxQ2,* (H'') outline of gene expression of H'. Unless otherwise specified embryos are imaged with fluorescence microscopy and DAPI-labeled nuclei (blue). Embryos are presented in a lateral view with the apical domain at the top (B,C,D with oral side on the right). Apical view (APV). See main text for descriptions of arrows.

expressed in distinct cells within the *foxQ2* positive central apical domain (figure 4.10 G white arrow). An apical perspective confirms that *dcry* has been downregulated in the majority of the apical domain. However, all *dcry* positive cells still appear to be co-expressed with *foxQ2* (figure 4.10 H) showing a "salt and pepper" expression pattern (see figure 4.10 H'' for outlines of expression domains). This is in sharp contrast to *delta*, which is also expressed in individual scattered cells, but adjacent to the *foxQ2* central apical domain (figure 4.10 F'').

Summary

In this section, I have used a series of double fluorescent WMISH to identify the position of several regulatory genes in the apical domain at late gastrula stage. At this stage, a number of interesting gene expression patterns and dynamics occur. The presence of *foxG* in the oral part of *foxQ2* shows that the ciliary band is formed from the most oral part of the central apical domain. *frizzled 5/8* does not form a simple concentric disk around *foxQ2* but rather is eccentric and positioned towards the oral side. In contrast to earlier stages *delta* is no longer expressed with *foxQ2* and *dcry* has started to become scattered, although is still with the *foxQ2* region. *zic2* and *fgfr1* are expressed at opposite ends of the apical domain.

4.3. Combinatorial gene expression studies of the apical domain at mid-gastrula stage

In this section, I present the results of a series of fluorescent WMISH that help to identify the different regulatory states and spatial domains that exist at mid-gastrula stage (36 hours). Interestingly, between early gastrula and mid gastrula stage, a dynamic change occurs in the expression of the apical organ landmark *foxQ2.* The domain of *foxQ2* shrinks from roughly 25 cells (5x5 arrangement) to 16 cells (an approximate 3x5 arrangement; figure 3.7). This restriction occurs along the oral-aboral axis and *foxQ2* is

cleared from the aboral half of the original central domain (Yaguchi *et al.,* 2011).

six3 expression

At mid-gastrula stage, s*ix3* expression levels (figure 3.8 - orange line) remain constant and the spatial expression shows that *six3* is expressed on either side of *foxQ2* but never co-expressed (figure 4.11 C). On one side of *foxQ2,* six3 is expressed with a much higher intensity (figure 4.11 C white arrow) than on the opposite side (figure 4.11 C turquoise arrow). The apical perspective confirms that *six3* and *foxQ2* are not co-expressed and that *six3* expresses strongly along one side of *foxQ2* (figure 4.11 D white arc), but has become more diffuse on the other sides (figure 4.11 D white arrowheads).

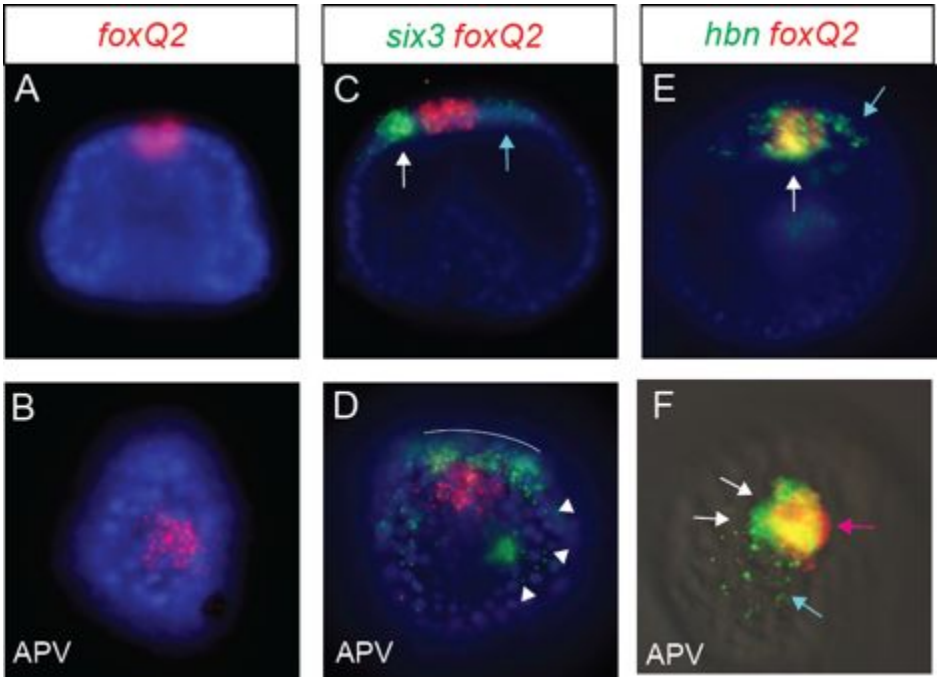

Figure 4.11. Expression analysis of *foxQ2, six3* and *hbn* at mid-gastrula stage
(A,B) Single fluorescent WMISH of *foxQ2*. (C,D) Double fluorescent WMISH of *six3* and *foxQ2*. (E,F) Double fluorescent WMISH of *hbn* and *foxQ2.* Unless otherwise specified embryos are imaged with fluorescence microscopy and DAPI-labeled nuclei (blue) or DIC. Embryos are presented in a lateral view with the apical domain at the top. Apical view (APV). See main text for descriptions of arrows.

hbn expression

The expression levels of *hbn* (figure 3.8 - green line) steadily increase to reach 742 transcripts per embryo by mid-gastrula stage (36 hours). Double fluorescent WMISH shows, that *hbn* has expanded its expression outside of *foxQ2* (figure 4.11 E turquoise arrow) and is now expressed in 10 cells (n=7) compared to 8 cells (at early gastrula stage; n=7), when viewed from a lateral perspective. However, *hbn* is still co-expressed with *foxQ2* in the central apical domain (figure 4.11 E white arrow). Viewing from an apical perspective show, that *hbn* is expressed on two sides of the *foxQ2* domain (figure 4.11 F white arrows), extends faintly along one side of the embryo (figure 4.11 F turquoise arrow) but is expressed right to the edge of *foxQ2* on the other (figure 4.11 F pink arrow)

frizzled 5/8 expression

frizzled 5/8 expression (figure 3.8 - blue line) remains constant from early gastrula stage (30 hours) to mid-gastrula (36 hours). At this stage, a vegetal view shows clear expression of *frizzled 5/8* in the oral ectoderm (figure 4.12 A black arrow) and in the oral half of gut (figure 4.12 A black arrowhead). A double fluorescent WMISH with *foxQ2* shows, that *frizzled 5/8* is expressed in 11 cells (n=14) across the apical domain and is co-expressed with *foxQ2* and in an equal number of cells on either side of *foxQ2* when viewed from an oral perspective (figure 4.12 B). An apical view shows that the disc of *foxQ2* is co-expressed with *frizzled 5/8,* but *frizzled 5/8* is expressed as a larger domain that is eccentric to *foxQ2* and shifted towards the oral side (figure 4.12 C). To understand the position of *frizzled 5/8* in more detail, I compared the outlines of their expression domains (figure 4.12 C''). This illustrates that *frizzled 5/8* is expressed equally on both lateral sides of *foxQ2* (as in figure 4.12 B'') but is shifted towards one side of *foxQ2* along the oral-aboral axis (figure 4.12 B'' compare white and turquoise bar). To further investigate *frizzled 5/8* expression relative to the oral-aboral axis, I carried out a double fluorescent WMISH with *nkx3.2*. This showed that *nkx3.2* is expressed towards the oral side of *frizzled 5/8* (figure 4.12 D white arrow). Finally, when viewed from an apical perspective, *nkx3.2* is expressed in a smaller circle inside a larger circle of *frizzled 5/8*, but is shifted towards the oral side (figure 4.12 E''' compare white bar to turquoise bar).

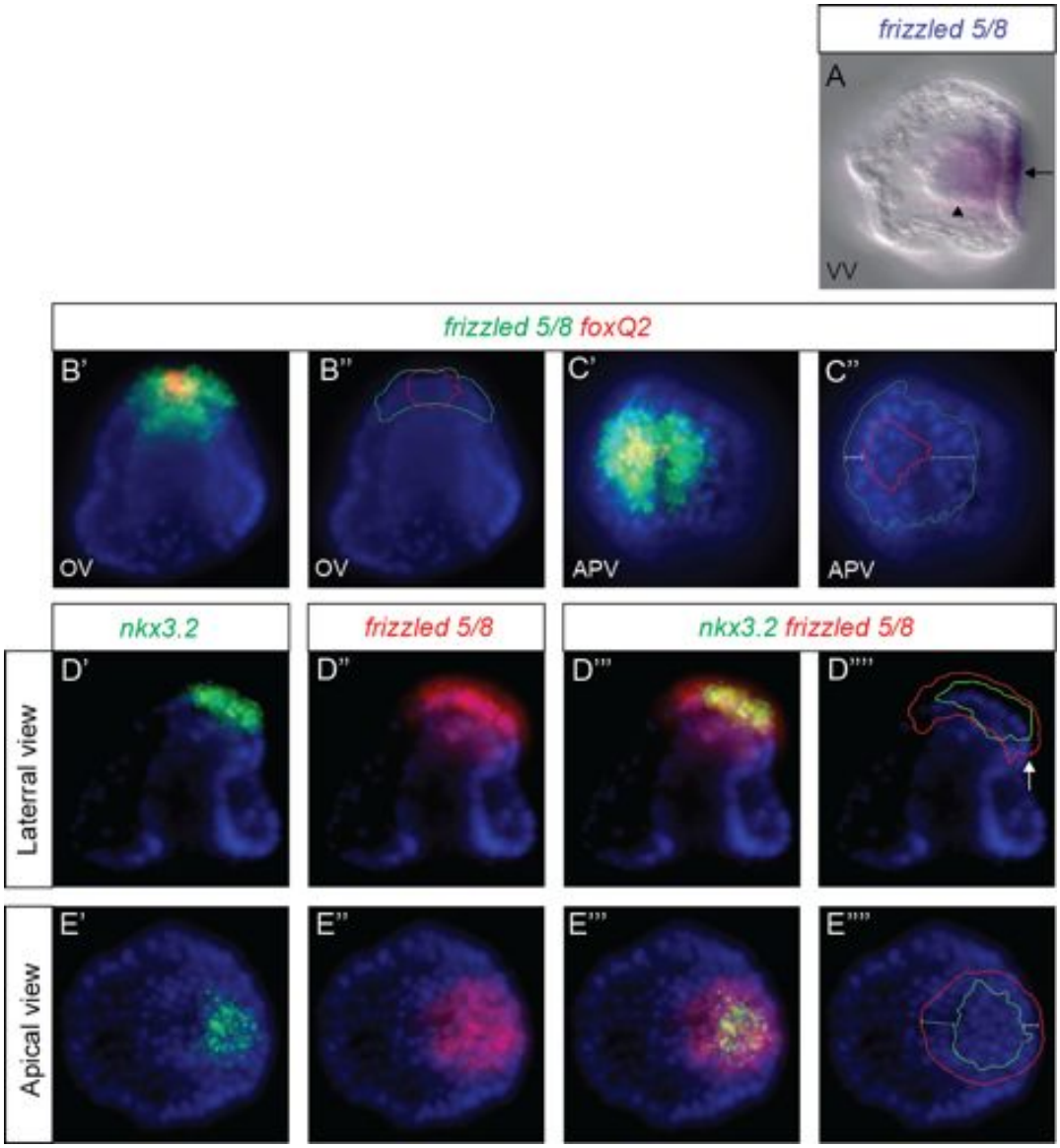

Figure 4.12. Expression analysis of *frizzled 5/8* and *nkx 3.2* at at mid-gastrula stage
(A) DIC images of a NBT/BCIP WMISH of *frizzled 5/8*. (B,C) Double fluorescent WMISH of *frizzled 5/8* and *foxQ2*,(B'') outline of gene expression of B' and (C'') outline of gene expression of C'. (D,E) Double fluorescent WMISH of *nkx3.2* and *frizzled 5/8* showing each channel individually and merged, (D''') outline of gene expression of D''' and (E'''') outline of gene expression of E'''. Unless otherwise specified embryos are imaged with fluorescence microscopy and DAPI-labeled nuclei (blue). Embryos are presented in a lateral view with oral side on the right and the apical domain at the top. Apical view (APV), Oral view (OV) ,vegetal view (VV). See main text for descriptions of arrows.

Expression of *fgf 9/16/20* and *fgfr1*

FGF signalling components continue to be expressed at mid-gastrula stage in domains relevant for the development of the apical organ. The expression of the ligand *fgf 9/16/20* (figure 4.1 - pink line) increases to 108 transcripts per embryo by mid-gastrula stage (36 hours). Double fluorescent WMISH with *foxQ2* at mid-gastrula stage, shows that *fgf 9/16/20* is expressed 2-3 cells (n=8) away from the *foxQ2* central apical domain (figure 4.13 A,B). As already described for the *P. lividus* species, *fgf 9/16/20* expression is also seen in the primary mesenchyme cells and adjacent ectoderm (figure 4.13 A), but they are not relevant for this study. Apical views clearly shows that *fgf 9/16/20* is not co-expressed with *foxQ2* (figure 4.13 B). On the other side, the expression of the receptor *fgfr1* (figure 3.8 - brown line) greatly increases from 2606 transcripts per embryo at early gastrula stage (30 hours), to 5298 transcripts per embryo by mid-gastrula (36 hours). At this stage, *fgfr1* can been seen as a broad band running down the entire oral ectoderm (figure 4.13 C). A double fluorescent *in situ* shows that *fgfr1* is co-expressed with *foxQ2* only in the oral half of the *foxQ2* domain (figure 4.13 C white arrow). Interestingly, *fgf 9/16/20* is expressed on either side of *fgfr1,* but there is no co-expression between the two genes (figure 4.13 D,E white circle in E'' represents the approximate location of *foxQ2*). Furthermore, a bilaterally symmetrical gap between the two domains of expression clearly visible.

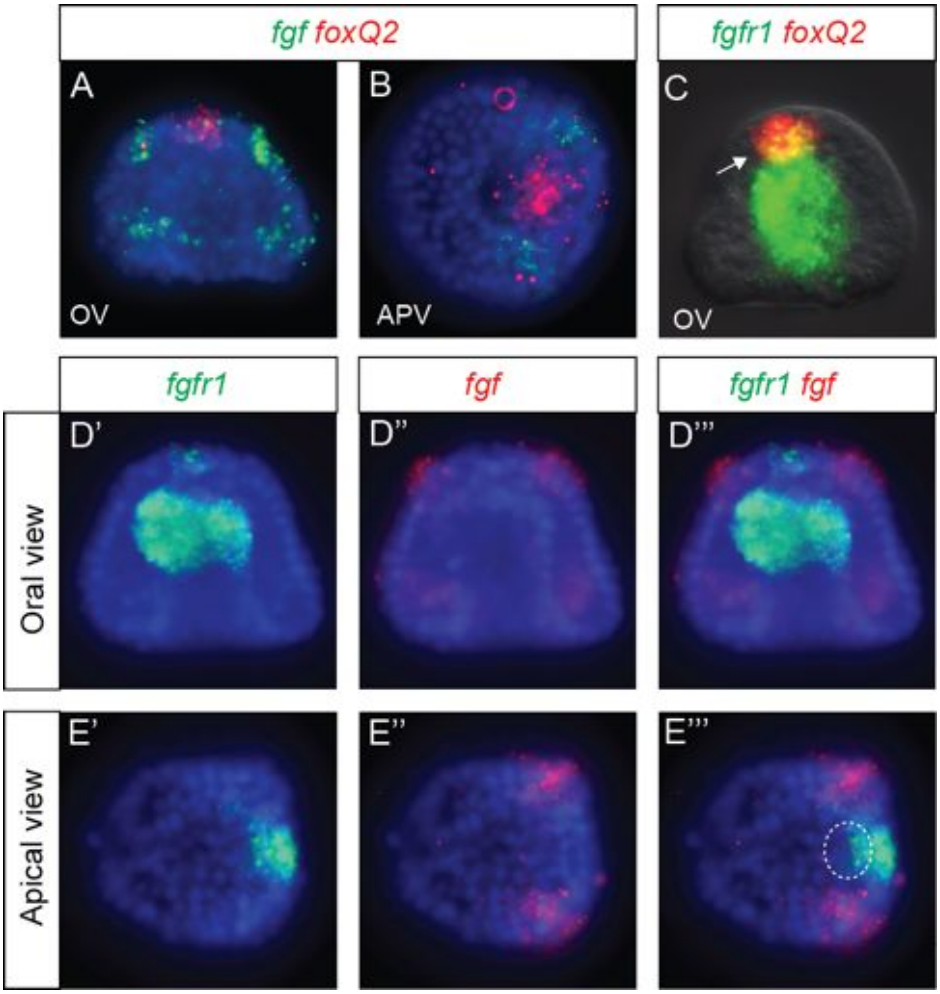

Figure 4.13. Expression analysis of *fgf 9/16/20* and *fgfr1* at mid-gastrula stage
(A,B) Double fluorescent WMISH of *fgf 9/16/20* and *foxQ2.* (C) Double fluorescent WMISH of *fgfr1* and *foxQ2.* (D,E) Double fluorescent WMISH of *fgfr1* and *fgf 9/16/20* showing each channel individually and merged. Unless otherwise specified embryos are imaged with fluorescence microscopy and DAPI-labeled nuclei (blue) or DIC. Embryos are presented in a oral view with the apical domain at the top. Apical view (APV) with oral side on the right. See main text for descriptions of arrows.

zic2 expression

zic2 expression (figure 3.8 - purple line) decreases slightly from 377 transcripts per embryo at early gastrula stage (30 hours) to 285 transcripts per embryo by mid-gastrula stage (36 hours). However, counting the number of positive cells shows that *zic2* has in fact, slightly expanded its expression across the apical domain from an average of 7 cells to 8 cells (n=10). Double fluorescent WMISH with *foxQ2* shows, that *zic2* is co-expressed with *foxQ2* in the central apical domain and in cells equally on

either side, when viewed from an oral perspective (figure 4.14 A white arrows). While a lateral view shows that *zic2* is co-expressed with *foxQ2* and also expressed in a few cells in the aboral apical domain (figure 4.14 B white arrow), similar to what has already been observed at early gastrula stage.

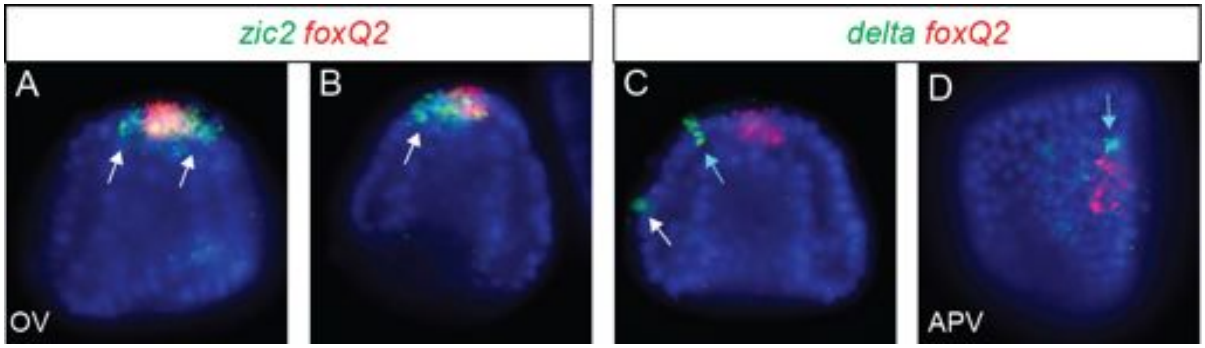

Figure 4.14. Expression analysis of *zic2* and *delta* at mid-gastrula stage
(A,B) Double fluorescent WMISH of *zic2* and *foxQ2.* (B,C) Double fluorescent WMISH of *delta* and *foxQ2.* Unless otherwise specified embryos are imaged with fluorescence microscopy and DAPI-labeled nuclei (blue). Embryos are presented in a lateral view with the oral side at the right and the apical domain at the top. Apical view (APV), oral view (OV). See main text for descriptions of arrows.

delta expression

In terms of transcripts per embryo, *delta* expression remains almost constant after the start of gastrulation (30 hours; figure 4.1 - brown line). However, the actual number of *delta* positive cells, increases considerably when early and mid-gastrula stage are compared. Similarly to what was observed at early gastrula stage, *delta* is not co-expressed with *foxQ2* but rather, is found in individual cells at the aboral edge of the *foxQ2* central apical domain (figure 4.14 C,D turquoise arrows). At mid gastrula stage, *delta* also begins to be expressed in individual cells in the ectoderm (figure 4.14 C white arrow) in a domain consistent with the ciliary band.

dcry expression

dcry expression (figure 3.8 - pink line) decreases to 178 transcripts per embryo by mid-gastrula stage (36 hours). *dcry* spatial expression continues to be highly dynamic. In fact, the majority of *dcry* positive cells are now expressed as individual cells outside the *foxQ2* domain (figure 4.15 A,B white arrows). This is quite a dramatic change from even a few hours earlier, when all *dcry* positive cells were found only within the *foxQ2* apical domain. However, in some embryos (n=13) *dcry* expression is still observed in a number of indistinct cells within the *foxQ2* apical domain (figure 4.15 B). The outlines of their expression domains (figure 4.15 B'') shows clearly that two distinct cells (white arrows) are expressed outside the *foxQ2* region, while some remaining expression of *dcry* is found within (turquoise arrow).

To expand my regulatory state analysis of *dcry,* I carried out a double fluorescent WMISH with either *mox,* a homeobox transcription factor expressed in the same cells as serotonin in the sea urchin (Poustka *et al.,* 2007) or *z167,* a transcription factor required for the differentiation of photoreceptor cells in *Drosophila* (Moses and Rubin, 1991). *mox* (figure 4.1 - orange line) begins to be expressed at mid-gastrula stage (30 hours) with half of embryos (n=12) showing a single *mox* positive cell and the remainder showing no expression (compare figure 4.15 C and D). However, embryos that do express a *mox* positive cell (figure 4.15 D'' white arrow) show clear co-expression with *dcry* (figure 4.15 D''' turquoise arrow). *z167* (figure 4.1 - green line) begins to be expressed at the beginning of gastrulation (30 hours) and is expressed in single cells in the apical organ (figure 4.15 E,F). At mid-gastrula stage, it is clear in embryos viewed from both a lateral and an apical perspectives, that *z167* postive cells (figure 4.15 E''', F''' white arrows) are not co-expressed with *dcry* (figure 4.15 E''',F''' turquoise arrow).

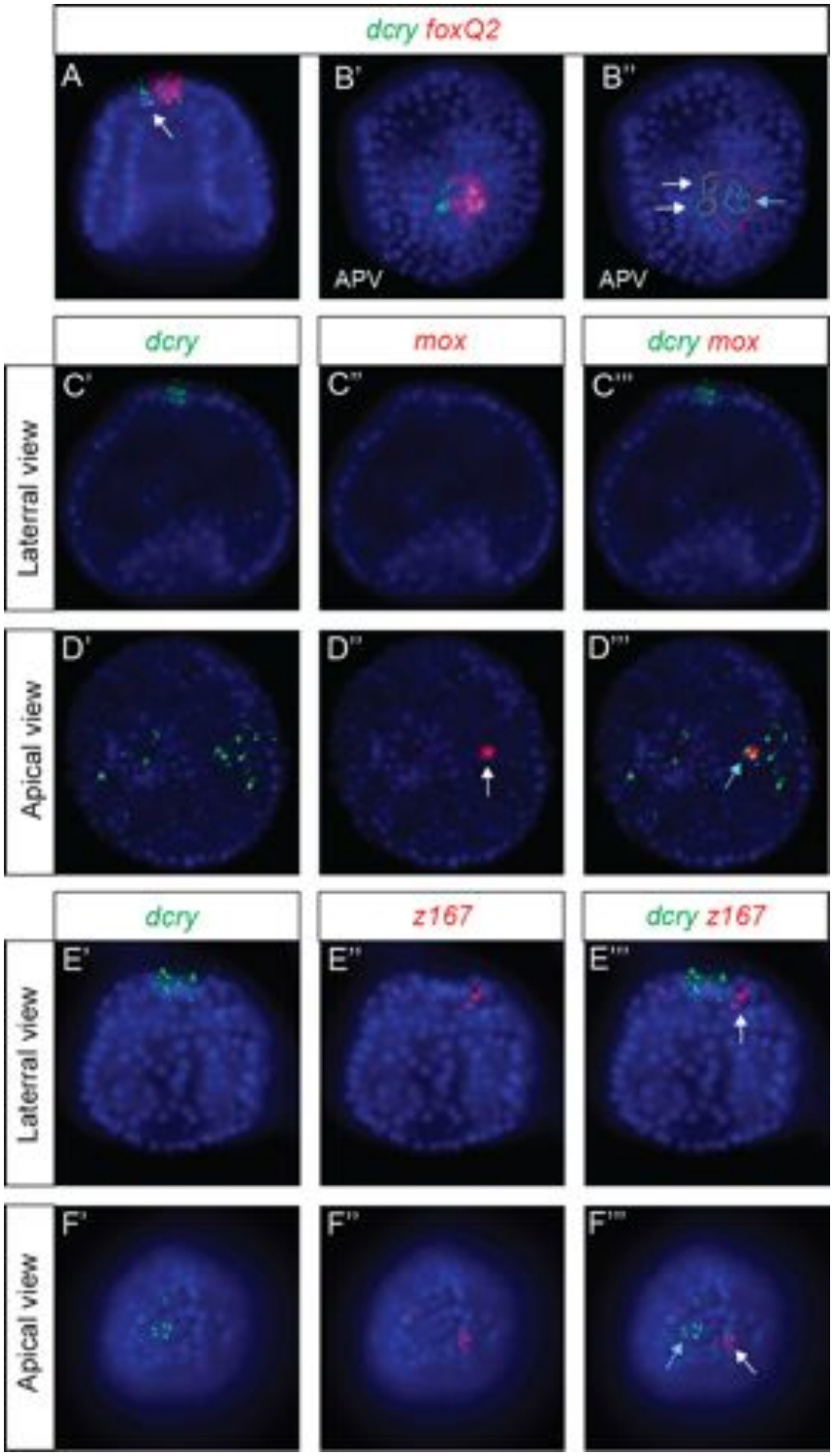

Figure 4.15. Expression analysis of *dcry, mox* and *z167* at mid-gastrula stage

(A,B) Double fluorescent WMISH of *dcry* and *foxQ2,* (B'') outline of gene expression of B'. (C,D) Double fluorescent WMISH of *dcry* and *mox* showing each channel individually and merged. (E,F) Double fluorescent WMISH of *dcry* and *z167* showing each channel individually and merged. Unless otherwise specified embryos are imaged with fluorescence microscopy and DAPI-labeled nuclei (blue). Embryos are presented in a lateral view with the apical domain at the top. Apical view (APV). See main text for descriptions of arrows.

Cellular maps and summary

In this section, I have used a series of double fluorescent WMISH to identify the position of several regulatory genes in the apical domain at mid-gastrula stage. All these data were combined, integrated and subsequently overlaid onto cellular maps. Figure 4.16 shows cellular maps for the eight regulatory genes studied at this stage. For many of the genes studies, their overall position in the apical organ has not changed greatly since early gastrula stage. The two most dynamic genes have been *foxQ2* itself, which has restricted its expression domain along the oral-aboral axis and *dcry* which at this stage is now expressed on the aboral edge of *foxQ2. dcry* and *mox* are found in the same cells but not *dcry* and *z167.*

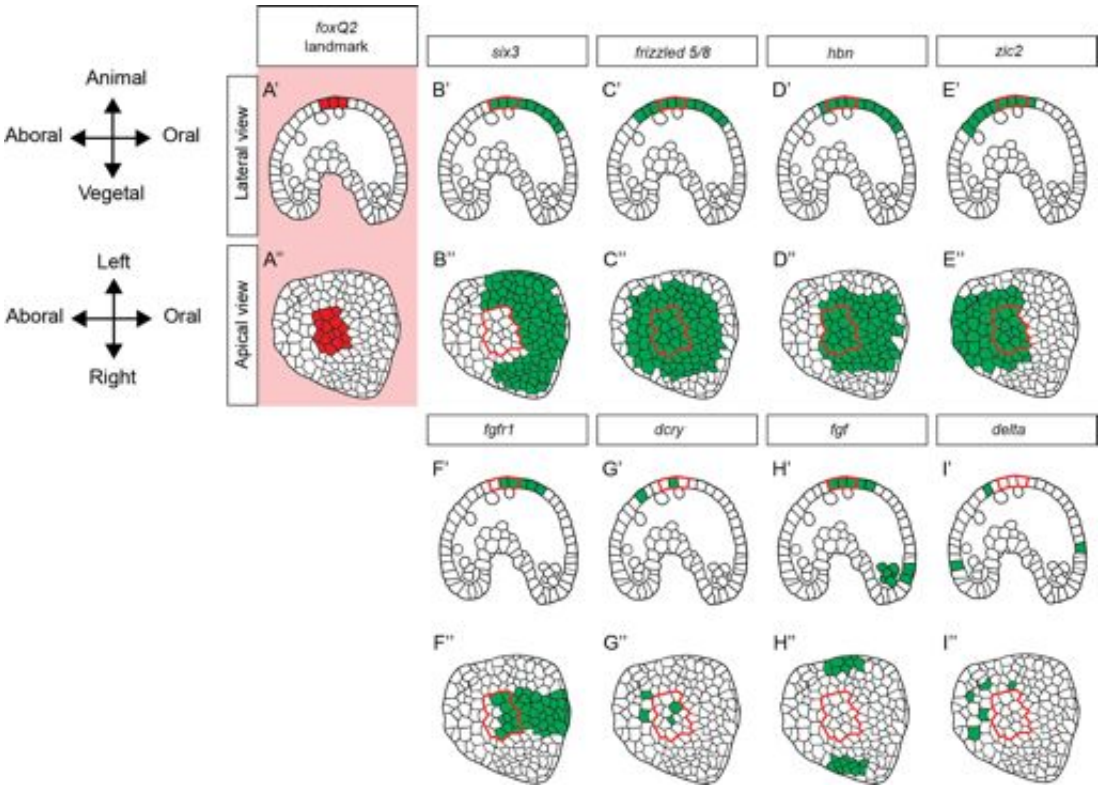

Figure 4.16. Cellular maps of gene expression at mid-gastrula stage
Lateral and apical view of mid-gastrula stage cellular maps. (A) *foxQ2* expression (red). (B-I) Expression of other regulatory genes (green) with outline of *foxQ2* (red line).

Chapter 5

Regulatory state analysis:

the late embryo

In this chapter, I extend my analysis of the apical domain regulatory states into the late embryo and in some cases the early pluteus larvae. The two developmental stages studied in this chapter are: (1) Late gastrula, which occurs at 48 hours and is characterised by a fully invaginated archenteron, which fuses with the oral ectoderm. The apical domain at this stage still retains an apical tuft, made by long cilia, and the first serotonin positive cells begin to appear; (2) Pluteus larva, which occurs around 72 hours and marks the end of embryonic development and the beginning of the fully differentiated larval stage in the life cycle. The apical organ is characterised by a thick epithelium, several serotonergic and non-serotonergic neurons and supporting cells. For the majority of the genes that have been studied so far, I conclude my gene expression analysis at late gastrula stage. However, a subset of genes that are potentially linked to the function of this neurosensory structure (*e.g.* the circadian photoreceptor *dcry*) are studied in more detail at both late gastrula stage and pluteus larva using immunohistochemistry and detailed confocal microscopy.

5.1. Combinatorial gene expression studies of the apical domain at late gastrula stage

foxG expression

foxG expression (figure 4.1 - blue line) remains quite constant during gastrulation (from 30 hours onwards), and is strongly expressed in the ciliary band at late gastrula (figure 5.1 C). Double fluorescent WMISH of *foxG* and *foxQ2* shows that *foxG* is co-expressed with only the oral cells of the *foxQ2* domain when viewed from a lateral perspective (figure 5.1 C white arrow). This is shown even more clearly in embryos imaged from an apical perspective (figure 5.1 D white dashed line). Hence the cells of the apical domain contribute to the ciliary band but only the most oral part of the *foxQ2* positive apical domain.

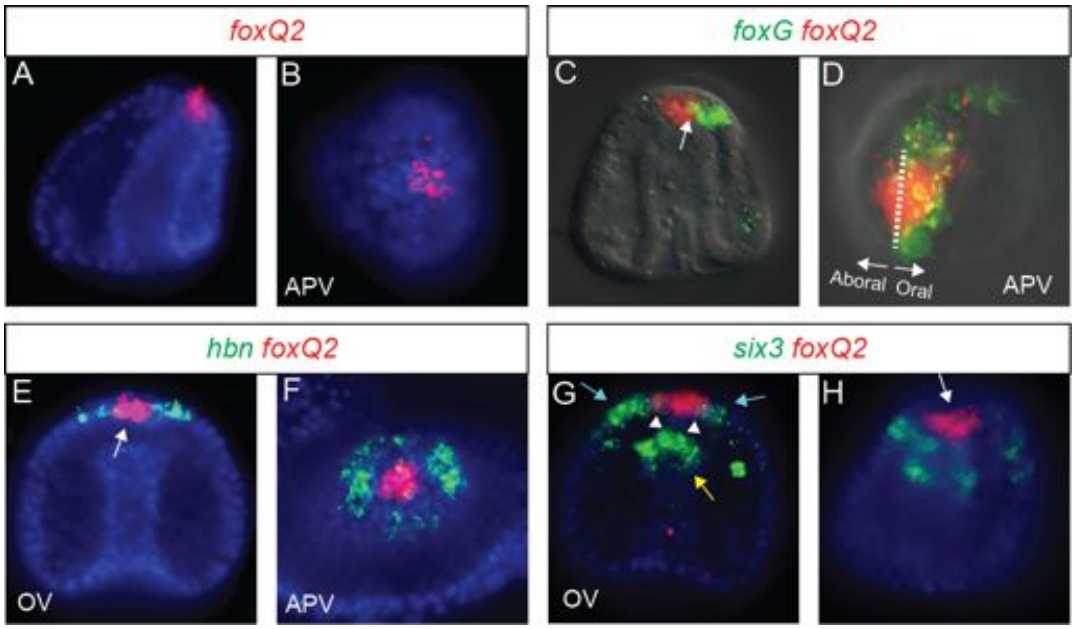

Figure 5.1. Expression analysis of *foxQ2, foxG, hbn* and *six3* at late gastrula stage
(A,B) Single fluorescent WMISH of *foxQ2*. (C,D) Double fluorescent WMISH of *foxG* and *foxQ2*. (E,F) Double fluorescent WMISH of *hbn* and *foxQ2.* (G,H) Double fluorescent WMISH of *six3* and *foxQ2.* Unless otherwise specified embryos are imaged with fluorescence microscopy and DAPI-labeled nuclei (blue) or DIC. Embryos are presented in a lateral view with the oral side at the right and the apical domain at the top. Apical view (APV), oral view (OV). See main text for descriptions of arrows.

hbn expression

hbn transcripts decrease (figure 3.8 - green line) from 724 transcripts per embryo at mid gastrula stage (36 hours), to 558 transcripts per embryo at late gastrula stage (48 hours). This is accompanied by a dramatic change in the spatial expression of *hbn* (compare figure 4.2 D,E with figure 5.1 E,F). Double fluorescent WMISH with *foxQ2* shows that in late gastrula stage, *hbn* clears completely from the central apical domain and is no longer co-expressed with *foxQ2* (figure 5.1 E white arrow). Viewing embryos from an apical perspective, clearly shows that *hbn* is expressed in a ring of 3 to 4 cells (n=5) wide surrounding *foxQ2* (figure 5.1 F).

six3 expression

The gene encoding the transcription factor *six3* (figure 3.8 - orange line) decreases in its expression from 1815 transcripts per embryo during mid-gastrula stage to reach 1457 transcripts per embryo at late gastrula (48 hours). At this stage, *six3* is expressed broadly but not in the centre of the apical domain marked by *foxQ2.* Fluorescent WMISH shows that *six3* is expressed in 5 to 6 cells (n=5) at either side of *foxQ2* (figure 5.1 G turquoise arrows) when viewed from an oral perspective. However, *six3* is still not co-expressed with *foxQ2* in the central apical domain (figure 5.1 G white arrowheads and figure 5.1 H white arrow) At this stage, six3 is also expressed at the tip of the archenteron (figure 5.1 G yellow arrow). A vegetal view (data not shown) shows that *six3* is expressed in the oral half of the archenteron and in the oral ectoderm. This is consistent with what is previously published (Wie *et al.,* 2009) and confirms previous suggestions that *six3* is not expressed in the most aboral side of the apical domain during development

frizzled 5/8 expression

frizzled 5/8 expression (figure 3.8 - blue line) remains constant from mid-gastrula stage (36 hours) to the end of gastrulation (48 hours). At this stage, *frizzled 5/8* is expressed in the apical domain and the tip of the archenteron (figure 5.2 A). Double fluorescent *in situ* with *foxQ2* shows that *frizzled 5/8* is expressed in a large domain of 12 cells (n=13) across the apical domain. It is co-expressed with *foxQ2* only in the central part of the domain and its expression extends on the oral and aboral sides of *foxQ2* (figure 5.2 A). At this stage, the morphology of the embryos allows us to distinguish between oral and aboral ectoderm without the necessity to use molecular markers. Different views confirm that *frizzled 5/8* is expressed in the apical domain as a larger disc than *foxQ2* (figure 5.2 B) and that it is co-expressed with *foxQ2* only in the centre. Together, this confirms that *frizzled 5/8* expression is more pronounced on the oral side of *foxQ2.* Double fluorescent WMISH between *fgf 9/16/20* and *frizzled 5/8* shows that *fgf 9/16/20* is expressed in two bilateral blocks either side of *frizzled 5/8* with no co-expression between them (figure 5.2 C). Apical views taken from a focal plane below the surface, show *frizzled 5/8* in the oral ectoderm, possibly showing some small overlap of expression with *fgf 9/16/20* expression (figure 5.2 D' white arrows). What seems likely is that the two domains are exactly adjacent to each other. Double fluorescent WMISH with *frizzled 5/8* and *nkx3.2,* shows that *nkx3.2* is co-expressed within the domain of *frizzled 5/8.* Although *nkx3.2* is expressed nearer to the oral side of *frizzled 5/8* (figure 5.2 E'' compare white bar-aboral side and turquoise bar-oral side). Viewing embryos from an oral perspective shows that *nkx3.2* is expressed in the central region of *frizzled 5/8* expression with *frizzled 5/8* expressed equally on both sides (figure 5.2 F'' white arrows). DAPI counterstaining, observed from an apical perspective, shows that *nkx3.2* is expressed in a disc roughly 5 cells by 7 cells (n=9) and that this disc of expression is eccentric and shifted towards the oral side of a larger disc of cells that express *frizzled 5/8* (figure 5.2 G white arrow marks the aboral side).

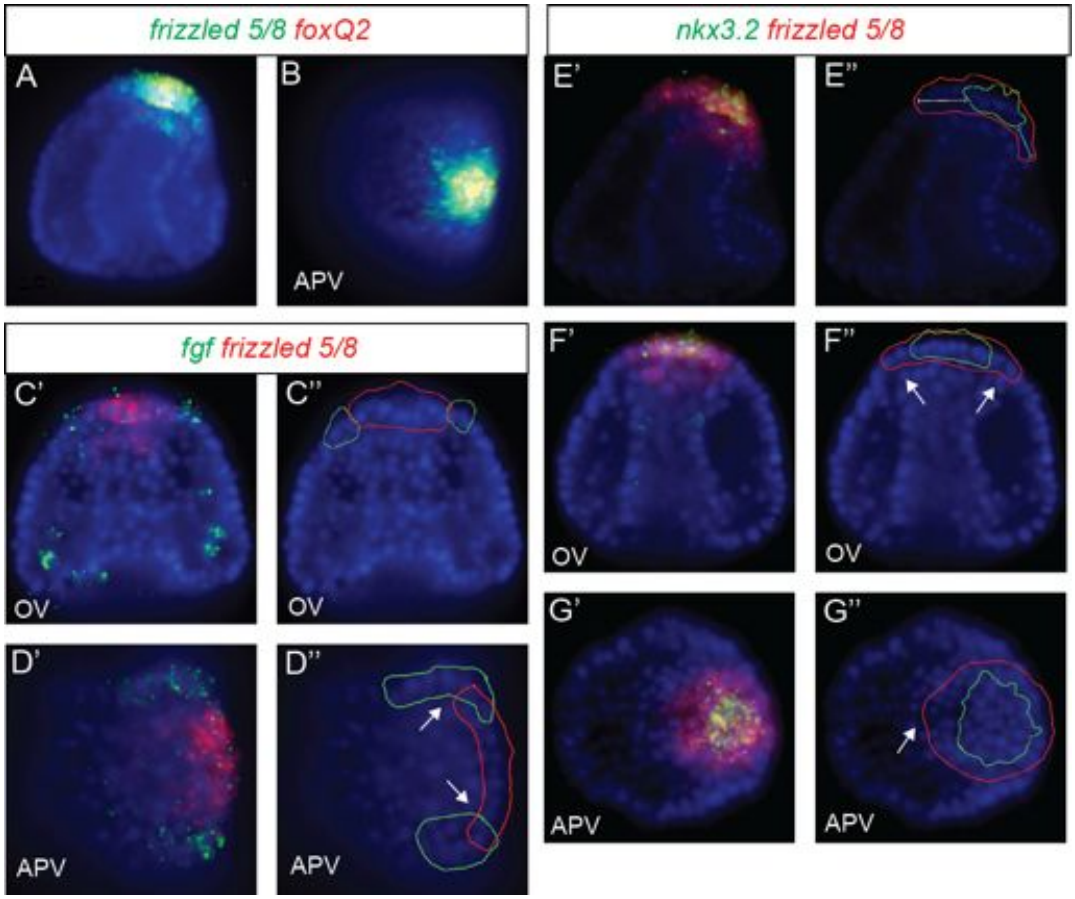

Figure 5.2. Expression analysis of *frizzled 5/8, fgf 9/16/20* and *nkx 3.2* at late gastrula stage
(A,B) Double fluorescent WMISH of *frizzled 5/8* and *foxQ2*. (C,D) Double fluorescent WMISH of *fgf* and *frizzled 5/8,* (C'') outline of gene expression of C' and (D'') outline of gene expression of D'. (E-G) Double fluorescent WMISH of *nkx3.2* and *frizzled 5/8,* (E'') outline of gene expression of E', (F'') outline of gene expression of F' and (G'') outline of gene expression of G'. Unless otherwise specified embryos are imaged with fluorescence microscopy and DAPI-labeled nuclei (blue). Embryos are presented in a lateral view with the oral side at the right and the apical domain at the top. Apical view (APV), oral view (OV). See main text for descriptions of arrows.

fgf 9/16/20 and *fgfr1* expression

fgf 9/16/20 expression (figure 4.1 - pink line) remains more or less constant during gastrulation. Double fluorescent *in situ* with the landmark *foxQ2* shows that *fgf* 9/16/20 is expressed on each side *foxQ2* and expression starts parallel to the aboral edge of *foxQ2* (figure 5.3 A white dashed line shows the domains share the same aboral boundary) and continues past the oral edge of *foxQ2* (figure 5.3 A yellow dashed line). Interestingly, a gap of 1-2 cells separates each side the *foxQ2* from the *fgf 9/16/20* expression domains. On the other hand, the gene encoding for the receptor *fgfr1* (figure

3.8 - brown line) increases its expression by ~ 1500 transcripts to reach 6937 transcripts per embryo at late gastrula stage (48 hours). *fgfr1* remains expressed through the gut (figure 5.3 B) and a double fluorescent WMISH with *foxQ2* show co-expression in a small domain within *foxQ2* (figure 5.3 B turquoise arrow). A lateral view shows that *fgfr1* is co-expressed with the oral most cells of the *foxQ2* domain (figure 5.3 C turquoise arrow). It is also weakly expressed in the oral ectoderm (figure 5.3 C white arrow) while it is completely cleared from the vegetal half of the oral ectoderm. Double fluorescent WMISH of *fgf 9/16/20* and *fgfr1* shows that *fgfr1* is expressed clearly in a small domain in the apical organ (figure 5.3 D', E' and F' white arrows). *fgf 9/16/20* is expressed in two domains either side of *fgfr1* and there is no co-expression between them (figure 5.3 E''' and F''').

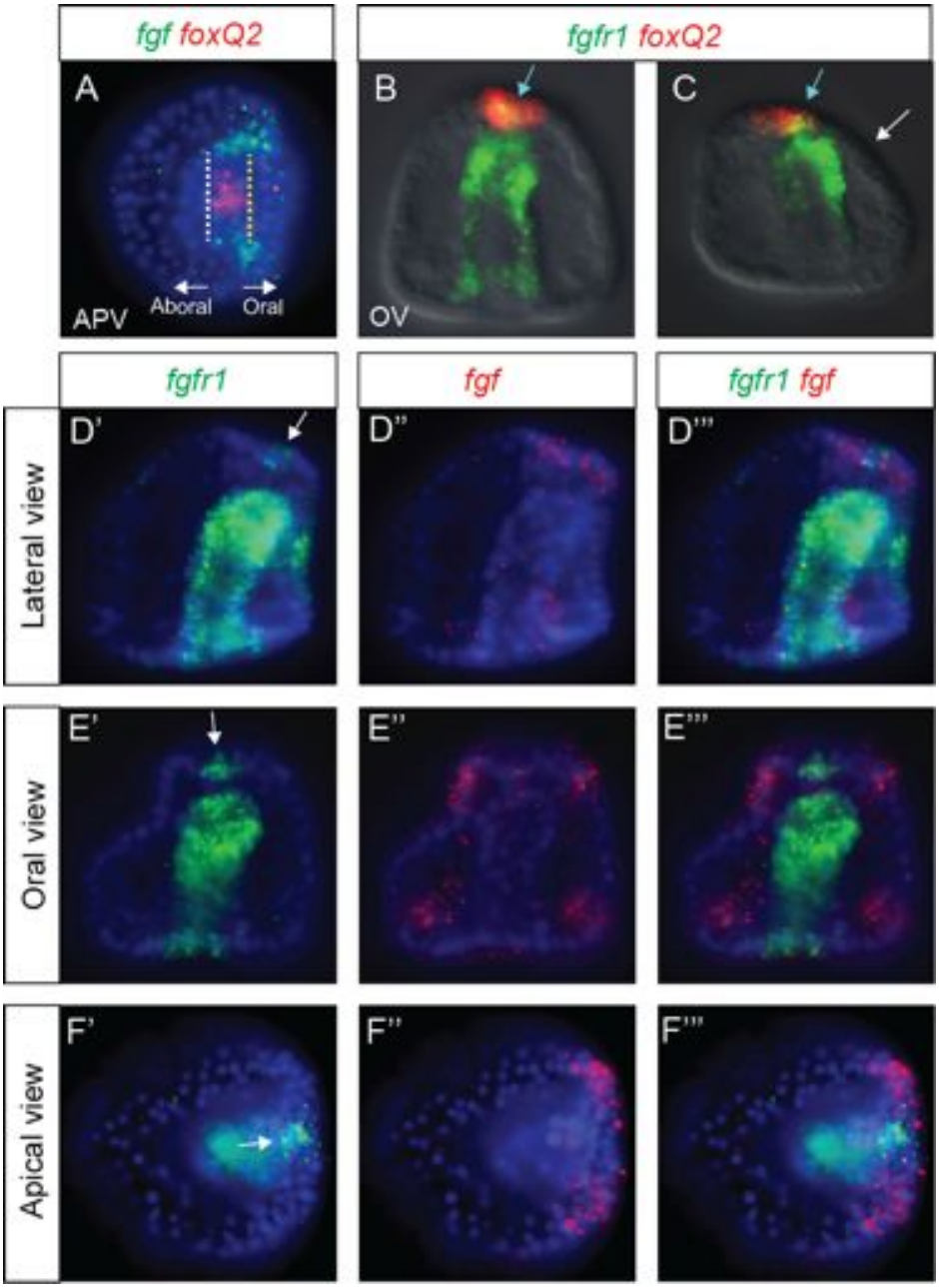

Figure 5.3. Expression analysis of *fgf 9/16/20* and *fgfr1* at late gastrula stage
(A) Double fluorescent WMISH of *fgf* 9/16/20 and *foxQ2*. (B,C) Double fluorescent WMISH of *fgfr1* and *foxQ2.* (D-F) Double fluorescent WMISH of *fgf* 9/16/20 and *fgfr1* showing each channel individually and merged. Unless otherwise specified embryos are imaged with fluorescence microscopy and DAPI-labeled nuclei (blue) or DIC. Embryos are presented in a lateral view with the oral side at the right and the apical domain at the top. Apical view (APV), oral view (OV). See main text for descriptions of arrows.

zic2 expression

zic2 expression (figure 3.8 - purple line) slightly decreases during gastrulation to reach 202 transcripts per embryo by late gastrula stage (48 hours). At this stage, *zic2* is partially co-expressed with *foxQ2,* but also expressed outside the foxQ2 domain distinctly on the aboral side (figure 5.4 A white arrow). An apical view shows that *zic2* is expressed only in the aboral half of the *foxQ2* domain (figure 5.4 B white arrow). Expression can also be seen on either of the lateral sides of *foxQ2* (figure 5.4 B pink arrowheads) and into the aboral apical domain (figure 5.4 B turquoise arrow). Double fluorescent WMISH with *fgfr1,* a marker for the oral apical domain, shows that *zic2* broadly expressed in the apical domain (Figure 5.4 E'), while *fgfr1* shows expression in a small region of the oral apical domain (Figure 5.4 E'' white arrow). The outlines of their expression domains shows that *zic2* and *fgfr1* are not co-expressed and border each other (Figure 5.4 E'''' white arrow). This is consistent with the result that *zic2* is expressed in the aboral half of *foxQ2* domain and *fgfr1* in the oral half.

delta expression at late gastrula

At this stage, *delta* is expressed in single cells in the apical domain and in the ciliary band. Double fluorescent WMISH with *foxQ2* shows that *delta* is expressed in scattered cells in the aboral apical domain outside the *foxQ2* domain (figure 5.4 C white arrow). Viewing embryos from a partial apical view confirms that *delta* is expressed in single scattered cells on the aboral side of *foxQ2* and are not co-expressed (figure 5.4 D white arrowheads).

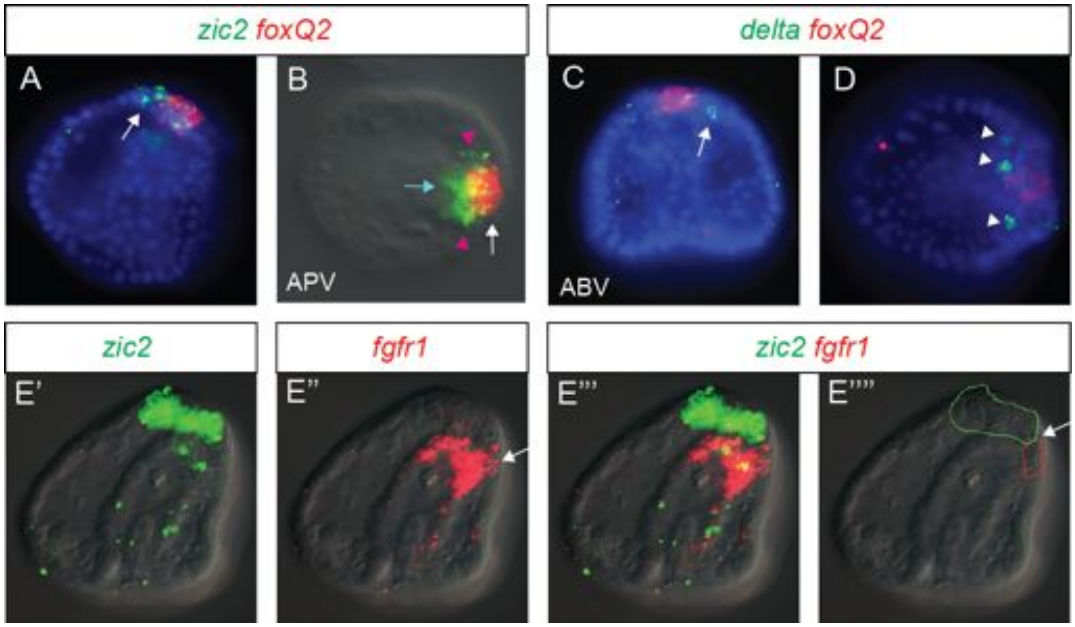

Figure 5.4. Expression analysis of *zic2, fgfr1,* and *delta* at late gastrula stage
(A,B) Double fluorescent WMISH of *zic2* and *foxQ2*. (C,D) Double fluorescent WMISH of *delta* and *foxQ2.* (E) Double fluorescent WMISH of *zic2* and *fgfr1* showing each channel individually and merged, (E'''') outline of gene expression domains of E'''. Unless otherwise specified embryos are imaged with fluorescence microscopy and DAPI-labeled nuclei (blue) or DIC. Embryos are presented in a lateral view with the oral side at the right and the apical domain at the top. Apical view (APV), aboral view (ABV). See main text for descriptions of arrows.

Cellular maps and summary

In this section, I have used a series of double fluorescent WMISH to identify the position of several regulatory genes in the apical domain at late gastrula stage. All these data were combined, integrated and subsequently overlaid onto cellular maps. Figure 5.5 shows cellular maps for the nine regulatory genes studied at this stage. The central apical domain is surrounded by a horseshoe pattern of *six3* and a ring of *hbn* cells. *foxQ2* is found inside a large disc of *frizzled 5/8* that is shifted towards the oral ectoderm. *zic2* is expressed in the aboral apical domain and *fgfr1* is expressed in the oral side. *dcry* and *delta* are expressed in scattered cells on the aboral side of *foxQ2. fgf 9/16/20* is expressed on either lateral side of foxQ2 and finally *foxG* is expressed in the ciliary band and overlaps with the oral most row of *foxQ2.*

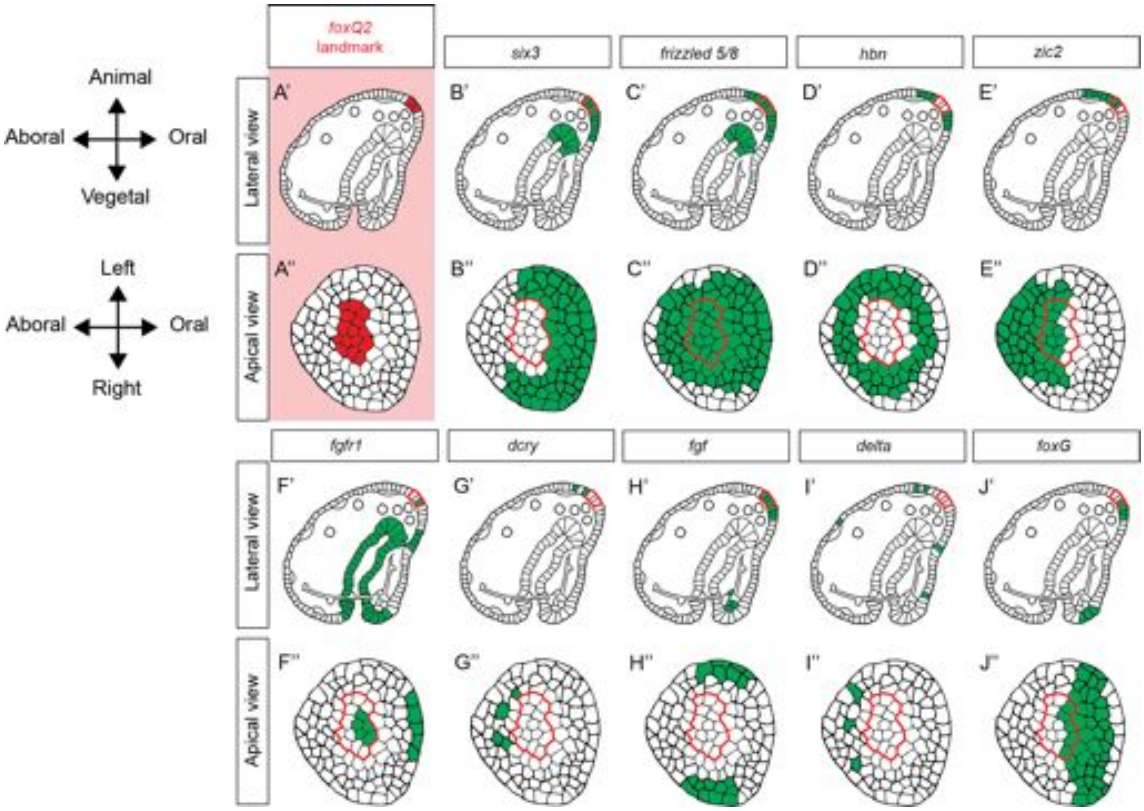

Figure 5.5. Cellular maps of regulatory gene expression at late gastrula stage
Lateral and apical views of late gastrula stage cellular maps. (A) *foxQ2* expression (red). (B-J) Expression of other regulatory genes (green) with outline of *foxQ2* (red line).

5.2. Combinatorial gene expression studies of *dcry, mox* and *z167* in the apical domain at late gastrula stage and pluteus larvae

dcry expression (figure 3.8 - pink line) decreases from 178 transcripts to 135 transcripts per embryo by late gastrula (48 hours). At this stage, a double fluorescent in situ with *foxQ2* shows that *dcry* is expressed in individual scattered cells on the aboral edge of *foxQ2* (figure 5.6 A,B white arrowheads). To investigate the regulatory state of these cells in more detail, I carried out double fluorescent WMISHs with two transcription factor genes expressed in single cells in the apical domain, *mox* and *z167*. At this stage, *mox* is consistently expressed in the same cells as *dcry* (figure 5.6 C yellow arrowheads). Similar expression pattern is seen for *z167* (figure 5.5 D white arrowheads) however, some *dcry* positive cells do not express *z167* (figure 5.5 C yellow arrowhead).

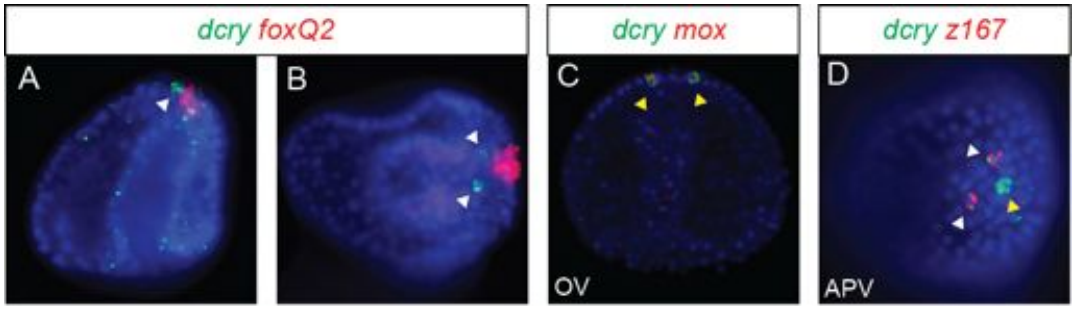

Figure 5.6. Expression analysis of *dcry, mox,* and *z167* at late gastrula stage
(A,B) Double fluorescent WMISH of *dcry* and *foxQ2*. (C) Double fluorescent WMISH of *dcry* and *mox.* (D) Double fluorescent WMISH of *dcry* and *z167.* Unless otherwise specified embryos are imaged with fluorescence microscopy and DAPI-labeled nuclei (blue). Embryos are presented in a lateral view with the oral side at the right and the apical domain at the to. Apical view (APV), oral view (OV). (B) is a partial apical view. See main text for descriptions of arrows.

To understand these results in more detail and confirm true co-expression, these double fluorescent WMISHs were analysed using single-slice confocal microscopy. In addition, to appreciate the relationship between these genes and serotonergic neurons, the embryos were stained for serotonin using immunohistochemistry. Double fluorescent WMISH confirmed that *mox* is co-expressed with *dcry* (figure 5.7 C' and C'' white arrowheads) and that all *z167* positive cells co-express *dcry* (figure 5.7 G' and G'' white arrowheads) but some *dcry* positive cells did not express *z167* (figure 5.7 G' yellow arrowhead and G'' pink arrowhead). In some embryos, a single serotonin positive cell is seen in the apical domain; in half of the embryos studied this cell expresses *dcry,* while the other half this serotonin cells does not express *dcry* or *z167* (n=6; figure 5.7 G'' pink arrowhead). Nuclei staining with DAPI can be used to count the number of cells that express each of the three genes being studied. A slice-by-slice analysis of confocal projections showed that on average in a late gastrula stage embryo, *dcry* is expressed in 4 cells (n=9), *mox* is expressed in 3 cells (n= 4) and *z167* is expressed in 2 cells (n=6). This leads to the conclusion that there are actually different sets of *dcry* positive cells, the ones that express *mox* and *z167* and the ones that express *mox* only. Alternatively, this could just be the result of very dynamic and transient expression of either *mox* or *z167*.

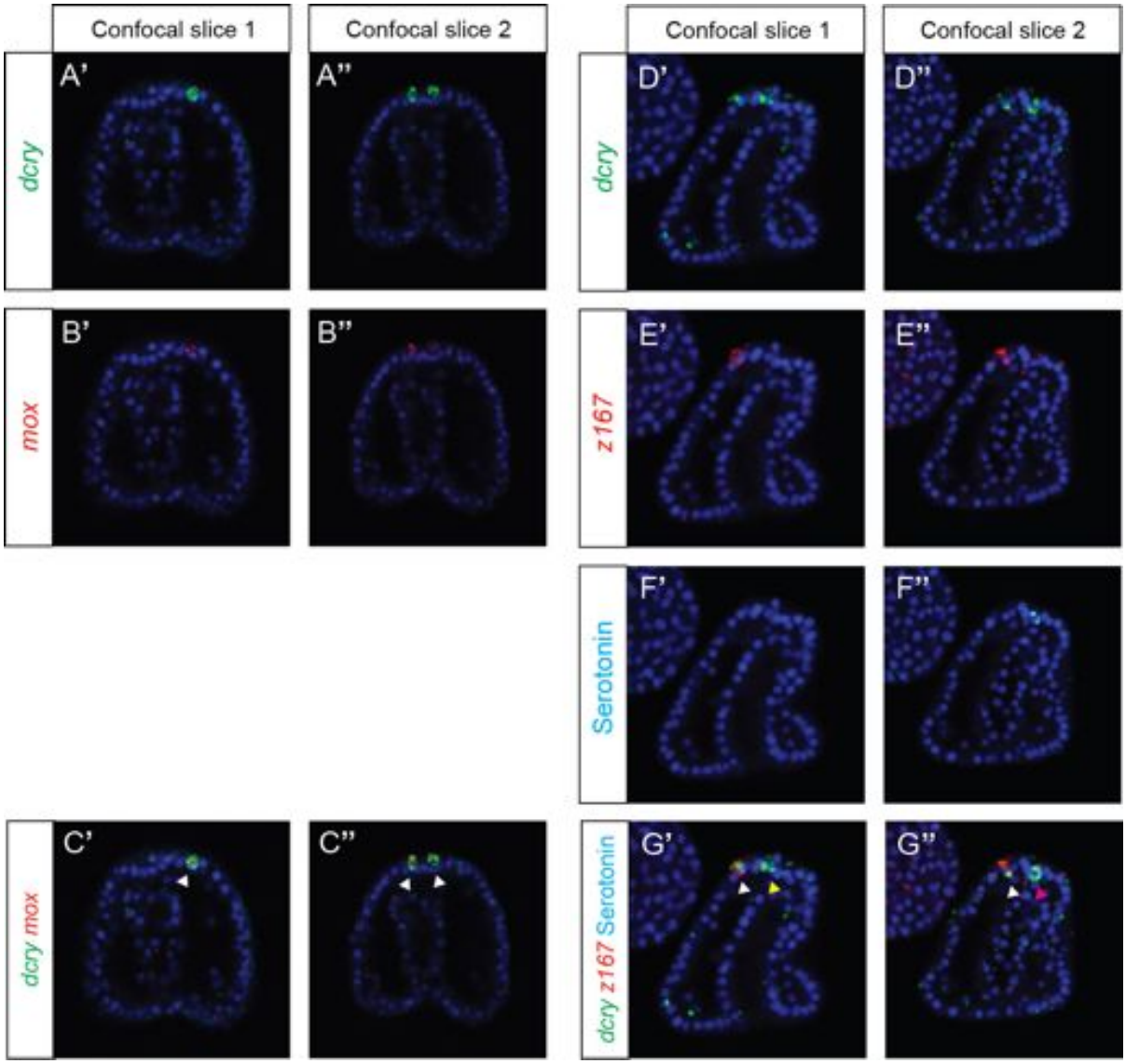

Figure 5.7. Analysis of single-slice confocal images of *dcry, mox,* and *z167* at late gastrula stage
(A-C) Double fluorescent WMISH of *dcry* and *mox*. Oral view showing individual and merged channels from two different single confocal slices. (D-G) Double fluorescent WMISH of *dcry* and *z167* combined with serotonin antibody staining. Lateral view (oral side to right) showing individual and merged channels from two different single confocal slices. DAPI-labeled nuclei (blue). See main text for descriptions of arrows.

The dynamic of expression of these three genes is quite dramatic and indeed by early pluteus larva the regulatory state of *dcry* cells has changed significantly. In contrast to late gastrula stage, *dcry* and *mox* are no longer co-expressed in pluteus larvae (figure 5.8 C white and yellow arrowheads) on the contrary *dcry* and *z167* are completely co-expressed (figure 5.8 G' yellow arrowhead and G'' pink arrowhead). Nuclei stained with DAPI were again used to count the number of cells that express each of the three genes being studied. A slice-by-slice analysis of confocal projections show that on average in

an early pluteus larvae, *dcry* is expressed in 2 cells (n=9), *mox* is expressed in 4 cells (n= 3) and *z167* is expressed in 2 cells (n=7).

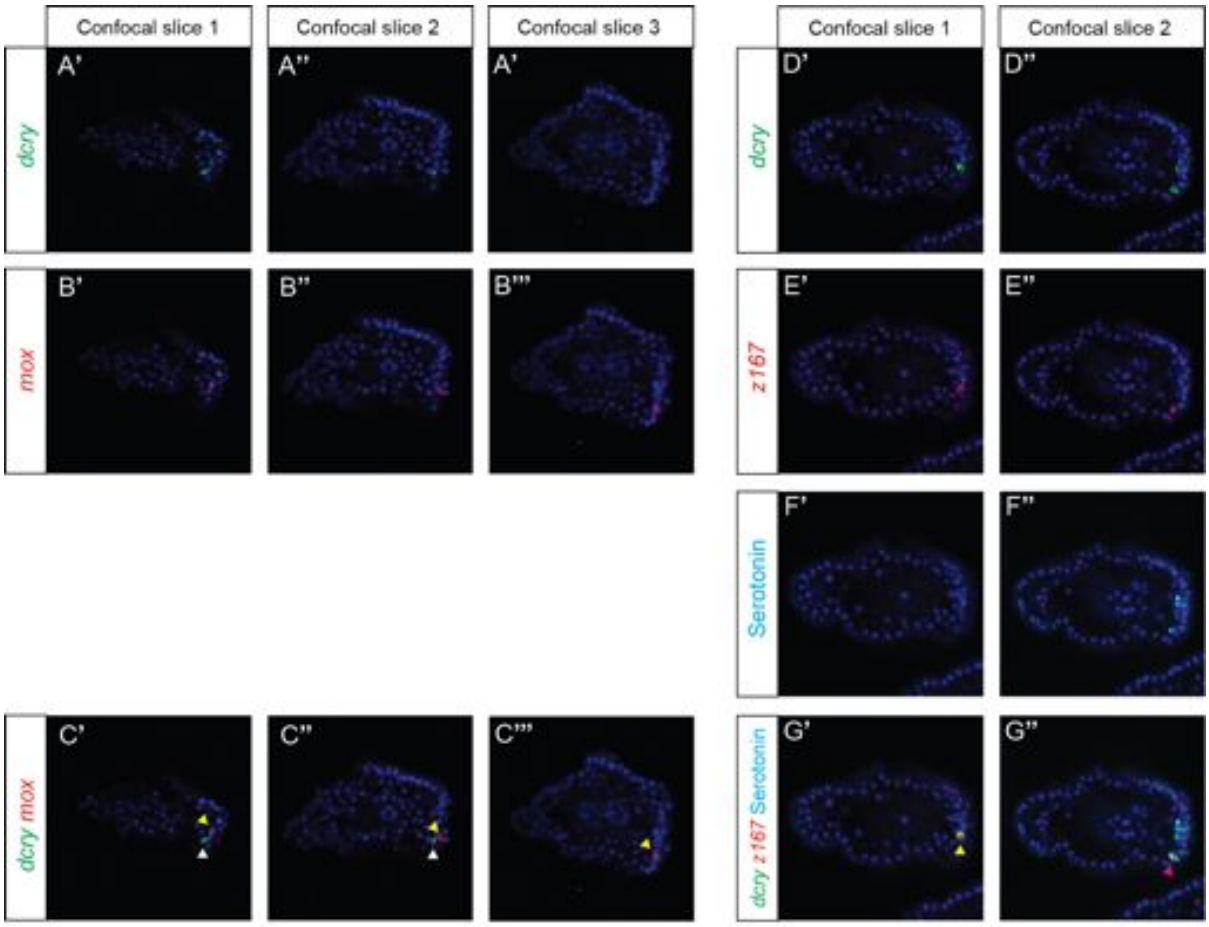

Figure 5.8. Analysis of single-slice confocal images of *dcry, mox,* and *z167* at pluteus larvae stage
(A-C) Double fluorescent WMISH of *dcry* and *mox*. Showing individual and merged channels from three different single confocal slices. (D-G) Double fluorescent WMISH of *dcry* and *z167* combined with serotonin antibody staining. Showing individual and merged channels from two different single confocal slices. DAPI-labeled nuclei (blue). See main text for descriptions of arrows.

dcry is expressed in the same location as serotonergic neurons and encodes for a protein that acts as a circadian photoreceptor (Cashmore *et al*., 1999). To see if cells that express *dcry* are also serotonergic neurons, I combined double fluorescent WMISH of *dcry* and *z167* with immunohistochemical staining for serotonin and analysed the resulting single-slice confocal images. The results show that in fact two clear and distinct types of serotonergic neurons exist in the sea urchin apical organ. The first type, here after named *Type 1 serotonergic neurons*, are defined as serotonin only and do not express either *dcry* nor *z167* (figure 5.9 A''' yellow arrow). The second type, hereafter named

Type 2 serotonergic neurons, are defined as serotonin cells that express both *dcry* and *z167* (figure 5.9 B''' yellow arrows). Interestingly, in figure 5.9 A' and A''' the white arrowheads shows a good example of a *dcry-z167* positive cell that does not express serotonin. Therefore, at pluteus stage, the sea urchin larva has cells that express just serotonin, cells that express *dcry* and *z167*, and finally cells that express serotonin as well as *dcry* and *z167.*

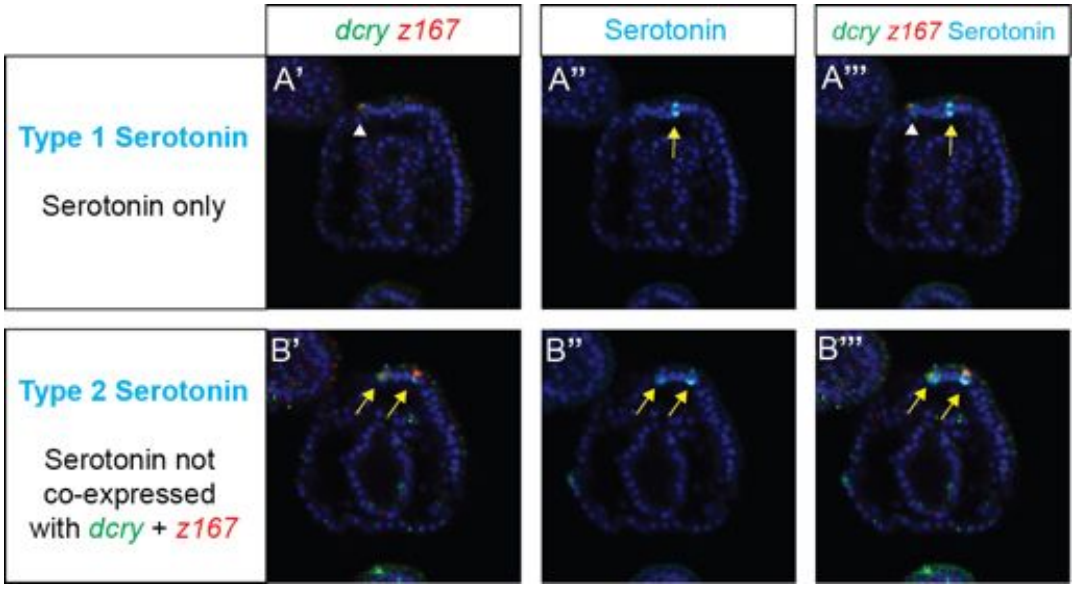

Figure 5.9. Analysis of single-slice confocal images showing two types of serotonergic neurons
(A) Double fluorescent WMISH of *dcry* and *z167* combined with serotonin antibody staining. Showing a cell that contains serotonin only (yellow arrow) and not *dcry* and *z167.* There is also a cell that expresses just *dcry* and *z167* but no serotonin (white arrowhead). (B) Double fluorescent WMISH of *dcry* and *z167* combined with serotonin antibody staining. Showing two cells that contains serotonin and both *dcry* and *z167* (yellow arrows). DAPI-labeled nuclei (blue). See main text for descriptions of arrows.

Chapter 6

FGF signalling and the apical organ:
a functional study

Aspects of this chapter were carried out with the help of undergraduate project student Isabelle Blomfield.

In the previous three chapters, I presented a detailed series of gene expression patterns that have helped illustrate different regulatory states and spatial domains that exist in the apical domain. While this knowledge is indispensable to building a GRN, it is only the preliminary stage. It is only through perturbing the normal function of a gene and monitoring the effects, that the functional linkages can be elucidated and the network constructed. In this chapter, I move away from analysing gene expression and begin to uncover functional aspects of apical organ development. I present three different functional studies, each of which investigates aspects of FGF signalling or its predicted targets.

6.1 Introduction

Since their discovery, FGF ligands and their receptors have been implicated in numerous biological phenomena and shown to regulate an abundance of developmental processes, including nervous system patterning, branching morphogenesis and limb development (Beenken and Mohammadi, 2009). Over the past decade or so, FGF signalling has been heavily implicated in the process of neural induction and has challenged the so-called

'default model' of neural induction. Briefly, neural induction is the process by which cells in the ectoderm make a decision to acquire a neural fate, rather than give rise to other tissues such as epidermis or mesoderm (Stern, 2006). The 'default model' suggests that ectodermal cells acquire neural fates by default, but this is normally inhibited in prospective endodermal cells by the action of BMPs (Wilson and Hemmati-Brivanlou, 1997; Schier and Talboti, 1998). However, there is evidence, especially in chicken embryo studies, that shows that inhibition of FGF signalling blocks neural induction (Streit *et al.,* 2000) and restores epidermal cell fate (Wilson *et al.,* 2000). This suggests that FGF signalling may be acting as an early competence factor for neural induction, providing the initial neuralising signal that prepares the ectoderm for further signals (Streit *et al.,* 2000; Wilson *et al.,* 2000; Sheng *et al.,* 2003). More generally, FGF signalling plays multiple roles in embryonic neural development, including neural patterning, placode formation, axon guidance and synaptogenesis (reviewed by Mason, 2007).

The FGF signalling pathway

The mammalian FGF family comprises 22 ligands, which signal through four highly conserved transmembrane tyrosine kinase receptors (Itoh and Ornitz, 2004). A fifth related receptor, FGFR5 (also known as FGFR like-1), can bind FGFs, but has no tyrosine kinase domain and does not transduce the signalling pathway as other classical FGF receptors (Bertrand *et al*., 2009). Ligand-dependent dimerisation of the FGF receptors leads to a conformational shift in the receptor structure, that activates the intracellular kinase domain. This results in intermolecular transphosphorylation of the tyrosine kinase domains. Phosphorylated tyrosine residues on the receptor, function as docking sites for adaptor proteins, leading to the activation of multiple signal transduction pathways (figure 6.1; Plotnikov *et al.,* 1999; Böttcher and Christof Niehrs, 2005). In order to gain a functional understanding of the FGF signalling, a number of inhibitors have been designed (reviewed by Beenken and Mohammadi, 2009). SU5402 is a widely used indolinone-based small molecule that selectively inhibits the specific tyrosine kinase activity of FGF receptors and hence disrupts FGF signalling (Grand *et al*., 2004; Byron *et al*., 2008; Meyer *et al*., 2008).

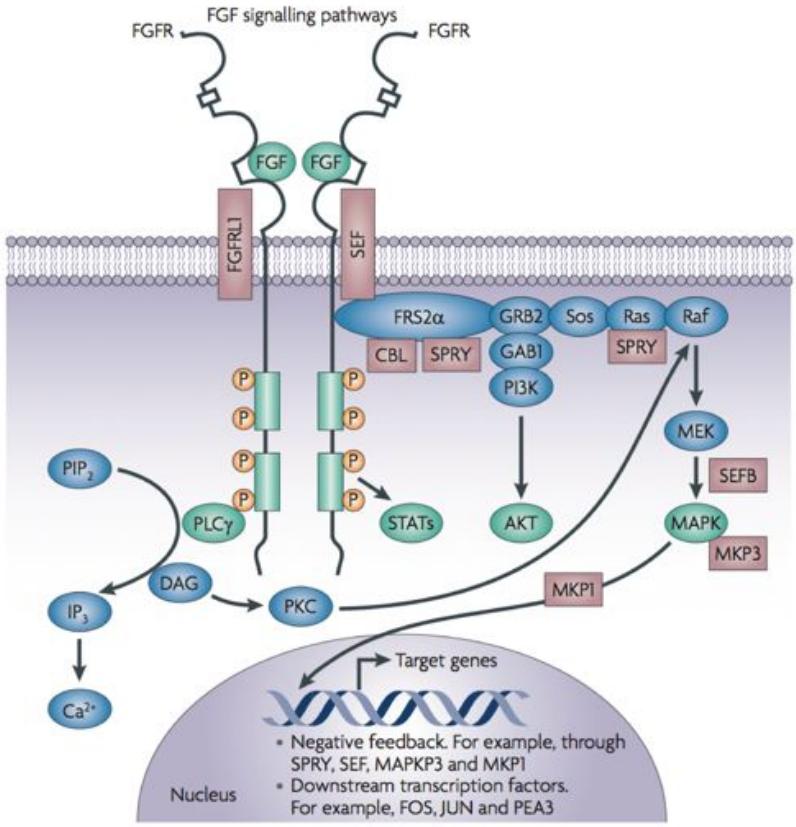

Figure 6.1. FGFR signalling network
The signal transduction network downstream of fibroblast growth factor (FGF) receptors (FGFRs). After receptor dimerisation, four key downstream intracellular signalling pathways are activated: RAS–RAF–MAPK, PI3K–AKT, STAT and PLCγ (adapted from Turner and Grose, 2010).

FGF signalling in the sea urchin embryo

It is thought that a complete set of FGF ligands and FGF receptors, have been identified in the sea urchin genome. A single FGF ligand, *fgf 9/16/20* has been shown to be expressed in the primary mesenchyme cells, the adjacent ectoderm and in two regions of lateral ectoderm either side of the apical domain (figure 6.2 A-D black arrows; Röttinger *et al.,* 2008). Two classical FGF receptors have also been identified in the sea urchin. The first, *fgfr1,* is expressed in a broad and dynamic fashion during development, expressed predominately in the oral ectoderm, but also in the precursors of both the primary mesenchyme cells, the non-skeletogenic mesenchyme, the apical domain (figure 6.2 F black arrow) and the gut (figure 6.2 E-H; Lapraz *et al*., 2006). The second, *fgfr2*, is expressed exclusively in the primary mesenchyme cells (figure 6.2 I-L; Röttinger *et al.,* 2008). A third FGF receptor has also been identified in the sea urchin genome

(Lapraz *et al.,* 2006) and is homologous to the human gene *fgfr like-1* (Zhuang *et al.,* 2009) but currently there are no data regarding its spatial expression. As mentioned above, FGFR like-1 is a fifth FGF receptor, and although they can bind FGFs, they have no tyrosine kinase domain so cannot signal (Bertrand *et al*., 2009). Several other genes have been shown to be expressed in an almost identical pattern to *fgf 9/16/20.* These include the FGF/MAP kinase modulator *sprouty* and the transcription factors *pax 2/5/8* and *pea3.* These genes are not expressed in the apical domain but all three of these genes are strongly downregulated when embryos are injected with an *fgf 9/16/20* MASO and suggests that they are downstream targets of FGF signalling in the sea urchin embryo (Rottinger *et al.,* 2008). Broadly speaking, little is known about the functional role of FGF signalling in sea urchin embryonic development. However, Röttinger *et al.,* (2008) have shown, that FGF 9/16/20 regulates directed migration of mesenchyme cells, morphogenesis of the skeleton and gastrulation during early development.

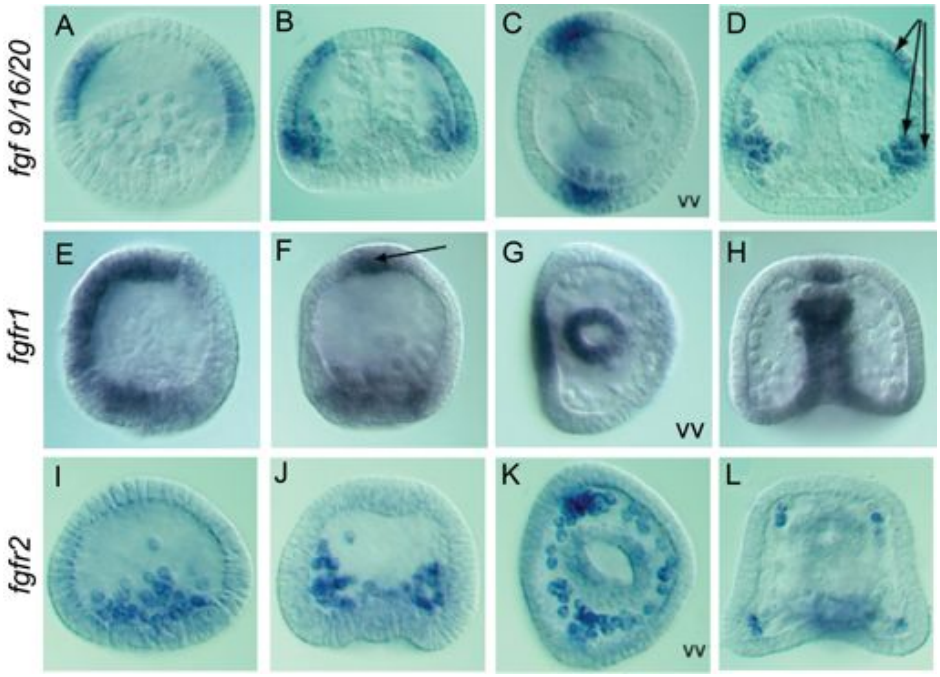

Figure 6.2. Expression of FGF signalling components in the sea urchin embryo
(A-D) *fgf 9/16/20* expression in (A) mesenchyme blastula stage, (B,C) early gastrula stage, (D) late gastrula stage. (E-H) *fgfr1* expression in (E) hatched blastulastage, (F) mesenchyme blastula stage, (G) early gastrula stage, (H) late gastrula stage. (I-L) *fgfr2* expression in (I) mesenchyme blastula stage, (J) early gastrula stage, (K, L) late gastrula stage. All embryos are *P. lividus,* and are shown from an oral perspective other than E (lateral view) and C, G, K (vegetal view, vv). In these cases the oral ectoderm is on the left hand side (adapted from Lapraz *et al.,* 2006; Rottinger *et al.,* 2008).

In conclusion, FGF signalling has a long standing role in neural induction and nervous system development in a diverse range of organisms. Furthermore, the combination of an FGF ligand expressed in the ectoderm surrounding the apical domain, and an FGF receptor expressed in the apical domain itself, is suggestive of a potential role of FGF signalling in the patterning of the apical domain. With this in mind, I performed a series of functional perturbation studies on FGF signalling, in order to investigate its role in the development of the apical domain.

6.2 Results

6.2.1 Disrupting FGF signalling

In this section, I start by describing the experimental strategy chosen to investigate FGF signalling. To determine 1) what genes are downstream of FGF and 2) to infer if any gene is a direct target of FGF signalling, I decided to disrupt FGF signalling at different developmental stages and thus dissect its function in greater detail. Both quantitative and qualitative methods were used to examine the perturbed embryos for any effects. Interestingly, the effects of the perturbation were inconsistent with the known expression patterns of FGF ligands and receptors. To explore these inconsistencies, I utilised a specific MASO knockdown of *fgfr1*.

Chemical disruption of FGF signalling: Pilot study and experimental strategy

To disrupt FGF signalling at different stages of development, I chose to use a chemical inhibitor of FGFR1 called SU5402, which can be applied to the embryo culture at the required stage. To determine a suitable concentration of SU5402 for the perturbation treatments, I carried out a pilot study (figure 6.3) using two different concentrations of SU5402. SU5402 was added at either 10μM or 20μM at hatching blastula stage (15

hours), and embryos were collected and visualised at mesenchyme blastula stage (24 hours) and pluteus larvae (72 hours). Two controls of either 0.1% DMSO (in which the drug is dissolved) or artificial sea water (ASW) were also used.

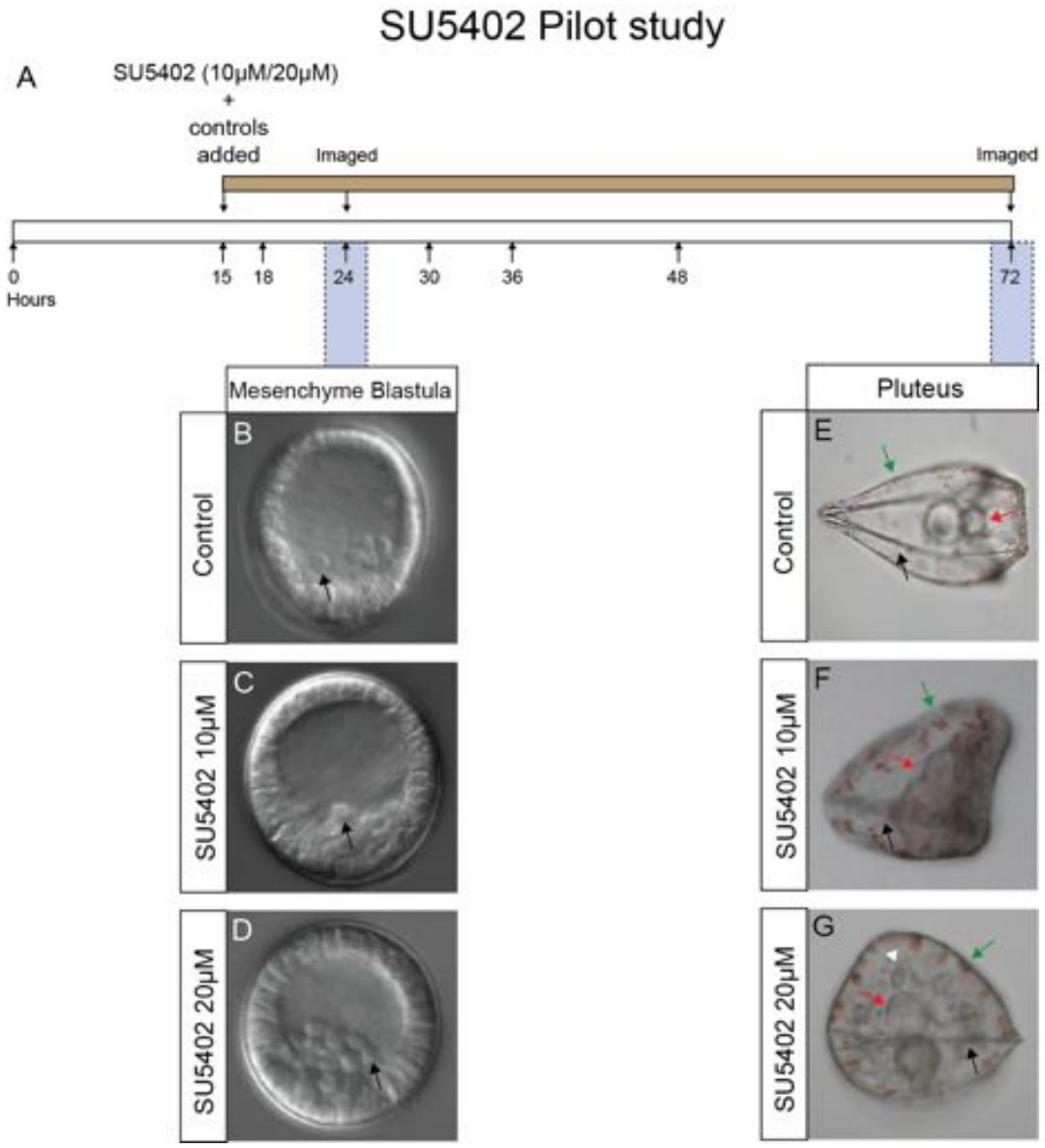

Figure 6.3. SU5402 pilot study and morphological effects
(A) A schematic diagram showing when SU5402 was added and at what time the embryos were collected. (B-D) DIC images showing morphology in control and SU5402 treated embryos at mesenchyme blastula stage. Ingressing primary mesenchyme cells can be seen (black arrows). Embryos are presented in a lateral view with the apical domain at the top. (E-G) DIC images showing morphology in control and SU5402 treated embryos in pluteus larvae. Important morphological details are marked: skeleton (black arrows), gut (red arrows), pigment cells (green arrows) and abnormally positioned mesenchymal cells (white arrowhead).

SU5402 treated embryos, showed a slight delay at mesenchyme blastula stage, with a thicker ectoderm and a smaller blastocoel, but contained primary mesenchyme cells that appeared to ingress normally (figure 6.3 B-D black arrows). In pluteus larvae, embryos treated with 10mM SU5402 had a smaller skeleton (figure 6.3 F black arrow), pigment cells that did not fully differentiate (figure 6.3 F green arrow), a normal but delayed gut (figure 6.3 F red arrow), and a fully developed apical organ. The effect was much more drastic with embryos treated with 20μM SU5402; the skeleton was very reduced and poorly positioned (figure 6.3 G black arrow), pigment cells did not fully differentiate (figure 6.3 G green arrow), the gut was reduced and not fully formed (figure 6.3 G red arrow), the non-skeletogenic mesoderm cells are abnormally positioned in the blastocoel (figure 6.3 G white arrowhead), and the apical organ is poorly developed. In contrast, control embryos develop into normal pluteus larvae, with a fully formed and extended skeleton (figure 6.3 E black arrow), fully differentiated pigment cells (figure 6.3 E green arrow), a fully differentiated tripartite gut (figure 6.3 E red arrow) and a perfectly formed apical organ. These results are consistent with previous work by Röttinger *et al*., (2008) who showed that FGF perturbation, results in problems with skeleton morphogenesis and delayed invagination of the archenteron. The embryos that best replicate these results were those treated with 20μM SU5402, and this was the concentration finally chosen and used for all subsequent experiments. SU5402 was chosen as an inhibitor of FGF signalling because it has certain advantages over other perturbation methods, such as morpholino knockdown or dominant negative gene knockdown. SU5402 as can be applied to an embryo culture at different times during development and can also be applied for a specific developmental window. Because *fgfr1* is also expressed in other cell types before the apical domain, removing FGF signalling from the start of development would results in unrelated developmental defects.

The temporal profile of *fgf 9/16/20* (figure 6.4 A) suggests, that there are three main phases of expression during embryonic development: (1) at hatched blastula stage, which is the initial start of expression (18 hours, green line); (2) at approximately gastrulation, where a second major increase of *fgf 9/16/20* expression occurs (27 hours, blue line); (3) and finally at mid-gastrula stage (36 hours, red line). To dissect the functional role of FGF signalling, I performed seven different SU5402 treatments

summarised in figure 6.4 B. In the first four treatments, SU5402 was added at different stages during development and embryos collected at 6 and 9 hours post incubation for quantitative analysis using QPCR. Extensive analysis has shown, that until 6 hours after the addition of SU5402, there is no significant effect on gene expression (see appendix C), this is presumably due to the time it takes for the inhibitor to make its way into the embryo and bind to the receptors. In addition to QPCR analysis, embryos were fixed for WMISH in order to study the spatial expression of affected genes in treated embryos (figure 6.4, treatment 3). The next three treatments used immunohistochemical methods, to study the effects of SU5402 treatment on cilia and serotonergic neurons, the two major features of the apical organ (figure 6.4, treatments 5-7). Embryos were imaged at the pluteus stage to observe the morphological effects of the SU5402 treatment. Figure 6.4 C shows DIC images of control and treated embryos from the first four treatments. It is clear that adding SU5402 later during development, reduces any detrimental effects as anticipated, given the hierarchical nature of embryonic development and the regulatory networks encoding for it.

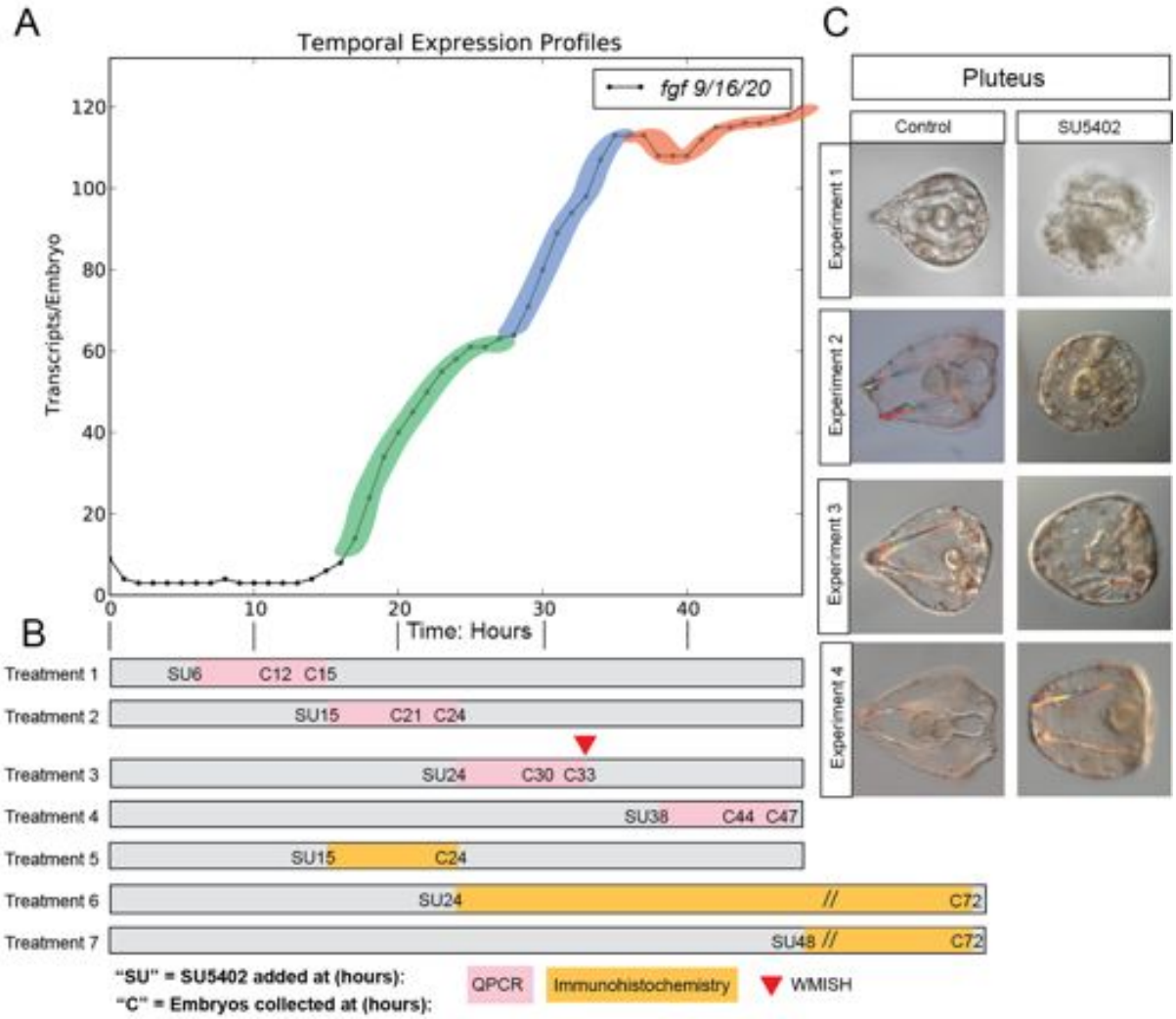

Figure 6.4. SU5402 experimental strategy and morphological assessment

(A) High-resolution temporal expression profile of *fgf 9/16/20* showing different phases of expression. Expression levels are given as number of transcripts per embryo and were quantified using Nanostring nCounter (Materna *et al.,* 2010). Phase one shows initial expression (green), phase two a second major increase (blue), phase three shows steady expression (red). (B) The 7 individual SU5402 treatments were carried out to dissect FGF signalling at different developmental stages. SU5402 was added at different times during development and embryos collected for QPCR, WMISH and immunohistochemical staining. (C) DIC images showing morphology in control and SU5402 treated embryos at pluteus larvae stage taken from the first four SU5402 treatments.

Assessment of the apical tuft and serotonergic neurons in SU5402 treated embryos

The apical tuft in sea urchin embryos is seen for the first time in the apical domain during blastula stages. To see if apical tuft formation is dependent on FGF signalling, embryos were treated with SU5402 at 15 hours (figure 6.4 treatment 5) and live embryos were viewed using dark-field microscopy to enable the cilia of the apical tuft to be visualised (figure 6.5 A,B). The results show that embryos treated with SU5402 retain an apical tuft (figure 6.5 B). When compared to controls (compare figure 6.5 A to B), it actually seems that the apical tuft as well as the other cilia are longer. To examine the cilia in the apical tuft in more detail, cilia were visualised using anti-acetylated α-tubulin antibody staining. Consistent with observations using dark-field microscopy, an apical tuft of long cilia is clearly visible (figure 6.5 C). A further noticeable difference between control embryos and those treated with SU5402, was a peculiar rounded morphology at the ciliary tip (figure 6.5 E) compared to the normal, smooth and elongated cilium of the controls (figure 6.5 D). This can be seen more clearly by focusing on the individual cilia of the embryo (figure 6.5 compare F to G).

The serotonergic neurons emerge in the apical domain in the late gastrula stage embryo. Because of the conserved role of FGF signalling in neuronal development, I was curious to see if FGF signalling was required for the formation of the serotonergic neurons in the sea urchin. Embryos treated with SU5402 at 24 hours (figure 6.4 treatment 6) formed pluteus larvae with no serotonergic neurons (figure 6.5 I), compared to controls that had normal serotonergic neurons (figure 6.5 H). However, embryos treated with SU5402 at 48 hours (figure 6.4 treatment 7), formed a normal pluteus larvae with a full complement of serotonergic neurons (figure 6.5 J). This suggests that FGF signalling may have a role in the early specification of the apical domain and thus serotonergic neurons, but by late gastrula stage, FGF signalling is no longer required for the differentiation of serotonergic neurons.

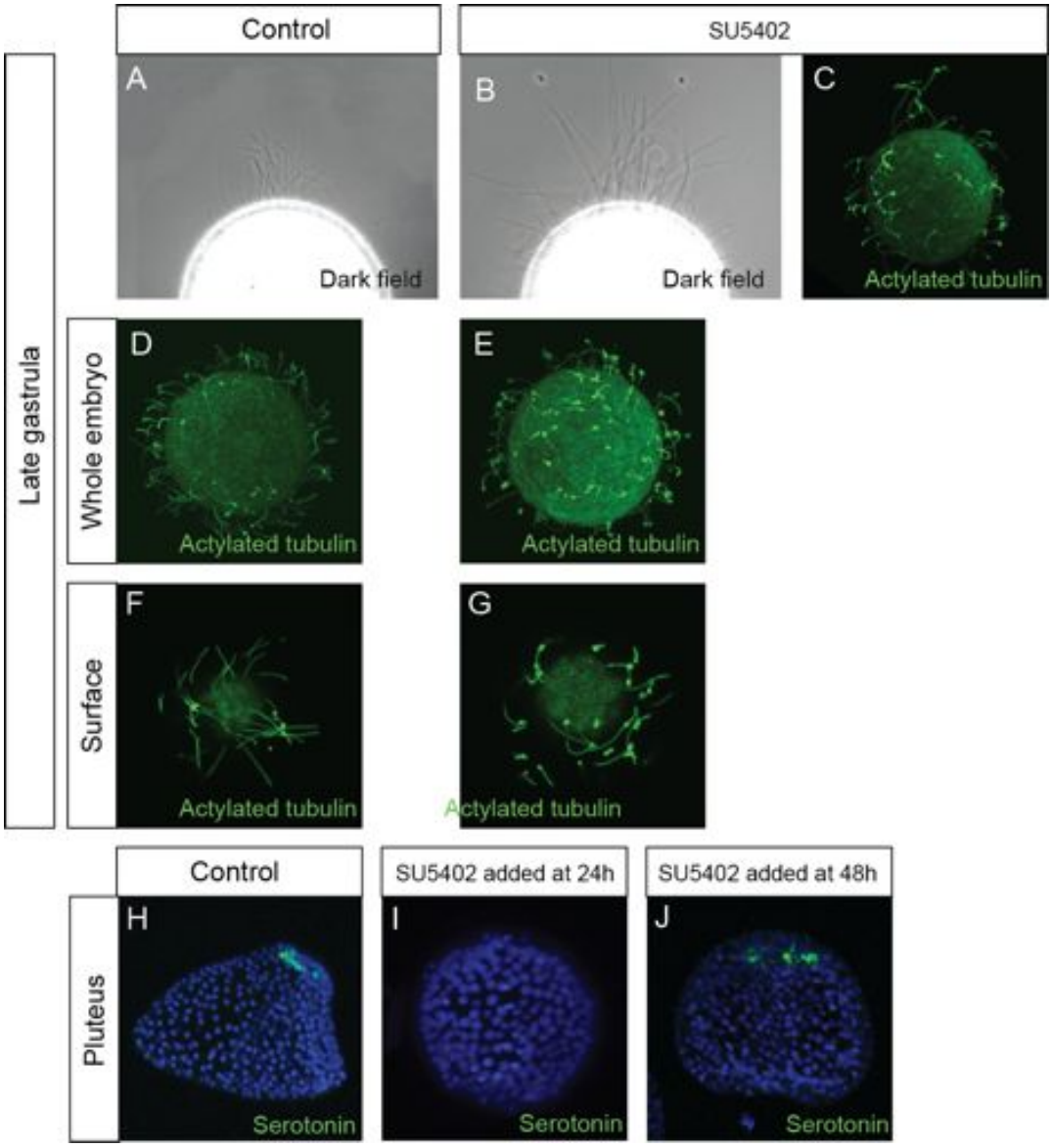

Figure 6.5. The effect of SU5402 treatment on the apical tuft and serotonergic neurons
(A,B) Apical tufts of control and SU5402 treated embryos visualised by dark field microscopy. (C-G) Cilia visualised using anti-acetylated α-tubulin antibody staining (green). (C) Apical tuft in an SU5420 treated embryo. (D,E) Full projection of merged confocal stacks showing cilia morphology in control and SU5402 treated embryos. (F,G) Projection of confocal stacks focusing on the cilia of the embryo surface. (H-J) Full projection of merged confocal stacks showing serotonin in control and SU5402 treated embryos Serotonin visualised using anti-serotonin antibody staining (green) and nuclei stain with DAPI (blue).

Quantitative analysis of embryos treated with SU5402

To dissect at a molecular level the role of FGF signalling in the development of the sea urchin apical organ, embryos treated with SU5402 at four different stages during development (see figure 6.4 treatments 1-4) were collected 6 and 9 hours after the addition of SU5402 and analysed using QPCR. To increase the chance of identifying a role for FGF, I checked over 70 apical organ (or potential apical organ) genes for up and downregulation (see appendix C for complete data table). For all QPCR experiments, technical repeats were carried out in triplicate or quadruplicate. Biological repeats were carried out for all genes in treatment 3 (SU5402 added at 24 hours) and for a number of genes in treatment 2 (SU5402 added at 15 hours). These two treatments are the most relevant to understanding the role of FGF signalling in the apical organ, especially as distinct expression of *fgf 9/16/20* is only seen from mesenchyme blastula stage (see chapter 4). Figure 6.6 shows detailed QPCR results for a selection of 34 regulatory and downstream genes, checked in embryos treated with SU5402 at 24 hours (treatment 3). The results show that a limited set of regulatory and downstream genes responded to SU5402 treatment. *sm30*, a gene encoding a spicule matrix glycoprotein crucial to the development of the sea urchin skeleton was selected as a positive control for SU5402 treatments. Rottinger *et al.,* (2008) showed that FGF signalling is required for skeletal morphogenesis and *sm30* is downregulated in both *fgfr1* and *fgfr2* MASOs. So too here, SU5402 treatment resulted in *sm30* being significantly and consistently downregulated (figure 6.6). *sm30* is also effected when SU5402 was added at 15 hours, but not at 6 and 38 hours, consistent with the normal temporal expression profile of *sm30* and confirms the efficiency of the SU5402 treatments in blocking the FGF signalling (see appendix C for complete SU5402 data table).

The initial, and perhaps the most striking result of the SU5402 treatments, was how the "classical cohort" of apical organ genes were not affected. These include key regulatory genes such as *foxQ2, six3, hbn, rx* and *ac-sc.* These are all expressed in the apical organ and are thought to operate at or near the top of an apical organ GRN (Burke *et al.,* 2006; Yaguchi *et al.,* 2008; Wei *et al*., 2009; reviewed by Angerer *et al.,* 2011). The major exception is the transcription factor *zic2.* Expressed solely in the central and aboral

apical domain, it is significantly and repeatedly upregulated by SU5402 treatment. This suggests that FGF signalling does not have a key role in apical organ specification, but actually provides a subtle repressive function of only a single transcription factor, *zic2*.

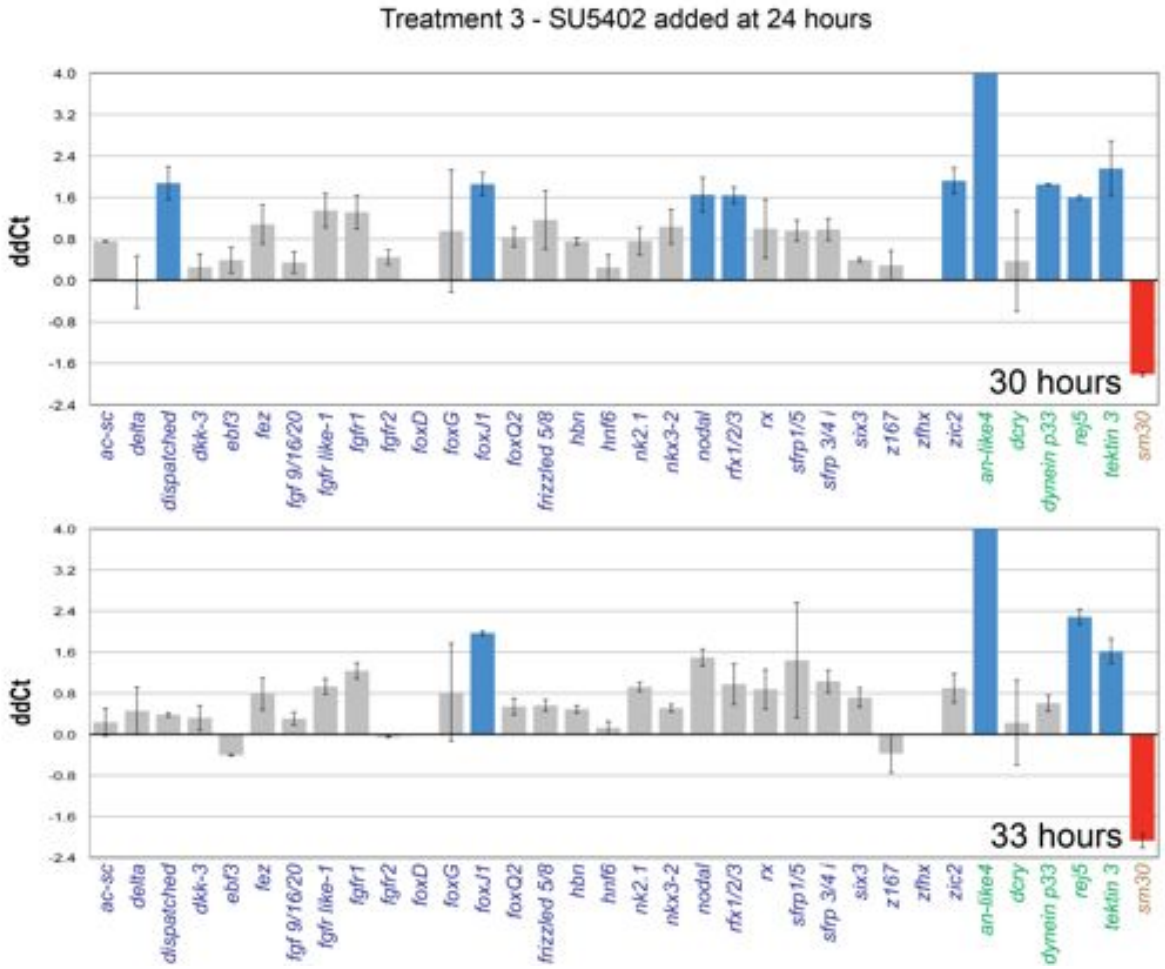

Figure 6.6. Quantitative analysis of SU5402 treated embryos

Perturbation analysis of SU5402 treated embryos. SU5402 added at 24 hours. Gene expression levels were quantified by QPCR at 30 and 33 hours. Differences of mRNA levels relative to controls are shown as ddCt. Significant threshold is a ddCt of + or -1.6, which is equal to ~3 folds of difference. Positive numbers indicate upregulation (significant upregulation, blue bar) and negative numbers indicate downregulation (significant downregulation, red bar) relative to controls. SU5420 treatments were repeated in different batches and the standard deviation is shown as error bars in the chart. The colour of the gene names indicate either a regulatory gene (blue), downstream gene (green) or positive control (brown). *an like-4* has a ddCt of 6.6 (30 hours) and 5.5 (33 hours).

There is, however, a limited set of regulatory and downstream genes that do respond to SU5402 treatment. Curiously, one gene that is drastically upregulated, is *an like-4.* Results show it is strongly affected during all four SU5402 treatments and at times, even reaching a massive hundred-fold increase when compared to controls (figure 6.6; see appendix C). Little is known about *an like-4*, although Angerer *et al*., (2006) reports that it is a PEgsl astacin metalloproteinase and expressed in scattered cells, mostly in the animal half of the embryo from mesenchyme blastula stage onwards.

nodal is also significantly and repeatedly upregulated during treatment 3 (figure 6.6). This is interesting, as the Nodal signalling pathway is an essential mediator of oral and aboral ectoderm specification in the sea urchin embryo (Li *et al*., 2012) and is excluded from the apical domain by *foxQ2* (Yaguchi *et al.,* 2008). Interestingly, *nodal* and *fgfr1* are co-expressed in the oral ectoderm, but not in the apical domain, however without more detailed WMISH analysis and further studies at different developmental stages, it is difficult to fully understand the regulation of nodal by *fgfr1*. Another signalling molecule affected by SU5402 treatment is *dispatched.* Thought to be expressed in the early apical domain (Wei *et al.*, 2009), it is a modifier of the Hedgehog signalling pathway (Burke *et al.,* 1999) and is significantly and repeatedly upregulated during the inhibition of FGF signalling at 24 hours (treatment 3, figure 6.6; and during treatment 1, see appendix C).

Overall, the largest group of genes affected by SU5402 treatment includes two ciliogenic transcription factors and several downstream structural cilia genes. The transcription factors *foxJ1* and *rfx 1/2/3* are significantly and repeatedly upregulated. *foxJ1* is initially expressed in the whole ectoderm and, by the start of gastrulation, is expressed exclusively in the apical domain together with *foxQ2* (Tu *et al.,* 2006 and Oliveri, unpublished data). Interestingly, *foxJ1* is thought to have a conserved regulatory role in the transcriptional program that controls the production of cilia (Yu *et al*., 2008), while *rfx* genes have been shown to be linked with *foxJ1,* but more specifically in the formation of sensory cilia (Dubruille *et al*., 2002). Unsurprisingly, several downstream genes that are involved in cilia structure are also upregulated during SU5402 treatment and include *dynein p33* and *tecktin 3,* both of which are expressed in the apical domain (Dunn *et al.,* 2007). However, what remains unclear, is the link between the upregulation

of cilia genes and the morphological effects seen in the cilia and the apical tuft. Another upregulated gene is *rej5,* which appears to be involved in sperm function (Butscheid *et al*., 2006), although what role it might be playing here is unclear. It is interesting to note that all the genes affected in these treatments are upregulated in the presence of the SU5402. As SU5402 specifically inhibits the transduction of FGF signalling, this suggests that the FGF signalling via *fgfr1* provides a repressive function in the apical domain for these genes.

Qualitative analysis of SU5402 treated embryos

To examine the spatial effects of SU5402 treatment on significantly upregulated genes, embryos were fixed at 33 hours (figure 6.4 treatment 3) and studied using WMISH (figure 6.7). Embryos treated with SU5402 are slightly delayed with a smaller blastocoel and thicker animal plate. To start, three genes, *foxJ1, an like-4* and *zic2,* were checked using WMISH.

(1) SU5402 treatment results in a three-to-four fold increase in the number of *foxJ1* transcripts (figure 6.6). During early gastrula stage (33 hours), *foxJ1* is usually expressed only in the apical domain, as seen in control embryos (figure 6.7 A,C), while in SU5402 treated embryos *foxJ1* expression has clearly expanded and there is ectopic expression in the oral ectoderm or ciliary band (figure 6.7 B,D). (2) SU5402 treatment results in an almost ninety-fold increase in the number of *an like-4* mRNA transcripts (figure 6.6). At this stage, *an-like 4* is expressed in random scattered cells in the animal half of the embryo, as seen in control embryos (figure 6.7 E,G), while in SU5402 treated embryos, *an like-4* expression is massively expanded and there is strong expression in the apical domain as well as ectopic expression in the entire ectoderm (figure 6.7 F,H). (3) SU5402 treatment results in a three-to-four fold increase in the number of *zic2* transcripts. During early gastrula stage (33 hours), *zic2* is usually expressed in the central and aboral apical domain, as seen in control embryos (figure 6.7 I,K), while in SU5402 treated embryos the intensity of *zic2* expression clearly increases, although there is little or no expansion of *zic2* expression (figure 6.7 J,L).

Two further genes were checked by WMISH: (4) *fgfr1* tends to be consistently upregulated, but below the significance threshold during most SU5402 treatments (see SU5402 data table in appendix C). To check for any spatial effects that might not be picked up by QPCR, a WMISH was carried out. *fgfr1* is expressed in the apical domain, oral ectoderm and invaginating archenteron of control embryos (figure 6.7 M,O) and this remains the same in embryos treated with SU5402 (figure 6.7 N,P) although the intensity of expression appears stronger, especially in the apical domain. However, the usual oral boundary is visible in the apical domain of the SU5402 treated embryos (figure 6.7 N). This is consistent with a small upregulation seen by QPCR. Finally (5) expression levels of *foxQ2,* like many other genes expressed in the apical organ, remains unaffected by SU5402 treatment, and was confirmed with WMISH. At 33 hours, *foxQ2* is expressed only in the central apical domain (Tu *et al.,* 2006; chapter 3) as can be seen in control embryos (figure 6.7 Q,S). Embryos treated with SU5402 showed little effect in *foxQ2* expression; there is possibly a small spatial increase, but without a more detailed spatial analysis using double WMISH and DAPI counter staining to allow cell counting, it is difficult to confirm such a subtle change.

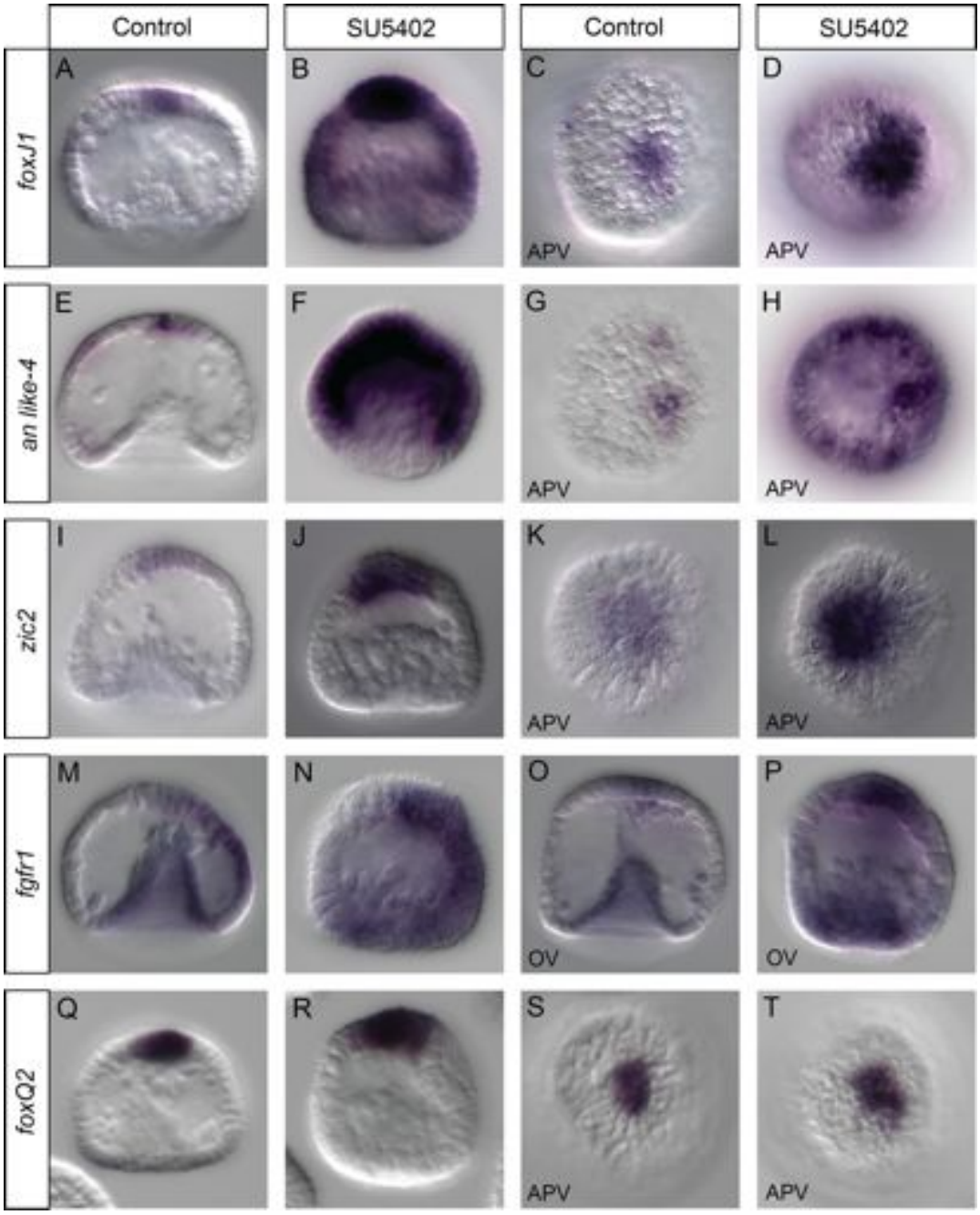

Figure 6.7. Spatial gene expression in SU5402 treated embryos

DIC images of NBT/BCIP WMISH on SU5402 treated embryos (SU5402 added at 24 hours) and control embryos. Embryos were collected and fixed at 33 hours. Controls and treated embryos were hybridised simultaneously and stained for the same amount of time. Unless otherwise specified embryos are presented in a lateral view with the oral side at the right and the apical domain at the top. Apical view (APV) and oral view (OV).

Spatial effects of SU5402 treatment inconsistent with *fgfr1* expression.

SU5402 treatment causes a vast expansion of the domain of expression of both *an like-4* and *foxJ1* (figure 6.7 A-H). *an like-4* especially, expands its expression from a few randomly scattered cells, found predominantly in the animal half of the embryo, to the entire ectoderm and is excluded only from the vegetal plate. This expansion is difficult to explain. SU5402 is a chemical inhibitor that binds to the ATP binding site of FGF receptors and disrupts normal signal transduction (Mohammadi *et al.,* 1997) therefore it is expected that only the cells expressing *fgfr1* and *fgfr2* should be affected by the presence of SU5402 and cease to function normally. However, *fgfr1,* and presumably the protein, is expressed in the oral half of the apical domain, the oral ectoderm and vegetal plate, and *fgfr2* is only in the skeletogenic mesoderm. Therefore, inhibiting the receptor in these locations does not explain the expansion of *an like-4* and *foxJ1* in territories that do not express any known FGF receptors. The question therefore remains: if inhibition of FGFR1 is not causing these results, what is? There are several possible explanations. Firstly, SU5402 could be inhibiting another tyrosine kinase receptor, either instead of, or together with FGFR1, with *an-like 4* and *foxJ1* downstream of this other receptor. In this scenario, the result has little or nothing to do with FGF signalling. Secondly, it is possible our knowledge of the FGF signalling family in the sea urchin is incomplete or wrong. Perhaps additional FGF ligands or receptors exist in the sea urchin that have yet to be discovered. Moreover, it is already well known that a third FGF receptor, *fgfr like-1,* exists. However, nothing is known about its spatial expression pattern, and although it does not have a tyrosine kinase domain, it may be playing a supporting role in mediating FGF signalling in the apical domain. Thirdly, given the fact that *fgfr1* is initially expressed ubiquitously, the possibility exists that the protein remains localised broadly across the ectoderm and could explain the spatial expansion of *an like-4* and *foxJ1.* In contrast the mRNA becomes quickly expressed in a more restricted pattern.

To investigate the specificity of SU5402, we specifically disrupted the function of *fgfr1* by injecting an *fgfr1* MASO. There were two main aims of this experiment. (1) To check if FGFR1 has a role in apical organ development by collecting embryos at 20 and 24 hours and checking for up or downregulation of apical organ genes using QPCR. (2) To check if the same genes upregulated in SU5402 treated embryos are also upregulated in *fgfr1*

MASO treated embryos collected at 30 hours. Two independent *fgfr1* MASOs were gratefully received from Dr Yi-Shien Su (Taiwan) and were injected after fertilisation (see appendix A and materials and methods). The results show that several apical organ genes were upregulated in 20 and 24 hour embryos (figure 6.8). Four genes significantly upregulated in both independent *fgfr1* MASOs at 24 hours were *fez, rx, ac-sc* and *nk2.1*. All of these genes are expressed in the apical domain during development; *nk2.1* plays a role in apical tuft formation (Tackas *et al.,* 2004; Dunn *et al.,* 2007) and the other three genes are involved in neurogenesis (Burke *et al.,* 2006).

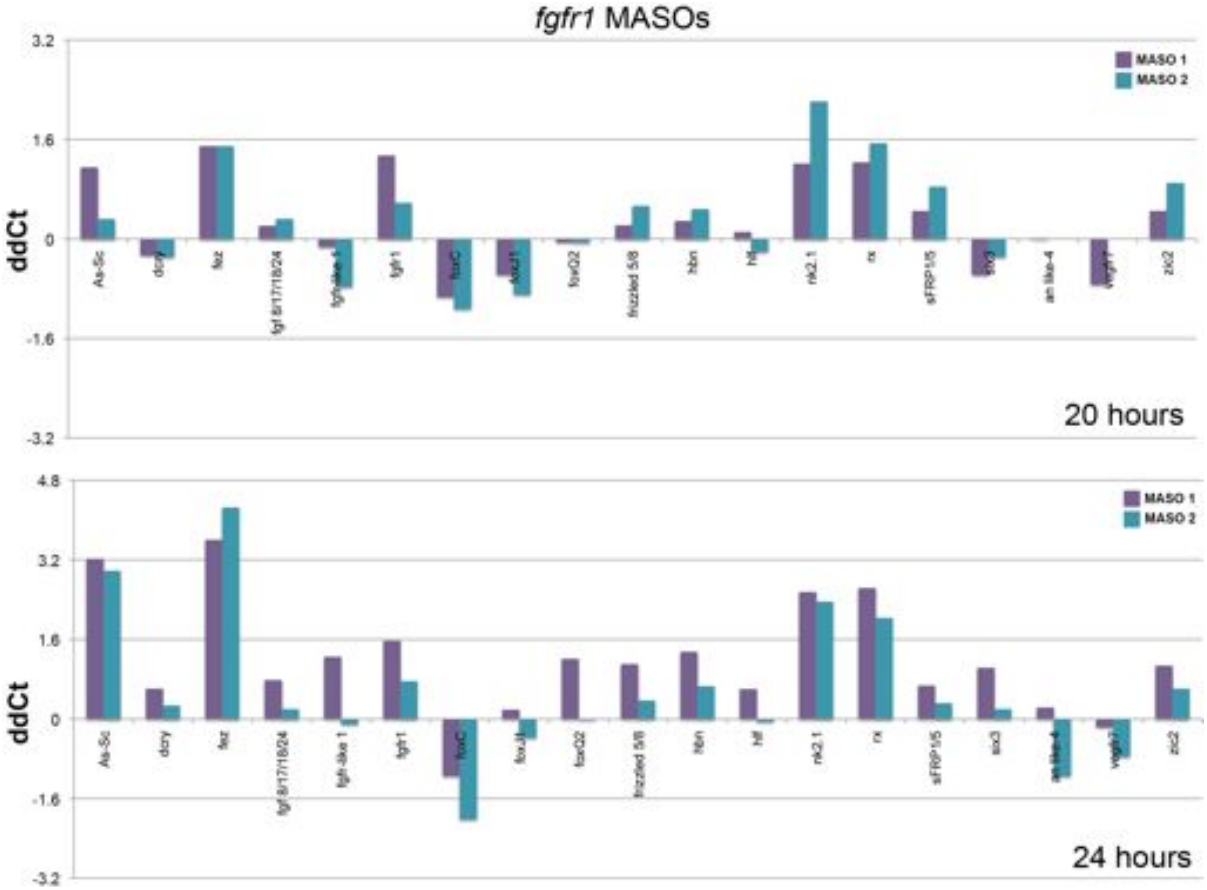

Figure 6.8. *fgfr1* MASO experiments at 20 and 24 hours
Perturbation analysis of two independent *fgfr1* MASOs. Gene expression levels were quantified by QPCR at 20 and 24 hours. Differences of mRNA levels relative to controls are shown as ddCt. Significant threshold is a ddCt of + or -1.6, which is equal to ~3 folds of difference. *fgfr1* MASO 1 (purple bar) and *fgfr1* MASO 2 (teal bar). Experiment carried out by Isabelle Blomfield.

Interestingly, this suggests a role for FGFR1 and FGF signalling in apical organ development, which is a distinctly different outcome from SU5402 treatment. Furthermore, the genes upregulated in the equivalent SU5402 treated embryos (figure 6.4 treatments 3; figure 6.6) were completely unaffected by the two independent *fgfr1* MASOs (figure 6.9). For example, *an like-4, foxJ1* and *zic2* are all upregulated in embryos treated with SU5402 but not strongly affected in embryos injected with *fgfr1* MASOs. *zic2* is repeatedly upregulated but always below the significance threshold. From the other perspective, *fez, rx, ac-sc* and *nk2.1* are all upregulated in *fgfr1* MASO but are not upregulated in embryos treated with SU5402. As a consequence of the divergent results between SU5402 treatment and *fgfr1* MASO knockdown, the conclusion was drawn that SU5402 and the *fgfr1* MASO knockdown are not targeting the same pathway(s). The consistent results of the two independent *fgfr1* MASOs suggest that the knockdowns are specific to *fgfr1.* Further confirmation of MASO specificity could be carried out by using a splice-blocking MASO against *fgfr1* or a FGFR1-GFP construct. The spatial expansion of *an like-4* and *foxJ1* suggest that SU5402 is not inhibiting FGFR1 exclusively, and is possibly binding to at least one other receptor. The use of phosphorylated forms of ERK1/2 would allow detection of FGF signalling readout in SU5402 treated and *fgfr1* MASO knockdown embryos and could help to further elucidate these conflict results. However, ERK1/2 is also a downstream target of other RTKs and thus might not be the most effective tool too study the specific readout of FGF signalling.

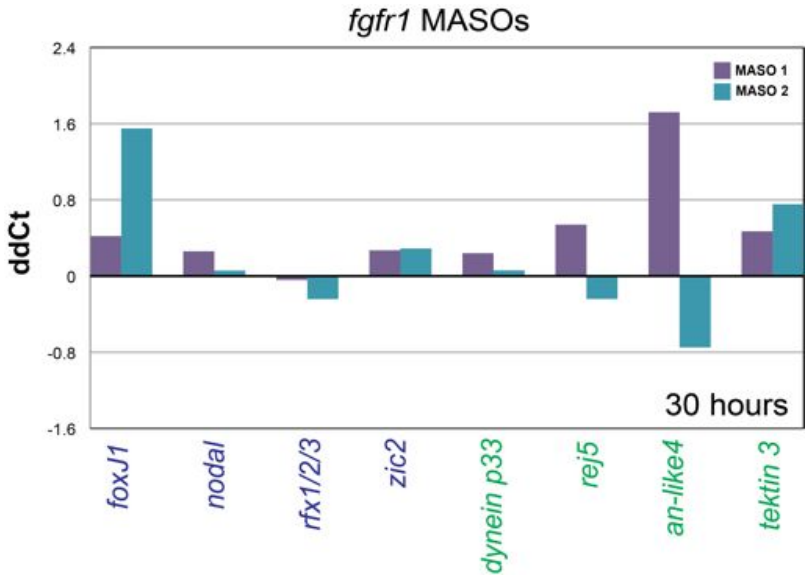

Figure 6.9. Effect of *fgfr1* MASOs on genes upregulated by SU5402 treatment
Perturbation analysis of two independent *fgfr1* MASOs. Gene expression levels were quantified by QPCR at 30 hours. Differences of mRNA levels relative to controls are shown as ddCt. Significant threshold is a ddCt of + or -1.6, which is equal to ~3 folds of difference. *fgfr1* MASO 1 (purple bar) and *fgfr1* MASO 2 (teal bar). Experiment carried out by Isabelle Blomfield.

.2.2 What else is SU5402 inhibiting?

The results from the previous section show how genes upregulated in SU5402 treated embryos are not upregulated in embryos treated with *fgfr1* MASOs. This suggests that, contrary to previous use in the sea urchin (Rottinger *et al.,* 2008), other systems (Grand *et al*., 2004; Byron *et al*., 2008; Meyer *et al*., 2008) and the manufacturers claims, SU5402 might not be an exclusive inhibitor of FGFR signalling. For this reason, I attempted to identify other possible targets of SU5402 to see if they can help explain the expanded expression domain of *an like-4* and *foxJ1.* Firstly, I searched the sea urchin genome for receptors that have a tyrosine kinase domain similar to FGFR1, and then used multi-alignments to identify which tyrosine kinase domains have a binding site that, in theory, could allow SU5402 to bind. Secondly, I used QPCR and WMISH to investigate the temporal and spatial expression patterns of these candidate genes, as well as their response to SU5402 treatment.

Mechanism and action of the chemical inhibitor SU5402

The interaction between SU5402 and human FGFR1 has been elucidated by x-ray crystallography and FGFR1 has been shown to have a two-lobe architecture typical of receptor tyrosine kinases (RTKs). ATP (or in this case, SU5402) binds to a hinge region that connects the two lobes (Mohammadi *et al.,* 1997). The FGFR1 hinge region comprises six residues and is highly variable between different RTKs. The specificity of SU5402 results from a hydrogen bond between the carboxyethyl group of SU5402 and an asparagine that is the final residue of the hinge region. The *S. purpuratus* FGFR1 hinge domain has conserved the essential amino acids required to bind SU5402.

In order to identify candidate receptors that could bind SU5402, I first characterised the *S. purpuratus* FGFR1 protein using PFAM and Prosite. Then, based on the amino acid sequence of the RTK domain, I used BLASTP to search the sea urchin genome for receptors with a similar RTK domain; the top results are presented in figure 6.10. To determine if any of the candidate RTKs could be inhibited by SU5402, I performed a multi-alignment of the hinge domain (figure 6.10). The results show that several RTK genes such as *tie 1/2*, *tk9, vegfr7* and *vegfr10* all encode proteins that could in theory bind with SU5402. To understand if any of these genes are expressed in a location that could help explain the results of *an-like* and *foxJ1*, I studied their spatio-temporal expression profiles and their expression levels in SU5402 treated embryos.

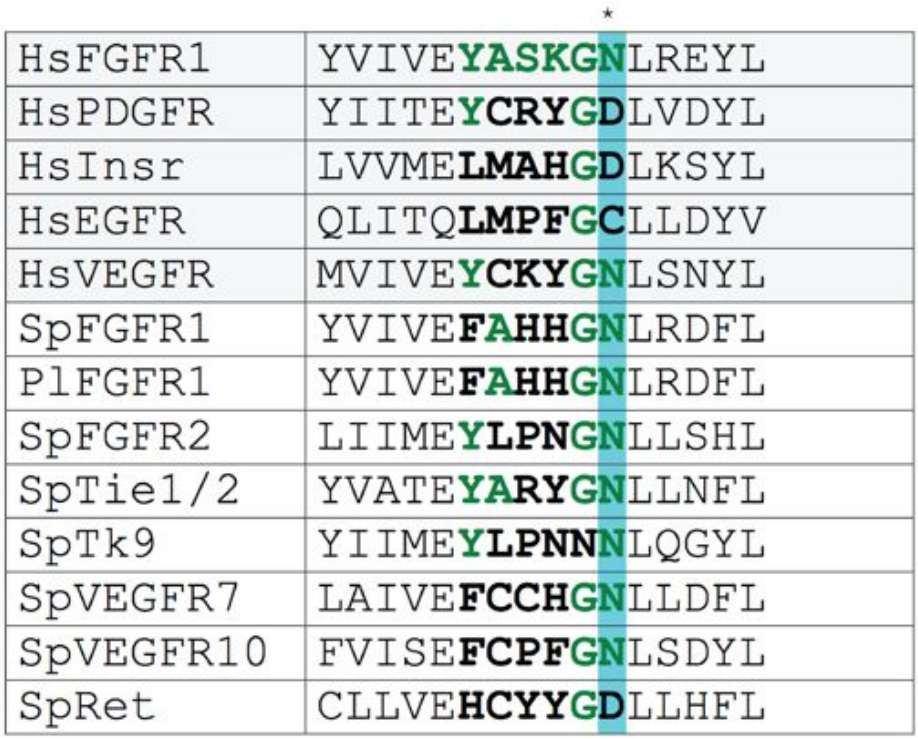

Figure 6.10. Multialignment of the hinge domain in several RTKs
Human FGFR1 and other RTKs are used as reference to show the key Asparagine (N) amino acid (*) residue that controls the binding specificity of SU5402. A multialignment was carried out using MEGA 5 and shows in bold the six residues that form the hinge domain. Amino acids conserved with human FGFR1 are in green. The key Asparagine residue is highlighted in turquoise. Species shown are *Homo sapiens* (Hs), *Strongylocentrotus purpuratus* (Sp), *Paracentrotus lividus* (Pl). The fifth and sixth amino acids of the hinge domain are highly conserved in all FGF and VEGF receptors, but also in other RTK receptors in the *S. purpuratus* genome.

Temporal and spatial expression patterns for *tie 1/2, tk9* and *vegfr7*

To determine if any of these receptors are expressed in a domain that could explain the surprising spatial expansion of *an-like 4* and *foxJ1* in SU5402 treated embryos, I set out to characterise the temporal and spatial expression profiles of our RTK candidates. *vegfr10* has been thoroughly characterised by Duloquin *et al.,* 2007 and shown to be expressed exclusively in skeletogenic mesoderm. Stevens *et al.,* (2010) previously characterised the temporal expression profile of *tie 1/2.* However, no spatial expression data exists for *tie 1/2* and for both *tk9* and *vegfr7* there are no expression data at all.

tie 1/2 expression only starts after mesenchyme blastula stage and climbs steeply, reaching a peak at mid-gastrula stage (40 hours), of 830 transcripts per embryo. Transcripts then reduce to 627 transcripts per embryo by late gastrula stage (48 hours), and increase again at pluteus larva (figure 6.11). During early gastrula stage, *tie 1/2* is expressed strongly in the non-skeletogenic mesoderm (figure 6.11 C). At mid-gastrula stage, *tie 1/2* continues to be expressed in non-skeletogenic mesoderm at the tip of the archenteron (figure 6.11 D) and in non-skeletogenic mesoderm cells that have begun to bud off and move into the blastocoel (figure 6.11 D,E). This expression pattern persists until the end of gastrulation (figure 6.11 E), and at pluteus stage it is expressed in blastocoelar cells (data not shown).

tk9 has a high level of maternal expression, which gradually decreases over the first 24 hours of development. Zygotic expression then begins after mesenchyme blastula stage (24 hours), and reaches its peak by late gastrula stage (48 hours), of 1414 transcripts per embryo (figure 6.11). Expression is ubiquitous until the start of gastrulation, when *tk9* begins to clear from the apical domain and from the oral ectoderm (figure 6.11 F-H). By late gastrula stage, *tk9* is expressed in the entire ectoderm except the oral ectoderm (figure 6.11 I-J).

vegfr7 expression starts during cleavage stages (9 hours) and climbs steeply, reaching a peak at hatching blastula stage (15 hours), of 3207 transcripts per embryo. Transcripts then fall drastically to 578 transcripts per embryo by hatched blastula stage (18 hours). *vegfr7* transcripts continue to reduce to 107 transcript per embryo by early gastrula stage (30 hours), after which expression slowly starts to increase again to 552 transcripts per embryo by late gastrula stage (48 hours; figure 6.11). *vegfr7* is expressed ubiquitously until after early gastrula stage (figure 6.11 K-L). From the start of gastrulation, *vegfr7* is expressed in the endomesoderm (figure 6.11 M) and interestingly is faintly expressed in the apical domain (figure 6.11 M white arrowhead). At mid-gastrula stage, *vegfr7* is expressed in the endoderm (figure 6.11 N), but can no longer be seen in the apical organ. Finally, at late gastrula stage, *vegfr7* is expressed in the foregut (figure 6.11 O white arrowhead) and faintly in the apical domain. This expression pattern persists through to pluteus larva stage (data not shown).

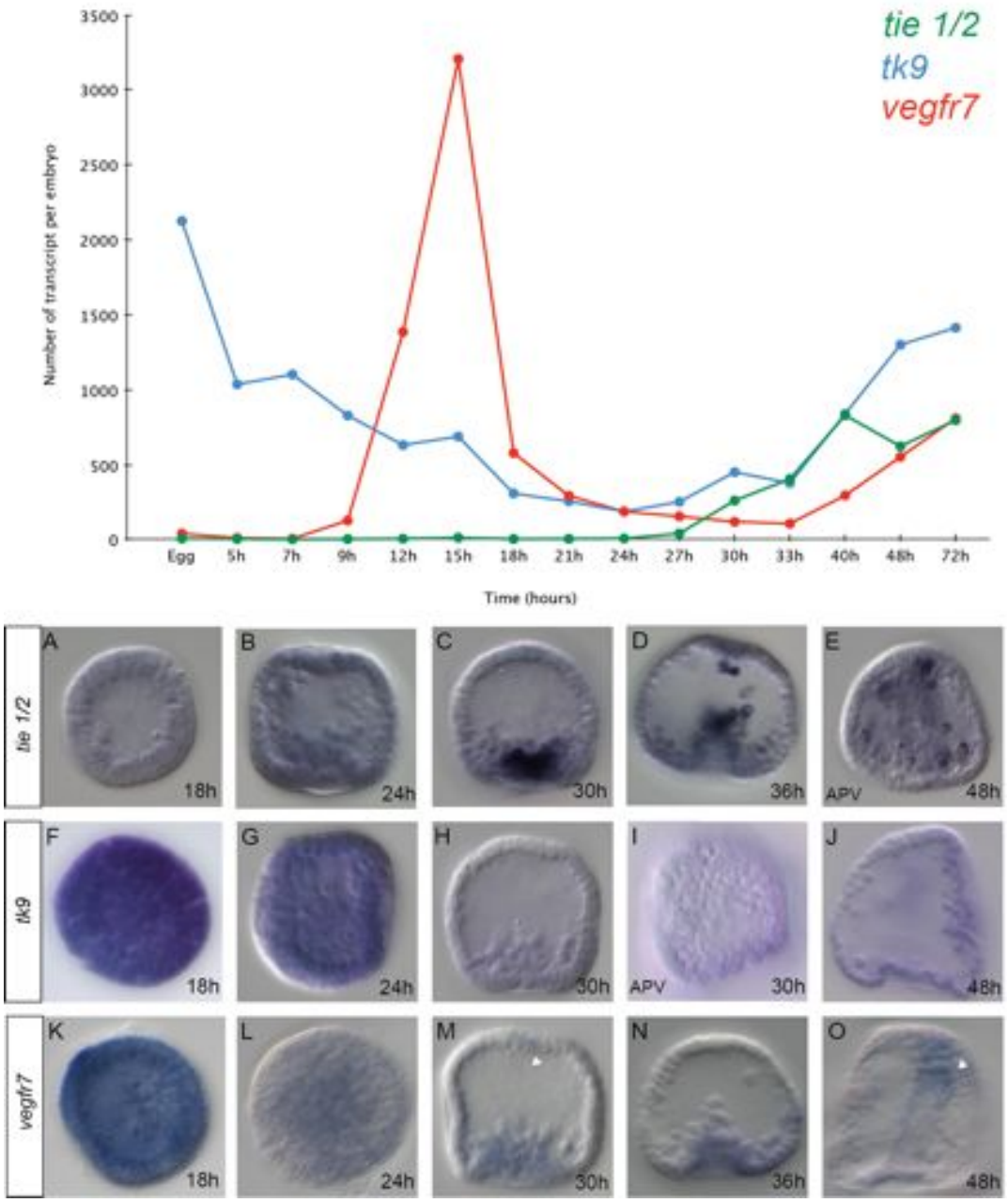

Figure 6.11. Temporal and spatial expression profiles for *tie 1/2*, *tk9* and *vegfr7*
Temporal expression profiles as revealed by QPCR and expression levels are given as number of transcripts per embryo. (A-I) Gene expression pattern of *tie 1/2* through development. Unless otherwise specified embryos are imaged with DIC and are presented in a lateral view with the oral side at the right and the apical domain at the top. Apical view (APV). See main text for descriptions of arrow.

In conclusion, *tie 1/2* is not expressed in a manner that could explain the result seen with *an like-4* and *foxJ1* in SU5402 treated embryos. The spatial expression patterns of *tk9* and *vegfr7* are less conclusive; both are ubiquitously expressed in early development. However, *tk9* is not expressed in the oral ectoderm and is expressed in the

vegetal plate. On the other hand, *vegfr7* expression is more strongly linked to the apical domain, although it still has quite a restricted expression pattern that is not totally consistent with the spatial expansion seen with *an like-4* and *foxJ1.* Ultimately, individual MASOs against both *tk9* and *vegfr7* are required to see if either of these two genes replicate the results seen in SU5402 treated embryos. QPCR was used to investigate if any of these receptors are upregulated in SU5402 treated embryos. The results show that both *tie 1/2* and *tk9* are not affected; Interestingly, *vegfr7* is repeatedly and significantly upregulated, increasing with exposure to SU5402 (see figure 6.12). This could suggest that *vegfr7* could be downstream of FGFR1 or that some autorepressive function exists.

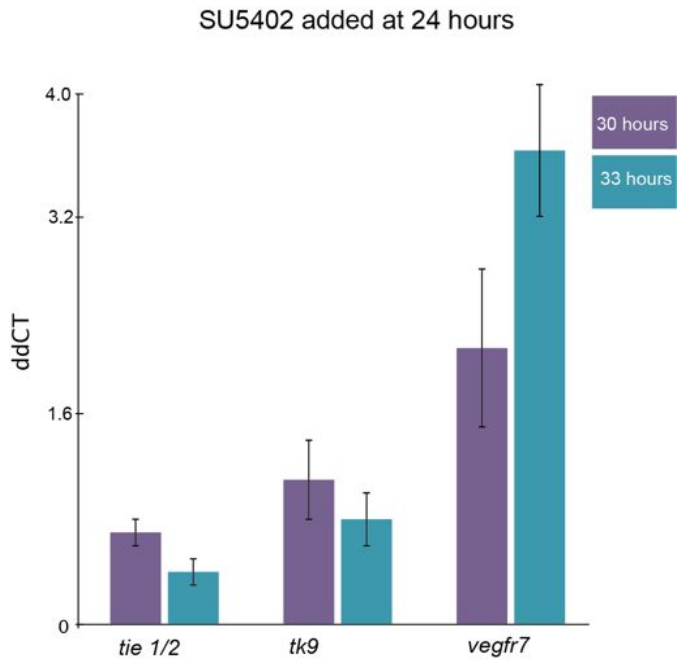

Figure 6.12. Quantitative analysis of RTK genes in SU5402 treated embryos
Perturbation analysis of SU5402 treated embryos. SU5402 added at 24 hours. Gene expression levels were quantified by QPCR at 30 (purple) and 33 (teal) hours. Differences of mRNA levels relative to controls are shown as ddCt. Significant threshold is a ddCt of + or -1.6, which is equal to ~3 folds of difference. SU5420 treatments were repeated in different batches and the standard deviation is shown as error bars in the chart. Experiment carried out by Isabelle Blomfield.

6.2.3 Characterisation of *fgfr like-1* and *fgf 8/17/18/24*

A second explanation for the spatial expansion of *an like-4* and *foxJ1* in SU5402 treated embryos, could be the unknown presence of FGF ligands or receptors. In this section, I extend the knowledge of FGF signalling components by characterising the temporal and spatial expression patterns of *fgfr like-1,* a so far uncharacterised FGF receptor. Next, using data from a recently published phylogenetic analysis of FGF ligands (Oulion *et al.,* 2012), I searched the sea urchin genome and transcriptome for novel FGF ligands.

***fgfr like-1* is expressed in the apical domain during development**

Besides the 4 classical FGF receptors, a fifth evolutionarily related protein, called FGFR-like-1 has been discovered in all major metazoan phyla (Bertrand *et al.*, 2009). Like other FGFRs, *fgfr-like 1* contains three extracellular Ig-like domains and a single transmembrane helix. However, in contrast to the other FGF receptors, it does not possess an intracellular RTK domain, but instead harbours a C-terminal domain of only 100 residues that cannot signal by transautophosphorylation, although it still has a functional role in organisms studied so far (Trueb, 2011). Interestingly, *fgfr like-1* is expressed in neural tissues and involved in nervous system development in a number of organisms. For example, in planarians, *fgfr like-1* is specifically expressed in the head region and loss of function studies results in ectopic expression of brain tissue throughout the body (Cebria *et al.,* 2002) and Xenopus shares a conserved expression of *fgfr like-1* in the anterior regions of the body (Hayashi *et al.,* 2004).

fgfr like-1 expression (figure 6.13 A - blue line) begins during cleavage stage (9 hours) and reaches 94 transcripts per embryo by hatching blastula stage (15 hours). Expression increases slowly, reaching 143 transcripts per embryo by early gastrula stage (30 hours) and then increases rapidly, reaching 348 transcripts per embryo by late gastrula stage (48 hours). Until the start of gastrulation, *fgfr like-1* expression is ubiquitous (figure 6.13 B), it then becomes restricted to the ectoderm and gut and is excluded from the vegetal plate (figure 6.13 C). From late gastrula stage, *fgfr like-1* is

expressed broadly in the apical domain and the foregut (figure 16.3 D). Expression can also be seen in the oral ectoderm (figure 16.3 E black arrowhead). In the pluteus larvae, *fgfr like-1* is expressed at high levels in the apical domain and the foregut, and a lower levels the oral ectoderm and midgut (figure 6.13 F). A double fluorescent WMISH of *fgfr like-1* and *foxQ2*, shows that *fgfr like-1* is expressed in a larger domain than *foxQ2* especially on the oral side (figure 6.13 G).

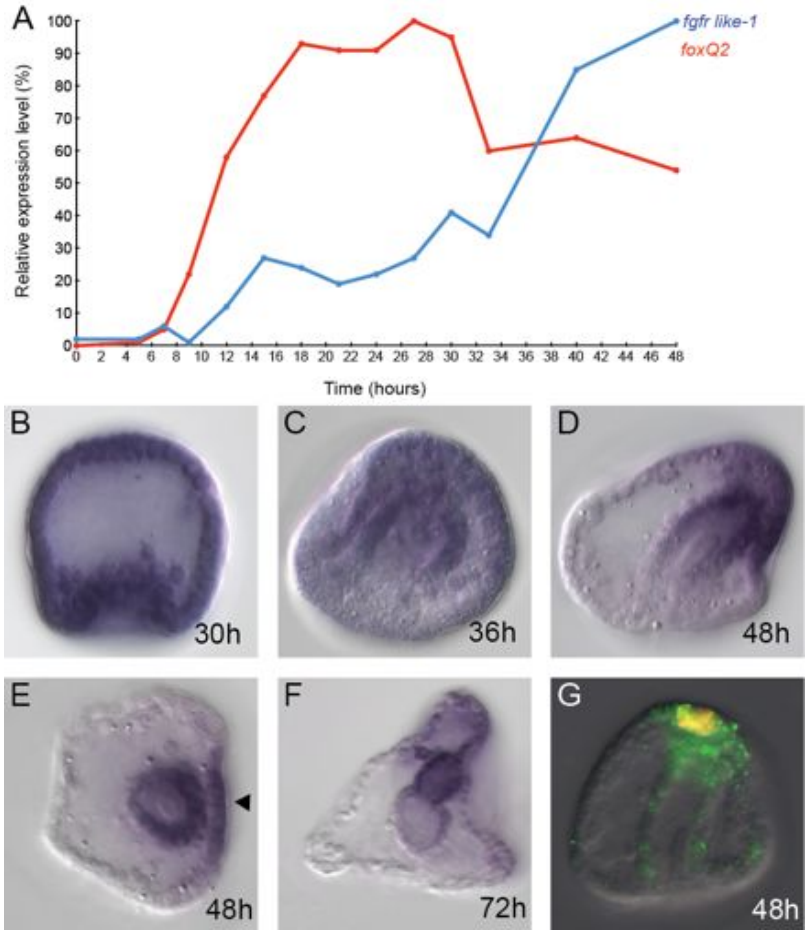

Figure 6.13. Temporal and spatial expression profiles for *fgfr like*-1
(A) Graph shows the temporal expression profile as revealed by QPCR. Expression levels are given as a fraction of peak expression. (B-F) DIC images of a NBT/BCIP WMISH of *fgfr like-1* at different stages of development. (G) Double fluorescent WMISH of *fgfr like-1* (green) and *foxQ2* (red). Unless otherwise specified embryos are imaged with DIC and are presented in a lateral view with the oral side at the right and the apical domain at the top. (E) is a vegetal view. See main text for descriptions of arrowhead.

Discovery of a novel FGF ligand in sea urchin

Currently available data, have always suggested that only a single FGF ligand exists in sea urchin (Mistry *et al.,* 2003; Itoh and Ornitz, 2004; Lapraz *et al.,* 2006; Poustka *et al.,* 2007; Rottinger *et al.,* 2008). Recently, Oulion and colleagues (2012), while still maintaining that sea urchin has a single FGF ligand, suggested that the common ancestor of Ambulacraria had at least three FGF ligands and that sea urchin had lost two of these and subsequently was left with a single FGF ligand.

With the recent publication of the sea urchin transcriptome (Tu *et al.,* 2012), I was able to search for the two additional FGF ligands predicted by Oulion *et al.* (2012), to have been lost in the sea urchin lineage. Using the protein sequence from *Saccoglossus kowalevskii* of two subfamilies of FGF ligands, FGF 8/17/18/24 and FGF 19/21/23, that have not been found in the sea urchin (for accession numbers see Oulion *et al.,* 2012), I used BLASTP to search the sea urchin transcriptome for possible matches. The results showed no matches for FGF 19/21/23 but one good match was found for FGF 8/17/18/24. Prosite and PFAM were used to search for conserved domains in the coding sequence, and confirmed the presence of an FGF superfamily conserved domain, authenticating it as putative FGF ligand. The transcriptome also showed that there were three different transcripts for this FGF 8/17/18/24 protein.

Temporal expression data were gathered for each transcript individually. *fgf 8/17/18/24* transcript 1 begins to be expressed around hatched blastula stage (18 hours) and steadily increases throughout development. *fgf 8/17/18/24* transcript 2 begins to be expressed at very low levels and only starts to be expressed after late gastrula (48 hours; data not shown). *fgf 8/17/18/24* transcript 3 is the most strongly expressed of all three transcripts, and starts at hatching blastula stage (15 hours) and continues to rise steadily until late gastrula stage (48 hours; figure 6.14). WMISH, designed to be informative for all three transcripts, was used to identify the spatial expression pattern of *fgf 8/17/18/24.* At hatching blastula stage, *fgf 8/17/18/24* is ubiquitously expressed (figure 6.14 A). From hatched blastula stage to the start of gastrulation, *fgf 8/17/18/24* is broadly expressed in the apical domain (figure 6.14 B-D). By mid-gastrula stage, the expression of *fgf 8/17/18/24* has become more restricted along the oral-aboral axis

(figure 6.14 E). At late gastrula stage, *fgf 8/17/18/24* forms a horseshoe shape that is cleared from the central and oral apical domains.

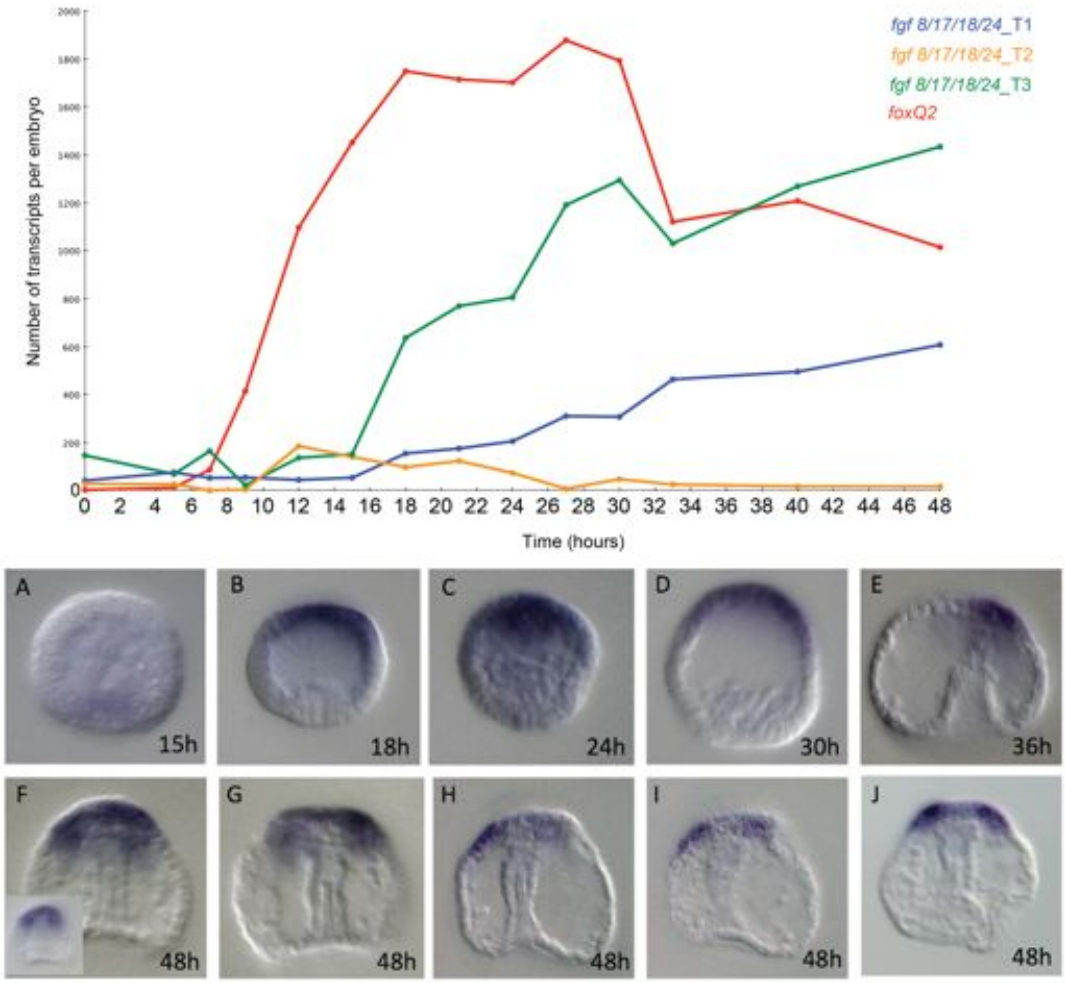

Figure 6.14. Temporal and spatial expression profile for *fgf 8/17/18/24*
Graph showing the temporal expression profile for each indivdual transcript as revealed by QPCR and expressed in number of transcripts per embryo. (B-J) DIC images of NBT/BCIP WMISH of *fgf 8/17/18/24* at different developmental stages. Unless otherwise specified embryos are imaged with DIC and are presented in a lateral view with the apical domain at the top. F,G,J are presented in an oral view. Experiment carried out by Isabelle Blomfield.

6.2.4 Functional analysis of *zic2*

Only a limited number of genes are affected by SU5402 treatment. One transcription factor that is significantly upregulated is *zic2.* Interestingly, *zic2* is expressed in the aboral half of the apical domain at late gastrula in the same location as serotonergic neurons (chapter 3-5) and is thought to have a conserved role in neuronal development. To investigate the role of *zic2* in (1) FGFR/unknown RTK signalling and (2) apical organ specification, embryos were injected with a *zic2* MASO.

zic2 represses itself and is required for serotonergic neurons

Embryos injected with *zic2* MASO show only minor morphological defects (figure 6.15 A-H). A slight delay in embryonic development can be observed at mesenchyme blastula stage when control and *zic2* MASO treated embryos are compared (figure 6.15 A,B). Dark-field microscopy confirms that no effect is seen in cilia and an apical tuft is retained (figure 6.15 C,D). Other than an initial delay, embryos develop as normal, gastrulate and form a regular skeleton (figure 6.15 E-H). Embryos treated with *zic2* MASO were collected at 16, 20 and 24 hours and analysed using QPCR to identify functional linkages with other apical organ genes (figure 6.15 I). Although expressed only in the apical domain, *zic2* MASO had almost no effect on all the "classical cohort" of apical domain gene such *foxQ2, six3, hbn, rx, ac-sc* etc*.* Two genes were affected, *nk2.1* and *zic2* itself. *nk2.1* is only upregulated at 16 hours but at no other time point, while *zic2* represses itself. Interestingly, *zic2* is required for a normal complement of serotonergic neurons and embryos treated with *zic2* have almost no serotonergic neurons when compared to controls embryos (figure 6.15 J-L). That *zic2* represses itself is very interesting, and can shed light on other results involving *zic2.* For example, in SU5402 treatments, *zic2* is often upregulated at the first time point but not at the second. Furthermore, in embryos treated with *fgfr1* MASO, *zic2* is consistently upregulated but always below the threshold. In both these cases, the autorepressive function of *zic2* may help explain these results in more detail.

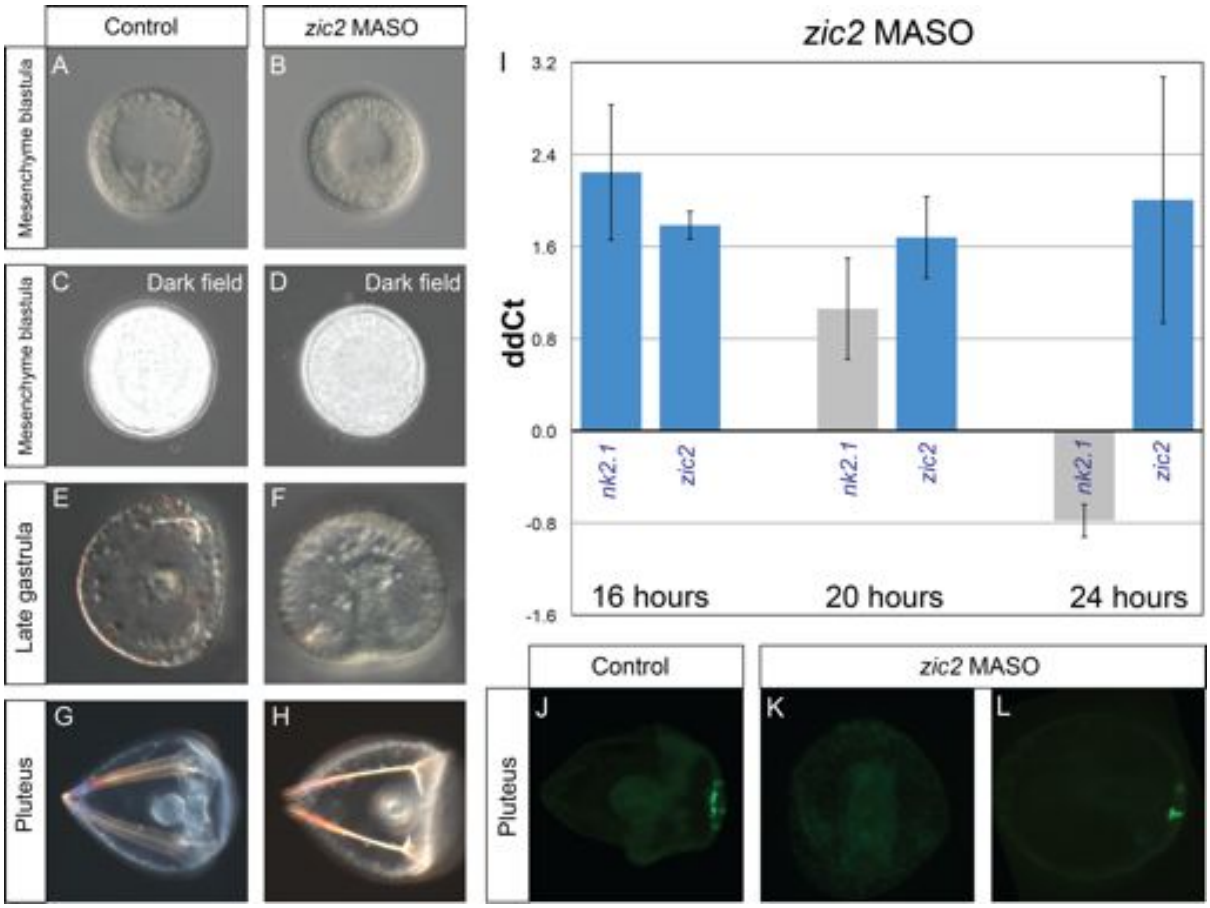

Figure 6.15. Morphological, molecular and immunohistochemical results of *zic2* MASO

(A-H) DIC images showing morphology in control and *zic2* MASO treated embryos. (C,D) Normal cilia can be seen using dark field microscopy in normal and *zic2* MASO treated embryos. (I) Perturbation analysis of *zic2* MASO treated embryos. Gene expression levels were quantified by QPCR at 4 hour intervals. Differences of mRNA levels relative to controls are shown as ddCt. Significant threshold is a ddCt of + or -1.6, which is equal to ~3 folds of difference. *zic2* MASO treatments were repeated in different batches and the standard deviation is shown as error bars in the chart. Significant upregulation (blue bar) and downregulation (red bar). (J-L) Serotonin immunohistochemistry (green) in control and *zic2* MASO treated embryos. Control embryos have on average 4 neurons (J, n=15) while *zic2* MASO show either no neurons (K, n=10) or an average of 2 neurons (L, n=37).).

6.3 Summary

In conclusion, in this chapter I have showed that embryos treated with SU5402 or *fgfr1* MASO upregulate a totally different set of genes. SU5402 treatment upregulates *an like-4* and several genes involved in cilia development, while embryos injected with *fgfr1* MASOs upregulate transcription factors initially expressed in the apical domain and

later in neurons. This implies that SU5402 is not a specific inhibitor of FGFR1. Three possible aberrant targets for SU5402 were identified and investigated but non showed an expression pattern that easily explains the spatial expansion of SU5402 targets. In light of this, additional components of the FGF signalling family were characterised. Gene expression patterns for both *fgf 8/17/18/24* and *fgfr like-1* are presented and show that are both are expressed in the apical domain during development. Finally, a functional analysis of *zic2* shows that it represses itself and *nk2.1.*

Chapter 7: Discussion

In this thesis, I set out to provide new insight and understanding into the development of the sea urchin apical organ. The primary focus of my thesis was to elucidate the dynamic regulatory states that exist in the apical organ, during development. To this end, high-resolution spatial and temporal expression profiles were integrated into cellular maps of the apical domain, at different developmental stages. This combinatorial gene expression analysis identifies the different sub-domains that exist in the apical domain and shows how different groups of cells have unique regulatory states (chapters 3-5). The secondary aim of my thesis was to begin to tease apart some of the regulatory interactions that form the apical organ GRN. To start, I presented a large-scale quantitative screen to identify possible downstream targets of FGF signalling, by using the FGFR-specific chemical inhibitor SU5402. Only a limited number of genes were recovered through this screen and the results, while interesting, were inconsistent with the spatial expression of known FGF signalling components. I therefore investigated the specificity of the SU5402 inhibitor by treating embryos with an *fgfr1* MASO and showed the results differed from the SU5402 screen. Finally, embryos were treated with a *zic2* MASO to investigate the role of *zic2* in the apical organ GRN (chapter 6).

This discussion is divided into the following sections: The first two sections form an overview and summary of the high-resolution mapping and regulatory state analysis; the third discusses the discovery of a novel FGF ligand and summarises what we know about apical organ expression of FGF signalling components; the fourth section provides a network perspective on the SU5402 and MASO experiments, integrating all the data to construct a preliminary GRN; in the fifth section, I take an evolutionary perspective of the work produced in this thesis and present some of the possible implications in a wider biological framework; in the final two sections, future directions are discussed and I finish with a few closing remarks.

7.1 Multiple dynamic regulatory states underlie the development of the apical organ

Regulatory state analysis: Its importance and some critiques of the strategy

A thorough understanding of a GRN allows us to understand what drives development forward and offers a mechanistic explanation for developmental events, such as specification and differentiation (Materna and Oliveri, 2008). Two important foundations are required to successfully build a GRN: the identification of as many relevant, regulatory genes as possible, and the subsequent characterisation of these genes at high-resolution in both space and time. This allows the characterisation of the cells' regulatory state and may suggest, although preliminarily, the flow of regulatory information (Materna and Oliveri, 2008). The existence, and more importantly, the progression of regulatory states through apical organ specification has not been studied systematically. However, such information is essential for determining the participants of the underlying GRNs, and for indicating order in the regulatory hierarchies (Materna *et al.,* 2013).

After producing an apical organ gene set, I used QPCR to complete high-resolution temporal expression data when required (see appendix B). High-resolution temporal expression data, in itself, is a very useful tool in the construction of a GRN, as it helps to understand the underlying regulatory logic. Bolouri and Davidson, (2003) have previously shown, using parameters measured for a number of regulatory and downstream genes in *S. purpuratus*, the typical gene cascade step time, *i.e*., the interval between activation of a regulatory gene and the activation of its direct transcriptional targets; for embryos developing at 15°C, this is about two to three hours. With this knowledge, the study of temporal expression profiles can give a useful insight into potential transcriptional network architectures.

To some extent, acquiring high-resolution temporal data is relatively straight forward, thanks to easily available and semi high-throughput technology, such as QPCR and the Nanostring nCounter (Materna *et al.,* 2010). Producing high-resolution spatial data, on

the other hand, is much more difficult and time consuming. A number of different strategies have been used in the sea urchin community to deal with the technical difficulties of acquiring spatial data for GRN construction. The first thing to consider is the number of genes under study. There is a need to balance the study of fewer genes at higher resolution and in more detail, (Li *et al.,* 2012; Materna *et al.,* 2013; de-Leon *et al.,* 2013) *versus* studying a greater number of genes but at a lower resolution and in less detail (Poustka *et al.,* 2007; Saudemont *et al*., 2010; Rafiq *et al.,* 2012). The second thing to consider when devising a GRN strategy, is what method should be used to obtain the actual spatial data. Essentially, the primary choice is between the less time consuming enzymatic WMISH and the more time consuming fluorescent WMISH, after which there exists a secondary choice; between single or double WMISH. It was clear to me that the benefits of double WMISH are immeasurable and have been put to excellent use recently by Li *et al.,* (2012) and de-Leon *et al.,* (2013), showing that both the oral and aboral ectoderm are spatially complex and contain more regulatory state sub-domains than previously thought. In contrast, when comparing two single enzymatic WMISH images, it is often difficult to discriminate if two gene expression patterns are the same or different. Double enzymatic WMISH, however, can show subtle differences in gene expression and suggest that multiple expression domains exist. The greatest power in discriminating gene expression patterns, comes through the use of double fluorescent WMISH. Furthermore, double fluorescent WMISH can be easily combined with immunohistochemistry and nuclei staining.

The biggest initial obstacle to the construction of an apical organ GRN, and generally for any embryonic structure, is the lack of detailed and systematic spatial information. At the start of this study, much of the available spatial data originated from large screens performed at the time the sea urchin genome was sequenced (Sodergren *et al.,* 2006) and often shows only a single developmental stage. Furthermore, a study of the literature shows the apical domain is treated as a simple, homogenous territory, much the same way that the oral and aboral ectoderm were (until recently) considered to be simple and homogenous territories (Li *et al.,* 2012; de-Leon *et al.,* 2013). Even the most recent studies (Yaguchi *et al.,* 2012; Range *et al.,* 2013) and reviews (Angerer *et al.,* 2011) still depict the apical domain as a simple territory with serotonergic neurons represented in diagrams by circles. To this end, I focused my efforts on elucidating the

spatial complexity of the apical organ during development. I decided to investigate a smaller number of genes and obtain spatial information using high-resolution double-fluorescent WMISH, combined with nuclei staining in order to increase the resolution of my results to the cellular level.

The apical domain is subdivided into many more domains than previously described

In the absence of any obvious morphological landmark in the apical domain, I decided to use *foxQ2* as a molecular landmark for the apical domain, to unequivocally position the expression of all other regulatory genes. I have presented in this thesis a series of combinatorial gene expression studies. Strikingly, the majority of the genes show considerably different spatial expression patterns, resulting in an increased number of regulatory state sub-domains within the apical domain. This is in sharp contrast to how the spatiality of the apical domain has been viewed so far. The apical domain is not a simple homogeneous region (as reviewed recently by Angerer *et al.,* 2011) or even a simple inner and outer ring, (as depicted in Wie *et al.,* 2009) but rather a complicated embryonic territory with different groups of cells that express unique sets of genes, and thus have unique regulatory states that likely drive the development of different cell types. Furthermore, this high level of regulatory complexity is present quite early in development; in fact the apical domain is already comprised of multiple regulatory state sub-domains by the end of cleavage and hatching blastula stage and increases in spatial complexity rapidly during development. As additional genes begin to be expressed in the apical domain, they not only illustrate the appearance of novel domains, but they also result in existing domains becoming refined and divided.

Figure 7.1 summarises the proposed regulatory states that exist in the apical domain between hatching blastula and late gastrula stage. For the stages between hatching blastula and mesenchyme blastula, I present both a lateral and apical map of the different regulatory states. The lateral perspective illustrates the regulatory states that exist along the oral-aboral axis, through the centre of the apical domain. For mid and late gastrula, the number of genes studied, and hence the number of regulatory states

and level of spatial complexity, is too great and beyond the scope of this thesis to be presented from an apical view; therefore, only the lateral view is shown. More advanced imaging and 3D modelling are required to be able to gain a full *apical view* appreciation of regulatory state complexity.

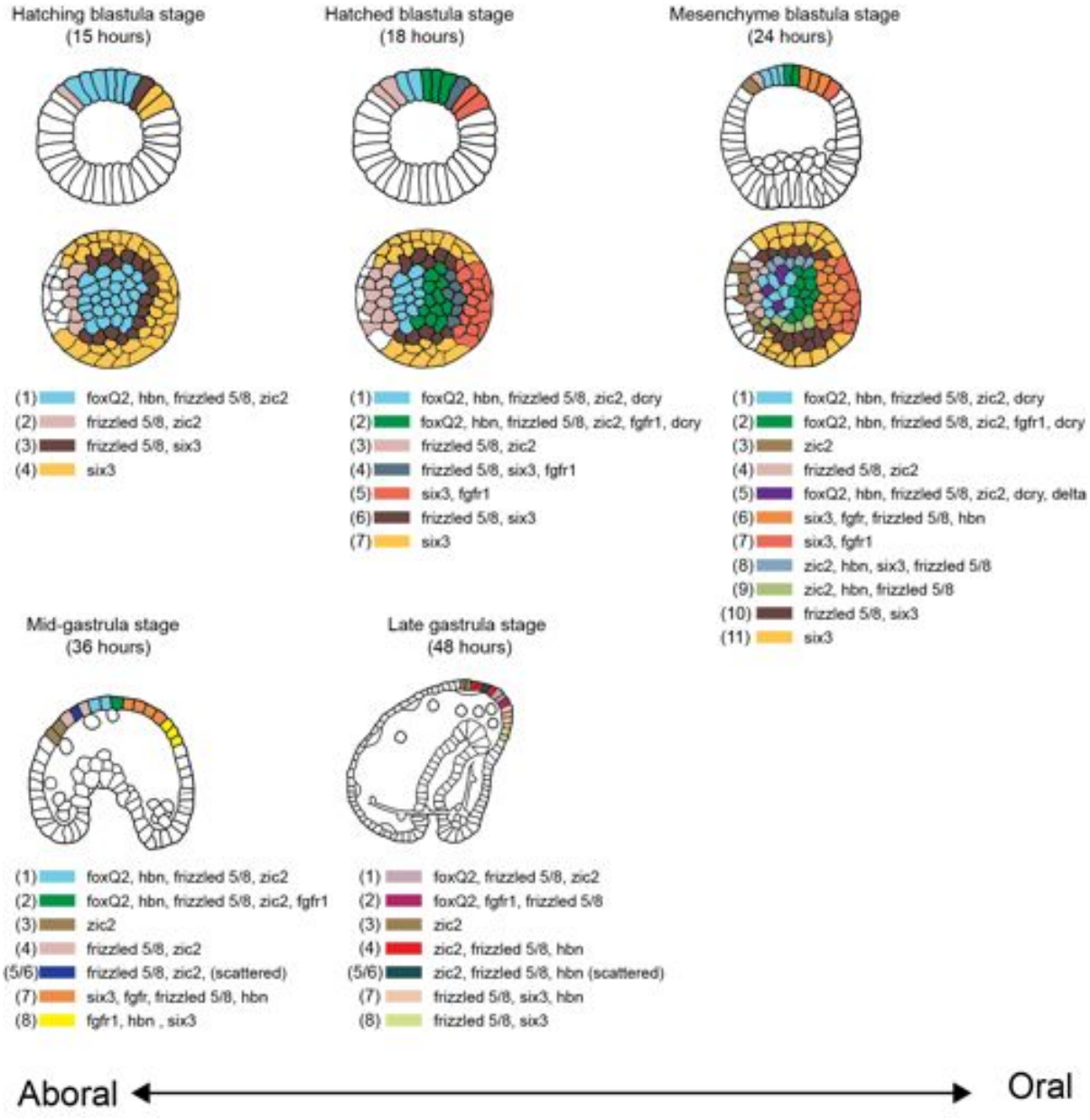

Figure 7.1. Apical domain regulatory states
Lateral and apical maps showing the apical domain regulatory states in hatching blastula, hatched blastula and mesenchyme blastula stages. Lateral maps showing the apical domain regulatory states in mid-gastrula and late gastrula stages. Each colour-coded cell represents a unique regulatory state in *time and space*. Cell in the same colour share the same regulatory state. All maps are presented with the oral side on the right.

Hatching blastula stage

At the end of cleavage stage and after an extensive series of signalling events, (Range *et al.,* 2013), the apical domain emerges and is formed by at least four regulatory states: (1) the *foxQ2* central apical domain that expresses *foxQ2, hbn, frizzled 5/8,* and *zic2*; (2) a cell row on the aboral edge of the *foxQ2* central apical domain that expresses *frizzled 5/8* and *zic2;* (3) an inner horseshoe-shape domain formed by one cell row outside *foxQ2* that is open on the aboral side and expresses *frizzled 5/8* and *six3;* (4) an outer and larger horseshoe domain that expresses just *six3*. This final domain likely to express additional oral and aboral ectodermal genes, that are not considered in this study.

Hatched blastula stage

The combinatorial gene expression identifies at least seven regulatory states by hatched blastula stage: (1) the aboral half of the *foxQ2* central apical domain that expresses *foxQ2, hbn, frizzled 5/8, zic2* and *dcry;* (2) the oral half of the *foxQ2* central apical domain that expresses *foxQ2, hbn, frizzled 5/8, zic2*, *dcry* and *fgfr1;* (3) the aboral edge of the *foxQ2* central apical domain that expresses *frizzled 5/8* and *zic2;* (4) a cell row on the oral edge of the *foxQ2* central apical domain that expresses *frizzled 5/8, six3,* and *fgfr1;* (5) the oral outer apical domain that expresses *six3* and *fgfr1;* (6) a cell row along the right and left edges of the *foxQ2* central apical domain that express *frizzled 5/8* and *six3;* (7) two additional cell rows to the right and left that express only *six3* and mark the outer boundary of the apical domain.

Mesenchyme blastula stage

At this stage, the complexity of the apical domain increases and at least eleven different regulatory states are identified: (1) the aboral half of the *foxQ2* central apical domain expressing *foxQ2, hbn, frizzled 5/8, zic2*, and *dcry*; (2) the oral half of the *foxQ2* central apical domain, expressing *foxQ2*, *hbn, frizzled 5/8, zic2*, *dcry* and *fgfr1,* (3) the aboral outer apical domain expressing just *zic2;* (4) the aboral edge of the *foxQ2* central apical domain, expressing *frizzled 5/8* and *zic2;* (5) scattered cells in the aboral half of the *foxQ2* central apical domain, expressing *foxQ2, hbn, frizzled 5/8, zic2, dcry* and *delta;* (6) the oral edge of the *foxQ2* central apical domain, expressing *six3, fgfr1, frizzled 5/8* and *hbn;* (7) the oral outer-apical domain, expressing *six3* and *fgfr1*; (8) a cell row along the left edge of the *foxQ2* central apical domain, expressing *zic2, hbn, six3* and *frizzled 5/8;*

(9) a cell row along the right edge of the *foxQ2* central apical domain, expressing *zic2, hbn* and *frizzled 5/8;* (10) an additional cell row on the right and left of the previous regulatory state and expressing *frizzled 5/8* and *six3;* (11) two additional cell rows to the right and left that express only *six3* and mark the outer boundary of the apical domain.

Mid-gastrula stage

The regulatory complexity of the apical domain during gastrulation dramatically changes. On a lateral representation, the apical domain along the oral-aboral axis, contains at least eight regulatory states by mid-gastrula stage: (1) the aboral half of the *foxQ2* central apical domain expressing *foxQ2, hbn, frizzled 5/8* and *zic2*; (2) the oral half of the *foxQ2* central apical domain, expressing *foxQ2, hbn, frizzled 5/8, zic2,* and *fgfr1;* (3) the aboral outer apical domain, expressing just *zic2;* (4) the aboral edge of the *foxQ2* central apical domain expressing *frizzled 5/8* and *zic2;* (5/6) the aboral apical domain expressing *frizzled 5/8, zic2* and "scattered" cells - at least two types of scattered cell exists i) *dcry* and *mox* ii) *z167* (7) the oral edge of the *foxQ2* central apical domain, expressing *six3, fgfr1, frizzled 5/8* and *hbn;* (8) the oral outer apical domain, expressing *six3, hbn* and *fgfr1*.

Late gastrula stage

At this stage, differentiation markers begin to be expressed and the different regulatory states reach the single cell resolution. On a lateral representation, the apical organ along the oral-aboral axis contains at least eight regulatory states: (1) the aboral half of the *foxQ2* central apical domain, expressing *foxQ2, frizzled 5/8* and *zic2*; (2) the oral half of the *foxQ2* central apical domain, expressing *foxQ2, frizzled 5/8,* and *fgfr1;* (3) the aboral outer apical domain, expressing just *zic2;* (4) the aboral edge of the *foxQ2* central apical domain, expressing *frizzled 5/8*, *zic2* and *hbn;* (5/6) scattered cells in the aboral apical domain, expressing *frizzled 5/8, zic2, hbn* and "scattered" cells - at least two types of scattered cell exists i) *dcry* and *mox* ii) *dcry, mox* and *z167;* (7) the oral edge of the *foxQ2* central apical domain, expressing *six3, frizzled 5/8* and *hbn;* (8) the oral outer-apical domain, expressing *six3* and *frizzled 5/8.*

Regulatory state highlights

(i) One of the most striking results to emerge from the regulatory state analysis is the spatial complexity that exists so early in development. Already by hatching blastula stage, the apical domain can be split into four regulatory state sub-domains, each expressing a unique combination of transcription factors and signalling molecules. (ii) The apical domain acquires oral-aboral polarity through the expression of *fgfr1* in the oral half of *foxQ2* central apical domain, already by hatched blastula stage. (iii) Looking at just eight regulatory genes at mesenchyme blastula stage, provides over 11 regulatory states. The genes studied here represent a small selection of early regulatory genes (compared to the complete gene set see table 3.1), and already the level of spatial complexity is high. (iv) *delta* marks the appearance of regulatory genes that are scattered in the apical domain already by mesenchyme blastula stage. (v) The additional regulatory states that exist just by looking at three scattered genes (*dcry, mox* and *z167).* (vi) Overall there is a sharp and defined difference between the oral regulatory states and the aboral regulatory states of the apical domain. This is particularly interesting, as the serotonergic neurons differentiate from the aboral apical domain, and the oral side forms part of the ciliary band, which itself is the location of other neurons.

7.2 Serotonergic neurons and neurosensory cells

The "scattered" regulatory state: an additional layer of spatial complexity in the apical organ

Many studies have shown that the sea urchin apical organ is home to the serotonergic neurons (Bisgrove and Burke, 1986, 1987; Yaguchi and Katow, 2003; Nakajima *et al*., 2004). The serotonergic neurons are physically located in scattered cells at the aboral edge of the *foxQ2* central apical domain (Yaguchi *et al.,* 2008). Regulatory and downstream genes that are expressed in scattered cells in and around the apical organ are reminiscent of these serotonergic neurons and are often thought to be linked to neurogenesis. Recent examples of this are *fez* and *zfhx1,* which both appear scattered in the apical domain during gastrulation (Yaguchi *et al.,* 2011; Yaguchi *et al.,* 2012). *fez*

controls the size of the apical domain and hence the number of serotonergic neurons (Yaguchi *et al.,* 2011), while *zfhx1* is expressed in the precursor cells of serotonergic neurons, and is required for their differentiation (Yaguchi *et al.,* 2012). Table 7.1 summarises a literature survey of regulatory genes, that are expressed in scattered cells in the sea urchin apical domain.

Table 7.1. "Scattered" regulatory genes in the sea urchin apical domain

The gene name and unique ID (SPU_0XXXX) is given for each gene. The type of regulatory gene, either transcription factor or signalling molecule is specified as well as the specific gene family.

Gene name	Gene ID	Gene type	Gene family	Reference
ac-sc	SPU_028148	Signalling molecule	bHLH	*Burke et al., 2006*
delta	SPU_016128	Signalling molecule	Delta/notch	*Walton et al. 2009*
ebf3/coe	SPU_004702	Transcription factor	bHLH	*Jackson et al., 2010*
egr/z60	SPU_015358	Transcription factor	Zinc-finger	*Materna et al., 2006*
ets1/2	SPU_002874	Transcription factor	Ets	*Rizzo et al., 2006*
fez/z133	SPU_027491	Transcription factor	Zinc-finger	*Yaguchi et al., 2011*
hbn	SPU_023177	Transcription factor	Homeodomain - paired	*Burke et al., 2006*
mox	SPU_025486	Transcription factor	Homeodomain	*Pouska et al., 2007*
pea	SPU_014576	Transcription factor	Ets	*Rizzo et al., 2006*
rx	SPU_014289	Transcription factor	Homeodomain - paired	*Burke et al., 2006*
z167	SPU_015362	Transcription factor	Zinc-finger	*Pouska et al., 2007*
zfhx1/z81	SPU_022242	Transcription factor	Zinc-finger	*Yaguchi et al., 2011*

Integrating the expression data that have been published about these scattered genes, allows several conclusions to be made. Yaguchi *et al.,* (2011) shows that *fez* is co-expressed with *tph* cells in late gastrula stage. Because TPH is the rate-limiting enzyme in serotonin synthesis, it is a specific marker for serotonergic neurons in sea urchin embryos (Yaguchi and Katow, 2003). *fez* also shows co-expression with *zfhx1* at gastrula stages (Yaguchi *et al.,* 2012). Like *fez, zfhx1* also shows co-expression with *tph* and interestingly also with *delta* (Yaguchi *et al.,* 2012). Finally, Wei *et al.,* (2009) shows that at late gastrula stage, the transcription factor *rx* is co-expressed in cells containing serotonin. Therefore, it is likely that at gastrula stages, there is a subset of cells that express *zfhx1, fez* and *tph* (and possibly *rx*).

An interesting consequence of regulatory genes acquiring a scattered expression pattern, is the drastic increase in both the spatial complexity of an embryonic territory and the number of its regulatory states. A good example of this is presented in this thesis. I present a detailed analysis of a small subset of scattered genes, thought to be involved in circadian light sensing and serotonergic neurogenesis.

From late gastrula stage onward, *dcry, mox* and *z167* are expressed in scattered cells in the aboral part of the apical domain. By this time, *dcry* is no longer co-expressed with *foxQ2* and is located on its aboral edge. This "expressed on the aboral edge of *foxQ2"* expression dynamic, appears to be characteristic of scattered genes and is seen with at least *dcry,* but also with *delta* (figure 5.4), *fez* (Yaguchi *et al.,* 2011) and *zfhx1* (Yaguchi *et al.,* 2012) and it seems likely to be shared with *mox* and *z167* as well. Figure 7.2. summarises the regulatory states, based on the expression patterns of three scattered genes; *dcry, mox* and *z167.*

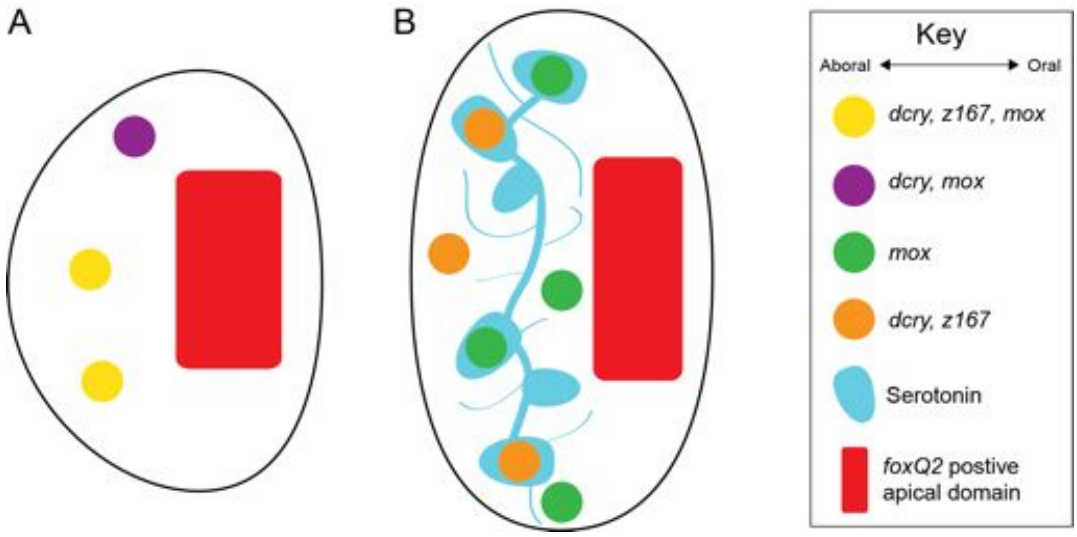

Figure 7.2. Example of scattered regulatory states
(A) Late gastrula (48 hours) shows that three genes; *dcry, mox* and *z167* form at least two cell types. (B) Early pluteus larvae (72 hours) shows that these three genes combine with serotonin to form at least five cell types.

Dynamic expression of *dcry*

I have identified a novel population of cells in the neuro-sensory apical organ that express *dcry,* a potential blue UV-A light photoreceptor. This is the first time a potential photoreceptor has been identified in the apical organ of the sea urchin embryo and suggests that embryos have the physical structures to sense environmental stimuli such as light. Towards the end of gastrulation, this population of cells begins to show co-expression with the zinc-finger transcription factor *z167*. Interestingly, *z167* is thought to be a sea urchin homologue of *glass* (Poustka *et al*., 2007), a zinc-finger transcription factor that is required for normal photoreceptor cell differentiation in *Drosophila* (Moses *et al*., 1989). Furthermore, I show for the first time that not all serotonergic neurons in the sea urchin embryo are the same and that a subset of neurons exists that share expression with both *dcry* and *z167*. This is in agreement with the morphological differences seen in serotonergic neurons in the late pluteus larva (Beer *et al.,* 2001).

dcry appears to have multiple and distinct phases of expression (see figure 7.3). (1) initially ubiquitous; (2) broad expression within the *foxQ2* central apical domain; (3) in individual cells, partially in the *foxQ2* central apical domain; (4) in a few individual cells at the aboral edge of the *foxQ2* central apical domain. Even from the start, the expression patterns of *dcry* and *foxQ2* do not perfectly coincide, making it clear that the expression of *dcry* will be driven by a precise regulatory state in which *foxQ2* could be one of the regulatory genes, but which also includes additional, spatially restricted inputs. Furthermore, late *dcry* expression is *foxQ2* independent, thus it is conceivable that *foxQ2* might provide a regulatory input into *dcry* expression from hatching, until the middle of gastrulation. Interestingly, similar regulatory control has recently been predicted for *fez*, which like *dcry,* is co-expressed with *foxQ2* from hatched blastula stage, becoming restricted after gastrulation, to a few individual cells in the aboral edge of the apical organ, and shown to be under regulatory control of *foxQ2* only between blastula and mid-gastrula stages (Yaguchi *et al*., 2011).

Slightly after the start of gastrulation, there begins a downregulation of *dcry* in most of the apical domain, but it is unclear how *dcry* positive cells are ultimately positioned on the aboral edge and no longer co-express with *foxQ2.* There are two explanations to help

explain the transformation of *dcry*. One option is that *dcry* is downregulated in the entire *foxQ2* positive domain and concurrently, a novel set of two-or-three cells begins to express *dcry* along the aboral edge of *foxQ2*. A second option is, that with the start of gastrulation, cells that express *foxQ2* downregulate *dcry*, and the oral restriction of *foxQ2* results in *dcry* cells being localised along the aboral edge of *foxQ2.*

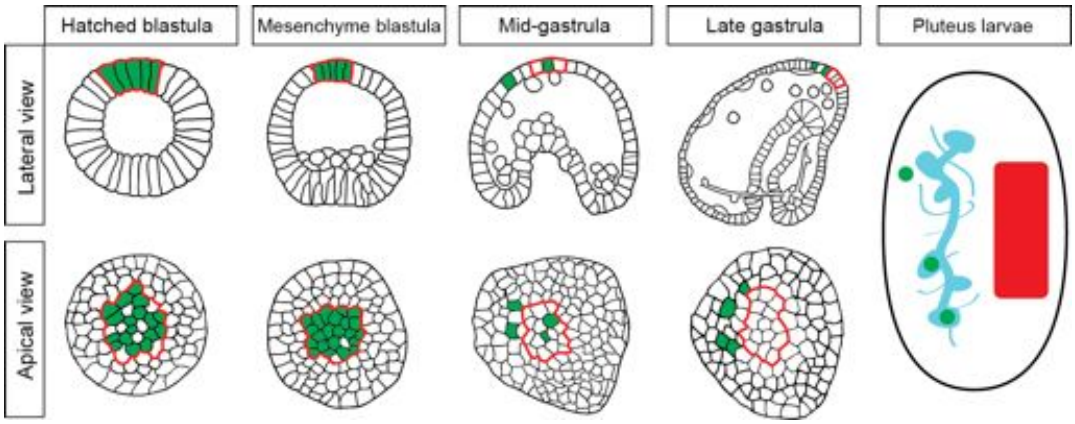

Figure 7.3. Dynamic expression of *dcry*
Cellular maps showing *dcry* expression between hatched blastula and early pluteus larvae. *dcry* is shown in green. The outline of *foxQ2* is in red. Serotonergic neurons are in turquoise. Maps are presented with the oral side at the right.

dcry shows a highly dynamic interrelationship with both *mox* and *z167* (figure 7.2). Ultimately, *dcry* is co-expressed with *z167* at pluteus larva. However, at late gastrula stage, all *z167* cells expressed *dcry* but not all *dcry* cells express *z167.* One explanation for this is that *dcry* cells not expressing *z167,* are in the process of being downregulated, and thus by pluteus larva, no longer exist, leaving *z167* and *dcry* to be fully co-expressed. *mox* and *dcry* are co-expressed at mid and late gastrula stages but not in pluteus larvae. Once again, it seems likely that *dcry,* is downregulated in these cells, between late gastrula stage and pluteus larva. The fact that the number of *mox* cells remains the same, from late gastrula stage to pluteus larva, while *dcry* deceases, would appear to support this.

Not all serotonergic neurons are the same

Until now, the expanding array of serotonergic neurons in the sea urchin pluteus larva were thought to be homogenous and thus share a common regulatory state. My results, however, show that the pluteus larva contains at least two forms of serotonergic neuron. *Type 1 serotonergic neurons* express only serotonin and not *dcry* or *z167*, while *Type 2 serotonergic neurons* express serotonin together with *dcry* and *z167*. This could suggest that *Type 2 serotonergic neurons* function as sensory neurons while *Type 1 serotonergic neurons* are non-sensory. In hemichordates, it has been reported that the serotonergic nervous system contains two morphologically distinct serotonergic neurons. The first, presumed sensory, are elongated and extend a process to the cell surface. The second are rounded with no extended process and presumed to have a non-sensory function (Nezlin and Yushin, 2004). This is consistent with our observation in the sea urchin pluteus larvae, whereby using immunohistochemistry, we have identified a set of large bottle-shaped serotonergic neurons located in the aboral side of the apical organ and reaching the surface, plus a set of serotonergic neurons with the typical shape of bipolar interneurons located more orally (Oliveri and Ward, unpublished data). It would be beneficial to pursue a more detailed study of the regulatory states and temporal expression of these morphologically distinct neurons. It is interesting to note that a similar combination of *dcry* and *z167* has been shown in *Drosophila*, where *glass (z167)* is co-expressed with *dcry,* in a subset of so-called "clock" (DN1) neurons in the brain, which function as pacemakers of the circadian clock (Klarsfeld *et al*., 2004). This inspires the suggestion that there exists a subset of serotonergic neurons in the sea urchin, that could be involved in linking the external environment to the internal circadian clock via the photoreceptor *dcry*, suggesting that the sea urchin apical organ has a role in light sensing.

7.3 The development of the apical organ is associated with multiple FGF signalling components

Novel FGF 8/17/18/24 discovered in the apical organ

Until now, only a single FGF 9/16/20 ligand was thought to exist in sea urchin (Lapraz *et al.,* 2006; Poustka *et al.,* 2007; Rottinger *et al.,* 2008). Recently, Oulion *et al.,* (2012; figure 7.4), taking advantage of the diverse range of publicly available metazoan genomes, undertook a phylogenetic analysis of FGF genes. The authors proposed a new classification of FGF ligands into 8 subfamilies, and presented a hypothesis explaining the evolutionary events leading to the present diversity of this gene family. They showed that, while a single FGF gene exists in the echinoderm *Strongylocentrotus purpuratus*, six FGF genes have been found in the hemichordate *Saccoglossus kowalevskii.* One of those genes can be clearly assigned to the FGF 8/17/18/24 subfamily, three genes are orthologs of the FGF9/16/20 subfamily, another is an ortholog of the FGF 19/21/23 subfamily and the final gene shows no clear relationship with any FGF gene subfamily. As hemichordates and echinoderms are sister groups, it means that their ancestor must have had FGF genes from at least three FGF subfamilies: 8/17/18/24, 9/16/20, and 19/21/23. With the recent publication of the *Strongylocentrotus purpuratus* transcriptome (Tu *et al.,* 2012), I decided to search for the presence of additional FGF ligands to confirm that the sea urchin has truly lost two out of three predicted FGF subfamilies. To my surprise, I discovered that a second FGF ligand, showing similarity to the FGF 8/17/18/24 family, exists in the sea urchin transcriptome and thus, contrary to what has been previously thought, was not lost in evolution. Furthermore, spatial analysis showed that it is expressed in the apical domain during development. This is particularly interesting because it means that there is an FGF ligand (FGF 9/16/20) that is expressed on the lateral edges of the apical organ and also an FGF ligand (FGF 8/17/18/24) that is expressed in the apical organ itself. This gives more confidence to the idea that FGF might be playing a conserved role in neural development.

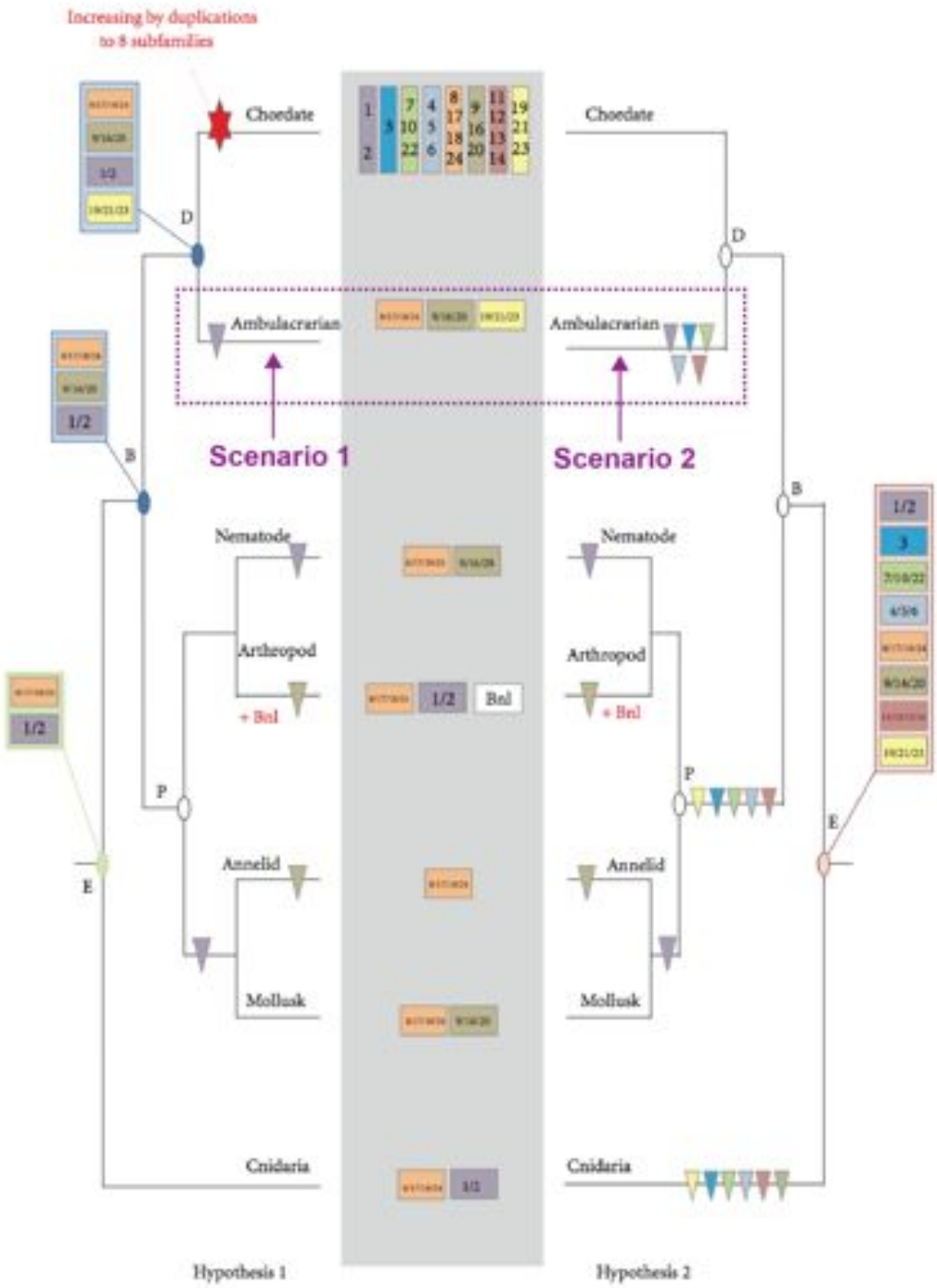

Figure 7.4. Evolutionary scenarios for FGF evolution in eumetazoans.

The minimum number of FGF ligands of each eumetazoan lineage is specified in the centre (grey box). Two evolutionary hypotheses are shown: Scenario 1 (left side), starting from a minimum gene set of two genes (green box) in the eumetazoan ancestor, diversity of the subfamily is acquired through chordate-specific duplications; Scenario 2 (right side), diversity of the subfamily was acquired very early in metazoan evolution, with 8 subfamilies in the eumetazoan ancestor (red box) and then numerous gene losses in the different lineages occurred. Ambulacrarians (purple dashed box). Gene losses are represented by triangles. E: eumetazoan ancestor; P: protostome ancestor; D: deuterostome ancestor and B: bilaterian ancestor. (adapted from Oulion *et al.,* 2012).

fgf 8/17/18/24 is expressed broadly in the apical domain during early stages of development, but then clears from the centre and oral side of the apical domain. This places it in a position where it is likely to be co-expressed with serotonergic neurons in the aboral apical domain. It appears to be co-expressed with *fgfr1,* at least early in development (data not shown), but its expression relative to the other FGF ligand (*fgf 9/16/20*) is unknown. Interestingly, *Nematostella* also has two FGF ligands expressed in the apical organ which work in conjunction with each other. One of these ligands is required for the formation of the apical organ, whereas the other counteracts the FGF signalling to prevent precocious and ectopic apical organ development (Rentzsch *et al.,* 2008).

fgfr like-1 is expressed in the apical organ

I present, for the first time, the spatial expression pattern for *fgfr like-1* in the sea urchin. It is expressed quite broadly in the apical organ after gastrulation, as well as in the tip of the archenteron. At late gastrula stage, co-expression studies with *foxQ2* show that *fgfr like-1* is co-expressed with *foxQ2* in the central apical domain, but is also expressed in the oral and aboral outer apical domain, as well as part of the oral ectoderm. This broad apical domain expression pattern is consistent with a potential role in modulating FGF signalling during neuronal development, in both the aboral apical organ together with the serotonergic neurons and the oral apical organ with the ciliary band neurons. However, its function in sea urchin development is unknown.

Like the other classical FGF receptors, FGFR like-1 contains three extracellular Ig-like domains but lacks the RTK domain, meaning it cannot initiate signal transduction by transphosphorylation. One hypothesis is that FGFR like-1 functions as a negative regulator of FGF signalling in one of two ways. It could either act as a dominant-negative FGFR by ligand-mediated dimerisation with a conventional FGF receptor, preventing transphosphorylation and therefore signal transduction. Alternatively, it could function as a decoy receptor and compete for FGF ligands binding with other FGFRs (Steinberg *et al.,* 2010). How this would function during sea urchin development is unclear. *fgfr like-1* is ubiquitously expressed until mid-gastrula stage, so is unlikely to play a specific role in

the overall patterning of the embryo. After gastrulation, *fgfr like-1* is expressed broadly in the apical domain and could be acting to 'soak up' both FGF 9/16/20 and FGF 8/17/18/24 ligands, thus modulating their effects. From the perspective of the apical organ, the only other FGF receptor that is spatially relevant is FGFR1 which is expressed in the oral half of the apical organ and oral ectoderm. FGFR like-1 could therefore be dimerising with FGFR1 in the oral half of the apical organ and inhibiting or dimming-down the signalling pathway. In our case, a transcription factor(s) downstream of the FGF signalling cascade acts to repress apical domain genes such as *nk2.1, fez, rx,* and *ac-sc*. The presence of FGFR like-1 in the apical domain leads to the hypothesis that it could modulate FGF signalling by reducing the ability of FGFR1 to function as effectively as normal, thereby reducing the inhibition on these downstream targets.

The state of the art: FGF signalling components in the sea urchin embryo

The work presented in this thesis has filled in some crucial gaps in our knowledge of FGF signalling in the development of the sea urchin embryo. The FGF toolkit in the sea urchin embryo, now consists of two FGF ligands: FGF 9/16/20 and FGF 8/17/18/24, and three FGF receptors: two classical FGF receptors, FGFR1 and FGFR2 as well an FGF receptor lacking an RTK domain, FGFR like-1. These FGF signalling components are expressed quite broadly throughout the embryo during development (Figure 7.5). *fgf 9/16/20* is expressed predominantely in regions on either side of the apical domain; in the vegetal ectoderm where the skeletal arms form and in the primary mesenchyme cells. *fgfr like-1* is ubiquitous until gastrulation, after which it is expressed broadly in the apical organ and in the tip of the archenteron. *fgfr1* is expressed exclusively in the primary mesenchyme cells. *fgfr1* is expressed in quite a complex manner; initially ubiquitous, it is later expressed in the oral half of the apical domain, the oral ectoderm and the gut. *fgf 8/17/18/24* is expressed in the apical domain, the oral ectoderm and in the gut.

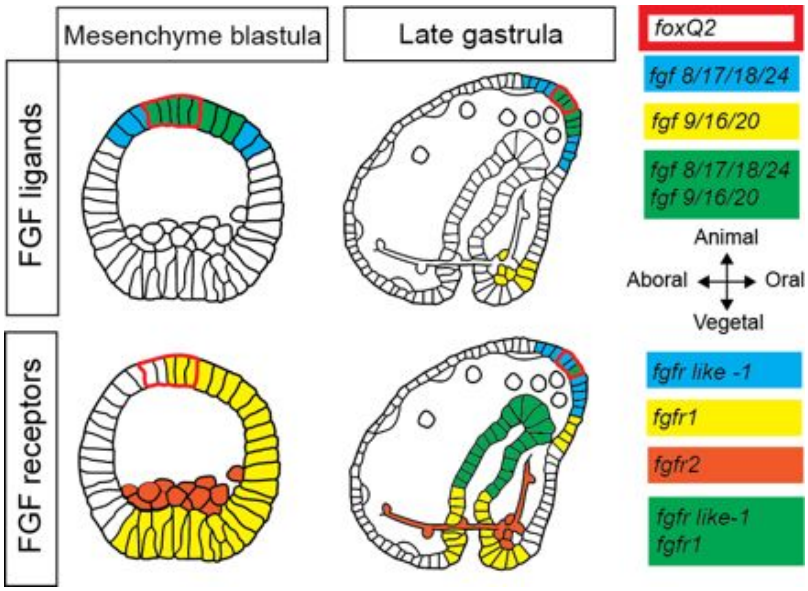

Figure 7.5. Gene expression summary of FGF signalling components in the sea urchin.
Expression data for FGF ligands and receptors was gathered from this thesis and Rottinger *et al.,* (2008), combined and summarised. Two stages are shown: mesenchyme blastula and late gastrula. Outline of *foxQ2* domain in red.

The functional roles of these components are emerging from this and other studies. FGF 9/16/20 together with FGFR1 and FGFR2 regulates directed migration of the primary mesenchyme cells and morphogenesis of the skeleton. FGF 9/16/20 and FGFR1 are required for normal invagination of the archenteron, regionalisation of the gut and formation of the stomodeum (Rottinger *et al*., 2008). Our results, presented in this thesis, suggest that FGFR1 might also play a role in repressing the expression of several apical organ genes. So far, this work has been purely quantitative in nature and therefore requires the study of spatial expression patterns in normal and MASO treated embryos,in order to differentiate more clearly the regulatory effects on genes in the apical organ and effects in the oral ectoderm or gut. The function of FGF 8/17/18/24 and of FGFR like-1 is currently unknown. The fact that they are expressed in the apical domain suggests they may play a role in its development, but further investigation is required. It is interesting to note though, that the simple sea urchin toolkit, formed by two FGF ligand and 3 FGF receptors, working with a precise spatio-temporal regulation can achieve a variety of effects in different cell types of the developing larva.

7.4 Functional linkages and a preliminary network downstream of FGF signalling.

SU5402 inhibition up-regulates a small sub-section of genes and represses serotonergic neurons.

The disruption of FGF signalling using SU5402 led to the conclusion that it is not a specific inhibitor of FGFR1 (see chapter 6). What is clear, however, is that the vast majority of apical organ genes are not affected. Furthermore, a "classical cohort" of genes such *foxQ2, six3, hbn, rx* etc that are expressed in the apical domain and thought to be important in the development of the apical organ, are not affected. Figure 7.6 summarises the network interactions downstream of FGFR1 and other RTK receptors after SU5402 treatment. The most strongly affected gene is *an like-4*, a metalloprotease that is expressed from the early blastula stage in scattered cells located in the animal hemisphere (Angerer *et al*., 2006). Co-expression studies with *foxQ2,* show that at least some of the *an like-4* positive cells in the animal hemisphere are co-expressed with *foxQ2* (data not shown). The function of *an like-4* is currently unknown in the sea urchin and attempts to ascertain this function have so far been unsuccessful (Angerer *et al*., 2006). The results of the SU5402 treatments show, that *an like-4* is up-regulated up to ninety times compared to controls, its expression pattern expands drastically to cover the entire ectoderm, but not the vegetal plate. None of the potential SU5042 target receptors analysed is expressed in a pattern that can easily explain this drastic expansion.

One of the most interesting results from the SU5402 treatments was the up-regulation of two transcription factors that are involved in ciliogenesis and several downstream genes, that are involved in building cilia. This is consistent with the phenotype observed, in which all the cilia of the embryo, especially the apical tuft, appear slightly longer (figure 6.5). *foxJ1* has been described as "key regulator of the motile ciliogenic program" (Yu *et al.,* 2008) and RFX genes are known to be important for the assembly of cilia in metazoans (Thomas *et al*., 2010). A set of downstream genes was also up-regulated and are all thought to be involved in the structure, assembly or function of

cilia. It is curious to note that both FGF signalling and FoxJ1 have recently been reported to be required for cilia in both zebrafish and *Xenopus* (Neugebauer *et al*., 2009). In sea urchin, however, there is no loss of cilia or apical tuft when embryos are treated with SU5402 (figure 6.5). This is in contrast to what has been seen in both vertebrates (Neugebauer *et al*., 2009) but also cnidarians (Rentzsch *et al.,* 2008).

***fgfr1* MASOs effect several apical organ regulatory genes.**

In contrast to SU5402 treatment, in which the strongest up-regulation was seen in ciliogenic transcription factors and downstream structural cilia genes, the genes up-regulated in embryos treated with *fgfr1* MASOs were *fez, rx, ac-sc* and *nk2.1*, the majority of which are specifically expressed in the apical domain and are generally involved in neurogenesis in other organisms. Yaguchi *et al.,* (2011) showed that *fez* represses *foxQ2* and is required to control the size of the apical domain and consequently the number of serotonergic neurons. Embryos treated with *fgfr1* MASOs show an increased number of *fez* transcripts and as a result, should have a larger apical domain and a greater number of neurons (Yaguchi *et al.,* 2011). However, without spatial analysis it is difficult to know if there is an expansion of the *fez* domain or if the number of transcripts is simply upregulated. *fez* is co-expressed with *foxQ2* in the central apical domain, while *fgfr1* is co-expressed with *foxQ2* in the oral apical domain. This means that *fgfr1* is co-expressed with the oral half of *fez.* This suggest that *fgfr1* is not acting as a simple repressor of *fez*, but a more complicated scenario exists, in which multiple inputs are involved in controlling *fez* expression.

Zic2 represses itself and is required for the differentiation of serotonergic neurons

zic2 is expressed in the central and the aboral parts of the apical domain until late gastrula. After this stage, it clears from the oral half of the *foxQ2* positive central apical domain and begins to transform its expression into scattered cells in the aboral apical domain (data not shown). This aboral expression means that from late cleavage stage,

zic2 is expressed in the future location of the serotonergic neurons. As mentioned above, *zic* genes are often expressed in neuroectodermal territories (Aruga *et al*., 1994; Nagai *et al*., 1997; Nakata *et al*., 1998) and also play a functional role in the development of the nervous system in many organisms (Nakata *et al*., 1998; Purandare *et al*., 2002; Wada and Saiga, 2002). Furthermore, *zic* genes play an important role in human health and disease (Grinberg *et al*., 2005). The perturbation analysis of *zic2* has brought to light an interesting sub-circuit architecture, wherein *zic2* represses itself in a negative feedback loop (figure 7.6) In addition, *zic2* represses *nk2.1*, although this is only seen at early stages of development (16 hours) with no effect observed by 20 and 24h. This can be explained by the fact that *zic2* represses itself and therefore the number of *zic2* transcripts increases as a consequence of MASO treatment and this can have a compensatory effect that will mask the knock–down effect with time. Another possibility is that the regulation of *nk2.1* changes with time and it responds to the repressive action of *zic2* only in the early phase of expression, while the late expression is under the regulation of other inputs. The auto-negative-feedback could also explain why the quantitative effects of the *fgfr1* MASOs on *zic2* show a consistent upregulation, but always slightly below the established threshold of significance. This is one of the justifications of including *zic2* in the cohort of genes downstream of the *fgfr1* signalling cascade.

Figure 7.6 is a preliminary GRN that combines all of the epistatic linkages that have been revealed so far in this study. At least two distinct groups of genes can be identified in this GRN. The first set includes the 'ciliogenic' genes and includes the transcription factor *nk2.1,* which activates *tecktin 3* and represses *dynein p33*, both of which are downstream cilia genes and expressed solely in the apical domain (Dunn *et al.,* 2007). Two further transcription factors are also known to have a conserved role in ciliogenesis, *foxj1* and *rfx 1/2/3* (Yu *et al.,* 2008; Thomas *et al*., 2010). These downstream cilia genes, such as *tecktin 3* and *dynein p33,* are thought to mirror the expression pattern of *foxJ1* though development (Dunn *et al.,* 2007). The second distinct group includes 'neurogenic' genes and includes the transcription factors *fez, ac-sc, rx* and *zic2.* I have shown here that *zic2* is expressed in the aboral apical domain and is required for serotonergic neuron differentiation. *fez, ac-sc* and *rx* are expressed at late gastrula stage and in pluteus larvae in scattered cells at the aboral edge of the *foxQ2*

apical domain and both *rx* and *fez* are known to be expressed in serotonergic neurons (Wei *et al.,* 2009; Yaguchi *et al.,* 2011). One could speculate that within the apical domain, two parallel GRNs exist: a neurogenic GRN and a ciliogenic GRN, which semi-independently encode for the two major characters of the apical domain, the apical tuft and the neurosensory cells. That is, both the neurogenic and ciliogenic GRNs act on the same physical part of the embryo (the apical domain) but from a network perspective, are largely independent and no (or limited) connections are present between both. This is in a way supported by the fact that some genes like *nk2.1* are expressed in the apical domain, but are not required for serotonergic neurons (Takas *et al.,* 2004). Furthermore, given the hierarchical architecture of GRN, it is conceivable that only very early genes such as *foxQ2*, *six3* and *hbn* might affect both networks and that later, they run in parallel.

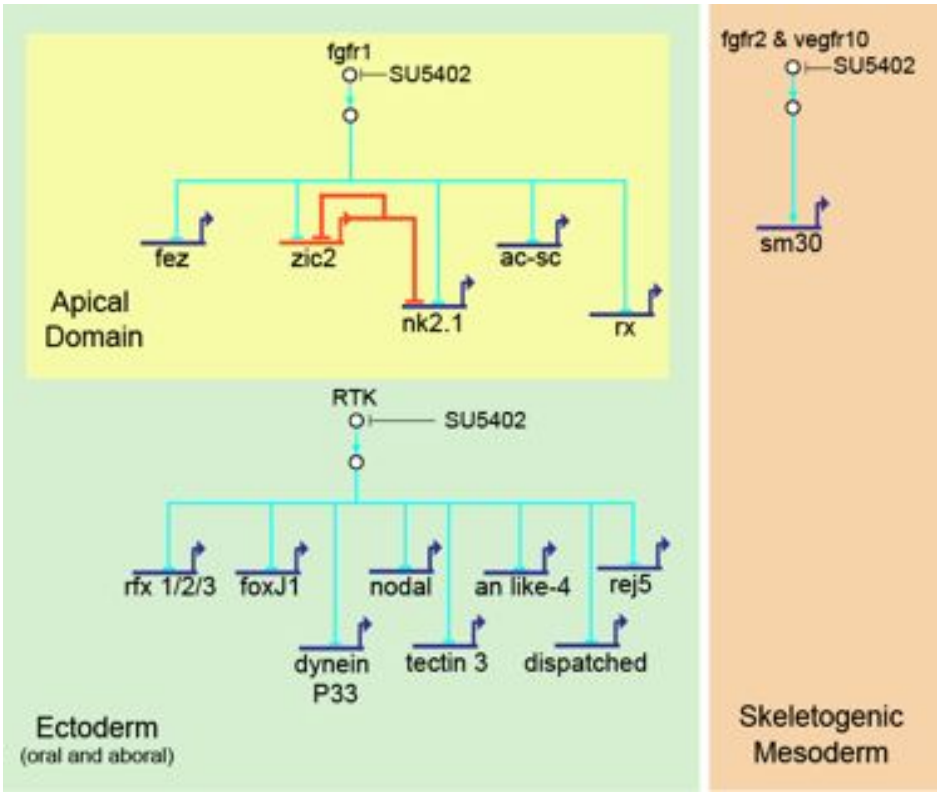

Figure 7.6. GRN diagram summarising the functional data presented in this thesis
The linkages are based on SU5402 treatments, *fgfr1* and *zic2* MASOs. Three domains are represented in the model, the ectoderm (green), representing the oral, aboral ectoderm as well as the apical domain (yellow) and the skeletogenic mesoderm (brown; *fgfr2* and *vegfr10* data from Rottinger *et al.,* 2008 and Duloquin *et al.,* 2007). The model is built in BioTapestry software (Longabaugh et al., 2005) and modified in Adobe Illustrator CS5.

7.5 Apical organs and evolution

The sea urchin and cnidarian apical organ: a gene expression comparison

Aspects of this chapter are currently in press: Sinigaglia, C., Busengdal, H., Lerner, A., Oliveri, P., Rentzsch, F. Molecular characterisation of the apical organ of the anthozoan *Nematostella vectensis. Front. Zool.* Submitted.

As described in the introduction, apical organs occur across a diverse range of metazoans and it has been proposed that apical organs could represent a simple brain of an early ancestor of the cnidarians and bilaterians (Nielsen *et al.,* 2005). Recently, Sinigaglia *et al.,* (2013) proposed the hypothesis that the apical organ at the anterior end of bilaterians and the apical organ in the aboral region of cnidarians are derived from the same domain of their last common ancestor and are therefore homologous. Moreover, *foxQ2* and *six3* are expressed early in sea urchin development in the apical domain and are thought to operate at the top of a sea urchin apical organ GRN (Burke *et al.,* 2006; Yaguchi *et al.,* 2008; Wei *et al.,* 2009). In a similar fashion, both *foxQ2* and *six3*/6 are expressed in the apical domain of *Nematostella* and are required for the development of a normal apical organ (Sinigaglia *et al.,* 2013).

To improve our understanding of the evolutionary origin of the apical organ, Sinigaglia and colleagues undertook a molecular characterisation of the cells constituting the apical organ in *Nematostella.* To identify genes that are specifically or predominantly expressed in the apical organ, they used microarray analysis to compare gene expression profiles of perturbed embryos, with an expanded or reduced apical organ and confirmed any predicted apical organ expression with *in situ* hybridisation. This produced a *Nematostella* apical organ gene set of 77 genes, all of which have been confirmed to be expressed in the apical organ.

In collaboration with Sinigaglia and colleagues, we wanted to test how many genes are expressed in common, between sea urchin and cnidarian apical domains. For this purpose, I used the newly assembled *Nematostella* apical organ gene set to query sequences in the *S. purpuratus* genome using a reciprocal BLAST strategy (Rivera *et al.,* 1998). The genomic search identified 51 putative sea urchin genes homologous to the genes in the *Nematostella* apical organ gene set. For an initial *in situ* hybridisation analysis, 19 genes were chosen, of which 9 showed an apical organ expression (two genes were expressed in the gut and for the remainder no expression was detected). A search of the literature identified many other genes that are expressed in both sea urchins and cnidarian apical organs. These include a number of developmental regulatory genes such as *foxQ2, frizzled 5/8, six3* and *sfrp1/5,* as well as regulatory and downstream genes involved in ciliogenesis such as *foxJ1* and *dynein heavy chain.*

It has emerged from this thesis, that both cnidarians and sea urchins have two FGF ligands in and around the apical organ (rather than, as previously thought, just the single FGF 9/16/20 ligand in sea urchin). It would be interesting to see if specific knockdowns of these two FGF ligands in sea urchin replicate the antagonistic function seen in *Nematostella* (Rentzsch *et al.,* 2008). Furthermore, in sea urchin and cnidarians, SU5402 treatment shows upregulation (sea urchin) and downregulation (cnidarians) of ciliogenic transcription factors and downstream genes. However, in *Nematostella*, SU5402 treatment results in the loss of the apical tuft, while in sea urchin this is not the case (figure 6.5; Rentzsch *et al.,* 2008). A further important difference in the apical organ of cnidarians and the apical organ of the sea urchin (and other bilaterians), is that bilaterian apical organs are characterised by a strong neuronal presence, especially serotonergic and FMRFamide neurons, whereas the cnidarian apical organ does not have a strong neuronal presence, nor is there an indication of the presence of a neuronal ganglion, as there is in the apical organ of many other species.

Interestingly, *foxQ2* and *six3* expression in the apical organ is conserved in cnidarians (Sinigaglia *et al.,* 2013). *foxQ2* is a highly conserved marker for the apical organ and is expressed not only in the sea urchin (Tu *et al.,* 2006) and cnidarians (Sinigaglia *et al.,* 2013), but also in the cephalochordate *Branchiostoma floridae* (Yu *et al*., 2003), the brachiopod *Terebratalia transverse* (Santagata *et al.*, 2012), and the arthropod

Drosophila melanogaster (Lee and Frasch, 2004); in fact in every invertebrate group apart from vertebrates. Santagata *et al.,* (2012) show that the brachiopod *Terebratalia transverse* expresses several genes (at least six) in its apical organ in a very similar manner to sea urchin, including *six3/6, nk2.1, hbn, fez,* and *foxQ2*, suggesting that the anterior pole of the bilaterian ancestor expressed these genes. Recently, Range *et al.,* (2013) showed the apical organ of the sea urchin embryo expresses many of the same transcription factors and secreted modulators of Wnt signalling, as the early vertebrate forebrain/eye field, such as *six3, frizzled 5/8, sFRP1/5, dkk1* and *dkk3.* Taken together, this strongly advocates a common evolutionary origin of the apical organ in bilaterians.

The sea urchin: a tale of a protostome vertebrate ….

Sea urchins, like all echinoderms, are invertebrate deuterostomes. There has been a growing trend in the sea urchin community to focus on the similarities that sea urchins share with vertebrates (e.g. recent publications Angerer *et al.,* 2011; Range *et al.,* 2013), to the exclusion of similarities held in common with other invertebrates and more importantly, with marine invertebrates that develop through a planktonic larva stage. While obviously the unique phylogenetic position of echinoderms means, by definition, it will share features in common with many metazoan phyla, it is important to resist taking a purely vertebrate-centric view of sea urchin evolution.

Aspects of this thesis bring to light certain invertebrate characteristics of the sea urchin embryo. The potential discovery of a special subset of serotonergic neurons that could function as light sensing “clock” neurons, suggests that sea urchins share a major aspect of circadian biology with protostomes. Circadian rhythms play an important role in a diverse range of biological phenomena. The internal circadian clock is entrained by light and other environmental cues, such as temperature, to link internal biological rhythms and functions to the external 24 hour period. The molecular nature of the key light-sensing molecule and organ, which inputs environmental signals into the molecular clockwork, is fundamentally different between invertebrates and vertebrates. In vertebrates, the photopigment responsible for photo-sensitivity in the clock is

melanopsin (Hankins *et al*., 2008) and the major organ is the eye while in invertebrates clock photosensitivity is provided by the type 1 cryptochromes, known as *dcry* after the *Drosophila* cryptochrome (Im & Taghert, 2011) and the cells are specific subset of neurons. *dcry* has only been found outside the protostomes in the sea urchin (Rubin *et al*., 2006) indicating the presence of *dcry* at least in the last common ancestor of bilaterians, furthermore *S. purpuratus dcry* is expressed in a specific subset of serotonergic neurons. In *Drosophila*, *glass*, a zinc finger transcription factor, is required for normal photoreceptor differentiation and *glass*-mutants lack photoreceptors in all sensory organs (Moses *et al*., 1989). It also plays a role in chemosensory neurons in *C. elegans* (Uchida *et al*., 2003). Interestingly, *glass* is co-expressed with *dcry* in a subset of clock (DN1) neurons in the *Drosophila* brain (Klarsfeld *et al*., 2004). I have shown that here too, with sea urchins, a specific subset of neurons expresses both *dcry* and *z167.* Without further study the function of these neurons can only be inferred, but this similarity is interesting. Furthermore, a genomic survey of *z167* showed that it is also only found in invertebrates. Although, the sea urchin is a deuterostome, its complement of clock genes and cellular localisation of these components shows that it may contain a circadian clock that has many protostome characteristics. Importantly, this strongly suggests a common origin in bilaterians, not only of the molecular clockwork underlying circadian rhythms, but also of the cellular components responsible for the interactions with the environment.

7.6 Future directions

The work presented in this thesis provides a deeper understanding of the regulatory states that characterise the apical domain during development. This insight into the developmental *time and space* of the apical organ forms an essential foundation for establishing an apical organ GRN, the ultimate goal for understanding its developmental program. What follows is a discussion of how these results can be expanded and brought forward to help in the next stage of building an apical organ GRN. It also highlights a number of interesting questions that have arisen during this work and makes some suggestions of how to clarify these issues.

Regulatory state analysis

One of the benefits of using double fluorescent WMISH is the ability to count individual nuclei and appreciate a cellular resolution of gene expression patterns. Technical difficulties resulting from the 3D volume of the embryo and epi-fluorescent microscopy makes it difficult to get accurate and repeatable counts of how many cells express a given gene in the apical domain. One solution would be to use confocal microscopy. This was employed to great benefit during the in-depth study of *dcry* and other scattered genes in the apical domain. Although more time consuming, confocal microscopy gives a highly accurate count of how many cells express a given gene and avoids problems of image perspective. Another interesting option would be to combine confocal data with recent advances in computational 3D modelling, that have shown excellent results in preliminary work carried out in the sea urchin (Flynn *et al.,* 2011).

The integration of the oral-aboral axis and the apical domain is a concept that has arisen numerous times, both during this work and previously in the literature (see chapter 1). So far, I have performed the combinatorial gene analysis using *foxQ2* as an apical domain marker and this has proved quite useful. It would be beneficial to expand this combinatorial analysis to include oral and aboral landmarks as well. This would then allow the triangulation of gene expression to the apical organ at a precise location along the oral-aboral axis.

The next goal for this project is the completion of the regulatory state analysis for the pre-gastrula apical domain. To do this, combinatorial gene analysis needs to be carried out on the remaining regulatory genes that make up the early apical domain gene set. These are the transcription factors *nk2.1*, *fez, ac-sc, rx* and the signalling molecule *sfrp1/5*. Furthermore, while a detailed knowledge of temporal and spatial expression profiles provides the foundations for building a GRN, only through perturbing the function of a regulatory gene and monitoring the effects on downstream genes, can this knowledge be converted into functional understanding and hence a GRN (Materna and Oliveri, 2008). Perturbation experiments between the network candidates will reveal the cause–effect linkages between regulatory genes and suggest a preliminary network architecture.

Scattered genes and function of *dcry*

One of the most interesting discoveries that emerged during this work, was that the gene *dcry* was found to be expressed early in development in the apical domain. Structural and functional studies are required to confirm that *dcry* in the sea urchin apical organ functions as a true photoreceptor and also to gain a functional understanding of how *dcry* interacts with the underlying transcriptional apparatus that controls the internal molecular clock. I also showed that *dcry* is co-expressed with *z167*. Knockdown experiments with *z167* would be helpful for understanding if *z167* plays a similar role in sea urchin photoreceptors, or if it is involved in circadian functions.

Furthermore, I have shown for the first time that not all serotonergic neurons in the sea urchin apical organ are the same and that a subset of neurons exists that share expression with both *dcry* and *z167*. Further analysis may help us understand if these neurons play a special role in linking the external environment to the internal circadian clock and form so called "clock" neurons. The study of the literature and results from the experiments presented here, show the existence of a whole subset of regulatory and downstream genes that are expressed in the apical domain in a scattered expression pattern (table 7.1). Understanding the regulatory states that occur due to genes being expressed in scattered cells, is a fascinating area of future study. Even more interesting will be elucidating the GRN in which these scattered genes function, and how they work together to control the production of neurons and other aspects of apical organ development.

FGF signalling in the apical organ

Preliminary results presented in this thesis suggest that FGF signalling may be playing a role in apical organ development as seen by embryos treated with *fgfr1* MASOs, that show an up-regulation in key apical domain genes. However, biological replicas are required to confirm these results. The discovery of a novel FGF 8/17/18/24 ligand in the sea urchin apical domain now means that there are two FGF ligands in and around the apical organ. Perturbation experiments of these two genes would allow us to

understand the specific roles of these two ligands and show if either of them is playing a role in apical organ development. This will also help us to understand if the FGF ligands in the sea urchin are playing a similarly antagonistic role as they are in cnidarians.

7.7 Concluding remarks

A fundamental feature in the transformation of a fertilised egg into a fully formed and functional adult, is the partitioning of the embryo into domains of specific regulatory state. This spatial information is encoded in the genome in the form of gene regulatory networks that define precisely when and where transcription factors and signalling molecules are expressed.

I have investigated this biological phenomenon in the embryonic development of the sea urchin apical organ, a fundamental part of the larval nervous system. Using combinatorial gene analysis to identify domains of regulatory state, I have shown that the spatial organisation of the sea urchin apical organ is far more complex than previously thought. Early patterning confers oral-aboral polarity and intricate gene expression patterns refine the apical domain into multiple regulatory state sub-domains.

Post-gastrulation, several genes begin to be expressed in scattered cells along the aboral edge of the *foxQ2*-positive central apical domain. Multiple regulatory states begin to emerge in a highly dynamic fashion in these individual cells and together with the appearance of the serotonergic nervous system, illustrate an additional layer of spatial complexity that exists in the apical organ. Furthermore, *dcry,* a potential circadian photoreceptor, has been identified in a subset of these cells, lending support for a specific sensory function of this structure. *dcry* shows partial co-expression with both *mox* and the transcription factor *z167*, and in the pluteus larva becomes restricted to a specific subset of serotonergic neurons, proving the existence of multiple types of serotonergic neurons in the sea urchin nervous system.

I have discovered a novel FGF 8/17/18/24 ligand in the sea urchin and shown that it is expressed in the apical domain during development. In addition, I have shown for the first time, that *fgfr like-1* is also expressed in the apical domain. Together, these results show that almost all of the sea urchin expanded repertoire of FGF signalling components are expressed in or surrounding the apical domain, and combined with functional studies, suggest that FGF signalling is involved in the development of this part of the larval nervous system.

I present in this work only a subset of the regulatory genes that are expressed in the apical organ during development. The true story, however, will inevitably be more complicated and show the existence of further regulatory state sub-domains and an even greater level of spatial refinement. Ultimately, all the information required for the embryo to carry out this highly specialised developmental task is situated in the strings of As, Ts, Gs, and Cs, that are encoded in the regulatory genome.

References

Alsmadi, O., Meyer, B.F., Alkuraya, F., Wakil, S., Alkayal, F., Al-Saud, H., Ramzan, K., and Al-Sayed, M. (2009). Syndromic congenital sensorineural deafness, microtia and microdontia resulting from a novel homoallelic mutation in fibroblast growth factor 3 (FGF3). Eur. J. Hum. Genet. 17, 14–21.

Altschul, S.F., Gish, W., Miller, W., Myers, E.W., and Lipman, D.J. (1990). Basic local alignment search tool. Journal of Molecular Biology 215, 403–410.

Andrew C, R., and Davidson, E. (1991). Cell type specification during sea urchin development. Trends in Genetics 7, 212–218.

Angerer, L.M., Oleksyn, D.W., Levine, A.M., Li, X., Klein, W.H., and Angerer, R.C. (2001). Sea urchin goosecoid function links fate specification along the animal-vegetal and oral-aboral embryonic axes. Development 128, 4393–4404.

Angerer, L.M., Yaguchi, S., Angerer, R.C., and Burke, R.D. (2011). The evolution of nervous system patterning: insights from sea urchin development. Development 138, 3613–3623.

Angerer, L., Oleksyn, D., Logan, C., McClay, D., Dale, L., and Angerer, R. (2000). A BMP pathway regulates cell fate allocation along the sea urchin animal-vegetal embryonic axis. Development 127, 1105–1114.

Angerer, L., Hussain, S., Wei, Z., and Livingston, B.T. (2006). Sea urchin metalloproteases: A genomic survey of the BMP-1/tolloid-like, MMP and ADAM families. Dev Biol 300, 267–281.

Arenas-Mena, C., Cameron, A.R., and Davidson, E.H. (2000). Spatial expression of Hox cluster genes in the ontogeny of a sea urchin. Development. 127(21), 4631-4643.

Arnone, M.I., and Davidson, E.H. (1997). The hardwiring of development: organization and function of genomic regulatory systems. Development. 124(10), 1851-1864.

Aruga, J., Yokota, N., Hashimoto, M., Furuichi, T., Fukuda, M., and Mikoshiba, K. (1994). A novel zinc finger protein, zic, is involved in neurogenesis, especially in the cell lineage of cerebellar granule cells. J. Neurochem. 63, 1880–1890.

Beer, A.J., Moss, C., and Thorndyke, M. (2001). Development of serotonin-like and SALMFamide-like immunoreactivity in the nervous system of the sea urchin *Psammechinus miliaris*. The Biological Bulletin 200, 268–280.

Beenken, A., and Mohammadi, M. (2009). The FGF family: biology, pathophysiology and therapy. Nature Reviews Drug Discovery 8, 235–253.

Ben-Tabou de-Leon, S., and Davidson, E.H. (2007). Gene regulation: gene control network in development. Annu Rev Biophys Biomol Struct 36, 191.

Ben-Tabou de-Leon, S., Su, Y.-H., Lin, K.-T., Li, E., and Davidson, E.H. (2013). Gene regulatory control in the sea urchin aboral ectoderm: Spatial initiation, signaling inputs, and cell fate lockdown. Dev Biol 374, 245–254.

Bertrand, S., Somorjai, I., Garcia-Fernandez, J., Lamonerie, T., and Escriva, H. (2009). FGFRL1 is a neglected putative actor of the FGF signalling pathway present in all major metazoan phyla. BMC Evol. Biol. 9, 226.

Bisgrove, B., and Burke, R. (1986). Development of serotonergic neurons in embryos of the sea urchin, Strongylocentrotus purpuratus. Development, growth & differentiation, 28(6), 569-574.

Bisgrove, B., and Burke, R. (1987). Development of the nervous system of the pluteus larva of Strongylocentrotus droebachiensis. Cell Tissue Res. 248.

Bolouri, H., & Davidson, E. H. (2003). Transcriptional regulatory cascades in development: initial rates, not steady state, determine network kinetics. Proceedings of the National Academy of Sciences, 100(16), 9371-9376.

Bolouri, H., and Davidson, E.H. (2010). The gene regulatory network basis of the "community effect," and analysis of a sea urchin embryo example. Dev Biol 340, 170–178.

Böttcher, R.T., and Niehrs, C. (2005). Fibroblast Growth Factor Signaling during Early Vertebrate Development. Endocrine reviews, 26(1), 63-77

Bourlat, S. J., Juliusdottir, T., Lowe, C. J., Freeman, R., Aronowicz, J., Kirschner, M., ... & Telford, M. J., 2006. Deuterostome phylogeny reveals monophyletic chordates and the new phylum Xenoturbellida. Nature, 444(7115), 85-88.

Bradham, C.A., Oikonomou, C., Kühn, A., Core, A.B., Modell, J.W., McClay, D.R., and Poustka, A.J. (2009). Chordin is required for neural but not axial development in sea urchin embryos. Dev Biol 328, 221–233.

Brinkmann, N., and Wanninger, A. (2008). Larval neurogenesis in *Sabellaria alveolata* reveals plasticity in polychaete neural patterning. Evolution & Development 10, 606–618.

Britten, R. J., and Davidson, E. H. (1969). Gene regulation for higher cells: a theory. Science, 165(891), 349-357.

Burke, R., Nellen, D., Bellotto, M., Hafen, E., Senti, K.-A., Dickson, B.J., and Basler, K. (1999). Dispatched, a Novel Sterol-Sensing Domain Protein Dedicated to the Release of Cholesterol-Modified Hedgehog from Signaling Cells. Cell 99, 803–815.

Burke, R.D., Angerer, L.M., Elphick, M.R., Humphrey, G.W., Yaguchi, S., KIYAMA, T., LIANG, S., MU, X., AGCA, C., Klein, W.H., et al. (2006). A genomic view of the sea urchin nervous system. Dev Biol 300, 434–460.

Burke, R., Angerer, L., Elphick, M., Humphrey, G., Yaguchi, S., Kiyama, T., Liang, S., Mu, X., Agca, C., and Klein, W. (2006). A genomic view of the sea urchin nervous system. Dev Biol 300, 434–460.

Butscheid, Y., Chubanov, V., Steger, K., Meyer, D., Dietrich, A., and Gudermann, T. (2006). Polycystic kidney disease and receptor for egg jelly is a plasma membrane protein of mouse sperm head. Molecular reproduction and development, 73(3), 350-360.

Byrne, M., Nakajima, Y., Chee, F.C., and Burke, R.D. (2007). Apical organs in echinoderm larvae: insights into larval evolution in the Ambulacraria. Evolution & Development 9, 432–445.

Cameron, R.A., Fraser, S.E., Britten, R.J., and Davidson, E.H. (1990). Segregation of oral from aboral ectoderm precursors is completed at fifth cleavage in the embryogenesis of *Strongylocentrotus purpuratus*. Dev Biol 137, 77–85.

Cameron, R. A., and Davidson, E. H. (1991). Cell type specification during sea urchin development. Trends in genetics 7(7), 212.

Cameron, R. A., Hough-Evans, B. R., Britten, R. J., and Davidson, E. H. (1987). Lineage and fate of each blastomere of the eight-cell sea urchin embryo. Genes & development, 1(1), 75-85.

Carroll, S.B. (2000). Endless forms: the evolution of gene regulation and morphological diversity. Cell 101, 577–580.

Carroll, S. B., Grenier, J. K., and Weatherbee, S. D. (2005). From DNA to diversity: Molecular genetics and the evolution of animal design. Malden, MA: Blackwell Pub.

Cashmore, A. R., Jarillo, J. A., Wu, Y. J., and Liu, D. (1999). Cryptochromes: blue light receptors for plants and animals. Science, 284(5415), 760-765.

Cebria, F., Kobayashi, C., Umesono, Y., Nakazawa, M., Mineta, K., Ikeo, K., ... & Agata, K. (2002). FGFR-related gene nou-darake restricts brain tissues to the head region of planarians. Nature, 419(6907), 620-624.

Chen, J.-H., Luo, Y.-J., and Su, Y.-H. (2011). The dynamic gene expression patterns of transcription factors constituting the sea urchin aboral ectoderm gene regulatory network. Dev. Dyn. 240, 250–260.

Chia, F.-S., and Koss, R. (1979). Fine structural studies of the nervous system and the apical organ in the planula larva of the sea anemone *Anthopleura elegantissima.* J. Morphol. 160, 275–297.

Coffman, J.A., and Davidson, E.H. (2001). Oral–Aboral Axis Specification in the Sea Urchin Embryo: I. Axis Entrainment by Respiratory Asymmetry. Dev Bio 230(1), 18-28.

Coffman, J. A., Coluccio, A., Planchart, A., & Robertson, A. J. (2009). Oral–aboral axis specification in the sea urchin embryo: III. Role of mitochondrial redox signaling via H2O2. Dev Biol 330(1), 123-130.

Cole, A.G., and Arnone, M.I. (2009). Fluorescent in situ hybridization reveals multiple expression domains for SpBrn1/2/4 and identifies a unique ectodermal cell type that co-expresses the ParaHox gene SpLox. Gene Expression Patterns 9, 324–328.

Conklin, E. G. (1897). The embryology of *Crepidula*: A contribution to the cell lineage and early development of some marine gasteropods. Boston: Ginn & company.

Conzelmann, M., Offenburger, S.-L., Asadulina, A., Keller, T., Münch, T.A., and Jékely, G. (2011). Neuropeptides regulate swimming depth of *Platynereis* larvae. Proceedings of the National Academy of Sciences, 108(46), 1174-1183.

Conzelmann, M., Williams, E.A., Tunaru, S., Randel, N., Shahidi, R., Asadulina, A., Berger, J., Offermanns, S., and Jékely, G. (2013). Conserved MIP receptor-ligand pair regulates *Platynereis* larval settlement. Proceedings of the National Academy of Sciences, 110, 8224–8229.

Croce, J. (2006). Frizzled5/8 is required in secondary mesenchyme cells to initiate archenteron invagination during sea urchin development. Development 133, 547–557.

Croce, J.C., and McClay, D.R. (2010). Dynamics of Delta/Notch signaling on endomesoderm segregation in the sea urchin embryo. Development 137, 83–91.

Dan, K. (1960). Cyto-embryology of echinoderms and Amphibia. International review of cytology, 9, 321-367.

Davidson, E.H., Cameron, R.A., and Ransick, A. (1998). Specification of cell fate in the sea urchin embryo: summary and some proposed mechanisms. Development 125, 3269–3290.

Davidson, E. (1989). Lineage-specific gene expression and the regulative capacities of the sea urchin embryo: a proposed mechanism. Development 105, 421-45

Davidson, E. H. (2001). Genomic regulatory systems: Development and evolution. San Diego: Academic Press.

Davidson, E. H. (2006). The regulatory genome: Gene regulatory networks in development and evolution. Burlington, MA: Academic.

Davidson, E.H. (2009). Network design principles from the sea urchin embryo. Current opinion in genetics & development. 19, 535–540.

Davidson, E.H. (2010). Emerging properties of animal gene regulatory networks. Nature 468, 911–920.

Davidson, E.H., and Erwin, D.H. (2006). Gene regulatory networks and the evolution of animal body plans. Science 311, 796–800.

Davidson, E.H., and Levine, M.S. (2008). Properties of developmental gene regulatory networks. Proceedings of the National Academy of Sciences, 105, 20063–20066.

Davidson, E.H., Rast, J.P., Oliveri, P., Ransick, A., Calestani, C., Yuh, C.-H., Minokawa, T., Amore, G., Hinman, V., Arenas-Mena, C., et al. (2002). A genomic regulatory network for development. Science 295, 1669–1678.

Driesch, H. 1891. Entwicklungsmechanische studien, I. Der werth der beiden ersten furchungszellen in der echinodermentwicklung. Experimentelle er- zeugen von theil— und doppelbildung. Zeitschr. Wissenschaft. Zool. 53:166-178. Abridged En- glish translation: B. Willier and J. M. Oppenhei- mer (eds.). 1974. Foundations of experimental embryology. Hafner Press, New York.

Duboc, V., Röttinger, E., Besnardeau, L., and Lepage, T. (2004). Nodal and BMP2/4 signaling organizes the oral-aboral axis of the sea urchin embryo. Dev. Cell 6, 397–410.

Dunn, E.F., Moy, V.N., Angerer, L.M., Angerer, R.C., Morris, R.L., and Peterson, K.J. (2007). Molecular paleoecology: using gene regulatory analysis to address the origins of complex life cycles in the late Precambrian. Evolution & Development 9, 10–24.

Dubruille, R., Laurençon, A., Vandaele, C., Shishido, E., Coulon-Bublex, M., Swoboda, P., ... and Durand, B. (2002). *Drosophila* regulatory factor X is necessary for ciliated sensory neuron differentiation. Development, 129(23), 5487-5498.

Duloquin, L., Lhomond, G., & Gache, C. (2007). Localized VEGF signaling from ectoderm to mesenchyme cells controls morphogenesis of the sea urchin embryo skeleton. Development, 134(12), 2293-2302.

Edgecombe, G. D., Giribet, G., Dunn, C. W., Hejnol, A., Kristensen, R. M., Neves, R. C., ... and Sørensen, M. V., (2011). Higher-level metazoan relationships: recent progress and remaining questions. Organisms Diversity & Evolution, 11(2), 151-172.

Ernst, S.G. (2011). Offerings from an Urchin. Dev Biol 358, 285–294.

Erwin, D.H., and Davidson, E.H. (2002). The last common bilaterian ancestor. Development 129, 3021–3032.

Erwin, D.H., and Davidson, E.H. (2009). The evolution of hierarchical gene regulatory networks. Nature Reviews Genetics 10, 141–148.

Ettensohn, C.A. (2013). Encoding anatomy: Developmental gene regulatory networks and morphogenesis. Genesis 1–27.

Flynn, C.J., Sharma, T., Ruffins, S.W., Guerra, S.L., Crowley, J.C., and Ettensohn, C.A. (2011). High-resolution, three-dimensional mapping of gene expression using GeneExpressMap (GEM). Dev Biol 357, 532–540.

Gilbert, S. F. (2006). Developmental biology. Sunderland, Mass: Sinauer Associates Publishers.

Glabe, C. G., and Vacquier, V. D. (1978). Egg surface glycoprotein receptor for sea urchin sperm bindin. Proceedings of the National Academy of Sciences, 75(2), 881-885

Gould, S. J. (1977). Ontogeny and phylogeny. Cambridge, Mass: Belknap Press of Harvard University Press.

Grand, E.K., Chase, A.J., Heath, C., Rahemtulla, A., and Cross, N.C.P. (2004). Targeting FGFR3 in multiple myeloma: inhibition of t(4;14)-positive cells by SU5402 and PD173074. Leukemia 18, 962–966.

Grinberg, I., and Millen, K.J. (2005). The ZIC gene family in development and disease. Clin. Genet. 67, 290–296

Geiss, G., Bumgarner, R., Birditt, B., Dahl, T., Dowidar, N., Dunaway, D., Fell, H.,Ferree, S., George, R., Grogan, T., James, J., Maysuria, M., Mitton, J., Oliveri, P., Osborn, J., Peng, T., Ratcliffe, A., Webster, P., Davidson, E., Hood, L., 2008. Direct multiplexed measurement of gene expression with color-coded probe pairs. Nature Biotechnology. 26, 317–325.

Gustafson, T., and Wolpert, L. (1961). Studies on the cellular basis of morphogenesis in the sea urchin embryo: Directed movements of primary mesenchyme cells in normal and vegetalized larvae. Experimental cell research, 24(1), 64-79.

Gustafson T, & Wolpert L. (1963). The cellular basis of morphogenesis and sea urchin development. International review of cytology. 15, 139-214.

Hadfield, M., Meleshkevitch, E., and Boudko, D. (2000). The apical sensory organ of a gastropod veliger is a receptor for settlement cues. The Biological Bulletin 198, 67.

Hankins, M. W., Peirson, S. N., & Foster, R. G. (2008). Melanopsin: an exciting photopigment. Trends in neurosciences, 31(1), 27-36.

Hayashi, S., Itoh, M., Taira, S., Agata, K., and Taira, M. (2004). Expression patterns o *Xenopus* FGF receptor-like 1/nou-darake in early Xenopus development resemble those of planarian nou-darake and Xenopus FGF8. Dev. Dyn. 230, 700–707.

He, J., and Deem, M.W. (2010). Hierarchical evolution of animal body plans. Dev Biol 337, 157–161.

Hertwig, O. (1876). Beitragezurkenntniss der bildung, befruchtung und theilung des thierischen eies. Morph. Jb. 1:347-432.

Holland, N.D. (2003). Early central nervous system evolution: an era of skin brains? Nature Review Neuroscience. 4, 617–627.

Hörstadius, S. (1973). Experimental embryology of echinoderms. Oxford. England: Clarendon Press.

Hörstadius, S., Josefsson, L., & Runnström, J. (1967). Morphogenetic agents from unfertilized eggs of the sea urchin *Paracentrotus lividus.* Dev Biol 16, 2, 189-202.

Howard-Ashby, M., Materna, S.C., Brown, C.T., Tu, Q., Oliveri, P., Cameron, R.A., and Davidson, E.H. (2006). High regulatory gene use in sea urchin embryogenesis: Implications for bilaterian development and evolution. Dev Biol 300, 27–34.

Huang, H.C., and Klein, P.S. (2004). The Frizzled family: receptors for multiple signal transduction pathways. Genome biology, 5(7), 2004-5.

Hylander, B. L., and Summers, R. G. (1982). An ultrastructural immunocytochemical localization of hyalin in the sea urchin egg. Dev Biol 93(2), 368-380.

Illies, M. R., Peeler, M. T., Dechtiaruk, A., and Ettensohn, C. A. (2002). Cloning and developmental expression of a novel, secreted frizzled-related protein from the sea urchin,Strongylocentrotus purpuratus. Mechanisms of development, 113(1), 61-64.

Im, S. H., and Taghert, P. H. (2011). Neuroscience. A CRY to rise. Science, 331(6023), 1394.

Itoh, N., and Ornitz, D.M. (2004). Evolution of the Fgf and Fgfr gene families. Trends in Genetics 20, 563–569.

Jackson, D.J., Meyer, N.P., Seaver, E., Pang, K., McDougall, C., Moy, V.N., Gordon, K., Degnan, B.M., Martindale, M.Q., Burke, R.D., et al. (2010). Developmental expression of COE across the Metazoa supports a conserved role in neuronal cell-type specification and mesodermal development. Dev. Genes Evol. 220, 221–234

Katow, H., Suyemitsu, T., Ooka, S., Yaguchi, J., Jin-nai, T., Kuwahara, I., Katow, T., Yaguchi, S., and Abe, H. (2010). Development of a dopaminergic system in sea urchin embryos and larvae. J. Exp. Biol. 213, 2808–2819.

Kenny, A.P., Kozlowski, D., Oleksyn, D.W., Angerer, L.M., and Angerer, R.C. (1999). SpSoxB1, a maternally encoded transcription factor asymmetrically distributed among early sea urchin blastomeres. Development 126, 5473–5483.

Kenny, A.P., Oleksyn, D.W., Newman, L.A., Angerer, R.C., and Angerer, L.M. (2003). Tight regulation of SpSoxB factors is required for patterning and morphogenesis in sea urchin embryos. Dev Biol 261, 412–425.

Klarsfeld, A., Malpel, S., Michard-Vanhée, C., Picot, M., Chélot, E., and Rouyer, F. (2004). Novel features of cryptochrome-mediated photoreception in the brain circadian clock of *Drosophila*. J. Neurosci. 24, 1468–1477

Kominami, T., and Takata, H. (2004). Gastrulation in the sea urchin embryo: a model system for analyzing the morphogenesis of a monolayered epithelium. Dev. Growth Differ. 46, 309–326.

Lacalli, T.C. (1994). Apical organs, epithelial domains, and the origin of the chordate central nervous system. Integr Comp Biol 34, 533–541.

Lapraz, F., Besnardeau, L., and Lepage, T. (2009). Patterning of the dorsal-ventral axis in echinoderms: insights into the evolution of the BMP-chordin signaling network. PLoS Biol. 7, e1000248.

Lapraz, F., Röttinger, E., Duboc, V., Range, R., Duloquin, L., Walton, K., Wu, S.-Y., Bradham, C., Loza, M.A., Hibino, T., et al. (2006). RTK and TGF-beta signaling pathways genes in the sea urchin genome. Dev Biol 300, 132–152.

Larkin, M. A., Blackshields, G., Brown, N. P., Chenna, R., McGettigan, P. A., McWilliam, H., ... and Higgins, D. G. (2007). Clustal W and Clustal X version 2.0. Bioinformatics, 23(21), 2947-2948.

Lee, H., and Frasch, M. (2004). Survey of forkhead domain encoding genes in the *Drosophila* genome: Classification and embryonic expression patterns. Dev. Dyn. 229, 357–366

Levine, M., & Davidson, E. H. (2005). Gene regulatory networks for development. Proceedings of the National Academy of Sciences of the United States of America, 102(14), 4936-4942.

Li, E., Materna, S.C., and Davidson, E.H. (2012). Direct and indirect control of oral ectoderm regulatory gene expression by Nodal signaling in the sea urchin embryo. Dev Biol 369 (2012) 377–385

Logan, C.Y., Miller, J.R., Ferkowicz, M.J., and McClay, D.R. (1999). Nuclear beta-catenin is required to specify vegetal cell fates in the sea urchin embryo. Development, 126(2), 345-357.

Longabaugh, W.J.R., Davidson, E.H., and Bolouri, H. (2005). Computational representation of developmental genetic regulatory networks. Dev Biol 283, 1–16.

Mason, I. (2007). Initiation to end point: the multiple roles of fibroblast growth factors in neural development. Nature Reviews Neuroscience, 8(8), 583-596.

Materna, S.C., and Davidson, E.H. (2012). A comprehensive analysis of Delta signaling in pre-gastrular sea urchin embryos. Dev Biol 364, 77–87.

Materna, S.C., and Oliveri, P. (2008). A protocol for unraveling gene regulatory networks. Nature Protocols 3, 1876–1887.

Materna, S.C., Howard-Ashby, M., Gray, R.F., and Davidson, E.H. (2006). The C2H2 zinc finger genes of *Strongylocentrotus purpuratus* and their expression in embryonic development. Dev Biol 300, 108–120.

Materna, S.C., Nam, J., and Davidson, E.H. (2010). High accuracy, high-resolution prevalence measurement for the majority of locally expressed regulatory genes in early sea urchin development. Gene Expr. Patterns 10, 177–184.

Materna, S.C., Ransick, A., Li, E., and Davidson, E.H. (2013). Diversification of oral and aboral mesodermal regulatory states in pregastrular sea urchin embryos. Dev Biol 375, 92–104.

McClay, D.R. (2011). Evolutionary crossroads in developmental biology: sea urchins. Development 138, 2639–2648.

McClay, D.R., and Logan, C.Y. (1996). Regulative capacity of the archenteron during gastrulation in the sea urchin. Development 122, 607–616.

McCoon, P.E., Angerer, R.C., and Angerer, L.M. (1996). SpFGFR, a new member of the fibroblast growth factor receptor family, is developmentally regulated during early sea urchin development. J. Biol. Chem. 271, 20119–20125.

Minokawa, T., Rast, J.P., Arenas-Mena, C., Franco, C.B., and Davidson, E.H. (2004). Expression patterns of four different regulatory genes that function during sea urchin development. Gene Expr. Patterns 4, 449–456.

Minokawa, T., Wikramanayake, A.H., and Davidson, E.H. (2005). cis-Regulatory inputs of the wnt8 gene in the sea urchin endomesoderm network. Dev Biol 288, 545–558.

Mistry, N., Harrington, W., Lasda, E., Wagner, E.J., and Garcia-Blanco, M.A. (2003). Of urchins and men: evolution of an alternative splicing unit in fibroblast growth factor receptor genes. RNA 9, 209–217.

Mohammadi, M., McMahon, G., Sun, L., Tang, C., Hirth, P., Yeh, B.K., Hubbard, S.R., and Schlessinger, J. (1997). Structures of the tyrosine kinase domain of fibroblast growth factor receptor in complex with inhibitors. Science 276, 955–960.

Morrill, J, B., Marcus, L. (2005). An atlas of the development of the sea urchin.

Moses, K., Ellis, M.C., and Rubin, G.M. (1989). The glass gene encodes a zinc-finger protein required by *Drosophila* photoreceptor cells. Nature 340, 531–536.

Moses, K., and Rubin, G.M. (1991). Glass encodes a site-specific DNA-binding protein that is regulated in response to positional signals in the developing Drosophila eye. Genes & Development 5, 583–593.

Nagai, T., Aruga, J., Takada, S., Günther, T., Spörle, R., Schughart, K., and Mikoshiba, K. (1997). The expression of the mouse Zic1, Zic2, and Zic3 gene suggests an essential role for Zic genes in body pattern formation. Dev Biol 182(2), 299.

Nakajima, Y., Kaneko, H., Murray, G., and Burke, R.D. (2004). Divergent patterns of neural development in larval echinoids and asteroids. Evolution and Development 6, 95–104

Nakajima, Y. (1986). Development of the nervous system of sea urchin embryos: formation of ciliary bands and the appearance of two types of ectoneural cells in the pluteus. Development, growth & differentiation, 28(6), 531-542.

Nakajima, Y., Burke, R. D., and Noda, Y. (1993). The structure and development of the apical ganglion in the sea urchin pluteus larvae of *Strongylocentrotus droebachiensis* and *Mespilia globulus*. Development, growth & differentiation, 35(5), 531-538.

Nakanishi, N., Renfer, E., Technau, U., and Rentzsch, F. (2012). Nervous systems of the sea anemone *Nematostella vectensis* are generated by ectoderm and endoderm and shaped by distinct mechanisms. Development 139, 347–357.

Nakano, H., Nakajima, Y., & Amemiya, S. (2009). Nervous system development of two crinoid species, the sea lily *Metacrinus rotundus* and the feather star *Oxycomanthus japonicus.* Development Genes and Evolution, 219(11-12), 565-576.

Nakata, K., Nagai, T., Aruga, J., and Mikoshiba, K. (1998). *Xenopus* Zic family and its role in neural and neural crest development. Mech. Dev. 75, 43–51.

Nemer, M., Rondinelli, E., Infante, D., and Infante, A. A. (1991). Polyubiquitin RNA characteristics and conditional induction in sea urchin embryos. Dev Biol 145(2), 255-265.

Neugebauer, J.M., Amack, J.D., Peterson, A.G., Bisgrove, B.W., and Yost, H.J. (2009). FGF signalling during embryo development regulates cilia length in diverse epithelia. Nature 458, 651–654.

Nezlin, L.P., and Yushin, V.V. (2004). Structure of the nervous system in the tornaria larva of *Balanoglossus proterogonius* (Hemichordata: Enteropneusta) and its phylogenetic implications. Zoomorphology 123, 1–13.

Nielsen, C. (2005). Larval and adult brains. Evolution and Development. Wiley Online Library. Evolution and Development.

Nielsen, C., and Hay-Schmidt, A. (2007). Development of the enteropneust *Ptychodera flava*: ciliary bands and nervous system. J. Morphol. 268, 551–570.

Nitabach, M.N., and Taghert, P.H. (2008). Organization of the *Drosophila* Circadian Control Circuit. Current Biology 18, R84–R93.

Oliveri, P., Carrick, D. M., & Davidson, E. H. (2002). A regulatory gene network that directs micromere specification in the sea urchin embryo. Dev Biol 246(1), 209-228.

Oliveri, P., & Davidson, E. H. (2004). Gene regulatory network analysis in sea urchin embryos. Methods in cell biology, 74, 775-794.

Oliveri, P., Davidson, E. H., and McClay, D. R., 2003. Activation of pmar1 controls specification of micromeres in the sea urchin embryo. Dev Biol 258, 1, 32-43.
Oliveri, P., and Davidson, E.H. (2004). Gene regulatory network controlling embryonic specification in the sea urchin. Current opinion in genetics & development. 14, 351–360.

Oliveri, P., Tu, Q., and Davidson, E.H. (2008). Global regulatory logic for specification of an embryonic cell lineage. Proceedings of the National Academy of Sciences of the United States of America, 105, 5955–5962.

Otim, O., Amore, G., Minokawa, T., and McClay, D.R. (2004). SpHnf6, a transcription factor that executes multiple functions in sea urchin embryogenesis. Dev Biol 273(2), 226-243.

Oulion, S., Bertrand, S., and Escriva, H. (2012). Evolution of the FGF Gene Family. International Journal of Evolutionary Biology, 2012.

Pehrson, J. R., & Cohen, L. H. (1986). The fate of the small micromeres in sea urchin development. Dev Biol 113(2), 522-526.

Peter, I.S., and Davidson, E.H. (2011). A gene regulatory network controlling the embryonic specification of endoderm. Nature 474, 635–639.

Pinho, S., Simonsson, P.R., Trevers, K.E., Stower, M.J., Sherlock, W.T., Khan, M., Streit, A., Sheng, G., and Stern, C.D. (2011). Distinct Steps of Neural Induction Revealed by Asterix, Obelix and TrkC, Genes Induced by Different Signals from the Organizer. PLoS ONE 6, e19157.

Plotnikov, A.N., Schlessinger, J., Hubbard, S.R., and Mohammadi, M. (1999). Structural Basis for FGF Receptor Dimerization and Activation. Cell 98, 641–650.

Poustka, A.J., Kühn, A., Groth, D., Weise, V., Yaguchi, S., Burke, R.D., Herwig, R., Lehrach, H., and Panopoulou, G. (2007). A global view of gene expression in lithium and zinc treated sea urchin embryos: new components of gene regulatory networks. Genome Biol. 8, R85.

Punta, M., Coggill, P.C., Eberhardt, R.Y., Mistry, J., Tate, J., Boursnell, C., Pang, N., Forslund, K., Ceric, G., Clements, J., et al. (2011). The Pfam protein families database. Nucleic Acids Research 40, D290–D301.

Purandare, S. M., Ware, S. M., Kwan, K. M., Gebbia, M., Bassi, M. T., Deng, J. M., ... & Casey, B. (2002). A complex syndrome of left-right axis, central nervous system and axial skeleton defects in Zic3 mutant mice. Development, 129(9), 2293-2302.

Rafiq, K., Cheers, M.S., and Ettensohn, C.A. (2012). The genomic regulatory control of skeletal morphogenesis in the sea urchin. Development 139, 579–590.

Range, R.C., Angerer, R.C., and Angerer, L.M. (2013). Integration of Canonical and Noncanonical Wnt Signaling Pathways Patterns the Neuroectoderm Along the Anterior–Posterior Axis of Sea Urchin Embryos. PLoS Biol. 11, e1001467.

Rast, J. P., Cameron, R. A., Poustka, A. J., & Davidson, E. H. (2002). *brachyury* Target Genes in the Early Sea Urchin Embryo Isolated by Differential Macroarray Screening. Developmental biology, 246(1), 191-208

Rentzsch, F., Fritzenwanker, J.H., Scholz, C.B., and Technau, U. (2008). FGF signalling controls formation of the apical sensory organ in the cnidarian *Nematostella vectensis.* Science Signaling 135, 1761–ec168.

Revilla-i-Domingo, R., Oliveri, P., and Davidson, E.H. (2007). A missing link in the sea urchin embryo gene regulatory network: hesC and the double-negative specification of micromeres. Proceedings of the National Academy of Sciences of the United States of America, 104, 12383–12388

Rizzo, F., Fernandez-Serra, M., Squarzoni, P., Archimandritis, A., and Arnone, M.I. (2006). Identification and developmental expression of the ets gene family in the sea urchin *(Strongylocentrotus purpuratus)*. Dev Biol 300, 35–48

Röttinger, E., Saudemont, A., Duboc, V., Besnardeau, L., McClay, D.R., and Lepage, T. (2008). FGF signals guide migration of mesenchymal cells, control skeletal morphogenesis [corrected] and regulate gastrulation during sea urchin development. Development 135, 353–365.

Rozen, S., and Skaletsky, H. (1999). Primer3 on the WWW for general users and for biologist programmers. In Bioinformatics methods and protocols (pp. 365-386). Humana Press.

Rubin, E.B., Shemesh, Y., Cohen, M., Elgavish, S., Robertson, H.M., and Bloch, G. (2006). Molecular and phylogenetic analyses reveal mammalian-like clockwork in the honey bee (*Apis mellifera*) and shed new light on the molecular evolution of the circadian clock. Genome Res. 16, 1352–1365.

Ruiz-Jones, G.J., and Hadfield, M.G. (2011). Loss of sensory elements in the apical sensory organ during metamorphosis in the nudibranch *Phestilla sibogae*. The Biological Bulletin 220, 39–46.

Santagata, S., Resh, C., Hejnol, A., Martindale, M.Q., and Passamaneck, Y.J. (2012). Development of the larval anterior neurogenic domains of *Terebratalia transversa* (Brachiopoda) provides insights into the diversification of larval apical organs and the spiralian nervous system. Evodevo 3, 3–21.

Saudemont, A., Haillot, E., Mekpoh, F., Bessodes, N., Quirin, M., Lapraz, F., Duboc, V., Röttinger, E., Range, R., Oisel, A., et al. (2010). Ancestral regulatory circuits governing ectoderm patterning downstream of nodal and BMP2/4 revealed by gene regulatory network analysis in an echinoderm. PLoS Genet. 6, e1001259.

Schier, A. F., & Talbot, W. S. (1998). The zebrafish organizer. Current opinion in genetics & development, 8(4), 464-471.

Schultz, J., Milpetz, F., Bork, P., & Ponting, C. P. (1998). SMART, a simple modular architecture research tool: identification of signaling domains. Proceedings of the National Academy of Sciences, 95(11), 5857-5864.

Sea Urchin Genome: Implications and Insights., 2006. Developmental biology, 300(1), 1-496.

Sea Urchin Genome Sequencing Consortium, Sodergren, E., Weinstock, G.M., Davidson, E.H., Cameron, R.A., Gibbs, R.A., Angerer, R.C., Angerer, L.M., Arnone, M.I., Burgess, D.R., et al. (2006). The genome of the sea urchin *Strongylocentrotus purpuratus.* Science 314, 941–952.

Sheng, G., Reis, dos, M., and Stern, C.D. (2003). Churchill, a zinc finger transcriptional activator, regulates the transition between gastrulation and neurulation. Cell 115, 603–613.

Simpson, P. (1990). Lateral inhibition and the development of the sensory bristles of the adult peripheral nervous system of *Drosophila*. Development. 109(3), 509-519.

Sinigaglia, C., Busengdal, H., Leclère, L., and Technau, U. (2013). PLOS Biology: The bilaterian head patterning gene six3/6 controls aboral domain development in a Cnidarian. PLoS Biol

Small S, Blair A, and Levine M. (1992). Regulation of even-skipped stripe 2 in the *Drosophila* embryo. The EMBO Journal. 11, 4047-57.

Steinberg, F., Zhuang, L., Beyeler, M., Kälin, R.E., Mullis, P.E., Brändli, A.W., and Trueb, B. (2010). The FGFRL1 receptor is shed from cell membranes, binds fibroblast growth factors (FGFs), and antagonizes FGF signaling in Xenopus embryos. J. Biol. Chem. 285, 2193–2202.

Steinmetz, P. R., Urbach, R., Posnien, N., Eriksson, J., Kostyuchenko, R. P., Brena, C., ... and Arendt, D. (2010). Six3 demarcates the anterior-most developing brain region in bilaterian animals. EvoDevo, 1(1), 1-9.

Stern, C.D. (2005). Neural induction: old problem, new findings, yet more questions. Development 132, 2007–2021.

Stern, C.D. (2006). Neural induction: 10 years on since the 'default model'. Current opinion in cell biology. 18, 692–697.

Stevens, M.E., Dhillon, J., Miller, C.A., Messier-Solek, C., Majeske, A.J., Zuelke, D., Rast, J.P., and Smith, L.C. (2010). SpTie1/2 is expressed in coelomocytes, axial organ and embryos of the sea urchin *Strongylocentrotus purpuratus*, and is an orthologue of vertebrate Tie1 and Tie2. Dev. Comp. Immunol. 34, 884–895.

Streit, A., Berliner, A.J., Papanayotou, C., Sirulnik, A., and Stern, C.D. (2000). Initiation of neural induction by FGF signalling before gastrulation. Nature 406, 74–78.

Su, Y.-H. (2009). Gene regulatory networks for ectoderm specification in sea urchin embryos. Biochim. Biophys. Acta 1789, 261–267.

Su, Y.-H., Li, E., Geiss, G.K., Longabaugh, W.J.R., Krämer, A., and Davidson, E.H. (2009a). A perturbation model of the gene regulatory network for oral and aboral ectoderm specification in the sea urchin embryo. Dev Biol 329, 410–421.

Su, Y.-H., Li, E., Geiss, G.K., Longabaugh, W.J.R., Krämer, A., and Davidson, E.H. (2009b). A perturbation model of the gene regulatory network for oral and aboral ectoderm specification in the sea urchin embryo. Dev Biol 329, 410–421.

Swalla, B.J., Sherrard, K., students of the Comparative Invertebrate Embryology course at FHL (2011). *Boltenia* embryos flash an orange crescent. Mol. Reprod. Dev. 78, 703.

Sweet, H.C., Gehring, M., and Ettensohn, C.A. (2002). LvDelta is a mesoderm-inducing signal in the sea urchin embryo and can endow blastomeres with organizer-like properties. Development. 129, 1945-1955 (2002)

Takacs, C.M., Amore, G., Oliveri, P., Poustka, A.J., Wang, D., Burke, R.D., and Peterson, K.J. (2004). Expression of an NK2 homeodomain gene in the apical ectoderm defines a new territory in the early sea urchin embryo. Dev Biol 269, 152–164.

Tamura, K., Peterson, D., Peterson, N., Stecher, G., Nei, M., & Kumar, S. (2011). MEGA5: molecular evolutionary genetics analysis using maximum likelihood, evolutionary distance, and maximum parsimony methods. Molecular biology and evolution, 28(10), 2731-2739.

Temereva, E., and Wanninger, A. (2012). Development of the nervous system in *Phoronopsis harmeri* (Lophotrochozoa, Phoronida) reveals both deuterostome- and trochozoan-like features. BMC Evol. Biol. 12, 121.

Thomas, J., Morlé, L., Soulavie, F., Laurençon, A., Sagnol, S., and Durand, B. (2010). Transcriptional control of genes involved in ciliogenesis: a first step in making cilia. Biol. Cell 102, 499–513.

Trimmer, J. S., & Vacquier, V. D. (1986). Activation of sea urchin gametes. Annual review of cell biology, 2(1), 1-26.

Trueb, B. (2011). Biology of FGFRL1, the fifth fibroblast growth factor receptor. Cell. Mol. Life Sci. 68, 951–964.

Tu, Q., Brown, C.T., Davidson, E.H., and Oliveri, P. (2006). Sea urchin Forkhead gene family: phylogeny and embryonic expression. Dev Biol 300, 49–62.

Tu, Q., Cameron, R.A., Worley, K.C., Gibbs, R.A., and Davidson, E.H. (2012). Gene structure in the sea urchin *Strongylocentrotus purpuratus* based on transcriptome analysis. Genome Research. 22, 2079–2087.

Turner, N., & Grose, R. (2010). Fibroblast growth factor signalling: from development to cancer. Nature Reviews Cancer, 10(2), 116-129.

Uchida, O., Nakano, H., Koga, M., and Ohshima, Y. (2003). The *C. elegans* che-1 gene encodes a zinc finger transcription factor required for specification of the ASE chemosensory neurons. Development 130, 1215–1224.

Wada, Y., Mogami, Y., and Baba, S. (1997). Modification of ciliary beating in sea urchin larvae induced by neurotransmitters: beat-plane rotation and control of frequency fluctuation. J. Exp. Biol. 200, 9–18.

Wada, S., and Saiga, H. (2002). HrzicN, a new Zic family gene of ascidians, plays essential roles in the neural tube and notochord development. Development, 129(24), 5597-5608

Wei, Z., Angerer, R. C., & Angerer, L. M. (2011). Direct development of neurons within foregut endoderm of sea urchin embryos. Proceedings of the National Academy of Sciences of the United States of America, 108(22), 9143-9147.

Walton, K.D., Warner, J., Hertzler, P.H., and McClay, D.R. (2009). Hedgehog signaling patterns mesoderm in the sea urchin. Dev Biol 331, 26–37.

Wei, Z., Yaguchi, J., Yaguchi, S., Angerer, R.C., and Angerer, L.M. (2009). The sea urchin animal pole domain is a Six3-dependent neurogenic patterning center. Development 136, 1179–1189.

Wikramanayake, A.H., Huang, L., and Klein, W.H. (1998). beta -Catenin is essential for patterning the maternally specified animal-vegetal axis in the sea urchin embryo. Proceedings of the National Academy of Sciences of the United States of America,95, 9343–9348.

Wilson, P.A., and Hemmati-Brivanlou, A. (1997). Vertebrate neural induction: inducers, inhibitors, and a new synthesis. Neuron 18, 699–710.

Wilson, S.I., Graziano, E., Harland, R., Jessell, T.M., and Edlund, T. (2000). An early requirement for FGF signalling in the acquisition of neural cell fate in the chick embryo. Current Biology 10, 421–429.

Wodicka, L. M., and Morse, D. E. (1991). cDNA sequences reveal mRNAs for two G {alpha} signal transducing proteins from larval cilia. The Biological Bulletin, 180(2), 318-327.

Wolpert, L., 2007. Principles of development. Oxford: Oxford University Press.

Wong, J.L., and Wessel, G.M. (2008). Free-radical crosslinking of specific proteins alters the function of the egg extracellular matrix at fertilization. Development 135, 431–440.

Yaguchi, J., Angerer, L. M., Inaba, K., & Yaguchi, S. (2012). Zinc finger homeobox is required for the differentiation of serotonergic neurons in the sea urchin embryo. Dev Biol 363(1), 74-83.

Yaguchi, S. (2006). Specification of ectoderm restricts the size of the animal plate and patterns neurogenesis in sea urchin embryos. Development 133, 2337–2346.

Yaguchi, S., Yaguchi, J., Angerer, R., and Angerer, L. (2008). A Wnt-FoxQ2-Nodal Pathway Links Primary and Secondary Axis Specification in Sea Urchin Embryos. Dev. Cell 14, 97–107.

Yaguchi, S., and Katow, H. (2003). Expression of tryptophan 5-hydroxylase gene during sea urchin neurogenesis and role of serotonergic nervous system in larval behavior. J. Comp. Neurol. 466, 219–229.

Yaguchi, S., Yaguchi, J., Angerer, R.C., Angerer, L.M., and Burke, R.D. (2010a). TGFβ signaling positions the ciliary band and patterns neurons in the sea urchin embryo. Dev Biol 347, 71–81.

Yaguchi, S., Yaguchi, J., Wei, Z., Jin, Y., Angerer, L.M., and Inaba, K. (2011). Fez function is required to maintain the size of the animal plate in the sea urchin embryo. Development 138, 4233–4243.

Yaguchi, S., Yaguchi, J., Wei, Z., Shiba, K., Angerer, L.M., and Inaba, K. (2010b). ankAT-1 is a novel gene mediating the apical tuft formation in the sea urchin embryo. Dev Biol 348, 67–75.

Yaklichkin, S., Vekker, A., Stayrook, S., Lewis, M., and Kessler, D.S. (2007). Prevalence of the EH1 Groucho interaction motif in the metazoan Fox family of transcriptional

regulators. BMC Genomics 8, 201.

Yu, J. K., Holland, N. D., and Holland, L. Z. (2003). AmphiFoxQ2, a novel winged helix/forkhead gene, exclusively marks the anterior end of the amphioxus embryo. Development genes and evolution, 213(2), 102-105

Yu, X., Ng, C.P., Habacher, H., and Roy, S. (2008). Foxj1 transcription factors are master regulators of the motile ciliogenic program. Nature Genetics 40, 1445–1453.

Yuh, C. H., Moore, J. G., & Davidson, E. H. (1996). Quantitative functional interrelations within the cis-regulatory system of the *S. purpuratus* Endo16 gene. Development, 122(12), 4045-4056.

Zhuang, L., Karotki, A., Bruecker, P., & Trueb, B. (2009). Comparison of the receptor FGFRL1 from sea urchins and humans illustrates evolution of a zinc binding motif in the intracellular domain. BMC biochemistry, 10(1), 33.

Appendix A:

Primers, morpholinos and clones

Presented below are tables of the primer sequences, morpholino sequences and clones used in this thesis. Table A.1. gives the sequences of the primers used to clone genes. Table A.2. gives the sequences of the primers used in QPCR. Tables A.3. gives the sequences used for the morpholinos. Table A.4. gives details of clones used in this study.

Table A.1. Sequence of cloning primers.

Gene name	Forward primer sequence	Reverse primer sequence
dcry	ATGGTCTCCGTCTCCATGAC	CAGTTGGGACACTGCAAGAA
fgf8	CCAATCATTCGGCGTAGTCT	CAGCTTTCGCCTCTGAATTT
fgfr like-1	GATAGAATGGCTCGGGTTTCGTC	AGCGTATGCTAGCAATGAAGAATG
fgfr1	GCCTGCCTGACCAATGTATG	GCATACGGACAACAGTCTCG
frizzled 5/8	GCTGCCTTCAGTGGAACAAT	CTCCCGAGTAATCTGTTGACG
hbn	TGAGAAATCCAATCGGGAAG	ACAGCAGGAGGAATCGCTTA
tie 1/2	CGTCAAGACGCTGAAAGATG	CACAATGTTGGGGTGTGTTC
tk9	GTCCCAGTGGCTACAGTGGT	AGGGATGCGATCCTAATGTG
vegfr7	TTGAGATTGGCGACAGTGAG	TGCGAGTTCATTTCCTCCTC
z167	TCAGGGATCAATCGACAGTG	GCTTCTGACCCGAGTGAATC
zic2	ACCACTATCACGCACACCAG	TTTGGCAGACGTACCATTCA

Table A.2. Sequence of QPCR primers.

Gene name	Forward primer sequence	Reverse primer sequence
ac-sc	TCAGCGGTGTCCTACATCAG	CTTCATCTTCAGGCGAGAGG
an-like4	CGAGTGCGACAATGAGTGTT	ATGGTGGTGTGGTGGTAGGT
bmp 2/4	CCAGCAAGGTCGAAGAACTC	CTCTACCCGACGACGATGAT
churchill1	AAGGACGATGGAGAGGAGGT	CCCACAAAGCATGCAGTACA
crim1-like	GTGCGCCAAAGTAGAAGGAG	CCTTGTTGAGGTTGGCTGTT
dcry	GGGTGTGCGTTATCTGACCT	CTCAATGCACTCGACCTTCA
delta	ACGGAGCTACATGCCTGAAC	TCACAATGGACCGAATCAGA
dispatched	GATCGCACGCTCTACAATGA	GCAGGATCATAATCGCACCT
dkk-3	ATGGCGATCTGGAAAGAGAA	CGATGACATCCACCGTAGTG
dynein heavy chain	CCATGGCTGAGCGGTACTAT	TGAATCTCCATGTCGGCTAC
dynein p33	TCGATGAGTTGATCCGTCAG	CCGAAGGCTACACTGCTTTC
e2f3	AATAGCGATCAAGGCACCAC	TTGATCCAGCTTCGGACTCT
ebf3	CCAGAGATGTGTCGTGTGCT	GCAGTTCTGGTTGCACTTGA
egr	CAATAGCGAGCACCTTGTGA	AGTTCTCCACGCCCAGTCTA
elipsa	CGATGATGTGGGTGAAGATG	CTTCGCCGTTCTCCTTACTG
fez	GGCTTTCCACCAGGTCTACA	CCCATTATCCGACGTCTTGT
fgf 9/16/20	CGTGTTGCTGCACAATCTCT	CGTCGACGAAGACGATGTAA
fgf8	AAGGGTAGACGCCAAAGGTT	TATTTATGCGTCAACGGCAA
fgf8_t1	CGTGGGAGGAAGACACATTT	CTTCTAGCCGCAGTTTGTCC
fgf8_t2	GCAGACGATCAGGTGGAGTT	GATGTGTGACGACGAACCTG
fgf8_t3	CACTTGCGAGGAAGGACCTA	TTTTCAGGGGTTTTCACTGG
fgfr1	CCTTCGGACAAACCAGACAT	TGATCCTGAGTGGGAGTTCC
fgfr2	AATGGCGGTGTCTACCAAAG	ACACCAGGGTACGGGTATGA
fgfr like-1	CGGCACCTACATGTGCATAG	ATGTTGTGCCTCCAAACTCC
foxa	CCAACCGACTCCGTATCATC	CGTAGCTGCTCATGCTGTGT
foxc	TAGCCCGATCCTTACCACAC	CATACCGCCGTAATGGTCTT
foxd	AGGTGGACATGACCCATGAT	GCTGTTTCCGATTTCGAGTC
foxg	CGCTCGAGTCCAGAGAAAAG	TGTCGAGGGACTTTCACAAA
foxj1	TAGGCAACCACGACCTTACC	TAGGCAACCACGACCTTACC
foxq2	CCGATTCGGATCATGAGTTT	CCGATTCGGATCATGAGTTT
frizzled 5/8	TAGGCAACCACGACCTTACC	CCGATTCGGATCATGAGTTT
geminin	CTGGGAAGAACTGGCTGAAG	GGCCATGACCTTGAGTTTGT
glass2	CAGCCGAACTTCCTCAACTC	GTGGAGACGAAGGGTGAGAC
gremlin	ATCCTGGCTGGGTCTACCTT	TCCAGGAGGGAACAATAACG
hbn	ACCACATTCCAACTGCATCA	CCAAACCTGGACTCGTGATT
hedgehog	GGCTTCGATTGGGTCAACTA	GTTGACCACGGCTACCTCAT
hlf	TGAAGGAGCGTCTCCTGTTT	CTCATTGGTGGTGGAGGACT
hnf6	TGCAGCTTCTCTGCATACCA	ACTCCAACATGCCTCCAAAC
hp1	GGCAGACCTTGAAAGAGCAC	CAACCTGGCTCCGTACAAAT
huntingtin	AAGTTCCTCACCACCCACTG	CCTTCCAGCTTCGTCAGTTC

(Table A.2. Continued)

id	ACCGGTATGATCACGGACTC	TGTTGCCTTACGTTGCTCTG
meg1	CTGTTGCCGTAGCACAAGAA	TCCTCTGCAGCTTCTTCACA
mox	GCTCGACCTAACAGCCAAAC	CCCACCTGTCTCTCGGTAAG
nk2.1	CGTGAGAGCTTCCCTACCTG	GAAGCTCCCTAGCTCGATGA
nkx3-2	ACTTGCCTTGCGTCTTCAAT	ACCGTCACGAAACGATTCTC
nodal	GACAACCCAAGCAACCACG	CGCACTCCTGTACGATCATG
pacrg	GACAGCATCGACTACGGACA	ATGCGTCGGAACCATGTACT
pacrg_like1	TCATCATTTGGACCTCCTCCT	TTCTGGTTTGTGAATGGATCA
pax2/5/8	CCAAAGGTGGTGTCGAAGAT	ATCGAGCTGACACTGGGAAC
pax6	CGGACTCTACCCGACAGAAG	AGCTACCCGAGGCTTACTCC
pitx2	TTTCGATGACGGCCTCTACT	CGGAGGGTTGAAACACATCT
radial spoke 3	ACCTTTCAATGGCACAGAGG	ACGGTTTCCATCTTCCTCCT
rbph	GATTCAATATTGCGCCCTCT	CTCTTTGTCAGGTGCGATCA
rej5	ATCGCAGCTTGCTCTGGTAT	CTTCCTGCTCCTCAGGTGTC
rfx1/2/3	TCTGATCGAGCACAAAGTGG	GAATTGACGGTTGCGGTAGT
rib74	TCGACGTCAACGAACTCAAG	CATGAACTCTGCGTGGCTTA
rsh p63	AAGATTGCAGCCAAGAGAGC	GCTTCCACATCTGCTTCCTC
rx	CGACAGTTACCCGCTCTCTC	GCTGCTGCTGTTGATGATGT
sfrp1/5	CATGTGCGAGAACTTGGAGA	TAACCGGTGTGTTGGTCTGA
sfrp3/4 i	ACCAGGACGTTGCCTATTTG	ACCTTGTGGGCTTGATTGAC
six3	TCAAAGAGAGAACGCGGAGT	AAACCAGTTTCCGACCTGTG
sm30	GTTCTCCGGTAGGCAAACA	ACATTTTGGGGCAAATGAAA
sm50	TAGCCTTTGCTACGGGTCAA	CTGAGGCGACGAAACTGAA
soxb1	TGGTGTGGTCAAGAGGACAA	GTAGTCCGGATGCTCCTTCA
soxb2	GGCATGATTTGGCTGGATAC	ATCCCATCTTGGTCAACAGC
sprouty	GGTTCTTCCAGCGAGTCATC	GGCTGGCTGTGTAAGGATGT
synaptogamin	GGAAAGCTCAATGTGGGTGT	CTGGGTTGAGGGTCTTTCTG
tecktin3	GAGTTGGGCCAAGTTTAGCA	CTTCCACTGAAGGCCACATT
tektin-2	GACAAGGACCTGGCAGAGAG	TCCTTGCCGACTTCTGAGTT
tph	GAATTTGCAGCAACCATCAA	GGTCAATTCGTCTCGGACAT
tubulin alpha 2	TGTCTCCTGTACCGTGGTGA	GACAGTGGGTGGCTGGTAGT
ubq	CACAGGCAAGACCATCACAC	GAGAGAGTGCGACCATCCTC
unc 44	CCAGACCAGAAGCACCATCT	TCTCGATGCCCTTCTCTGTT
vegfr7	GTCCTGTCTTGGCCATTGTT	CTTCATGCGTCTTTCACTGC
vitellogenin2	AATGCCAAGACCAGGTTCAC	CACGATCAACTGAGGCAGAA
z167	CCCAAGACCGCTACATCAGT	AGCGTAAGCGTCGAGTTGAT
zfhx1	GATGACTTGGAGCCGGATAA	TTGCTGTATCACTGCGGTTC
zic2	CCAGCGACCGTAAGAAACAT	ACTGCTGTCGTTGGCTTCTT

Table A.3. Morpholino details: Morpholino name, sequence and morpholino type.

Morpholino name	Sequence	Morpholino type
*fgfr1*_MASO 1	TCCTCGGACAACGCGGCAGACTCAT	Translation blocker
*fgfr1*_MASO 2	CGTGGCTGACCGAAGCATAGTTTTC	Translation blocker
*zic2*_MASO	ACCACTATCACGCACACCAG	Translation blocker

Table A.4. Clone details: Gene name, vector used for cloning , clone size and RNA polymerase used to produce antisense probe.

Gene name	Vector	Clone size	For antisense
six3	pSport1_Sfi	2.1 kb	SP6
frizzled 5/8	pGEM-T Easy	1586 bp	T7
hbn	pGEM-T Easy	1159 bp	SP6
zic2	pGEM-T Easy	1664 bp	SP6
fgfr1	pGEM-T Easy	2668 bp	SP6
dcry	pGEM-T Easy	1523 bp	SP6
fgf 9/16/20	pSport1_Sfi	1.3 kb	SP6
nkx3.2	pSport1_Sfi	1.8 kb	SP6
delta	pSport1	Oliveri *et al.*, 2002	
foxG	pSport1	556 bp	SP6
foxQ2	pSport1	526 bp	T7
mox	pGEM-T Easy	2.0 kb	SP6
z167	pGEM-T Easy	1196 bp	SP6
fgfr like-1	pGEM-T Easy	1468 bp	SP6
fgf 8/17/18/24	pGEM-T Easy	2600	T7
an like-4	pGEM-T Easy	1.9 kb	SP6
tie 1/2	pGEM-T Easy	2826	SP6
tk9	pGEM-T Easy	1182	SP6
vegfr7	pGEM-T Easy	1078	SP6
foxj1	pSport1	1509 bp	SP6

Appendix B:

Nematostella apical organ gene set, number of embryos counted and temporal expression profiles.

Table B.1. gives a list of apical organ genes found in *Nematostella* (supplied by Chiara Sinigaglia and Fabian Rentzsch) and the closest match in sea urchin. Table B.2. gives the numbers of embryos counted for each gene during the mapping experiments. Table B.3. presents temporal expression profiles with exact number of transcripts per embryos. The majority of the temporal expression data were produced from QPCR analysis of different apical organ genes and for some the data is gathered from Nanostring nCounter (Tu *et al.,* 2010).

Table B.1. *Nematostella* apical organ gene set and sea urchin homologues. Table shows *Nematostella* gene names, unique identifier "Nvseq ID" and sea urchin homologues names and gene IDs

Nematostella		Sea urchin	
Gene Name	**Nvseq ID**	**Gene Name**	**Gene ID**
Transcription factor, contains HOX domain	153628	Sp-Mlx1	SPU_011297
Dyneins, heavy chain	224165	Sp-DNAH8	SPU_030027
Uncharacterized conserved protein	113661	SpPARCG-like1	SPU_012917
Uncharacterized conserved protein	182272	Sp_PACRG	SPU_004619
Kinesin-like protein	30871	Sp-Kif16L	SPU_026237
Acetylcholine receptor	199721	Sp-Nachrα2_1	SPU_001774
Annexin	96324	Sp-AnxA7	SPU_019139
NvGremlin	95464	Sp_Gremlin	SPU_020030
uncharacterized	81173	Not annotated	SPU_005437
Flavin-containing monooxygenase	235461	Sp-FMO6L	SPU_007044
Spondins, extracellular matrix proteins	79471	Sp-Spon2L1	SPU_029584
Trypsin	53190	Sp-Mamdc4	SPU_015727
Fibroblast/platelet-derived growth factor receptor	41471	SP-Tie 1/2	SPU_024044
Dynein-associated protein Roadblock	237378	Sp-Rbgh	SPU_003137
FOG: Armadillo/beta-catenin-like repeats	31543	Sp-Armc4-2	SPU_007521
Beta tubulin	245773	Sp-BetaTubulin3	SPU_030062
Trypsin	147392	Sp-Arvlike	SPU_004114
Meprin A metalloprotease	131533	Sp-Arvlike	SPU_004114
Fibroblast growth factor	212596	Sp-FGF	SPU_006242
Smoothened and related G-protein-coupled receptors	200285	Sp-Dhp1/5	SPU_011271
Smoothened and related G-protein-coupled receptors	183962	Sp_Frizzeled 5/8	SPU_022916
Transcription factor of the Forkhead/HNF3 family	65436	Sp-FoxJ1	SPU_027969
TBX2 and related T-box transcription factors	165815	tbx 2-3	SPU_023386
Transcription factor zerknüllt and related HOX domain proteins	81249	Sp-Lox	SPU_026099
Kinesin-like protein	234547	Sp-Kif9L2	SPU_000875
Acetylcholine receptor	110265	Sp-Nachα6	SPU_001774
Chromatin assembly factor-1	188814	Sp-Cccb81	SPU_021664
Uncharacterized conserved protein, contains BTB/POZ domain	164988	Sp-Btbd16	SPU_015356
Projectin/twitchin and related proteins	240082	Sp-Titin	SPU_005613
FOG: RCC1 domain	89190	Sp-Nek9-2	SPU_019063
Annexin	96179	Sp-AnxA7	SPU_019139
Annexin	34056	Sp-AnxA7	SPU_019139
tektin	195162	Sp-Ccdc105	SPU_002424
Myosin class II heavy chain	93943	Sp-Ccdc105	SPU_002424
Ran GTPase-activating protein	218953	SP-RanGAP1	SPU_004276
uncharacterized	205233	Not annotated	SPU_004496
uncharacterized	59658	Not annotated	SPU_004558
Cyclin-dependent kinase 2-associated protein	86457	Not annotated	SPU_004653
uncharacterized	11327	Not annotated	SPU_005267
LRR-containing protein	24768	Sp-C14orf166b	SPU_005282
LRR-containing protein	212934	Sp-C14orf166b	SPU_005282
LRR-containing protein	3074	Sp-C14orf166b	SPU_005282
Protein phosphatase 1, regulatory subunit, and related proteins	244589	Sp-Lrrc48	SPU_006598
Aldehyde dehydrogenase	249626	Sp-Aldh2	SPU_007284
Uncharacterized conserved protein	143747	Sp-Hypp_517	SPU_007461
Ca2+-permeable cation channel OSM-9 and related channels (OTRPC family)	81127	Sp-Kcat2	SPU_007504
Translation initiation factor 5B (eIF-5B)	240906	Sp-Hypp_1772	SPU_008203
N-acetylglucosaminyltransferase I	191253	Sp-Pomgnt1	SPU_008219
uncharacterized	242786	Tenascin1	SPU_009640
uncharacterized	240540	Not annotated	SPU_010239
Adenylate kinase	98446	Not annotated	SPU_010767
Uncharacterized conserved protein	238199	Sp-Hypp_1972	SPU_011316
testicular haploid expressed gene product	172654	Sp-Thegl	SPU_011786
G protein-coupled receptors	237703	Sp-Egf like	SPU_012362
Protein phosphatase 1, regulatory subunit, and related proteins	208307	Sp-Caskin1	SPU_012637
Dual-specificity tyrosine-phosphorylation regulated kinase	120202	Sp-Dyrk4	SPU_012899
uncharacterized	182410	Sp-Agpx1	SPU_013076
sperm associated antigen 17	224084	Sp-Spag17	SPU_013103
Malate dehydrogenase	90973	Sp-Mdh1b	SPU_015928
Cdc4 and related F-box and WD-40 proteins	218233	Sp-Fbxw7L	SPU_015976
uncharacterized	209931	Not annotated	SPU_017778
uncharacterized	245069	Sp-C20orf26L	SPU_018537
SNF2 family DNA-dependent ATPase	237587	Sp-Hypp_2392	SPU_018584
Uridylate kinase/adenylate kinase	232309	Sp-Adk	SPU_019553
MYM type Zn finger	239479	Sp-Kdm1L_7	SPU_021568
endoglucanase	83869	Sp-eGas	SPU_021602
Spermatogenesis-associated protein 17	223606	Sp-Spata17	SPU_023743
WD40-repeat-containing subunit of the 18S rRNA processing complex	183356	Sp-Wdr49	SPU_026011
uncharacterized	233391	Sp-C1orf177L	SPU_026146
Myosin class II heavy chain	93609	Not annotated	SPU_026595
uncharacterized	160170	Sp-Hypp_2578	SPU_026963
Tetraspanin family integral membrane protein	171968	Sp-Thspn_22	SPU_027747
uncharacterized	237330	Sp-Hypp_2955	SPU_028435
Ca2+/calmodulin-dependent protein kinase, EF-Hand protein superfamily	117995	Sp-Drak	SPU_029549
Taurine catabolism dioxygenase TauD/TfdA, bacterial	242938	No match	
GTPase-activating protein	245865	No match	
Fibroblast growth factor	196402	No match	
Transcription factor, contains HOX domain	84003	No match	

Table B.2. Number of embryos used in counting experiments. During mapping experiments, DAPI staining was used to count the individual nuclei that expressed a given gene using epiflourscent microscopy. The number of embryos (n) counted for each gene at each developmental stages is shown.

	Hatching blatsula	Hatched blastula	Mesenchyme blastula	Mid-gastrula	Late gastrula	Other stages	Total embryos counted
fgf 9/16/20	-	-	12	8	10	5	35
fgfr1	8	4	8	6	6	9	41
foxQ2	16	22	23	13	31	8	113
frizzled 5/8	32	10	19	14	13		88
hbn	5	12	7	7	5	7	43
nkx3.2	-	-	5	7	9		21
six3	14	9	8	8	5		44
zic2	13	7	6	10	5	17	58
							443

Table B.3. Temporal expression profiles. Values are given as number of transcripts per embryo and are shown for different developmental stages. Results are colour coded to represent levels of expression: red (0-50 transcripts), orange (50-150 transcripts), yellow (150-500 transcripts), green (500-1500 transcripts), turquoise (1500-5000 transcripts), blue (5000-15000 transcripts), dark blue (>15000).

Name	SPU	0	5	7	9	12	15	18	21	24	27	30	33	36	48	hours
		Data gathered using QPCR (this thesis)														
armadillo	SPU_004121	93	31		304	127	682	832	407	522	715	403	463	868	389	
churchill1	SPU_013399	50	44	31	21	15	34	9	11	16	28	39	24	55	54	
crim1-like	SPU_027369	0	0	3	8	20	4	4	3	4	19	38	28	179	245	
dory	SPU_000282	154	225	123	133	81	27	71	78	135	148	189	159	178	135	
dispatched	SPU_020459	5	1	1	2	6	0	0	0	0	0	0	1	1	6	
dkk-3	SPU_012506	0	0	6	70	75	110	70	94	75	115	118	78	166	119	
dynein heavy chain	SPU_030227	13058	8219	10079	12470	30083	19449	28814	31165	30641	30571	18147	27751	37896	32837	
dynein p33	SPU_015320	13058	8219	10079	12470	30083	19449	28814	31165	30641	30571	18147	27751	37896	32837	
ebf3/coe	SPU_004702	162	117	207	117	63	23	12	6	8	24	38	29	167	190	
egf2	SPU_013932	22	18	12	266	3670	14250	28347	45142	57787	65674	73398	72238	60303	43273	
egflike	SPU_012362	6	8	27	28	46	19	50	127	97	143	273	139	451	80	
fgfr like-1	SPU_020680	8	238	30	5	43	94	62	67	77	95	143	117	295	348	
fgfr1	SPU_020677	715	358	334	269	194	397	1579	2019	2109	2034	2606	8068	5268	6937	
fgfr2	SPU_004747	0	23		4	0	1	3	2	16	99		309	121	64	
frizzled 5/8	SPU_022916	718	607	352	827	1339	1332	644	557	665	741	1010	837	1002	1030	
frzb1	SPU_026015	0	0	4	7	23	49	28	19	27	25		18	20	30	
geminin	SPU_005762	4524	4494	6091	5003	1609	869	413	280	250	244	90	279	234	2642	
glass2	SPU_007599	0	0	1	2	1	0	0	1	1	1	2	26	59	235	
gremlin	SPU_020330	2	0		28	42	3	34	4	1	97	1	23	699	73	
hp1	SPU_012728	619	381	422	431	591	687	609	679	610	818	1058	695	734	798	
huntingtin	SPU_011485	49	53	41	33	14	11	17	26	47	56	61	69	64	67	
meg1	SPU_002300	3826	1827		1301	861	4609	9457	12204	5041	8572		3203	2158	737	
mox	SPU_025486	1	0	5	1	31	19	9	4	8	1	3	2	22	63	
neurod	SPU_024918	1	10	1	14	196	30	7	7	0	9	6	1	1	8	
neurogenin	SPU_007147	1	3	2	1	2	3	2	3	4	5	6	7	8	14	
nkx3-2	SPU_013047	0	0	3	5	3	1	24	35	45	62	89	84	272	251	
obelix	SPU_026487	18	5	18	26	46	37	45	47	81	98	75	150	232	136	
pacrg	SPU_004619	6599	2512		2014	1073	4491	10346	7628	3336	3169		1727	2038	618	
pacrglike1	SPU_012917	27	26		38	26	56	37	21	18	20	28	14	22	37	
paxc	SPU_000276	2	2	4	5	2	2	1	1	2	2	8	12	187	284	
radial spoke 3	SPU_014801	319	278	326	324	477	502	508	382	351	286	348	223	399	302	
rbph	SPU_003137	48	27		63	46	40	79	72	72	88	102	71	118	121	
rej5	SPU_023615		12	1	34	196	293	98	91	29	79	56	115	55	51	
rfx1/2/3	SPU_007611	12816	9735	12903	10897	8825	6127	6060	3110	2093	1860	1349	2814	3915	4175	
rib74	SPU_021429	4067	1317		679	265	971	2190	2480	1393	1669		2037	819	313	
rsh p63	SPU_012045	491	31	126	8	748	1081	709	453	606	578	226	620	519	10	
sfrp	SPU_026015	6	8	3	11	6	13	9	16	16	13	18	17	87	74	
sfrp1/5	SPU_011271	194	185	159	183	330	239	151	176	219	277	477	383	780	1089	
sfrp3/4 i	SPU_004062	25	17	62	678	2694	4266	3144	2442	2647	2524	1994	1498	2344	1966	
sn like-4	SPU_004117	24	134	375	7864	20867	104998	4792	5175	6695	9262	5314	6913	13524	41650	
sprouty	SPU_025676		168	62	259	323	625	473	1109	383	2198	694	2928	988	1958	
synaptotagmin	SPU_005854	639	374	290	217	370	558	295	415	319	354	286	407	636	461	
tektin 3	SPU_023618	478	110	89	124	1052	874	624	470	362	517	390	404	404	321	
tektin-2	SPU_020728	1675	377	701	547	1938	2604	1633	716	367	385	183	395	210	388	
tph	SPU_003725	0	0		5	15	6	3	12	22	20	49	72	446	447	
tubulin alpha 2	SPU_04143	12871	5059	6665	5644	14798	28035	32671	43131	46718	58573	51395	42447	36901	34769	
unc 44	SPU_024961	7	6	7	9	8	8	13	79	204	252	406	516	604	603	
unc4.1	SPU_001739	14	6	90	525	4228	3047	2639	2683	2765	2995	3633	2667	4546	4980	
unk9	SPU_017609		1182	675	1053	1026	903	758	808	717	1311	1519	1186	1150	944	
vlpv rna pol	SPU_027021		0	1	17	38	276	279	404	142	287	145	223	128	79	
z142	SPU_022841	22	43	27	71	11	6	7	11	10	11	10	23	19	21	
z167	SPU_015362	0	1	1	1	2	1	3	1	1	2	2	384	205	21	
zfhx1/z81	SPU_022242	67	63	80	641	1340	228	210	395	386	364	443	492	490	416	
		Data gathered from NanoString nCounter (Tu et al., 2010)														
delta	SPU_016128	15	19	26	107	329	336	298	217	153	141	155	164	151	162	
fgf 9/16/20	SPU_006242	6	1	1	3	1	6	24	45	58	63	80	88	138	120	
foxg	SPU_009771	2	2	3	3	3	11	76	143	174	227	350	432	377	392	
foxq2	SPU_019002	3	12	66	414	1096	1451	1748	1714	1701	1877	1792	1120	1207	1014	
hbn	SPU_023177	3	2	4	58	204	450	621	711	703	592	646	672	724	558	
six3	SPU_018908	27	27	51	661	1752	1273	1340	1513	1874	1844	1804	1982	1815	1457	
zic2	SPU_028583	2	2	4	58	160	447	506	418	371	339	341	377	285	202	

Appendix C:

SU5402 positive control (SM30) and complete SU5402 data table

Below are presented additional results of SU5402 perturbations. Figure C.1. shows that no significant effect is seen on gene expression until 6 hours after SU5402 is added. Table C.1. shows ddCT values for all SU5402 perturbation experiments carried out.

Figure C.1. Effect of SU5402 perturbation on the expression of *sm30* (positive control). Embryos collected at 0 hours, 3 hours, 6 hours and 9 hours after SU5402 was added. Differences in mRNA levels relative to controls are shown as ddCt. Significant threshold is a ddCt of +/-1.6. Positive numbers indicate upregulation and negative number downregulation relative to controls (significant downregulation, red bar). It is clear that SU5402 does not have a significant effect on gene expression until 6 hours after SU5402 is added.

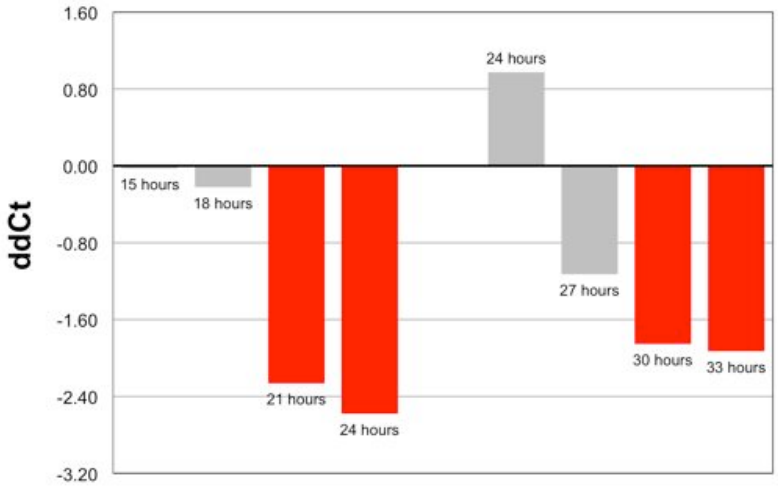

Table C.1. SU5402 perturbation data table. Differences in mRNA levels relative to controls are shown as ddCt. Significant threshold is a ddCt of +/-1.6. "R" = repeat.

SU5402 added at:	6 hours		15 hours				24 hours				38 hours	
Embryos collected at:	12 hours	15 hours	21 hours		24 hours		30 hours		33 hours		41 hours	44 hours
			R1	R2	R1	R2	R1	R2	R1	R2		
ac-tc	NE	NE	-0.9		-0.6		0.8	0.8	0.0	0.5	-0.2	0.6
an-like4	1.3	3.2	4.8	2.4	4.6	2.5	6.1	5.0	6.2	4.2	4.5	3.4
bmp 2/4	NE	NE	-0.3		-1.0		1.4	0.9	1.1	-0.2	0.7	0.5
churchill1	1.0	0.9	-0.3		0.9		1.4	1.7	1.2	1.8	0.8	1.1
crim1-like	NE	NE	0.8		-0.1		0.5	0.9	1.0	0.1	-0.2	-0.2
dcry	1.9	1.8	0.9	0.5	1.4	-0.8	1.3	-0.6	1.1	-0.6	1.2	1.1
delta	0.0	0.0	0.8	0.5	1.5	0.9		0.5		0.9	-0.9	-0.2
dispatched	1.1	1.7	0.7		-0.5		2.2	1.6	0.4	0.3	1.5	0.9
dkk-3	-0.4	-1.0	0.4		-0.5			0.5	0.6	0.1	2.0	0.6
dynein ji33	-0.1	0.0	0.9	0.4	2.0	0.9	1.9	1.8	0.8	0.5	1.2	1.0
dynein heavy chain	NE	NE	1.9		2.4			2.1		3.8	3.6	
e2f3	-1.3	-1.1	0.5		-0.1		0.9	0.2	0.9	-0.2	0.0	1.1
ebf3	1.4	2.5	0.6		-0.2		0.9	0.1	-0.4	-0.4	0.4	-0.1
egr	1.0	1.3	0.0		0.2		1.5	0.9	0.9	1.8	1.7	0.8
elipse	0.3	0.3	-0.1		0.4		1.3		0.3		1.4	0.6
fez	NE	NE	-0.7		-0.3		1.5	0.7	1.1	0.5		
fgf 9/16/20	NE	NE	-0.9		-0.6		0.6	0.1	0.4	0.2	0.0	0.7
fgfr like-1	0.2	0.2	0.1		0.8		1.7	1.0	1.1	0.9	1.3	1.3
fgfr1	0.9	-0.2	1.1	1.7	1.9	0.8	1.8	1.0	1.4	1.1	0.9	1.3
fgfr2	NE	NE	1.9		1.3		0.6	0.3	-0.1	0.0	0.3	-1.0
foxd	NE	NE	NE	NE	NE	NE	NE	NE	NE	NE	0.1	0.3
foxg	NE	NE	0.2		0.6			-0.2		-0.1	0.7	0.5
foxj1	0.9	2.1	1.2	0.8	2.0	0.8	2.1	1.6	1.9	2.0	1.5	2.1
foxq2	1.1	0.1	0.1	0.4	0.5	-0.2	1.0	0.7	0.7	0.4	0.8	-0.3
frizzled 5/8	0.9	0.9	0.3		0.6		1.7	0.6	0.5	0.7	0.8	1.3
geminin	0.6	1.9	1.0		1.5		1.4		0.3		1.1	0.7
z167	NE	NE	NE	NE	NE	NE	0.6		-0.6		-0.2	0.5
hbn	-1.3	-1.2	0.0		-0.4		0.7	0.6	0.4	0.6	0.6	0.2
hlf	-0.5	-0.3	0.0		0.7		2.2	0.4	1.9	0.5	0.3	0.7
hnf6	1.1	0.6	0.8	0.7	1.0	0.9		0.5		0.3	0.1	0.8
hp1	0.1	0.3	0.8		1.6		1.7	1.0	1.9	1.1	1.3	1.5
huntingtin	NE	NE	0.0		-0.8			1.2		0.8	0.8	0.7
id	0.1	0.5	0.7		0.6			0.8		0.9	0.5	0.6
meg1	-0.2	0.2	-0.5		1.1		1.8	1.2	1.6	1.1	0.9	1.6
mox	NE	NE	NE	NE	NE	NE	-0.3	0.5	0.1	-0.6	0.3	0.4
nk2.1	NE	NE	-0.5		0.2		1.0	0.5	1.0	0.9	0.4	0.5
nkx3-2	NE	NE	-0.9		-0.8		1.4	0.7	0.4	0.6	0.9	0.8
nodal	0.4	1.1	-0.6	0.7	2.2	1.3	2.0	1.3	1.7	1.3	1.3	1.0
pairg	-0.8	-0.6	0.9		1.5		1.6	0.6	0.8	0.9	1.3	1.3
pacrg_like1	0.4	0.8	0.4		1.2			1.0		1.3	0.8	0.8
pax2/5/8	NE	NE									-2.4	-2.4
pax6	NE	NE	0.8		-0.2			0.3		0.4	0.3	0.3
p5x2	NE	NE	0.3		-0.6			0.4		0.4	-0.5	0.6
radial spoke 3	-0.2	-0.1	1.3		1.4		2.0	1.2	0.5	1.1	1.2	1.1
rbph	0.3	0.2	0.5		1.2			1.1		1.1	0.9	0.8
rej5	-0.9	0.4	0.1		1.3		1.8	1.6	2.1	2.4	1.4	1.3
rfx1/2/3	0.8	0.3	2.2		2.3		1.8	1.5	0.6	1.4	1.4	0.7
rib74	-0.2	-0.1	0.7		1.1		1.4	n	0.9		0.8	0.8
rsh p53	-0.7	0.4	0.7		1.9		1.5	?	0.5		0.6	1.2
rx	NE	NE	-1.2		-0.6		0.4	1.6	0.5	1.3	0.7	0.9
sfrp1/5	1.1	0.7	0.0		0.2		1.2	0.8	2.6	0.3	0.6	0.4
sfrp3/4 /	-0.3	0.1	1.0		2.1		1.2	0.8	1.3	0.9	0.9	0.2
six3	0.8	0.6	0.9	0.1	-1.5	-0.1	0.4	0.4	0.5	0.9	-0.8	-0.1
sm30	NE	NE	-2.3	-1.9	-2.6	-2.7	-1.9	-1.8	-1.9	-2.2	0.0	-0.2
sm50	0.8	0.5	-0.1		-0.0		0.6		0.4		0.0	0.0
soxb1	0.4	1.1	-0.3		0.4		0.7	0.1	0.6	0.2	0.0	0.9
sprouty	-0.2	0.2	0.3		0.0		0.7		0.4		-0.2	-0.5
synaptogamin	0.1	0.2	0.8		1.4			1.5		1.0	0.9	0.1
tektin 3	-1.0	-0.4	0.0		2.1		2.7	1.6	1.4	1.9	1.6	1.8
tektin-2	-0.4	0.2	-0.1		1.7		1.8	0.9	0.7	1.0	1.1	1.1
tubulin alpha 2	-0.8	-0.6	-0.2		-0.5		1.2		0.8		0.8	0.7
unc 44	-0.9	-1.1	0.6		0.3		1.8	1.2	1.1	1.2	0.9	0.7
vitellogenin2	-0.4	0.3	-0.2		0.0						0.2	0.4
zic2	-0.7	-1.4	1.2	2.0	1.7	0.3	2.2	1.7	0.8	1.2	2.2	1.3